# STUDIES ON CELLULOSE ACETATE AND POLYAMIDE BASED OSMOTIC MEMBRANES FOR TREATMENT OF AQUEOUS STREAMS

*By*

**Ms. Bitan Ghosh**

[CHEM01201304015]

**Bhabha Atomic Research Centre**

*A thesis submitted to the*

*Board of Studies in Chemical Sciences*

*In partial fulfillment of requirements*

*for the Degree of*

**DOCTOR OF PHILOSOPHY**
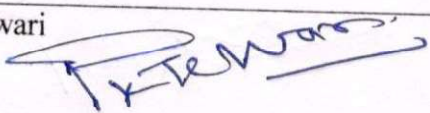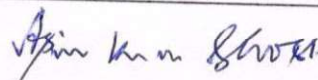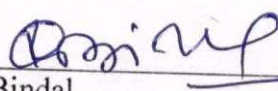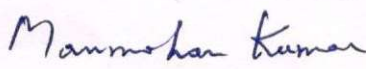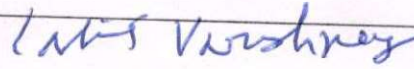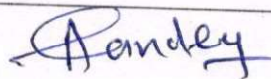
*of*

**HOMI BHABHA NATIONAL INSTITUTE**



**October, 2018**

# Homi Bhabha National Institute

## Recommendations of the Viva Voce Committee

As members of the Viva Voce Committee, we certify that we have read the dissertation prepared by **Ms. Bitan Ghosh** entitled **"Studies on Cellulose Acetate and Polyamide Based Osmotic Membranes for Treatment of Aqueous Streams"** and recommend that it may be accepted as fulfilling the thesis requirement for the award of Degree of Doctor of Philosophy.
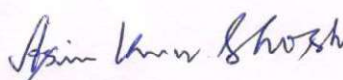
Chairman – Prof. P.K. Tewari

Date: 22/10/2018

Guide / Convener – Prof. A. K. Ghosh

Date: 22/10/18

Examiner – Prof. Parag Nemade

Date: 22/10/18

Member 1- Prof. R.C. Bindal

Date: 22.10.18

Member 2- Prof. Manmohan Kumar

Date: 22/10/18

Member 3- Prof. Lalit Vershney

Date: 22/1-/18

Member 4- Prof. A.K. Pandey

Date: 22.10.2018

Final approval and acceptance of this thesis is contingent upon the candidate's submission of the final copies of the thesis to HBNI.

I/We hereby certify that I/we have read this thesis prepared under my/our direction and recommend that it may be accepted as fulfilling the thesis requirement.

Date: 22/10/2018

Place: HRDD, Anushaktinagar

(Signature)
Guide

# STATEMENT BY AUTHOR

This dissertation entitled **"Studies on Cellulose Acetate and Polyamide based Osmotic Membranes for Treatment of Aqueous Streams"** has been submitted in partial fulfillment of requirements for an advanced degree at HomiBhabha National Institute (HBNI) and is deposited in the Library to be made available to borrowers under rules of the HBNI.

Brief quotations from this dissertation are allowable without special permission, provided that accurate acknowledgement of source is made. Requests for permission for extended quotation from or reproduction of this manuscript in whole or in part may be granted by the Competent Authority of HBNI when in his or her judgment the proposed use of the material is in the interests of scholarship. In all other instances, however, permission must be obtained from the author.

*Bitan Ghosh* 22.10.18

(Ms. Bitan Ghosh)

# DECLARATION

I, hereby declare that the investigation presented in the thesis entitled **"Studies on Cellulose Acetate and Polyamide based Osmotic Membranes for Treatment of Aqueous Streams"** has been carried out by me. The work is original and has not been submitted earlier as a whole or in part for a degree / diploma at this or any other Institution / University.

*Bitan Ghosh, 22.10.18*

(Ms. Bitan Ghosh)

# LIST OF PUBLICATIONS

**Journal:**

a. <u>Published:</u>

1. Effect of Addition of Iron Salt in Amine Solution on Performance of Polyethylene Imine-Isophthaloyl Chloride (PEI-IPC) based Polyamide-Polysulfone Composite Reverse Osmosis (RO) Membranes. **Bitan Ghosh**, A.K. Ghosh, R.C. Bindal, P.K. Tewari, *Journal of Polymer Materials*, 3 (2014) 29-38

2. Studies on Concentration of Simulated Ammonium Diuranate Filtered Effluent Solution by Forward Osmosis using Indigenously Developed Cellulosic Osmosis Membranes. **Bitan Ghosh**, A.K. Ghosh, R.C. Bindal, P.K. Tewari, *Separation Science and Technology*, 50 (2015) 324-331

3. Preparation of High Flux Aliphatic –Aromatic Based Polyamide Thin-Film Composite Osmosis Membranes by Addition of Inorganic Metal Salts with Amine Reactant, **Bitan Ghosh**, A.K. Ghosh, R.C. Bindal, *Separation Science and Technology* (in press), *https://doi.org/10.1080/01496395.2018.1532963*

4. High Flux Thin–film composite polyamide (TFCP) Forward Osmosis membranes for Concentration of Simulated Cesium and Strontium bearing Effluent solution, **Bitan Ghosh**, A.K. Ghosh, V.S. Mamtani, R.C. Bindal, *Separation Science and Technology (accepted)*

b. <u>Communicated:</u>

1. Development of Performance Enhanced Cellulose Triacetate Based Forward Osmosis Membranes by Incorporation of Nanomaterials, **Bitan Ghosh**, A.K. Ghosh, R.C. Bindal (Under communication)

2. Development of Polyimide Based Solvent Resistant Membranes and their Application in Complexation Nanofiltration Using Organic Solvents, **Bitan Ghosh**, T.K. Dey, R.C. Bindal (Under communication)

3. Development of Polyamide Membranes for Treatment of Simulated Ammonium Di Uranate Effluent Solution, **Bitan Ghosh**, A.K. Ghosh, R.C. Bindal (Under communication)

## Conferences:

1. Concentration of Solution and Recovery of water by Forward Osmosis using Composite Polyamide Membranes; **Bitan Ghosh**, A.K.Ghosh, R C Bindal and P.K. Tewari ; Proceedings of International Conference on Water Desalination, Treatment and Management *(InDACON-2013), Jaipur*

2. Concentration of Simulated Ammonium-diuranate Filtered Effluent solution by Forward Osmosis using Composite Polyamide Membranes; **Bitan Ghosh**, A.K. Ghosh, R.C. Bindal, P.K. Tewari; Proceedings of DAE-BRNS Theme Meeting on Membrane Separations for Fuel Cycle Applications *(MEMSEP-2013), BARC, Mumbai*

3. Development of Thin-film Composite (TFC) Reverse Osmosis (RO) membranes with Enhanced Separation Performance by in-situ Polymerization of Magnesium-complexed Polyethylene imine and Isophthaloyl chloride; **Bitan Ghosh**, A.K. Ghosh, R.C. Bindal, P.K. Tewari; Proceedings of Symposium of Emerging Trends in Separation Science and Technology *(SESTEC 2014), BARC, Mumbai*

4. Performance Enhancement of Cellulose triacectate based Forward Osmosis Membranes by incorporation of Nanomaterials; **Bitan Ghosh**, A.K.Ghosh, R C Bindal, Proceedings of International Conference of International Conference on Nanostructured Polymeric Materials and Polymer Nanocomposites (ICNPM 2015), *MGU, Kerala*

5. Development of Polyimide Based Solvent Resistant Membranes and Their Application in Complexation Nanofiltration using Different Organic Solvents; **Bitan Ghosh**, T.K. Dey, R. C. Bindal, Proceedings of Interdisciplinary Symposium on  Materials Chemistry *(ISMC-2016), BARC, Mumbai.*

6. High Flux Thin–film composite polyamide (TFCP) Forward Osmosis membranes for Concentration of Simulated Cesium and Strontium bearing Effluent solution ; A. K. Ghosh, **Bitan Ghosh**, V.S. Mamtani, R.C. Bindal, Proceedings of Emerging Trends in Separation Science and Technology *(SESTEC-2018), BITS Pilani, Goa (2018).*

*Bitan Ghosh* 22.10.18

(Ms. Bitan Ghosh)

*Dedicated*

*to*

*My Parents*

# ACKNOWLEDGEMENTS

# GLOSSARY OF ABBREVIATIONS

| Abbreviation | Full form |
|---|---|
| AFM | Atomic force microscope |
| BSE | Back scattered electrons |
| CA | Cellulose acetate |
| CAB | Cellulose acetate blend |
| CSA | Camphor sulfonic acid |
| CTA | Cellulose triacetate |
| DLS | Dynamic light scattering |
| DMAc | N,N-dimethyl acetamide |
| DMF | N,N-dimethyl formamide |
| EDX | Energy dispersive X-ray |
| FEG | Field emission gun |
| FO | Forward osmosis |
| IP | Interfacial polymerization |
| IPC | Isophthaloyl chloride |
| LMD | Liter per meter square per day |
| LMH | Liter per meter square per hour |
| MPD | m-Phenylenediamine |
| NF | Nanofiltration |
| NMP | N-methyl 2- pyrrolidone |
| PA | Polyamide |
| PEG | Polyethylene glycol |
| PEI | Polyethylene imine |
| PEO | Polyethylene oxide |
| PES | Polyethersulfone |
| PSf | Polysulfone |
| PVDF | Polyvinylidenefluoride |
| PVP | Polyvinyl pyrrolidone |
| PWP | Pure water permeability |
| RO | Reverse osmosis |

| | |
|---|---|
| SEM | Scanning electron microscope |
| SFE | Surface free energy |
| SR | Solute rejection |
| SRNF | Solvent resistant nanofiltration |
| TEA | Triethyl amine |
| TFC | Thin film composite |
| TFC-PA | Thin film composite Polyamide |
| TMC | Trimesoyl chloride |
| TOC | Total organic carbon |
| UF | Ultrafiltration |
| VRF | Volume reduction factor |

# CONTENTS

# SYNOPSIS

In the present thesis an attempt has been made to develop cellulose acetate and polyamide based membranes for treatment of different aqueous streams. The thesis consists of six chapters and the contents of each chapter are briefly outlined below. Towards this purpose, asymmetric membranes from cellulose acetate, cellulose triacetate and cellulose acetate blend has been developed targeting application on concentration of simulated Ammonium Di Uranate (ADU) filtered solution. Nanocomposite cellulosic membranes with enhanced performance were developed by incorporation of silica, silver and silver-silica nanoparticles onto cellulose triacetate. Thin film composite polyamide membranes were developed by in situ poly condensation reaction between amine and acid chloride and different inorganic salts were incorporated for performance enhancement of the overall membranes under standard desalination condition. Polyimide membranes were prepared from commercially available Lenzing P 84 polymer followed by chemical crosslinking to make them stable in harsh organic environment containing NMP, DMF and DMAc. The thesis consists of six chapters and the contents of each chapter are briefly outlined below.

## Chapter 1: Introduction

Osmosis is a phenomenon that has been exploited by human beings since the early days of mankind and later extensively studied by scientists in various disciplines of science and engineering. Following the progress in membrane science in the last few decades, especially for reverse osmosis (RO) applications, the interests in engineered applications of osmosis has been spurred. Osmosis, or as it is currently referred to as forward osmosis (FO), has new applications in separation processes for wastewater treatment, food processing, and seawater/brackish water desalination etc. However, RO and FO being two complementary membrane processes use similar kind of polymer materials for preparation of membranes. Cellulosic and polyamide

polymers are used worldwide for development of osmotic membranes depending upon their field of applications. Both the membrane processes and the types of membranes have advantages and disadvantages in their own way and development of application specific osmotic membranes are the biggest challenge of membrane sciences in current era.

FO is emerging as a potential membrane process used in many applications nowadays where RO dominated for several decades (1, 2).. It has advantages like operation at low or no hydraulic pressure, high rejection for wide range of contaminants, may have lower irreversible fouling than pressure-driven membrane processes (3). "Concentrate-and- contain" is one of the principles employed in the radioactive waste management. FO is one of the most favorable membrane process used to concentrate a desired stream but its application in this area is completely a new topic till date. The major challenges of FO processes are choice of ideal draw solution and high-performance membranes (4) for a particular application and the same could be true for application on concentration of radioactive solution. In case of concentration of radioactive solution, the radiation stability of the membrane is an additional requirement as the level of radioactivity increases with time as concentration increases. As per the membrane development status is concerned, cellulose acetate (CA) based membranes are most commonly used for osmosis applications and membranes from cellulose acetate (CA), CTA, CA-CTA blend, poly vinyl alcohol (PVA) modified cellulose acetate (CA) polymeric systems etc. has been developed in laboratory scale (5-7). Hence, some of the low level radioactive solution has been chosen which needs to be concentrated to keep in smaller volume. One such example is the filtered solution of the ammonium diuranate (ADU) precipitate which contains radio contaminants associated with uranium and its daughter products, and significant quantities of ammonium nitrate (about 40000 ppm) at around pH 7.5.

Development of high performance FO membranes is one ofthe priority research topics in the FO area (8-14). performance of existing commercial FO membranes [asymmetric cellulose

triacetate (CTA) membranes from Hydration Technology Inc. (HTI)] shows that asymmetric CA based membranes have (i) low to moderate water permeability in FO mode & (ii) more prone to biofouling. Nanocomposite membranes, a new class of membranes fabricated by combining polymeric materials with nanomaterials, are emerging as a promising solution to these challenges.

In reverse osmosis, the driving force for water permeation through the membrane is applied external pressure and not the osmotic pressure gradient.. Thin film composite (TFC) polyamide membranes are preferred over cellulosic membranes for all kind of applications in RO. The support layer of TFC membrane imparts the mechanical stability to the membrane whereas the thin active layer is responsible for flux and rejection properties and these two layers can be tailored independently to develop a high performance osmotic membrane. Development of high performance osmotic membranes is thereby emerging as a new field in membrane sciences (17–25). TFC polyamide membranes can be prepared by polycondensation reaction between m-Phenylenediamine (MPD) and trimesoyl chloride (TMC) or between Polyethylene imine (PEI) and Isophthaloyl chloride (IPC). The advantage of PEI/IPC based membranes is stability and reusability of amine with the disadvantage of its low water permeability under standard operating condition of RO. It is thereby intended to develop high flux PEI/IPC based membranes by incorporation of some metals salts and changing the reaction kinetics of interfacial polycondensation reaction.

Most of the polymers suitable for preparation of membranes used for different pressure driven processes being soluble in polar protic solvents like N,N-Dimethyl acetamide (DMAc), N-methyl pyrrolidone (NMP) and N,N-dimethyl formamide (DMF), offers a challenge to the current researchers to develop stable high performance membranes suitable for use either in pure organic medium or aqueous/organic mixed environment containing common solvents like DMAc, DMF, NMP etc. in long run. So far little work has been reported on development of

solvent resistant nanofiltration (SRNF) membranes (26-28) suitable for use in harsh polar aprotic organic environment with good rejection. In the present work, effort have been made to develop SRNF membranes by chemically crosslinking the polyimide membranes making them stable in harsh organic environment with high rejection of complexed and uncomplexed polar protic solvent.

## Chapter 2: Experimental

Cellulosic membranes are prepared by dissolving prerequisite amount of the polymer [cellulose acetate (CA) and/or cellulose triacetate (CTA)] into suitable solvent (mixture of acetone/dioxan with a trace amount of methanol in case of CTA only). In case of nanocomposite membrane preparation, nanoparticles are dispersed into the solvent by ultrasonication prior to addition of the polymer. The homogeneous polymer solution formed in casted over a nonwoven fabric, thickness maintained by doctor's knife followed by evaporation of solvent for 30 seconds. The whole setup is immersed into deionized water bath at ambient temperature where solvent-nonsolvent exchange takes place resulting in formation of asymmetric cellulosic membranes. The gelled membranes are then washed thoroughly to remove any excess solvent and annealed in hot water bath for 15minutes. The membranes are kept in refrigerator cooled water till further use.

Thin film composite (TFC) polyamide membranes are prepared in two steps. In first step polysulfone support membrane is prepared by phase inversion technique. Prerequisite amount of polymer beads are dissolved in N-Methyl pyrrolidone (NMP) to prepare a homogeneous polymer solution which is subsequently casted over nonwoven fabric by doctors knife followed by immediate immersion into water bath. In the second step, the polysulfone membranes were immersed into the aqueous amine solution with and without metal salts of known

iv

concentrations for 2 minutes. The amine saturated membranes are then dipped into 0.25% isophthaloyl chloride in hexane. Polycondensation reaction between amine and acid chloride takes place at the interface resulting in formation thin polyamide film. The resultant composite polyamide membrane is then heat cured for 10minutes under IR lamp and stored in a desiccator till further use.

Asymmetric polyimide membranes are prepared by phase inversion technique similar as discussed earlier. In order to make these membranes stable in harsh organic environment, the integrally skinned membranes are chemically crosslinked by ethylene diamine in methanol followed by thorough rinsing by methanol and EDI water.

Hydrophilicity of all the membranes are determined by measuring pure water contact angles using the sessile drop method on a standard drop shape analysis system (DSA100, KRüSSGmbH,Germany). Surface average roughness of the membranes are measured in semi contact tapping mode by using atomic force microscope, AFM (NT-MDT-Multimode 3, Ireland),equipped with standard silicon nitride cantilever.

Performance of the membranes are evaluated bydetermination of water permeability and percentage (%) salt rejection at 225 psig (1551 kPa) pressure using 2000ppm NaCl solution as feed (standard BWRO condition). Permeate flux is reported as $L.m^{-2}.d^{-1}$ (LMD) [Flux = volumetric flow rate of permeate (Liters)/active area of membrane ($m^2$) × operation time (day)] andSalt rejection (S.R) by each membrane is determined according to % S.R = [(1 − $C_p$/$C_f$) ×100] where $C_f$ and $C_p$ are the salt concentrations of feed and permeate solutions.

The performance of the membranes is further evaluated using a lab-scale FO test system. Both feed and draw solutions are circulated by variable speed pumps to minimize concentration polarization. The change in volume and back-diffusion of the salt from draw solution side to feed water is measured and reported.

**Chapter 3: Development of Cellulosic and Polyamide Osmosis Based Forward Osmosis Membranes Suitable for Simulated Low Level radioactive Waste Treatment:**

Cellulosic osmosis membranes for concentration of simulated ADU filtrate are prepared using CA, CTA and cellulose acetate blend (CAB) [blending of CA and CTA] by phase inversion technique. Composition of each system is optimized in way that all the membranes show similar salt rejecting properties (~90%) under standard brackish water reverse osmosis (BWRO) condition. All the membranes were characterized by water contact angle determination, surface roughness analysis and surface image analysis by SEM. The performance of the membranes in terms of volume reduction factor for concentration of solution containing 40,000 ppm of $NH_4NO_3$ and 20 ppm uranium increases in the order of CTA<CAB<CA membranes with negligible (0.45-0.56%) leaching of uranium to the draw solution side for all the membranes. Three different draw solutions, viz. $NH_4NO_3$, $NH_4HCO_3$ and $CaCl_2$ of 4(M) concentration were used for similar set of experiment. It was found that because of higher osmotic pressure exerted by $CaCl_2$ solution, volume reduction factor is highest in this case.Effect of concentration of draw solutions were monitored by taking 3 different concentrations [2(M), 3(M) & 4(M)] of $NH_4NO_3$& $CaCl_2$ solutions. By increasing the draw solution concentration, the volume reduction factor is increased invariably at a cost of back diffusion of draw solution resulting in contamination of feed side. Hence, in the case of low to medium level radioactive waste treatment, FO can offer a means for concentrating the activity in smaller volumes (concentrated feed) and making the larger volumes (diluted draw solution) suitable for direct disposal. Membrane pouch is a simple device that can be used for concentration of desired stream with proper choice of the membrane.

**Chapter 4: Performance Enhancement of Cellulose triacetate based Forward Osmosis Membranes by incorporation of Nanomaterials:**

The objective of this work is to develop high performance CA based FO membranes by incorporation of porous silica nanoparticles and silver nanoparticles to the polymer matrix. Porous silica nanoparticles are expected to provide extra channels for water passage and lower the overall S value by decreasing tortuosity resulting to mitigate the effect of internal concentration polarization (ICP) whereas Ag nanoparticles are expected to impart antibiofouling property to the membranes. Composite cellulose triacetate membranes are prepared by incorporation of silica and/or silver nanoparticles with intention to increase product permeability and biofouling resistance behavior. Polymer dope solutions were prepared by dissolving known amount of polymer in a mixture of Acetone, Dioxan and Methanol solvents. Phase inversion by solvent/nonsolvent exchange into the gelling media forms the asymmetric cellulosic membrane which is subsequently annealed in hot water to make the membranes suitable for FO applications. Membranes are characterized in terms of surface hydrophilicity, surface morphology and product permeation rate & salt rejection for NaCl feed under standard BWRO testing condition (2000ppm NaCl feed at 1551kPa pressure).Porous silica nanoparticles provide extra channels for permeation of water as well as salt, thereby increase flux at the expense of rejection as compared to our control membrane. CTA-silica-Ag nanocomposite membranes show somewhere intermediate result in similar line of control. A very interesting result is obtained from CTA-Ag nanocomposite membranes. No such tradeoff between flux and rejection is noticed in this case, these membranes are showing highest water permeability without any compromise in rejection (over 93% rejection is obtained under standard BWRO condition).Hydrophilic silica nanoparticles enhance the overall hydrophilicity of the membranes thereby decreasing their water contact angle value from 47° to 37.3°. Hydrophilicity of the membranes increases in the order CTA-blank<CTA-Ag<CTA-slica-

Ag<CTA-silica. Performance of the membrane in terms of volume reduction factor using UF water as feed and 0.5(M) NaCl as draw solution shows increase VRF in the order CTA<CTA-silica-Ag=CTA-silica<CTA-Ag with <2% back diffusion of salt from draw solution side to feed side. By increasing draw solution concentration, volume reduction factor can be increased but that may result in more back diffusion. Hence incorporation of porous nanoparticles may lead to formation of membranes with enhanced water permeability of low flux asymmetric cellulosic membranes.

**Chapter 5: Development of Performance Enhanced Aliphatic-Aromatic Polyamide Thin-film Composite Osmotic Membranes by Addition of Inorganic Metal Salts with Amine Reactant:**

Addition of metal salts in amine solution for modification of PEI by complexation and thereby changing the polymer globule size may impact on the performance of ultimate TFC RO membranes. Inorganic metal salts we have used with PEI reactants for preparation of TFC membranes are $CuSO_4$, $NiSO_4$, $MgSO_4$ and $Al_2(SO_4)_3$. Complexation of PEI with metal ions results in formation of smaller size globules in presence of metal ions which ends up affecting polycondensation reaction kinetics between amine and acid chloride. Addition of inorganic salts also changes the ratio of primary, secondary and tertiary amine groups resulting in changing the polycondensation reaction kinetics. All the membranes were characterized using water contact angle and atomic force microscopy studies. Performances of the TFC membranes were evaluated both in reverse osmosis mode using 2000ppm NaCl as feed under 15bar operating pressure and in forward osmosis mode using deionized water as feed and 0.5 (M) NaCl solutions as draw solution. It was found that with increase in concentration of all the metal salts, the performance of TFC membranes were enhanced up to a certain concentration of the metal ions followed by significant decrease in salt rejection with further increase in salt

concentration. The optimum metal salt concentration was identified for all the metal salts for maximum performance enhancement and it is found to be 2m(M) for $MgSO_4$ & $Al_2(SO_4)_3$ and 0.8m(M) for $CuSO_4$ & $NiSO_4$. At optimum concentration of metal ion, the effects of different anions for same metal ion and different molecular weight of PEI were also evaluated on composite polyamide membrane performances. To understand effect of molecular weight of polymeric amine, two different molecular weight of amine (viz. 50KDa and 600KDa) of same concentration are prepared with and without addition of metal sulfates. It can be seen that both the permeate flux and NaCl rejection are more for the membranes prepared using high molecular weight PEI (PEI-600KDa) than the membranes prepared with lower molecular weight PEI (PEI-50KDa) and the trend remains same even after addition of metal salts in PEI solution. Addition of metal salts invariably enhances performance of the membranes in terms of water permeability and salt rejection. To study the effect of lower molecular weight of PEI on membrane performance keeping the metal ion concentration fixed, 0.8m(M) $Ni^{+2}$ salt is taken with PEI-2KDa and the composite membrane performances are compared with that of membranes prepared using PEI-50KDa and PEI-600KDa. Water permeability and salt rejection data follows the trend PEI-2KDa> PEI-600KDa> PEI-50KDa and PEI-600KDa> PEI-50KDa> PEI-2KDa. Addition of metal salts increases water permeability with no significant change in rejection keeping the trend same. To observe the effect of change of anion keeping the cation fixed, three different (sulfate, chloride and nitrate) salts of $Mg^{2+}$ and two different (sulfate and nitrate) salts of $Cu^{2+}$ are added to the amine solution. It is found that for both the cases when anion changes from sulfate to nitrate keeping the metal ion same, the product flux of the composite polyamide membrane increases significantly with almost no change in salt rejection and gives more hydrophilic membrane with smoother surface. Nitrate being the monovalent ion, increases the overall ionic strength of the amine solution as compared to the addition of bivalent ion and it is reported that with increase in ionic strength of the solution, hydrodynamic

radius of PEI decreases and thus diffusion of PEI through initially formed polyamide layer becomes faster resulting in change in physicochemical properties as well as separation performance of the overall polyamide membrane. EDX data of blank TFC (prepared using only PEI), TFC- $CuSO_4$ (prepared with PEI &0.8 milimolar $CuSO_4$) and TFC-$Cu(NO_3)_2$[prepared with PEI + 0.8 milimolar $Cu(NO_3)_2$] membranes confirms that $Cu^{2+}$ is not there in both TFC-$CuSO_4$ and TFC-$Cu(NO_3)_2$ membranes. As it is the $Cu^{2+}$-PEI complex which took part in polycondensation reaction with acid chloride and not the free PEI, it can be concluded that the metal ion gets de-complexed from PEI during polycondensation reaction and leaches either to the aqueous solution inside the pores of polysulfone support or to the bulk organic solution of isophthaloyl chloride. Based on the new findings, a conceptual model was proposed to explain the role of metal ion in amine solution on the resulting characteristics of aromatic-aliphatic type polyamide-polysulfone composite membrane.

Similar set of experiment has been carried out with a range of concentration of $FeSO_4$ in PEI solution to determine the optimum concentration of $FeSO_4$ (0.8 m(M)). Surface roughness analyses shows that the membrane becomes rougher with increase in concentration of Fe-salt with a marginal change in hydrophilicity. Effect of molecular weight of polymeric amine in presence of 0.8 m(M) of $FeSO_4$ follows the trend as discussed earlier. Addition of $FeSO_4$ invariably enhances the membrane performance in terms of water permeability with marginal increase in salt rejection. Variation in reaction time confirms addition of metal salts decreases the time required to complete polycondensation reaction because of decrease in hydrodynamic radius of polymer globules which in turn makes the diffusion of PEI faster. Thus the optimum time of reaction is 60seconds for only PEI whereas the same is somewhere around 15-30 seconds for PEI/$FeSO_4$ system. The same may be attributed to the higher surface roughness value of PEI/$FeSO_4$as compared to that of blank PEI system.

**Chapter 6: Development of Polyimide Based Solvent Resistant Membranes and Their Application in Complexation Nanofiltration using Different Organic Solvents:**

It is hereby intended to develop high performance solvent resistant nanofiltration type membranes with minimum or no swelling for use in media containing harsh polar aprotic organic media like DMAc, NMP and DMF. Lenzing P-84 polyimide based nanofiltration membranes with different extent of cross linking have been developed for high performance complexation nanofiltration application involving a set of organic solvents. The membrane casting and cross linking conditions as well as evaporation time, concentration of crosslinker and time of cross linking are optimized to achieve membranes with high organic rejection with very high stability in these harsh environments. Membranes after crossinking show up to about 6times flux enhancement as compared to their controls withoutsignificant compromise in solute rejection (<90%) under standard nanofiltration condition. Decrease in glass transition temperature (Tg) after crosslinking of membranes infers some molecular relaxation which in turn enhances the water permeability by 6 fold. Surface roughness analysis indicates the membranes become smoother with increasing time of crosslinking whereas almost no change in water contact angle value indicates no significant change in hydrophilicity of the membrane due to crosslinking. Crosslinked membranes show upto 85% rejection for DMAc complexed with HCl. Further complexation of the DMAc/HCl with iron containing ligands results in very high rejection (97%) of the organic molecule as confirmed by UV-Vis spectrophotometric analysis. Similar results have also been obtained with identical complexes of other polar aprotic organic solvents like DMF and NMP.

## 7. Conclusions and Future Recommendations:

The conclusions of each studies carried out as a part of the thesis is summarized in this chapter. Indigenously developed cellulosic membranes can be used for concentration of simulated ADU filtrate developed and by proper choice of draw solutes and its concentration. Performances of asymmetric cellulosic membranes are enhanced successfully by incorporation of nanoparticles in laboratory. Addition of metal salts results in performance enhanced TFC polyamide membranes due to complexation of PEI with metal ions. Incorporation of metal salts decreases the hydrodynamic volume of PEI which in turn makes the diffusion of amine faster resulting in lowering of time of polycondensation reaction. Optimized crosslinking of lenzing P84 makes the membranes highly stable in harsh organic media with very high rejection of complexed and uncomplexed polar aprotic solvents in aqueous streams.

### References:

1. Cath, T.Y.; Childress, A.E.; Elimelech, M. Forward osmosis: principles, applications, and recent developments, J. Membr. Sci. 2006, 281, 70–87.

2. Shannon, M.A.; Bohn, P.W.; Elimelech, M.; Georgiadis, J.G.; Marinas, B.J.; Mayes, A.M. Science and technology for water purification in the coming decades, Nature 2008, 452, 301–310.

3. Lee,S.;Boo,C.;Elimelech,M.;Hong,S.Comparisonoffoulingbehavior in forward osmosis (FO) and reverse osmosis (RO), J. Membr. Sci. 2010, 365, 34–39.

4. Zhao, S.; Zou, L.; Tang, C.Y.; Mulcahy, D. Recent developments in forward osmosis: Opportunities and challenges, J. Membr. Sci. 2012, 396, 1–21.

5. Li, G.; Li, X.M.; He, T.; Jiang, B.; Gao, C. Cellulose triacetate forward osmosis membranes: preparation and characterization, Desalination and Water Treatment 2013, 51, 2656–2665.

6. Wang, K.Y.; Ong, R.C.; Chung, T-S. Double-skinned forward osmosis membranes for reducing internal concentration polarization within the porous sub layer, Ind. Eng. Chem. Res. 2010, 49, 4824–4831.

7. Ahn, H.R.; Tak, T.M.; Kwon, Y-N. Preparation and applications of poly vinyl alcohol (PVA) modified cellulose acetate (CA) membranes for forward osmosis (FO) processes, Desalination andWater Treatment2013, doi: 10.1080/19443994.2013.834516.

8. Chung, T.S.; Su, J.C.; Yang, Q.; Teo, J.F. Cellulose acetate nanofiltration hollow fibermembranes for forward osmosis processes, J. Membr. Sci. 2010, 355, 36–44.

9. Wang, R.; Shi, L.;Tang, C.Y.Y.; Chou, S.R.; Oiu, C.; Fane, A.G. Characterization of novelforward osmosis hollow fiber membranes, J. Membr. Sci. 2010, 355, 158–167.

10. Chou, S.R.;, Shi, L.; Wang, R.; Tang, C.Y.Y.; Oiu, C.Q.; Fane, A.G. Characteristics andpotential applications of a novel forward osmosis hollow fiber membrane,Desalination, 2010, 261, 365–372.

11. Yip, N.Y.; Tiraferri, A.; Philip, W.A.; Schiffman, J.D.; Elimelech,M. High performancethin-film composite forward osmosis membrane, Environ. Sci. Technol.2010, 44, 3812–3818.

12. Elimelech, M.; Tiraferri, A.; Yip, N.Y.; Phillip, W.A.; Schiffman, J.D. Relating performanceof thin-film composite forward osmosis membranes to support layerformation and structure, J. Membr. Sci. 2011, 367, 340–352.

13. Wei, J.; Oiu, C.Q.; Tang, C.Y.Y. Wang, R. Fane, A.G. Synthesis and characterizationofflat-sheet thin film composite forward osmosis membranes, J. Membr. Sci.2011, 372, 292–302.

14. Qi, S.; Oiu, C.; Tang, C.Y. Synthesis and characterization of novel forward osmosismembranes based on layer-by-layer assembly, Environ. Sci. Technol. 2011, 45, 5201–5208.

15. Chou, S.; Wang, R.; Shi, L.; She, Q.; Tang, C.Y.;Fane, A.G.Thin-film composite hollowfiber membranes for pressure retarded osmosis (PRO) process with high powerdensity, J. Membr. Sci. 2012, 389, 25–33.

16. Qi, S.; Oiu, C.;Zhao, Y.; Tang, C.Y. Double-skinned forward osmosis membranesbased on layer-by-layer assembly − FO performance and fouling behavior, J.Membr. Sci. 2012, 405–406, 20–29.


17.Jeong B.H.; Hoek, E.M.V.;Yan, Y.; Subramani, A; Huang, X.; Hurwitz, G.; Ghosh, A.K.; Jawor ,A. Interfacial polymerization of thin film nanocomposites: a new concept for reverse osmosis membranes, J. Mmembr. Sci. 2007, 294(1-2), 1-7.

18. Kong, C.; Koushima, A.; Kamada, T.; Shintani, T.; Kanezash, M.; Yoshioka, T.; Tsuru, T. Enhanced performance of inorganic-polyamide nanocomposite membranes prepared by metal-alkoxide-assisted interfacial polymerization, J. Membr. Sci. 2011, 366(1-2), 382-388.

19. Kulkarni, A.; Mukherjee, D.; Gill, W.L. Flux enhancement by hydrophilization of thin film composite reverse osmosis membranes, J. Membr. Sci. 1996, 114(1), 39-50.

20. Lind, M.L.; Suk, D.E.; Nguyen, T.V.; Hoek, E.M.V. Tailoring the structure of thin film nanocomposite membranes to achieve seawater RO membrane performance, Environ. Sci. Technol.2010, 44(21), 8230-8235.

21. Lu, X.; Castrillon, S.R.V.; Shaffer, D.L.; Ma, J.; Elimelech, M. In situ surface chemical modification of thin-film composite forward osmosis membranes for enhanced organic fouling resistance, Environ. Sci. Technol. 47(21), 12219-12228.

22. Park, J.; Choi, W.; Kim, S.H.; Chun, B.H.; Bang, J.; Lee, K.B. Enhancement of chlorine resistance in carbon nanotube based nanocomposite reverse osmosis membranes, Desalination and Water Treatment, 2010, 15(1-3), 198-204.

23.Pendergast, M.T.M.; Nygaard, J.M.; Ghosh, A.K.; Hoek, E.M.V. Using nanocomposite materials technology to understand and control reverse osmosis membrane compaction, Desalination, 2010, 261(3), 255-263.

24.Petersen, R.J. Composite reverse osmosis and nanofiltration membranes, J. Membr. Sci. 1993, 83(1), 81-150.

25.Ramachandhran, V,; Ghosh, A.K.; Prabhakar, S.; Tewari, P.K.Preparation and Separation Performance Studies on Composite Polyamide Membranes using different Amine Systems and Support Membranes ,J. Polym. Mater. 2009, 26, 177-185.

26. Zwijnenberg, H.J.; Dutczaka, S.M.; Boerrigtera, S.E.; Hempenius, M.A.; Luiten-Olieman, M.W.J.; Benes, N.E.; Wessling, M.; Stamatialise, D. *Important factors influencing molecular weight cut-off determination of membranes in organic solvents*, J. Membr. Sci. 2012, 390–391, 211–217.

27. Darvishmanesh, S.; Taselli, F.; Jansen, J.C.; Tocci, E.; Bazzarelli, F.; Bernardo, P.; Luis, P.; Degrève, J.; Drioli, E.; Bruggen, B.V. *Preparation of solvent stable polyphenylsulfone hollow fibre nanofiltration membranes*, J. Membr. Sci. 2011, 384, 89–96.

28. Zhang, H.; Zhang, Y.;Li, L.; Zhao, S.; NI, H.; Cao, S.; Wang, J. *Cross-linkedpolyacrylonitrile/polyethyleneimine–polydimethylsiloxane composite membrane for solvent resistant nanofiltration*, Chem. Engg. Sc. 2014, 106, 157-166.

# LIST OF FIGURES

# LIST OF FIGURES

# LIST OF TABLES

# LIST OF TABLES

# CHAPTER – I

# INTRODUCTION

## 1.0. Background

Over the past few decades, membrane processes have been adopted to perform a variety of separation operations in process industries. The main advantages of membrane technology as compared with other unit operations in separation processes are related to its unique separation principle, i.e. the transport selectivity of the membrane. These ambient temperature operations do not require additives and do not involve phase changes like other conventional separation techniques such as distillation, crystallization, evaporation etc. Also, upscaling and downscaling of membrane processes as well as their integration into other separation or reaction processes are easy. A membrane is an inter-phase between two adjacent phases acting as a selective barrier, regulating the transport of substances between the two compartments. It can be conceived as a three dimensional macromolecular porous network with symmetric or asymmetric morphology which restricts the mobility of various permeating constituents by virtue of their differing nature and extent of interaction. The absolute rate at which a permeate transverses through a membrane is known as permeability and the rate at which two different species permeate relative to one another is called selectivity. Permeability and selectivity of membranes are the two fundamental properties which determine the productivity of a given membrane process. Depending on the nature of the membrane, the driving force required to effect separation across the membrane and the species separated, various membrane processes have been recognized. The membrane processes are rate governed involving single step continuous molecular separation of species under the influence of an applied external field across the barrier. The commercially significant membrane processes are driven by only three forces namely, gradients of concentration, electricity and pressure. Characteristics of some of the commercially significant membrane processes are given in Table 1.1.

However, in subsequent discussion, only forward osmosis of concentration gradient driven and pressure driven membrane processes are discussed in this thesis.

Pressure driven membrane processes, namely, reverse osmosis (RO), nanofiltration (NF), ultrafiltration (UF) and microfiltration (MF) separate suspended or dissolved particles of different sizes by utilization of polymeric membranes of specific functional characteristics with controlled surface pore structure and surface morphology. In order of decreasing pore size, the membrane processes are microfiltration (MF), ultrafiltration (UF), nanofiltration (NF) and reverse osmosis (RO). In the FO process, the water flows from the feed solution (lower osmosis pressure) to the draw solution (higher osmosis pressure) across the designed semi-permeable membrane without any external energy consumption. FO uses only osmotic pressure as the driving force for mass transport. This osmotic gradient in FO is achieved by placing a higher osmotic pressure solution ("draw" solution) on the permeate side of the membrane. Therefore, FO process possesses unique advantages of high energy efficiency, high water recovery, low fouling tendency, simplicity and reliability, compared to other pressure-driven membrane separation processes, such as nanofiltration (NF) and reverse osmosis (RO) [1, 2]. A summary of these processes is given in Table 1.2.

The synthesis of the membrane is the first step for membrane process because membranes are the heart of the membrane systems. The theoretical basis on which a polymer is chosen to be appropriate as membrane material is well documented. However, the choice of polymeric candidates for membrane synthesis for use in above process is largely guided by functional utility, processibility and cost factors. Membranes can be prepared from polymer which can be natural, semisynthetic or fully synthetic. Naturally occurring polymers, such as cellulose was used commonly as membrane barrier after a suitable chemical modification. The history of synthetic

membranes began after the invention of first semisynthetic polymer, cellulose nitrate by Schonbein [3]. Cellulose nitrate membranes were used after this by different groups in several studies [4, 5]. Integrally-skinned cellulose acetate hyperfiltration membranes were reported by Loeb and Sourirajan [6] in 1960. Noncellulosic reverse osmosis membranes were developed by Orofino et.al. [7] in order to get superior mechanical, thermal, chemical and microbial resistance than cellulosic polymers. The significant progress of polymeric membranes is listed in Table 1.3. Both natural and synthetic polymeric membranes are widely used in the field of membrane but synthetic polymeric membranes are studied henceforth.

**Table 1.1: Characteristics of commercially practiced membrane processes.**

| Process | Driving force | Objective |
|---|---|---|
| Gas, vapor and organic liquid permeation | Concentration gradient (pressure, temperature assisted) | Product enriched in a desired component |
| Forward Osmosis | Concentration gradient | Concentration of a desired component with dilution of draw solution |
| Dialysis | Concentration gradient | Solutions of macro-solutes free of micro-solutes |
| Electrodialysis (ED) | Electrical potential | Solvent free of ionic solutes, removal or concentration of ionic solutes, ion replacement and electrolyte fractionation. |

| Microfiltration (MF) | Pressure | Sterilization, particulate removal |
|---|---|---|
| Ultrafiltration (UF) | Pressure | Separation and concentration of macrosolutes |
| Nanofiltration (NF) | Effective pressure | Removal of organic dyes, separation of multivalent ions, fractionation of electrolytes |
| Reverse osmosis (RO) | Effective pressure | Desalination, effluent water treatment and salt concentration |

**Table 1.2: Summary of pressure driven separation processes and membranes.**

| Process features | | | Membrane characteristics | | |
|---|---|---|---|---|---|
| Process | MWCO (Daltons) | Operational pressure $(Kg/cm^2)$ | Structure | Porosity (%) | Pore size range (A) |
| MF | > 100,000 | $1 - 2$ | Several types (all skinless) | ~ 70 | $10^3 - 10^5$ |
| UF | >750 | $2 - 5$ | Integrally skinned | ~60 | $20 - 100$ |
| NF | <750 | $10 - 15$ | Integrally skinned and thin film composite | ~50 | $10 - 20$ |
| RO & FO | <300 | $20 - 60$ (no pressure in FO) | Integrally skinned and thin film composite | ~40 | $1 - 10$ |

**Table 1.3: Some significant developments of synthetic polymeric membranes.**

| Development | Period | Significance |
|---|---|---|
| Noncellulosic homopolymer membranes | 1963 – 1980 | Superior mechanical, thermal and environmental resistance |
| Ionomer membranes | 1970 – 1980 | Superior performance characteristics |
| Copolymer membranes | 1970 – 1980 | Tailor – made polymers |
| Blend membranes | 1965 - 1980 | Economical alternative to copolymer membranes |
| Interfacial thin-film polycondensates | 1980 | In situ high performance thin films from monomers |

MWCO = Molecular weight cut-off

## 1.1 Essential polymer characteristics for use as a membrane material

The search for suitable synthetic polymers for membrane applications is basically aimed at improving the selectivity and service life of the membranes in comparison to existing membrane materials. An overview of the various essential physicochemical and structural parameters of polymers for forward osmosis and pressure driven membrane applications is given below.

## 1.1.1 Molecular weight and molecular weight distribution

The polymers are unique from other compounds because of their fibrous nature and large size which make them suitable for use as ideal membrane material. A convenient way of describing macromolecular size is in terms of degree of polymerization (DP), the number of monomer units contained in the polymer. A polymer is not a single monodisperse species of a given molecular weight (MW), but a polydisperse mixture of species with a distribution of molecular weights. The processing and end-use characteristics of the membranes are greatly influenced not only by the average molecular weight (MW) but also by the breadth and shape of the molecular weight distribution curve of the constituent polymer. Higher molecular weight polymer grade is obviously suited for membrane making as membrane integrity tends to increase with molecular weight. Excessively high molecular weight polymer grades are not suitable for membrane applications as the solubility of such grades may be inadequate. Narrow molecular weight distributions are preferable because the broader the molecular weight distribution, the greater the amount of low molecular weight material, and presence of even a small amount of the latter adversely affects the mechanical properties of a polymer and membrane. Optimum molecular weight with narrow molecular weight distribution is necessary from the point of view of processing. The membrane casting formulation requires sufficient viscosity which cannot be permitted by simply increasing the polymer concentration for obvious performance consideration. The molecular weight of polymer is related to intrinsic viscosity by Mark-Houwink equation as:

$$[\eta] = KM^a$$

The values of the Mark–Houwink parameters, a and K, depend on the particular polymer-solvent system.

8

For practical purposes the inherent viscosity values are often used rather than molecular weight as such.

## 1.1.2 Molecular architecture

In addition to molecular weight and molecular weight distribution, polymers are also characterized by their molecular architecture which greatly influence the permeability and selectivity. Polymers with steric irregularities at the molecular levels, tend to be amorphous because they prohibit intermolecular association. They are characterized by two transition temperatures, the glass transition temperature ($T_g$) and the crystalline melting temperatures ($T_m$). $T_g$ signifies transition from rigid glassy state to the flexible rubbery state and $T_m$ signifies transition from rubber to the liquid state. In the rubbery state, considerable segmental motion is possible and time - temperature dependent interchain oscillations result in transient pores of significant size. As a result, permeability becomes generally high with low selectivity. Moreover permeability is time dependent in such cases. In the glassy state, motion is restricted to bond vibrations and the state is often encountered in dense skin layers of highly permselective membranes. Glassy state is less dense than the crystalline state and the difference between the volume occupied by the completely crystalline polymer and that by a polymer in glassy state is known as the free volume. It is through this free volume that permeation takes place and actual sorption sites are associated with gaps between the chain segments. High selectivity is therefore associated with polymers in glassy state with rigid polymer chain backbones with small intersegmental gaps and reduced free volume. $T_g$ is an essential property for amorphous polymers and molecular architecture influence the value of $T_g$. On the molecular level, the nature of the groups which comprise the polymer backbone, the nature and size of the side chain

groups which increase the energy required for rotation, MW, MW distribution and other steric and cohesive forces which affect intermolecular association, influence the value of $T_g$. Presence of aliphatic $-C-C-$, $-C-O-$, or $-OSiO-$ bonds in the polymer chain leads to flexibility (and hence low $T_g$) because of the ability of these atoms to rotate more or less freely about these bonds. Any factor which hinders free rotation decreases flexibility and increases $T_g$. The introduction of ring structure, particularly planner aromatic rings, greatly increases chain stiffness. Similarly hydrogen bonding is among the strongest of the secondary valence forces which act to increase $T_g$. The crystalline state is the most dense state of polymer aggregation. Since a perfect crystallite is devoid of free volume, it is generally recognized that little permeation may occur through crystallites themselves.

### 1.1.3 Structural rigidity

The mechanical properties are the result of structure and orientation of the chemical groups present in the polymers. The elastic modulus, stress at yield, stress at break, elongation at yield and elongation at break are the principal tensile properties of interest. The elastic modulus is an indication of stiffness which is the ability to withstand stress without dimensional change. Stress at yield is related to elasticity, which is the ability to undergo stress without suffering a permanent set. This is the point at which elastic deformation changes to plastic flow. The stress at break is the ultimate tensile strength (UTS) of the material and is a measure of its ability to carry a dead load. The mechanical properties of desalting membranes under compression are of particular interest since they are related to the stresses encountered by the membrane under operating conditions. Compressive yield data of membrane polymers are related to permeability decrease during reverse osmosis. Membrane

polymers with high compressive yield are known to suffer less permeability decline with time whereas polymers with lower compressive yield suffer from permeability decline with time. The phenomena of compaction which desalting membranes undergo during long term use at high pressures is greatly reduced for membrane polymers of high mechanical strength. The presence of rigid aromatic ring in the polymer backbone increases its mechanical strength whereas aliphatic moieties with no polar groups are mechanically weak polymers.

### 1.1.4  Hydrophilicity / hydrophobicity (polarity)

All chemical differences between prospective polymeric materials can be ascribed to their differences in polarity. Polarity is attributable to unevenness in electron distribution. It is quantitatively described in terms of charge density, dipole moment and hydrogen bonding capacity, as well as by bulk electrical properties such as the dielectric constant and ion exchange capacity and by surface properties such as critical surface tension. Since polarity strongly influences solubility and permeability, all these are in turn related to the Hildebrand solubility parameter ($\delta$) and its various components. Membranes which are destined for aqueous based separation require polymers with hydrophilic character. Empirically, it has been found that hydrophobic polymers yield nearly impermeable or totally unselective membranes. This behavior is typical of all polyolifines, aliphatic nylons with long hydrocarbon segments (nylon 12) as well as some fully substituted cellulose esters. On the other hand highly hydrophilic polymers such as polyvinyl alcohol, polyacrylic acid, polyvinyl pyrrolidone etc. show large permeability to water (or sometimes they are water soluble) but are also unselective towards ions. A balanced hydrophilic character and hydrophobic character is considered adequate for polymer suitability with respect to water desalting

11

applications. Hydrophilicity and hydrophobicity has been expressed in various ways by different authors. A simple way of describing polar / nonpolar character of polymer is percent moisture regain by polymer at appropriate relative humidity and temperature.

### 1.1.5   Stability in acid, alkali, organic solvent and free chlorine environments

With all the above criteria, another criteria is of course the polymer should have enough stability in highly acidic, alkaline and free chlorine environments. In case of applications in aqueous − organic medium (solvent resistant nanofiltration), the polymer should be organic solvent resistant. Hence the selection of candidate polymer should be carefully made keeping the various aspects in mind and the ultimate application for which the membrane is needed.

## 1.2 Polymer materials used in forward osmosis & various pressure driven membrane processes

Selection of right kind of polymeric material and synthesis of suitable membrane with controlled pore size characteristics and thickness are the two essential stages of membrane development. Synthesis of suitable membrane with controlled pore size by different techniques and mechanism of pore formation of our concern are discussed in the next chapter. Various polymeric materials normally used in forward osmosis and different pressure driven membrane processes are given in Table 1.4.

**Table 1.4: Polymer materials typically used in forward osmosis and different pressure driven membrane processes.**

| Process | Membrane material |
|---|---|
| MF | Regenerated cellulose, cellulose acetate (CA), polysulfone (PSf), polycarbonate (PC), polypropylene, polytetrafluroethylene (PTFE), polyvinyl difluoride (PVDF), aromatic polyamide (PA), polyvinyl chloride (PVC) |
| UF | Regenerated cellulose, cellulose acetate (CA), aromatic polyamide (PA), polyamide hydrazide (PAH), polyacrylonitrile (PAN), polyimide, polysulfone (PSf), polyvinyl difluoride (PVDF) |
| NF | Modified polyamide and polysulfones, polyamide hydrazide (PAH), cellulose acetate blend, polyvinyl alcohol derivatives, polyamide, polyimide, polydimethyl siloxane (PDMS) |
| RO | Cellulose triacetate (CTA), cellulose acetate blend, polyamide, polyimide, polyamide hydrazide, polyurea (composite) |
| FO | Cellulose acetate & its blend, polyamide, modified polyamide |

Application of polymeric materials in the field of membrane science and technology for separation and purification has grown tremendously with the development of novel membranes with higher selectivity and permeability. Cellulose esters of optimum degree of substitution (particularly cellulose diacetates and triacetates) and their blends, aromatic polyamide group polymers, polysulfones either as such or in other chemically

13

modified forms are widely used as membrane materials for RO, NF, UF and MF applications because of their physicochemical film forming properties and immediate availability. But these polymers have some of the shortcomings like limited chemical stability, suffering from bacterial attack, poor tolerance towards chlorine and other oxidizing agents, lack of adequate selectivity for closely related molecular species, fouling on membrane surface and pressure induced long terms effects etc. though they satisfied the other criteria for use as a membrane material. Similarly, cellulose-based membranes are the most popular and commercialized FO membranes because of their high hydrophilicity and vast availability [8]. However, their relatively low salt rejection and biodegradation tendency severely limit their wide applicability. Later, the thin film composite (TFC) membranes have drawn extensive concerns in osmotic processes in virtue of its high water flux, superior salt rejection, good mechanical strength, long-term stability, and good applicability in practical processes [9, 10]. Development of high performance osmotic membranes is emerging as a new field in membrane sciences [11-19]. Current research in the area of synthetic membrane science mainly concentrate on development of newer membrane materials mainly from the modification of existing polymers to overcome the above mentioned shortcomings. Modifications of the polymers can be done either by introducing functional groups to change the surface charge characteristics of the membrane and increase the polymer hydrophilicity or by physically blending of a miscible hydrophililic polymer with a chemically or thermally stable hydrophobic polymer for achieving stable polymeric materials with improved hydrophilicity. However, the choice of polymers is limited since only a few polymers form homogeneous blends. Another widely investigated method is to modify the surface of an existing membrane by chemical reaction, plasma treatment and adsorption coating so that the surface has the desired characteristics for productive membrane [20-24].

Latest studies revealed that incorporation of nanoparticles into polymeric membranes has been brought to synergies the advantages of organic polymers and the inorganic filler materials and it gives new degrees of freedom on development of next generation membrane materials. Nanocomposite membranes exhibit higher permeability with the same rejection as pure polymeric membranes and can additionally have compaction resistant and surface fouling resistance capability for wide spectrum of membrane processes [25-33].

## 1.3 Literature status on membranes used for FO, RO and solvent resistant NF

### 1.3.1 Cellulosic polymers

The first commercial FO membranes were developed by Hydration Technology Inc. (HTI) using cellulose triacetate (CTA) polymer over a very thin polyester mesh [34]. Subsequently, cellulose acetate (CA) based membranes became the most commonly used ones in osmosis applications and membranes from cellulose acetate (CA), CTA, CA-CTA blend, poly vinyl alcohol (PVA) modified cellulose acetate (CA) polymeric systems etc. had been developed in lab scale [35-37] over the time. Cellulose is the omnipresent naturally occurring polymer which consist of anhydroglucose units joined each other by β- 1,4 glucosidic linkages. The anhydroglucose moiety has a cyclic structure in the chair conformation. All of its pendent groups, the single primary and the two secondary hydroxyl, and the β-glucosidic oxygen are in the equatorial position. Cellulose derivatives or cellulosics can be synthesized by reactions between suitable monomers and the active hydrogen of its three side chain hydroxyl groups. Since there are three potential sites for monomer addition, a range of derivatives with varying degree of substitution is possible. Cellulose esters with optimum degree of substitution are very versatile polymer candidates for membrane preparation because of its low cost, availability in a

wide variety of viscosity grades and reasonable resistance to oxidation by chlorine. However, these polymers have borderline glass transition temperature which limits their utility at elevated temperature and pressure. The other weaknesses are tendency to undergo hydrolysis particularly in alkaline media and lack of resistance to attack by microorganisms.

In order to overcome these shortcomings several trials have been made to modify cellulose acetate either by blending with some suitable compatible polymer, chemically modifying or by grafting with something. Cellulose acetate (CA) was grafted with styrene [38] for improvement of compaction at high pressure and modification of CA with monomer containing quarternary ammonium group increases its inhibition towards biodegradation [39] but the resultant membranes show lower permeate flux than the membrane from CA alone. In order to produce membranes having good permeability and excellent mechanical strengths, there have been many studies on blends of cellulose with other compatible polymers like polyacrylonitrile (PAN) [40], poly(4-vinyl pyridine) [41] and so on. Regenerated cellulose membrane from cuoxam / zincoxene blend was made with significantly improved mechanical strength by Zhang et al . Blend membranes of cellulose cuoxam / casein were prepared by Zhang et al [42] for better thermal stability, mechanical strength and permeability than the regenerated nonblended cellulose membrane.

High cyanoethylation cellulose (HCEC) was synthesized by Guo et.al [43] with the aim of improving the microbial resistance and the UF membrane made of HCEC had a good chemical stability and excellent microbial resistance but the permeate flux was low. For the purpose of improving cellulose triacetate (CTA) membrane properties, such as chemical stability and resistance to microbial degradation, UF membranes from HCEC and CTA blended system were reported by Guo et al [44]. Blend

16

membranes of CA and polysulfone blend were prepared and tested for pure water permeability and separation of metal ion in aqueous medium by Sivakumar et al. [45]. Akhtar et al. [46] used phospholipid grafted CA membranes for filtration of BSA solution and they found that the treated UF membrane had increased flux and a lower rate of flux decline for BSA. The UF membranes were prepared from CA-polyurathane blend by Sivakumar et al [47] for better results for the separation of proteins and metal ions.

Influenced by Hydration Technology Innovations' (HTI) FO membranes, the use of cellulose acetate (CA) and cellulose triacetate (CTA) for FO membranes received more attention. A unique double-skinned CA FO membrane was invented which was capable of mitigating the effect of internal concentration polarization (ICP) within the membrane and reducing fouling propensity by the introduction of a second "skin" to the membrane [36, 48]. Double-skinned hollow fibres made of CA and CTA were then developed accordingly for FO processes [11, 49, 50]. Ong et al. used cellulose esters with different degrees of substitution of hydroxyl, acetyl, propionyl, and butyryl functional groups to fabricate better flux asymmetric FO membranes via nonsolvent induced-phase inversion process [51]. Sairam et al. used phase inversion method to develop flat sheet FO membranes with cellulose acetate using lactic acid, maleic acid and zinc chloride as pore-forming agents and casted the membrane onto nylon fabric at different annealing temperatures [52].


### 1.3.2. Polyamides

Polyamides are the step reaction products of diamines and dibasic acids /acid chlorides and the general formula is $—[HN—R—NHCO —R'—CO]_n—$ . The most important feature of polyamides is the $—CONH—$ group, the amide linkage which has a strong capacity for hydrogen bonding. Polyamides of three classes are

commercially available : fully aliphatic (both R & R$^/$ are aliphatic), aromatic (R is aliphatic and R$^/$ is aromatic) and fully aromatic (both R & R$^/$ are aromatic ring). Aromatic rings are more susceptible for chemical substitution. Fully aromatic polyamide polymers have emerged as promising materials for RO/NF/UF applications. A number of fully aromatic polyamides namely, polyimide [53] polyamidehydrazide [54], polyetheramidehydrazide [55], polyurea, polybenzimidazole and polysulfonamide based membranes have been studied extensively [56-58] and shown to be useful as potential candidates having exceptional chemical, thermal, hydrolytic stability and permselectivity. But all these polymers lack chlorine resistance due to N- chlorination through amide nitrogen and electrophilic substitution of aromatic rings by chlorine which disrupt intermolecular hydrogen bonding resulting in increasing permeability and reduced selectivity [59].

Many attempts have been made to synthesize chlorine resistant polyamide membranes. Parrini [60] described preparation of a variety of tertiary amide polymers generally classified as polypiperazineamides. These polymers display high levels of chlorine resistance evidently resulting from the absence of N—H linkages. Kawaguchi and Tamura [61] reported preparation of chlorine – resistant polyamide RO membranes from polyethylene trimesamide which are resistant to fouling by nonionic surfactants. New composite RO membranes based on m-phenylene diamine/1,2,3,4- cyclopentane tetra carboxylic acid polyamide have been developed by Ikeda and Tomaschke [62]. These cyclopentane tetra carboxylic acid polyamide composite membranes are also resistant to chlorine attack. Fully aromatic polyamide membranes were nitrated to improve their resistance to chlorine was studied by Singh [63].

Most of the TFCRO membranes available commercially are prepared by in-situ polycondensation reaction between 1, 3-diamino benzene or metaphenylene diamine (MPD)

18

and 1, 3, 5- benzene tricarbonyl chloride or trimesoyl chloride (TMC) over a porous support membrane. In order to improve the highest achievable separation performance of these membranes, research is directed towards introduction of new monomeric systems other than MPD & TMC [62, 64-66], incorporation of additives into the reactants [67-69], surface modification etc. [70-73]. The concept of a mixed-matrix polyamide membrane by impregnation of a small amount of nanoparticle filler into the entire polymeric matrices is developed recently to improve mechanical, chemical, and thermal stability of the membranes alongwith their enhanced separation and sorption capacity [26, 74-80].

The composite membranes by combining polyamide with polysulfone have been reported by Chan et al. [57] and Gao et al. [81]. Hosch and Staude [82] reported about heterogeneously modified polyamide UF membranes for separation of human serum albumin (HAS). The membranes made from aromatic – aliphatic polyamide were heterogeneously reacted with glycidyl methacrylate to obtain epoxy groups on the membrane surface. These epoxy groups were further reacted with trimethyl amine and iminodiacetic acid to get positively and negatively charged groups, respectively.

In development of FO membrane, aiming to improve the water flux, many researchers shifted their asymmetric membranes made of the conventional phase inversion process to thin film composite (TFC) membranes fabricated via interfacial polymerization (IP). The pioneering TFC membranes for FO were synthesized by forming a thin polyamide (PA) selective layer on polysulfone and polyethersulfone (PES) porous substrates [12, 14]. Flat sheet TFC membranes were then fabricated by various research groups using different porous substrates such as polysulfone (PSf) [15, 16], electrospun polyethersulfone (PES)/PSf and PES nanofibers [83, 84], polydopamine (PDA)-modified commercial PSf RO membranes with PET fabrics removed [85], fully sponge-like macrovoid-free sulfonated polymer [86], PES/sulfonated PSf (SPSf) [87], cellulose acetate propionate substrates [88] and also zeolite

embedded PA thin film on PSf substrates [89]. Later, hollow fibre TFC polyamide membranes have been fabricated for FO applications [12, 13] and afterwards Song et al. developed a type of nanofibre TFC FO membrane through electrospinning followed by interfacial polymerization (ES-IP) [84]. They reported that the nanocomposite FO membrane had improved FO performance mainly due to its low tortuosity and high porosity, which significantly reduced the membrane structural parameter.

Darvishmanesh *et.al* reported [90] high performance polyamide type solvent resistant nanofiltration membranes with <80% rejection with polar protic solvents like Ethanol, Methanol, Isopropyl alcohol. Current state-of-the-art solvent resistant polyamide/imide membranes are being prepared by breaking up the imide rings of polymer backbone followed by successive formation of crosslinking bonds between two polymer chains [91, 92] by diamine crosslinker either during phase inversion [93] or post-synthetically [94, 95]. One such example is preparation of diamine-crosslinked commercial Matrimid® 5218 membranes using [96] ethylenediamine (EDA) or 1,6-hexanediamine (HDA) crosslinker. Apart from diamines, diisocyantes [97] has also been employed successfully for preparation of commercial solvent resistant polyamide-imide PAI Torlon® membranes. Commercial Matrimid based crosslinked membranes with high rejection of low molecular weight dyes like Methyl Orange and Bengal Rose has also been reported recently [94, 96]. High flux TFC-PA membranes in solvents like methanol, DMF and DMSO has been developed by compositional modification of reactant solution owing to addition of triethylamine/ camphorsulfonic acid into the amine solution and post treatment of the membrane with glycerol/SDS (sodium dodecyl sulfate) solution [98]. Thin film nanocomposite (TFN) membranes of high solvent stability as well as increased thermal and mechanical resistance were developed by incorporation of nanoparticles such as $TiO_2$ [99] or aminopropyldiethoxymethylsilane (APDEMS) modified $SiO_2$ [100].

### 1.3.3. Other polymers & composites

Apart from the conventional asymmetric membranes and TFC membranes, layer-by-layer (LbL) FO membranes were developed by assembling polyelectrolytes of opposite charges [17, 19, 101]. The LbL membranes showed a high FO water flux, using only a 0.5 (M) $MgCl_2$ draw solution. By using glutaraldehyde (GA) as the cross-linker and further photocross-linking under ultraviolent (UV), LbL polyelectrolyte FO membranes with good rejection towards NaCl were developed [102]. Biomimetic membranes embedded with aquaporin Z have also been explored and shown to have a phenomenally high water flux with a low reverse salt flux, using a 2 (M) NaCl draw solution [103]. The biomimetic concept has been proven feasibly for FO processes, but the difficulties in large-scale production and poor mechanical strength are its major shortcomings. Then some chemical modification methods have also been employed to prepare new FO membranes. Arena et al. used polydopamine (PDA) as a novel bio-inspired hydrophilic polymer to modify the support layers of commercial TFCRO membranes for engineered osmosis applications [85]. The modified membrane had reduced ICP and improved water flux in FO tests. Setiawan et al. developed a type of hollow fibre FO membrane with a positively charged NF-like selective layer by polyelectrolyte post treatment of a polyamide-imide (PAI) microporous substrate using polyethyleneimine (PEI) [104]. Additionally, Tang and co-workers novelly used the layer-by-layer assembly method to fabricate FO membranes [17, 101]. In their studies, polyacrylonitrile (PAN) substrate was prepared via phase inversion, and then post-treated by sodium hydroxide to enhance the surface negative charge density and hydrophilicity. Poly(allylamine hydrochloride) (PAH) and poly(sodium 4-styrene-sulfonate) (PSS) were, respectively, used as the polycation and polyanion.

Nanocomposite membranes, a new class of membranes fabricated by combining polymeric materials with nanomaterials, are emerging as a promising solution to current challenges of high performance membrane development. The advanced nanocomposite membranes could be designed to meet specific water treatment applications by tuning their structure and physicochemical properties (e.g. hydrophilicity, porosity, charge density, and thermal and mechanical stability) and introducing unique functionalities (e.g. antibacterial, photocatalytic or adsorptive capabilities). Inorganic nanoparticles are potentially used as fillers in recent times to improve the properties of microporous ultrafiltration (UF) membranes [105-107] with respect to water permeability, fouling propensity, mechanical and thermal properties, provided the quantity of nanoparticles added was not overloading which may give rise to agglomeration of nanoparticles, losing their specific properties and resulting in no performance enhancement of the mixed matrix nanocomposite membranes. Silver nanoparticles (AgNPs) are one of the most extensively studied biocides, which are effective against various aquatic microorganisms including bacteria, fungi, algae, and etc. [108]. They may affect the cell integrity and metabolism by direct interaction with cell membranes, releasing dissolved silver species, and/or generating reactive oxygen species (ROS) [109, 110]. AgNPs have been incorporated into nanocomposite microfiltration (MF) [111, 112], ultrafiltration (UF) [29, 113], nanofiltration (NF) [114] and reverse osmosis (RO) [115] membranes via various methods including membrane surface modification [112], phase-inversion [29, 113] and interfacial polymerization [115].

Polydimethyl siloxane (PDMS) is the most extensively used polymer for development of solvent resistant NF membranes [116-120]. Apart from this, polymers like polyurethane [121], polypyrrole (PPy) [122, 123] and poly[1-(trimethylsilyl)-1-propyne] (PTMSP) [124] were studied as coating materials on polymeric supports for development of stable solvent resistant (SRNF) membranes. Shao et al. [123] embedded GO nanosheets into PPy

membranes by dispersing them into the polymer dope solution prior to polymerization reaction to form a selective barrier layer over a hydrolyzed polyacylonitrile (PAN-H) support. A thinner layer formed by the 2-D structure of the GO nanosheets enhances the permeability of polar protic organic solvents like methanol, ethanol and isopropanol without any compromise in rose bengal dye (RB) rejection. Incorporation of rGo (reduced graphene oxide) into the polymer matrix forms membranes with higher selectivity towards acetone, xylene, toluene, pyrene owing to smaller interlayer spacing of the carbon sheets [125].

Use of multilayered polyelectrolyte complex (PEC) membranes for applications in SRNF was first reported by Li et al. [122]. The PEC membranes formed by deposition of poly(diallyldimethylammonium chloride) (PDDA)/SPEEK onto a PAN-H support exhibited excellent stability in IPA, THF and DMF. As the concentration of NaCl added to the polyelectrolyte solution increases from 0-0.5 (M), permeability of isopropanol through the PEC membrane was found to increase gradually from 0.6 to 9.8 $L·m−2·h−1 ·MPa−1$ [126]. Thermal crosslinking followed by aerial oxidation of polyaniline (PANi) membranes was reported to enhance their stability in various solvents like acetone, MeOH, DMF, NMP and THF [52, 127-129]. Attempts were made with polymers of sulfone family like polysulfone and polyethersulfone to make them stable in organic media by modifying different parametric variables for membrane preparation conditions like judicial choice of solvent, evaporation time of volatile solvents and incorporation of different molecular weight [130-132] additives. A longer evaporation time was reported to increase the solute rejection at the expense of water permeability and the membranes were found to get stabilized in harsh environment when exposed to a much longer evaporation time. Addition of small amount (5 wt%) of high molecular weight additives like PEG and higher amount (25%) low molecular weight additives like dimethyl ether, diethylene glycoldiethyl ether, acetone, 2-butanol and acetic acid were found to form polymeric sulfonic membranes with more than 90% RB rejection.

Literatures are available with reports on development of very stable crosslinked polybenzimidazole (PBI) membranes [133, 134]. PBI membranes crosslinked with α,α′-dibromo-p-xylene (DBX) were found to show high to moderate stability even in corrosive environments like solutions containing polar aprotic solvents or strongly acidic and basic media.

## 1.4 Literature status on application of cellulosic and polyamide membranes for treatment of aqueous streams

One of the major challenges to sustain the modern civilization is to secure adequate water resources of desirable quality for various designated uses. To address this challenge, membrane water treatment is expected to play an increasingly important role in areas such as drinking water production, brackish & sea water desalination, and waste water treatment & reuse.

### 1.4.1 Radioactive waste treatment

Nuclear power industry providing more than 11% of the world's total energy leads to generation of a good quantity of radioactive waste [135] that needs to be decontaminated properly for safe disposal [136, 137]. Radioactive wastes are generated at diverse stages of nuclear fuel cycle, starting from uranium ore mining and milling to spent fuel reprocessing through fuel fabrication, reactor operation [138, 139]. Recovery of radioisotopes from these radioactive wastes are equally important for their use medicine [140, 141], industry [142] and agriculture [143]. The management of radioactive waste thus involves decontamination and recovery [144]. The methods deployed worldwide for treatment of radioactive wastes depending upon the nature and concentration of radio nuclei present, are, (i) dilute and disperse, (ii) delay and decay and (iii) concentrate and contain. Separation processes like

evaporation, adsorption, distillation, precipitation, ion exchange etc. are used generally for treatment of radioactive waste by different means [145]. However, membrane based processes are fetching enormous attraction in the field of separation and recovery of radioactive chemical species because of following reasons; (i) Separation can be carried out in continuous [146], (ii) Low energy consumption [147], (iii) can be coupled with other processes [148, 149], (iv) Scalability [150, 151], (v) Requirement of no additives.

Reverse osmosis has already been successfully used for treatment of low to intermediate level radioactive waste of moderate pH by 'Concentrate-and-contain' method [152]. Nowadays forward osmosis (FO) is used extensively as a sustainable alternative to this high pressure operated reverse osmosis (RO) process especially for concentration of 'low volume - high value' products [153]. Once the total radioactivity of the effluent stream is confined into a smaller volume, further treatment of the same by an ion exchange column becomes easier. In spite of being the most energy efficient process, lack of availability of suitable membrane for FO application is the major obstacle in further advancement of the process for concentration of low to intermediate level radioactive waste. The main challenges of FO applications are proper choice of draw solution and high-flux membranes [154]. Development of high performance FO membranes in terms of high permselectivity and chemical as well as radiation stability for their application in treatment of radioactive waste is one of the main concerns of the current researchers working in this area of membrane application.

The challenges with inorganic/ceramic membranes which are highly stable under radioactive environment [155] are, (i) difficulty of fabrication because of their inherent brittleness and (ii) limitation to fine tuning of pore sizes. Polymeric membranes, on the other hand, has drawn significant attention due to higher flexibility, ease of processability, ability to tailor-make the membranes for specific application by functionalization, uncomplicated modification in the internal structure (pores/porosity, internal network etc) and moderate stability (thermal,

chemical or mechanical stability) etc. [156]. However, the relatively low radiation stability of polymeric membranes narrows their application to a limited extent.

Although, FO is one of the best suited membrane process for treatment of radioactive waste by concentrating a desired stream, its application in this area is still a very new topic. Lack of optimized membranes and an effective recovery process for the draw solutions [157] are still the major challenges in FO for a particular application and the same are applicable for concentration of radioactive solutions by membrane processes. Additional challenges pertaining to these kind of membrane application is radiation stability of the polymeric system, as the concentration of radio nuclei increases as a function of time leading to increase in the radiation dose onto the membrane in contact with the active solution. In a recent work, the radiation stability of common polymeric membranes like polytetrafluoroethylene (PTFE), polysulfone (PSf), polyethersulfone (PES), polyacrylonitrile (PAN), polyvinylidenefluoride (PVDF) has been evaluated and it was found that PTFE membranes are poorly stable towards ionizing radiations whereas membranes made of PSf, PES, PAN and PVDF are stable up to an absorbed dose of 20MRad [158]. Also, a number of reports are available on the radiation stability of polymers [137, 158, 159] which confirm that most of the polymeric membranes can be used easily for concentration of low level to intermediate level radioactive solutions.

Now an ideal draw solute of forward osmosis must have characteristics of high osmotic pressure, minimal reverse draw solute flux, zero toxicity, easy recovery and low cost. Enormous kinds of draw solutes like volatile compounds [160, 161], nutrient compounds [162, 163], inorganic [164] as well as organic salts [165], synthetic materials and nanoparticles [166-169] etc. have been used for different applications of forward osmosis. A comprehensive review on the progress of use of draw solution for FO processes elucidating the advantages and limitations of the existing draw solutes, their challenges and future research directions for molecular design of better draw solutes has been published recently

[170]. Proper choice of the draw solution is subject to the balance between osmotic pressure and reverse flux, the purpose of FO and its subsequent applications. Similarly, an ideal FO membrane should be capable of providing high water permeability, high solute rejection, low internal concentration polarization (ICP) along with the high chemical, thermal and mechanical stability depending on the field of application.

## 1.4.2 Desalination of aqueous streams

Nowadays, desalination process plays an important role in addressing the challenges of water scarcity worldwide [171]. Although existing desalination technologies like thermal distillation, freezing desalination, electrodialysis have contributed significantly to the success of sea water and/or brackish water desalination, their high energy consumption still remains as a concern to many, particularly when most of the energy consumed is derived from non-renewable sources [172]. Membrane based water desalination involves no phase change during the separation process and hence can be deployed as a potential energy efficient alternative of the trivial desalination techniques. In spite of very less energy consumption, forward osmosis is not used extensively for water desalination because of very low product permeation rate. Thus FO can be the proper choice for concentration of high value low volume species whereas other process like reverse osmosis or nanofiltration are being used worldwide for treatment of larger volume aqueous streams. The first successful TFCRO membrane with high salt rejecting properties was prepared by in-situ polycondensation reaction between polyethylenimine (PEI) and m-tolulene-2, 4-diisocyanate (TDI) on a porous polysulfone (PSf) support [173] membrane. The major breakthrough in the field of thin-film composite reverse osmosis (TFCRO) membrane is development aromatic-aromatic based polyamide composite membranes using 1, 3-diamino benzene, commercially known as metaphenylenediamine (MPD) and 1, 3, 5- benzene tricarbonyl chloride or trimesoyl chloride

27

(TMC) as reactive monomers by Cadotte and co-workers [174, 175]. Prior to this invention, most widely used polyamide membranes (NS 101) were being prepared by condensation reaction between polyethylene imine (PEI) and 1, 3-benzene dicarbonyl chloride or isophthaloyl chloride (IPC) [58]. Although these aliphatic-aromatic composite membranes (NS-101) show sufficiently high salt rejecting properties, aromatic-aromatic MPD-TMC based TFCPA membranes are preferred over them because of their higher product permeation rate. Most of the research works were there by directed to the performance enhancement of MPD-TMC based polyamide membranes in terms of their productivity and selectivity by employing different methods including surface modifications [70-73], altering the reacting monomers [64-66, 176], incorporation of extra additives into the reactants [67-69], impregnation of functional nanoparticles in polyamide top layer [25, 26, 72, 73, 76, 177-181] etc.

## 1.4.3 Decontamination of organic solvents from waste water

The major chunk of membrane based separation processes generally involve their application in aqueous media especially for removal of ionic or small organic solutes using reverse osmosis and nanofiltration or separation of macromolecular solutes using ultrafiltration or particulate matters using microfiltration. However, much less works has been carried out for treatment involving nonaqueous streams containing hazardous organic solvents. To achieve highly efficient decontamination process, it is necessary to design and fabricate membranes with high stability in harsh organic environment, capable of exerting high permeate flux and solute rejection and long term stability in the medium of interest. Solvent resistant nanofiltration (SRNF) is a relatively recently developed pressure driven membrane technology that allows efficient separation of solutes present in organic media as well as separation of organic solvents from aqueous streams [182-184]. Commonly used SRNF

membranes can be classified into two categories: (i) hydrophobic, like polydimethylsiloxane (PDMS)-based and (ii) hydrophilic like polyimide (PI)-based membranes. PDMS-based membranes can be applied successfully in system containing polar solvents with moderate solvent flux and solute rejection but the polymer chain tends to swell or dissolve in extreme situation, resulting in high flux but poor solute rejection in nonpolar solvents. In contrary, PI-based membranes have been successfully employed in treatment of nonpolar solvents but undergo severe swelling with low solute rejection in polar solvents [93]. Modification of PDMS/PI structures [93, 184] either by (i) preparing hybrid membrane: to adjust the free volume and chain mobility by impregnating inorganic fillers (e.g., zeolite, silica) or by (ii) cross-linking the membranes to restrict chain mobility and create cross-linked network of polymer chains by chemical reaction are capable to overcome such type of problems.

Advantages of using SRNF membranes for waste water treatment containing organic pollutants, recovery of organic solvents from industrial waste, recovery of catalysts from organic sewage etc. are (i) low energy consumption of the process operated in low to moderate pressure which makes itself a cost effective one & (ii) longibity of the membranes by reducing fouling even in harsh organic environments. As a promising energy efficient process [183, 185, 186] solvent resistant nanofiltration has triggered increasing attention in both academic as well as industrial fields and applied successfully in wide field of industrial applications such as treatment of petrochemical, food, semi-conductor and chemical industry sewage streams [183]. However, so far very little work has been reported on development of SRNF membranes suitable for use in harsh polar aprotic organic environment with good rejection. Most of the polymers suitable for preparation of membranes used for different pressure driven processes are soluble in polar aprotic solvents like N,N-Dimethyl acetamide (DMAc), N-methyl pyrrolidone (NMP) and N,N-dimethyl formamide (DMF), thus offers a

challenge to the current researchers to develop stable high performance membranes suitable for use in DMAc/DMF/NMP environments in long run.


## 1.5 Present work

In the present thesis, an attempt has been made to develop cellulose acetate and polyamide based membranes for treatment of different aqueous streams. Towards this purpose, asymmetric membranes from cellulose acetate, cellulose triacetate and cellulose acetate blende has been developed targeting application on concentration of simulated Ammonium Di Uranate (ADU) filtered solution. A new formulation of reactants was investigated to develop high flux TFC membranes & the potential of these high flux osmosis membranes for concentration of simulated cesium and strontium bearing effluent solution were evaluated at practical scale followed by demonstration of volume reduction of simulated cesium and strontium bearing effluent solution. Nanocomposite cellulosic membranes with enhanced performance were developed by incorporation of silica, silver and silver-silica nanoparticles onto cellulose triacetate. Thin film composite polyamide membranes were developed by in situ poly condensation reaction between amine and acid chloride and different inorganic salts were incorporated for performance enhancement of the overall membranes under standard desalination condition. Polyimide membranes were prepared from commercially available Lenzing P 84 polymer followed by chemical crosslinking to make them stable in harsh organic environment and performance of these membranes were evaluated in terms of their separation behavior for complexation nanofiltration of an aqueous stream containing polar aprotic solvent DMAc.

So the present work deals with:

(i)     Development of cellulosic and thin film composite (TFC) osmosis membranes and studies on the performance of the membranes in terms of volume reduction factor for concentration of solution containing 40,000 ppm of ammonium nitrate and 20 ppm uranium by forward osmosis.

(ii)    Preparations of high flux thin-film composite polyamide (TFCP) FO membranes in spiral configuration and evaluation of their potential for concentration of simulated cesium and strontium bearing effluent solution.

(iii)   Development of high performance CTA based FO membranes by incorporation of porous silica nanoparticles and silver nanoparticles into the polymer matrix.

(iv)    Development of performance enhanced aliphatic-aromatic polyamide thin-film composite osmotic membranes by addition of inorganic metal salts with amine reactant. Performances of the TFC membranes were evaluated both in reverse osmosis mode and forward osmosis mode.

(v)     Development of polyimide based solvent resistant membranes and their application in complexation nanofiltration using organic solvent.

(vi)    Thorough characterization of all the developed membranes using up to date instrumental techniques as well as the characterization with respect to separation characteristics under standard test conditions.

# CHAPTER 2


# PREPARATION AND CHARACTERIZATION TECHNIQUES OF CELLULOSIC AND POLYAMIDE BASED MEMBRANES

## 2.1. Introduction

The most commonly used polymers for development of osmotic membranes can either be cellulosic type or polyamide type. Cellulosic type membranes are asymmetric in nature and can be prepared by phase inversion method whereas polyamide membranes are mostly prepared by *in-situ* polycondensation method over an asymmetric support membrane and thus the generated polyamide membranes are composite in nature. Methodologies of both the processes are discussed in the trailing section of this chapter.

Any membrane developed under a new set of conditions (like compositions, temperature, relative humidity etc.) is a new membrane and needs to be characterized properly to ensure the area of application best suited for the membrane. Even a very small change in parametric variables involved in membrane preparation may bring quite a significant alteration in membrane structure and surface morphology, which in turn changes the separation characteristics of the membrane. Comprehensive characterization of a membrane by different suitable methods, subsequent to membrane preparation, is thereby of utmost interest and required to be carried out for determination of various physicochemical features of a given membrane in order to acquire appropriate knowledge about the constitutional and morphological features of the membrane. This further helps in proper selection of membrane suitable for a specific application, controlling the membrane quality and predicting the membranes' separation behavior for different substances.

The different characterization methods described in this chapter are well applicable for all the types of membranes including porous, nonporous, nanocomposites etc.

The membrane characterization methods can be classified [187] in general into the following categories:

- Instrumental technique for determination pore size and pore size distribution

- Spectroscopic methods to know the membrane structure in its molecular level

- Micrographic methods to have surface morphology

- Drop shape analysis (contact angle measurements) to determine hydrophilicity/ hydrophobicity of membrane surface

## 2.2. Preparation of Cellulosic and Polyamide Membranes

### 2.2.1. Preparation of cellulosic membranes by phase inversion technique

Asymmetric cellulosic membranes are prepared by solvent-non solvent exchange method commonly known as phase inversion technique [188]. In the first step the polymer beads are dissolved in suitable solvent or a mixture of solvent by incessant agitation until a homogeneous solution is formed. The viscous polymer solution is kept for overnight to remove any trapped air bubble that may make the final membrane defective due to formation of pin-holes in the subsequent steps. The polymer solution is spread over a fabric (acts as the mechanical support) under a steady casting shear, using a knife edge maintaining uniform thickness. The membrane is kept in air for pre-optimized time for evaporation of volatile solvent(s) followed by complete immersion of the total assembly in the precipitation bath where solvent-non solvent exchange takes place. The gelling bath is basically comprised of a liquid in which the solvent is soluble but the polymer is insoluble, the solvent, thereby leaches out into the gelling media and the polymer is precipitated out to form the membrane. Temperature of the gelling bath can be varied depending upon the requirement to change the precipitation kinetics of the polymer.
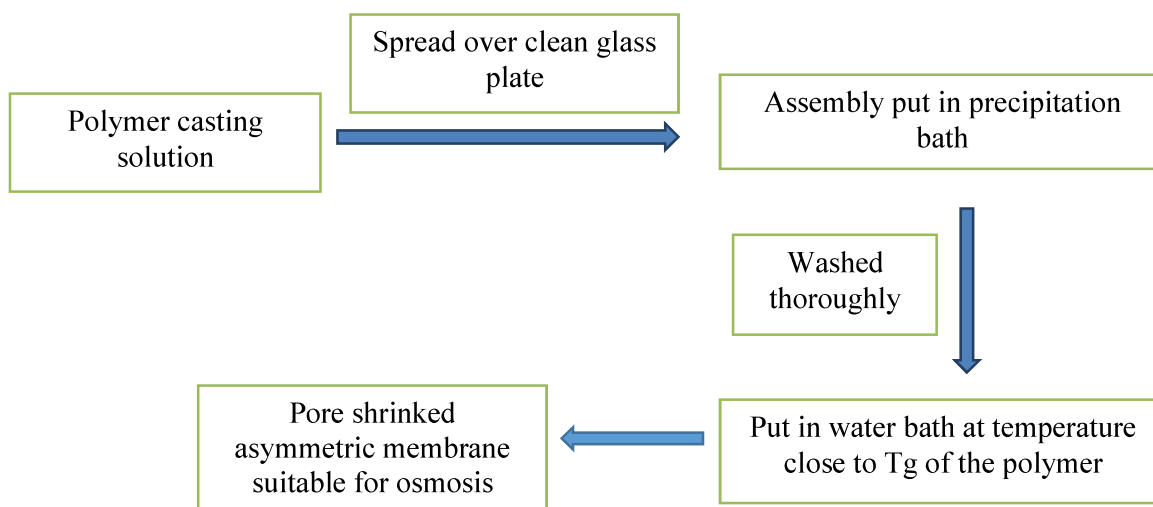
*Figure 2.1: Schematic representation of preparation of asymmetric membrane by phase inversion technique.*

The gelled membrane is washed thoroughly to remove any residual solvent from the membrane matrices and subsequently put in a water bath maintaining temperature near to the glass transition temperature (Tg) of the polymer. The method is called annealing in which the polymer chain become more labile at their near-Tg temperature and reorient themselves to form a tighter membrane with smaller pore size. The membranes after washing with adequate water, are stored in refrigerator cooled water (~6°C) till further use. The entire preparation process is performed in an environmentally controlled atmosphere maintaining temperature 25±3°C with relative humidity 35-40%. The whole membrane preparation process is schematically depicted in Fig. 2.1. Laboratory facility for preparation of asymmetric membranes by continuous casting machine is shown in Fig. 2.2.

*Figure 2.2: Laboratory facility for preparation of asymmetric membranes by continuous casting machine.*

## 2.2.2. Preparation of thin film composite polyamide membranes by *in-situ* poly-condensation reaction

The submicron level thickness of the thin barrier layer of a composite polyamide type membrane cannot be controlled mechanically and hence TFCPA membranes are prepared by *in-situ* poly condensation reaction. This is a two-step technique, the first step of which involves preparation of support membrane by phase inversion technique. The method is similar as described in the previous section (2.2.1) of this chapter except the requirement of solvent evaporation and annealing. As the support membrane of a TFCPA membrane is ultrafiltration type, its pore size is much bigger (2-50 nm) and the steps involving pore shrinking of the membranes can thus be discarded. In a second step, an ultrathin polyamide

sub-layer is deposited onto the support membrane by reaction between an amine and an acid derivative. Acid derivative are chosen over the corresponding simple acids because of their higher reactivity with amines.
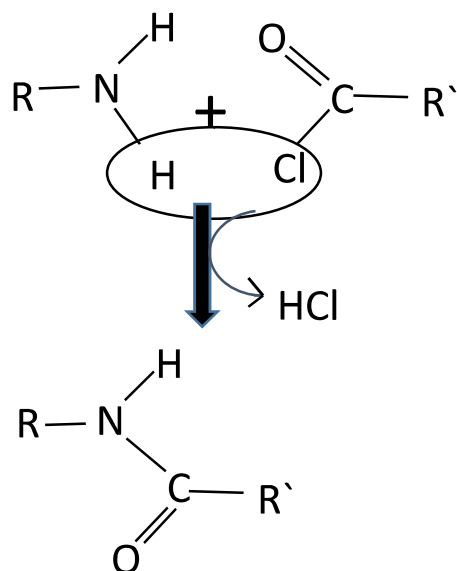


*Figure 2.3: Condensation reaction scheme.*

In this step the UF-type support membrane is made saturated by amine solution by immersing the membrane into pre-optimized concentration of amine solution. Excess amine from the surface of the membrane is removed by squeezing it with a soft rubber roller, taking care of not to damage the membrane surface. The amine saturated membrane is dipped into a solution of acid chloride in organic media. As the amine is residing only inside the pores of the support membrane while the acid chloride remains in bulk, the concentration of these two solution are to be taken in 1:20 (amine: acid chloride) ratio. Reaction between amine and acid chloride takes place (Fig. 2.3) at the interface of the two immiscible solvents (water in which amine is dissolved & organic for acid chloride) and a very thin polyamide film is formed. The step by step method is schematically presented in Fig. 2.4 to get a better overview of the process.

**Step-I**
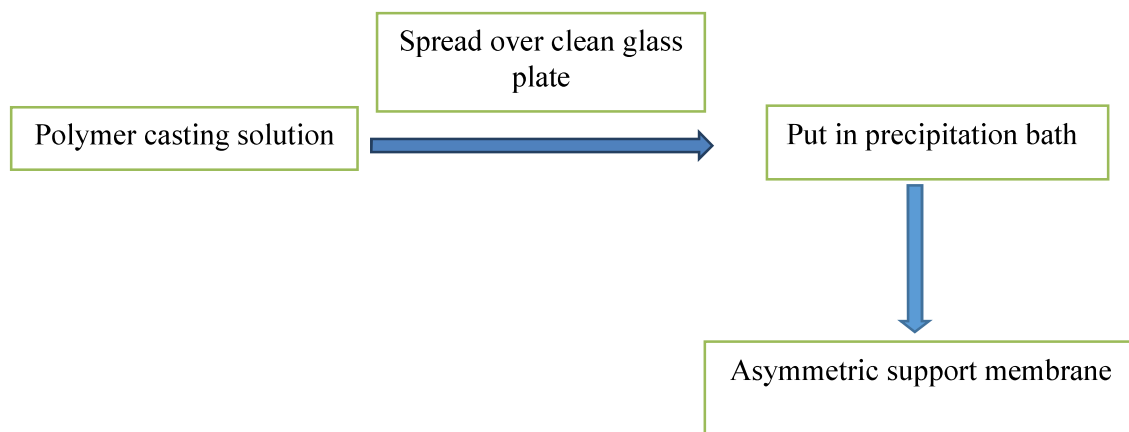


**Step-II**
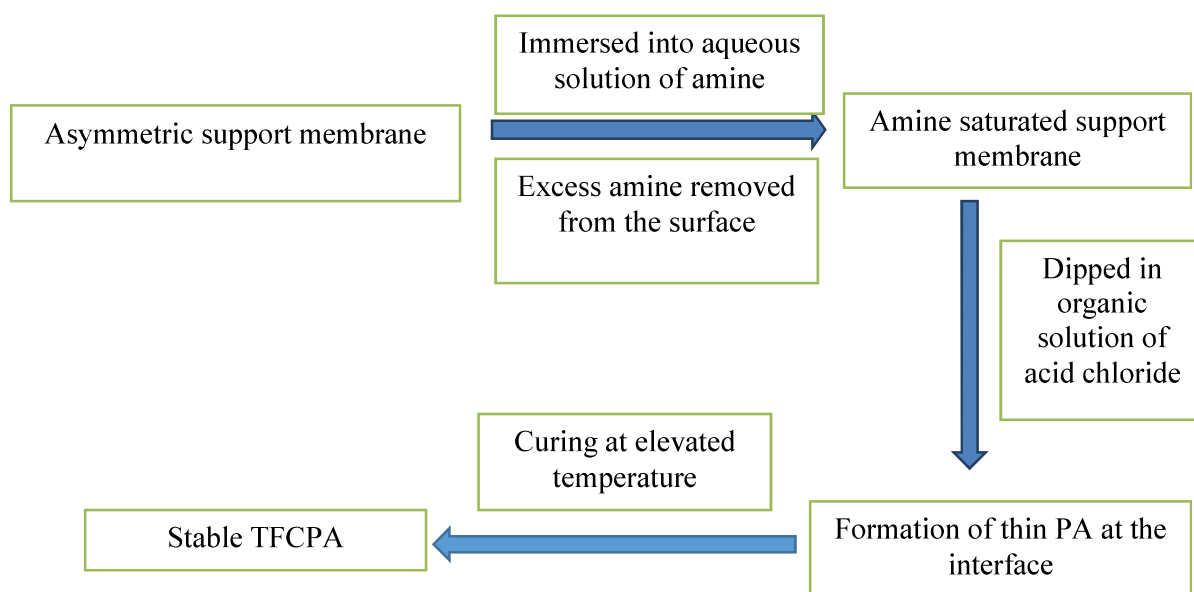


*Figure 2.4: Schematic representation of TFCPA membrane preparation by in-situ*

*polycondensation reaction.*

The reaction is self-limiting in nature because once the thin film is formed at the interface, it becomes difficult for the amine molecules to diffuse through it to come in contact with the bulk acid chloride for further reaction. The membrane is removed from the non-aqueous

medium and subsequently heat cured (under IR lamp/ oven). Heat curing is absolutely essential for such of membranes for (i) removal of excess solvent as well as small molecules (HCl in case of reaction between R-NH$_2$ and R`-COCl) generated at the time of reaction, (ii) ensure complete crosslinking for branch polymers and (iii) making the thin polyamide film strongly adhered to the support membrane to avoid the chances of peeling off during handling. Laboratory facility for preparation of long sheet TFCPA membranes (by step-II of Fig. 2.4) is given in Fig. 2.5. The membranes are stored in a desiccator till further use. The entire membrane preparation process is performed in an environmentally controlled atmosphere maintaining temperature 25±3°C with relative humidity 35-40%.



*Figure 2.5: Laboratory facility for preparation of long sheet TFCPA membranes by coating machine.*

41

## 2.3. Characterization of Cellulosic and Polyamide Membranes

### 2.3.1. Instrumental technique for determination pore size and pore size distribution

Positron annihilation lifetime spectroscopy (PALS) is a well-known technique for measuring free volume size, density and its size distribution in the polymeric membranes [189].

In this technique, positrons generated from a radioactive source ($^{22}$Na) are implanted into the polymeric matrix where a fraction of thermalized positrons form a bound state with an electron. The positron-electron bound state, known as positronium (Ps), can occur in two different spin states, singlet (anti parallel) and triplet (parallel), depending on the orientation of electron and positron. The singlet spin state is also terms as *para*-positronium (*p*-Ps) and the triplet state is known as *ortho*-positronium (*o*-Ps). This two spin states are generated with a relative abundance of 1:3 (*p*-Ps:*o*-Ps).

In polymeric membrane, the positronium trapped in a free volume (membrane pore) any annihilate by interacting with an opposite spin electron other than its bound partner. This process is commonly known as pick-off annihilation and eventually reduces the intrinsic lifetime of *p*-Ps (125 ps) and *o*-Ps (142ns). The extent of reduction in lifetime of the positrnium depends on the frequency of collision with the surface atom of the pores.

Assuming the pores of the membranes to be perfectly spherical with radius R, and behaving like a finite potential well in which the *o*-Ps atom is trapped, the *pick-off* lifetime, $\tau_3$ (ns), of *o*-Ps can be expressed by Tao-Eldrup equation [190, 191] (Eqn. 2.1).

$$\tau_3 = \frac{1}{2}\left[1 - \frac{R}{R+\Delta R} + \frac{1}{2\pi}\sin\left(\frac{2\pi R}{R+\Delta R}\right)\right]^{-1}$$

(2.1)

42

Where, $\Delta R = 0.166$ nm, empirically determined using materials with very well defined free volume sizes.

The measured intensity, $I_3$, is directly related to the fractional free volume assuming no other chemical moiety is present in the matrix capable of quenching the positronium formation.

The PALS spectrometer is consisted of a fast-fast coincidence set up coupled to plastic scintillation detectors. The time resolution (254 ps) of the spectrometer was measured by $^{60}$Co while maintaining the energy windows of discriminators according to prompt gamma (~1274 keV) and annihilation gamma (511 keV) photons from a $^{22}$Na positron source. The time calibration of multichannel analyser was 0.0244 ns/channel.
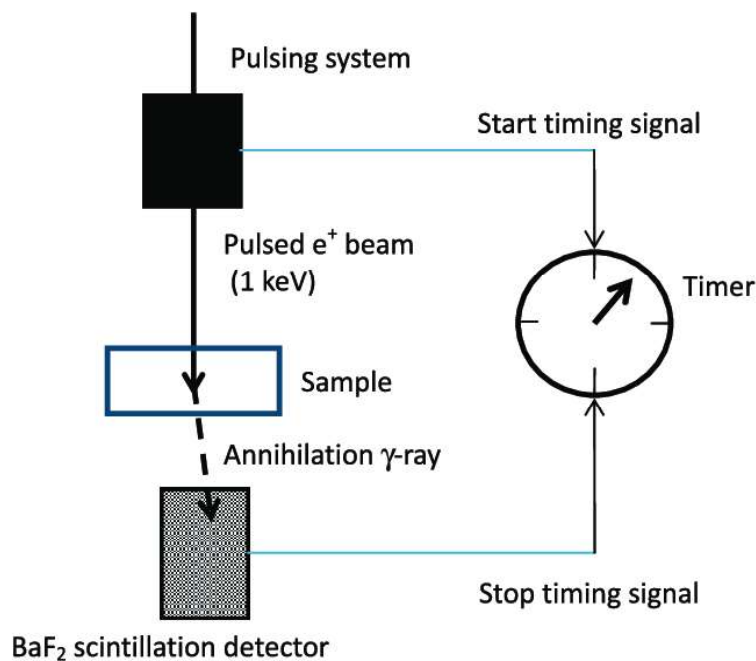


*Figure 2.6: Block diagram of PALS operation.*

The PALS measurements for membrane samples are carried under laboratory atmosphere using a $^{22}$Na positron source with 0.37 MBq radioactivity. The positron source is deposited between two polyimide kapton films each having ~7μm thickness. The whole assembly including the $^{22}$Na source is sandwiched between two stacks (~ 1.5 mm thick each) of the

43

membrane films to ensure complete annihilation of positron with the sample. Si single crystal reference is used to evaluate the fraction of positrons annihilated within the source and kapton films. Analysis of PALS spectra of the samples is done using PATFIT-88[192], a data-processing system for Positron Annihilation Spectra. The block diagram of PALS set up is given in Fig. 2.6.

## 2.3.2. Micrographic methods to have surface morphology

The following techniques are widely used to get the actual surface micrographs of a membrane for better understanding of correlation between structure and performance of the same.

- Atomic Force Microscopy
- Scanning Electron Microscopy

## 2.3.2.1. Atomic force microscopy

The surface morphology of a membrane can be characterized by topographical analysis using standard atomic force microscopy (AFM) instrument. The technique provides us two dimensional as well as three-dimensional surface features of a membrane. An important advantage of use of this technique is thus the study of surface properties of membranes, and quantifiable analyses of surface topography and followed by correlation the same with membranes performances.

A standard AFM instrument is capable of producing topographical images of membrane surfaces by scanning the desired surfaces with a microscopic probe, attached at the tip of a cantilever (Fig. 2.7). The cantilever is typically made up of highly chemically inert silicon nitride with a tip radius of curvature in the order of few nanometers. When the tip is brought

into close proximity of a sample surface, weak dispersion forces operating between the tip and the sample lead to a deflection of the cantilever following Hooks law. Depending on the type of sample, these dispersion forces that are measured in AFM can be mechanical contact forces, van der Waals forces, London forces, capillary forces, chemical forces, electrostatic forces, magnetic forces, solvation forces, etc. If the tip height is kept constant during scanning, a risk would prevail of collision of the tip with the surface, causing damage to it. Hence, a feedback mechanism is employed in most cases, where tip-to-sample distance adjusted so as to maintain a constant force between the tip and the sample. Traditionally, the sample is mounted on a small stage over a piezoelectric tube that can move the sample in the $z$ direction for maintaining a constant force, and the scanning is executed in $x$ and $y$ directions of the sample. Alternatively a 'tripod' configuration of three different piezo crystals may be employed, where each of the crystal is responsible for the scanning in x, y and z directions. This eliminates some of the distortion effects which arise while using a tube scanner. In recent models of the instrument, the tip is mounted on a vertical piezo scanner and the sample is being scanned in X and Y by employing another piezo block. The resulting map of the area represented as $z = f(x, y)$ gives the actual image of surface topography of the sample. The movement of the probe is measured by the deflection of a laser spot getting reflected from the top surface of the cantilever into an array of position sensitive detertors (photodiodes). This photodetector measures the difference laser intensities between the upper and lower photodiodes and subsequently converts the signal into voltage and a three dimensional map of surface topography can be generated by a computer.
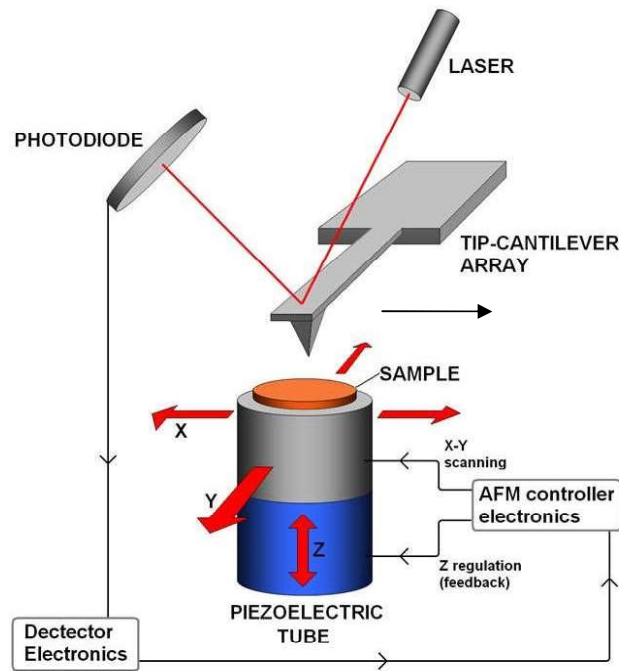
*Figure 2.7: Schematic of AFM operation.*

There are three commonly used AFM techniques: contact mode, noncontact mode and semicontact mode. In contact mode, the probe scans the surface in close contact with the sample and the interatomic forces operating between the sample and the probe is repulsive in nature with a typical value of $10^{-7}$ N. The problem associated with contact mode is excessive tracking forces exerted by the probe onto the sample surface and thereby contact mode is not an apt option for scanning of soft materials like polymeric membrane surfaces. Non-contact mode is used in cases where the contact of probe may alter the surface morphology of the sample. In non-contact mode the tip keeps a distance of about 50–150 Å above the sample surface while scanning and the weak attractive inter-atomic forces ($\sim 10^{-13}$ N) between the probe and the sample are measured to get topographic images of the surface. As the operating attractive forces are very weak in contact mode of operation, the cantilever is driven to oscillate near its resonance frequency. The changes in intrinsic resonance frequency of the tip as a result of the interaction between probe and sample surface are measured, the method is

46

commonly known as dynamic detection method. Presence of a contaminant layer onto the sample surface may interfere with the oscillation frequency of the cantilever and low resolution surface images can be recorded in such cases. In semicontact mode, the tip is alternatively brought to close contact with the sample surface to provide high resolution followed by lifting the same behind to avoid dragging it across the surface, thus a high resolution image is recorded by tapping the probe onto the sample surface. . Thus, during scanning, the vertically oscillating probe contacts the surface and lifts off in an alternate fashion at a typical frequency of 50,000–500,000 cycles per second. In this mode the cantilever assembly is oscillated at or very near to its resonance frequency using a piezoelectric crystal which enhances the amplitude of frequency very largely (typically greater than 20 nm) as compared to the non-contact mode. During this tapping motion of the cantilever, as soon as oscillating cantilever intermittently contacts the surface, its oscillation is reduced due to energy loss caused by the tip contacting the surface and the reduction in oscillation amplitude is used to diagnose the surface features.

Three dimensional surface analysis technique furnish specific 3D roughness parameters that can be categorized as *amplitude parameters* (based on comprehensive height of the surface) like average roughness ($R_a$), root mean square roughness ($R_{rms}$) etc. A brief theoretical knowledge of the various amplitude parameters, obtained from the 2D and 3D topographic image analysis, can be useful in characterizing the surface morphology of the membranes by implying the surface roughness dependent properties of the film. The topographic image extracted through AFM corresponds to a measured height value, *z(x,y)* for a given surface area, A, in a surface plane, x-y. Each height value is allied to a pair of surface coordinates, (x,y), and the image is depicted by a matrix with *N* number of rows and *M* number of columns which corresponds to the surface (x,y) points being the matrix elements the height *z(x,y)*.

The average roughness value represents the average deviation of the roughness from the mean plane, the plane in which scanning is executed. Average roughness parameter ($R_a$) is empirically expressed by the following mathematical expression (Eqn. 2.2):

$$R_a(N, M) = \frac{1}{NM} \sum_{x=1}^{N} \sum_{y=1}^{M} \left( z(x, y) - \bar{z}(N, M) \right) \qquad (2.2)$$

The root mean square roughness ($R_{rms}$) represents the standard deviation of the surface heights from the average planes within the area of interest and a more accurate picture of surface morphology can be depicted from rms roughness values as compared to the average roughness values. $R_{rms}$ can be mathematically expressed (Eqn. 2.3) as:

$$Rrms(N, M) = \sqrt{\frac{1}{NM} \sum_{x=1}^{N} \sum_{y=1}^{M} \left( z(x, y) - \bar{z}(N, M) \right)^2} \qquad (2.3)$$

## 2.3.2.2. Scanning electron microscopy

A scanning electron microscope (SEM) employs a high energy electron beam for scanning of a sample to acquire the surface images. The electrons interact with the atoms of the sample surface to generate signals that contain information about the surface morphology, composition and electrical conductivity of the substrate surface.

The signals produced during operation include secondary electrons, back-scattered electrons (BSE), characteristic X-rays, light (cathode luminiscence), specimen current and transmitted electrons. All the types of emissions coming from the sample during image acquisition are schematically represented in Fig. 2.8 & 2.9.
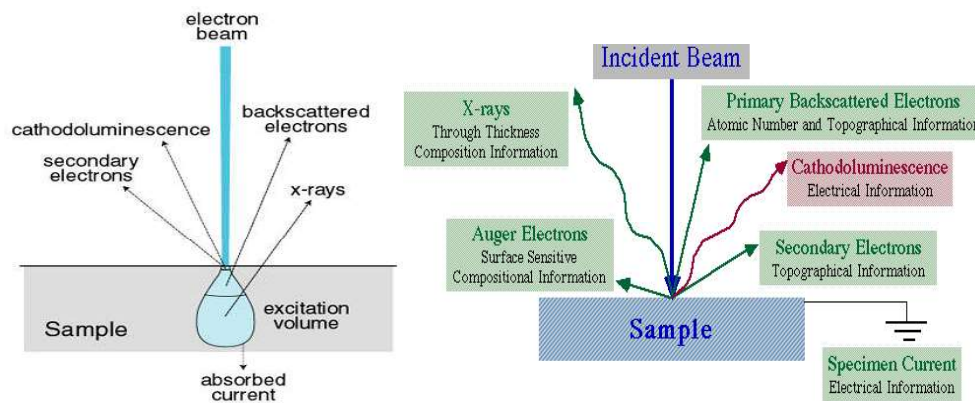
*Figure 2.8 & 2.9: Schematic diagram of electronic interaction with sample and generation of signals.*

Most of the SEM instruments deploy secondary electron detectors and it is not very common for a single machine to have detectors for all possible signals. The signals recorded originate from interactions of incident electron beam with surface and/or near to surface atoms of the sample. In most commonly used standard detection mode, images with resolution as high as 1nm are recorded by secondary electron imaging (SEI).The very narrow width of the probe electron beam helps the SEM micrographs to have a large depth of field and makes them useful for imaging of a characteristic three-dimensional appearance. A wide range of magnifications, from around 10 times (equivalent to a powerful hand lens) to about 500,000 (250 times the magnification of best optical microscopes) is possible. A fraction of the incident electron beam gets reflected from the sample surface by elastic scattering with the sample surface atoms and the reflected beam is termed as back scattered electrons (BSE). BSE are often used in elemental analysis of the sample in addition to the spectral analysis made from the characteristic X-rays. Intensity of the BSE signal is strongly dependent on the atomic numbers (Z) of the atoms, BSE images can thereby provide information about the elemental distribution of the sample. For the same reason, BSE imaging can be used for imaging of colloidal goldimmuno-labels of 5 or 10 nm diameters which is difficult or

impossible to be detected in secondary electron images in biological specimens. When the incident electron beam removes an electron from inner shell of an atom, a higher energy electron jumps into the vacant orbital and energy is released in form of characteristic X-ray. These characteristic X-rays are used to qualitative as well as quantitative analysis of elements present in the sample.

Thermionic emission from an electron gun having energy 0-40keV attached to a tungsten filament cathode is the source of probe electron beam of a typical SEM instrument. Tungsten being the highest melting metal with lowest vapor pressure is used in thermionic electron guns. These two properties make the metal suitable to be heated for emission of electron. Few other metal compounds like lanthanum hexaboride ($LaB_6$) in standard W filament SEM with upgraded vacuum system, Zirconium oxide (thermally assisted Schottky type) or single crystal tungsten sharpened to a tip radius of about 100 nm (field emission gun/ FEG) are also used as electron sources in different SEM instruments. The collimated electron beam is subsequently focused by the condenser lenses (as shown in Fig. 2.10) to a spot of ~0.4-5.0 nm diameter. The beam passes to the final lens through pairs of deflector plates that deflects the beam in x and y axes so that scanning in a raster fashion over a rectangular sample surface can be executed.
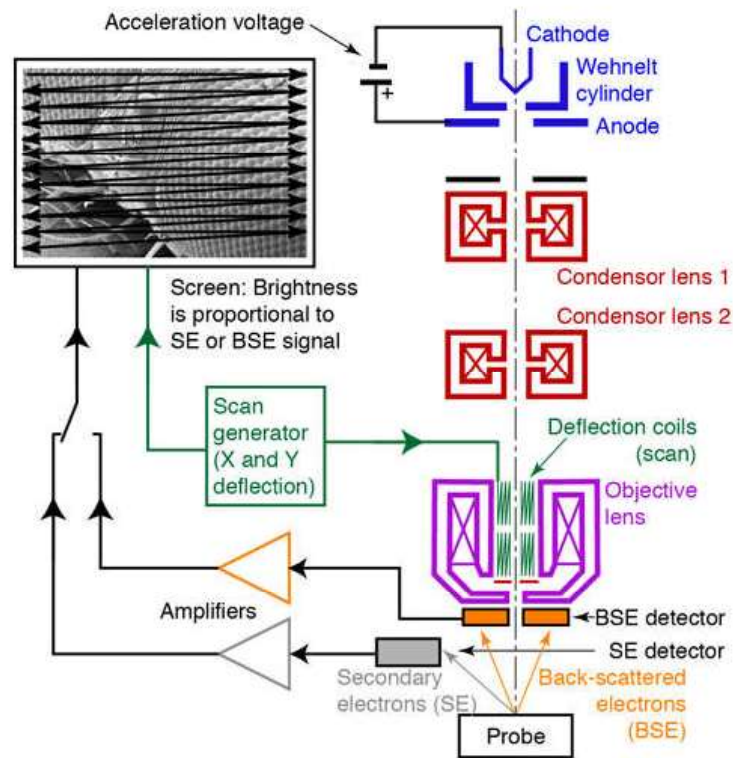
*Figure 2.10: Schematic diagram of SEM.*

Electrons of the primary electron beam lose energy by repeated random scattering and absorption within the interaction volume. The teardrop shaped interaction volume can extend from 100nm to 5µm into the surface depending upon the incident electrons' energy, density and atomic number of the specimen. Energy loss of the incident electron beam owing to elastic scattering of the high energy electrons from sample surface, secondary electron emission by inelastic collision, emission of characteristic X-ray can be measured by detecting each of the processes by specific detectors. Signals generated as variation of brightness on cathode ray tube are amplified by different electronic amplifiers. The raster scanning of the incident beam is synchronized with that of the cathode ray tube (CRT) display and this makes the resulting image a true representative of distribution map of intensity of the signals emitted

51

from the area of specimen under scan. A high resolution CRT is capable of capturing the image by photography, however in modern machinery; the image is digitally captured and stored in the hard disk of the computer.

### 2.3.3. Elemental analysis of membrane surfaces – Energy Dispersive X-ray

In Energy Dispersive X-ray (EDX) spectroscopy, the sample is bombarded with a collimated beam of electrons and the emitted x-ray spectrum is recorded for localized elemental analysis. The method is capable of detecting all the elements of atomic number 4 (Be) to 92 (U), but some instruments may not be equipped for detecting low Z (<10) elements. Identification of emitted X-ray lines characteristics of each element makes the technique a simple one for qualitative elemental analyses. Concentration of each element present in sample can be quantitatively determined by analysing the intensity of each line corresponding to every element. The instrument is calibrated prior to the elemental analyses of the sample using some standards of known composition having the same elements as present in the sample.EDX maps can also be generated by raster scanning of the beam onto the sample and displaying the intensity of selected X-ray lines, to get idea about the elemental distribution in sample of interest.Surface topography of the sample can also be revealed imaging the electrons collected from the top of the sample. Thus, qualitative as well as quantitative elemental analysis of the sample surface and mapping can be done by an energy dispersive X-ray spectrometer (EDX) coupled withanSEM, equipped with an ultrathin beryllium window and 20 $mm^2$ Si detectorand micro analysis system byemploying a certain accelerating voltage to the focused electron beam at specific magnification.

## 2.3.4 Drop shape analysis (contact angle measurements) to ensure hydrophilicity/ hydrophobicity of membrane surface

An instrument commonly known as a Contact Angle Goniometer or Drop Shape Analyzer is used to measure the static or dynamic contact angle value and surface energy of a solid surface with respect to polar and/or non-polar solvents. Static contact angle measurement of the membrane samples are carried out by employing sessile drop method at ambient temperature. A standard contact angle measuring instrument (DSA 100 of KRUSS Gmbh, Germany) with DSA 1v 1.92 software uses high resolution cameras and software suitable for capturing and analysis of the drop shape. Contact angle ($\theta$) of a sample surface with respect to a particular liquid is defined as the angle formed with the solid within the liquid at three phase boundary of the sample where the liquid, vapor and solid intersect. The value of contact angle depends on resultant effect of interfacial tensions between the solid& liquid, liquid & vapor and vapor & solid.

The change in contact angle values can also be explained by cohesive/adhesive forces operating at the different interfaces. Cohesive force is the intermolecular forces that resist separation in a liquid. This attractive force exists between molecules of the same substance. Adhesive forces, generated by the mechanical of electrostatic forces between two molecules, are the attractive forces between two different substances. Contact angle gives us a quantitative measurement of cohesion vs. adhesion forces. The value of contact angle close to zero signifies the liquid droplet wets the solid surface completely by spreading over it and adhesive forces are dominating over cohesive forces. In contrary, a very high value of contact angle indicates the prevailing effect of cohesive forces that resist the droplet to spread over the surface. An example of such case is the beading up liquid drop onto a lotus leaf. Higher is the contact angle of a surface lower is its tendency to get wet by that particular liquid.

Similarly lower contact angle value reflects the higher wettability of the surface by that particular liquid.

The chemical potential of a system, having surface free energy $\gamma_{sv}$ at solid-vapour interface, interfacial energy $\gamma_{sl}$ at solid-liquid interface and surface tension $\gamma_{lv}$ at liquid-vapor interface, must be zero under equilibrium condition and the Young's equation is to be satisfied by the system. Young's equation of such a system under equilibrium can be expressed by Eqn. 2.4.

$$\gamma_{sv} - \gamma_{sl} - \gamma_{lv}\cos\theta_c = 0 \qquad (2.4)$$

Where, $\theta_c$ is the equilibrium contact angle.

Static contact angle measurements of a system give static information about the interfacial tensions between the solid, liquid and gas, while dynamic (both advancing and receding) contact angles give some idea about the dynamic interaction of the three phases. An advancing contact angle is measured by pushing a droplet slowly and steadily out of a pipette onto a solid surface. As the liquid is purged slowly onto the sample surface by the pipette, volume of the initially formed droplet enhances and the contact angle increases from its initial value keeping its three phase boundary stationary until a sudden outward jump. The contact angle formed by the droplet immediately before its jumping outward is known as the advancing contact angle. The receding contact angle is measured by sucking the liquid back out of the droplet. As the volume of droplet decreases, contact angle decreases but the three phase boundary is kept stationary until a sudden inward jump, and the contact angle the droplet had immediately before jumping inward is known as the receding contact angle.

The pictorial representation (Fig. 2.11) of advancing and receding contact angle formation is given below

54
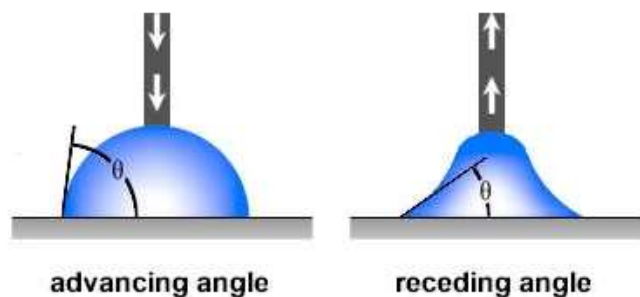
*Figure 2.11: Pictorial representation of advancing and receding contact angle*

*measurements.*

The difference between advancing and receding contact angles of a sample is termed as its contact angle hysteresis. Contact angle hysteresis can be used to characterize the surface heterogeneity, roughness, and mobility.

The contact angle can also be employed to calculate the hydrophilicity and surface free energy (SFE) along with its polar and dispersive components of membrane skin surfaces using two or more different solvents (water, ethylene glycol and diodomethane) of well-defined surface tension values ($\gamma_s$, $\gamma_s^p$ and $\gamma_s^d$, Table 2.1).

**Table 2.1: Polar ($\gamma_s^p$) and dispersive ($\gamma_s^d$) components of the surface tension ($\gamma_s$) values (subscript s stands for solvent; superscript p and d refer to the polar and dispersive components, respectively) of the probe solvents: water, ethylene glycol and diiodomethane.**

| Solvent | $\gamma_s$ (mN/m) | $\gamma_s^p$ (mN/m) | $\gamma_s^d$ (mN/m) |
|---|---|---|---|
| Water | 72.8 | 51.0 | 21.8 |
| Ethylene glycol | 48.0 | 19.0 | 29.0 |
| Diiodomethane | 50.8 | – | 50.8 |

Fowkes method [193] is one of the methods that can be employed to calculate the SFE with its polar and dispersive components from contact angle values of the membrane surfaces with different probe solvents and their corresponding surface tension values.

## 2.4. Determination of Polymer Globule Size by Dynamic Light Scattering

Size of the polymer globules can be determined by the process dynamic light scattering (DLS) using an instrument called particle size analyzer in which the random change in intensity of the light scattered by the particles of a solution is measured. Dynamic light scattering is also known as called photon correlation spectroscopy (PCS) and quasi-elastic light scattering (QELS). Quasi-elastic light scattering has been the old terminology of DLS and was commonly used in literature published in 1980s'. Random thermal motion executed by small particles in solution or suspension is known as Brownian motion. This random motion of the particles can be mathematically expressed by Stokes-Einstein equation. The form most often used for particle size analysis is given below (Eqn. 2.5):

$$D_h = \frac{k_B T}{3\pi\eta D_t}$$

(2.5)

Dh is the hydrodynamic diameter of the suspended particles

Dt is the translational diffusion coefficient (determined by dynamic light scattering)

$k_B$ is Boltzmann's constant

T is temperature at which the analysis is carried out

$\eta$ is viscosity of the solvent

The important points to be noted from Stokes-Einstein equation are the importance of knowing the sample temperature accurately, at it appears directly in the equation. Moreover, viscosity being a stiff function of temperature it also adversely changes the translational

diffusion coefficient with a small change in sample temperature. The analyst must keep it in mind that the particle size determined by this technique is the hydrodynamic size and not the actual size of the particle. However, in polymer sciences hydrodynamic volumes of the polymer molecules represent the size of the molecules in aqueous medium and DLS can be used as an important tool to it. The determined particle size is the size of a sphere that diffuses the way as your particle. The incident light emitted by the laser light source illuminates the sample in the sample compartment and the intensity of the scattered light al is collected with one of two detectors as signal (Fig. 2.12), either at a 90 degree (right angle) or 173 degree (back angle) scattering angle. The provision of two detectors gives more flexibility to the analyst in choosing measurement conditions. Particles can be dispersed in any solvent inter towards them under the analytical condition. All that needs to be known about the solvent are its viscosity and refractive index to interpret the measurement results.
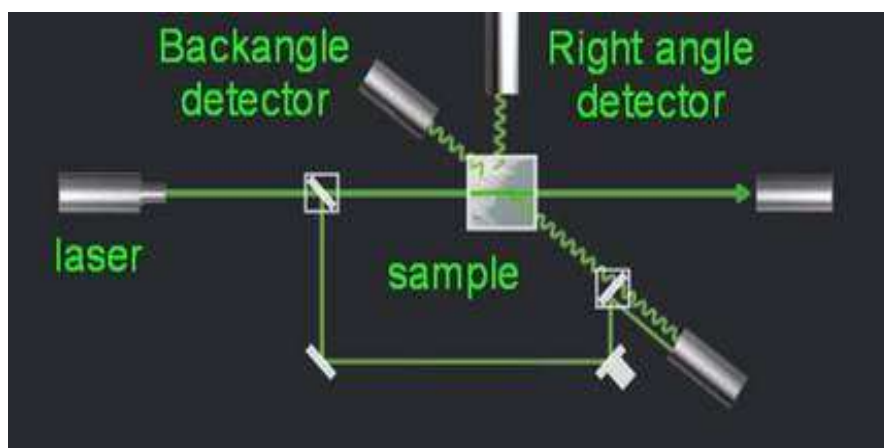


*Figure 2.12: Schematic representation of particle size analyzer.*

As the particles executing Brownian motion, randomly changes their relative positions, the obtained optical signal also shows random changes in intensity. This random change in signal intensity is termed as "noise". The noise generated from the particle motion is used to extract

the particle size. DLS measurements, in contrast to laser diffraction method, are typically made at a single angle, although data acquired at several angles can also be helpful. Moreover, the technique is entirely noninvasive which means that the particle motion continues whether or not it is being probed by DLS.

The random signal recorded as noise can be interpreted in terms autocorrelation function to extract the particle motion. A digital signal processing device, known as a correlator is employed to process the incoming data in real time to extract autocorrelation function as a function of delay time ($\tau$). For a sample with uniform particle sizes, the autocorrelation function, C, after baseline correction, can simply be is written as (Eqn. 2.6):

$$C = \exp(-2\Gamma\tau)$$
(2.6)

$\Gamma$ can be readily derived by a curve fit of the experimental data. The diffusion coefficient ($D_t$) is calculated following the equation $\Gamma = D_t . q^2$ where the scattering vector (q) = $(4\pi n/\lambda)\sin(\theta/2)$. The refractive index of the solvent is n and the incident laser lights of $\lambda$ is scattered by the polymer globules at an angle $\theta$. Inserting the value of Dt in Stokes-Einstein equation (Eqn. 2.8) gives the particle size to the analyst.

Dynamic Light scattering (DLS) measurements were performed using Autosizer 4800 (Malvern Instruments, UK) which employs a Malvern 7132 digital correlator. He-Ne laser operated at 632.8 nm with a power output of 15 mW was used as the light source. All measurements were carried out at $25^{\circ}$C using a peltier controlled water bath. Measurements were made at a scattering angle of $90^{\circ}$ and samples were placed in a cylindrical quartz cell of 25 mm diameter.

## 2.5. Performance Evaluation of Indigenously Developed Membranes

### 2.5.1. Performance Evaluation of FO membranes

Performance of the indigenously developed membranes in FO mode is determined by evaluating volume reduction factors (VRF) following Eqn. 2.7.

$$\text{VRF} = V^i_{feed} / V^f_{feed} \qquad (2.7)$$

Where, $V^i_{feed}$ = initial volume of feed and $V^f_{feed}$ = volume of concentrate feed left at the end of experiment.

The % back diffusion of salt from draw solution side to feed side can be mathematically calculated using Eqn. 2.8.

$$\% \text{ back diffusion} = \left[ 1 - \frac{C^f_{draw} \cdot V^f_{draw}}{C^i_{draw} \cdot V^f_{draw}} \right] \times 100 \qquad (2.8)$$

Where, $C^f_{draw}$ is the final concentration of draw solution with volume $V^f_{draw}$ at the end of experiment and $C^i_{draw}$ is the initial concentration of draw solution with volume $V^i_{feed}$. $C^i_{draw}$ and $C^f_{draw}$ can be calculated by measuring the specific conductance of the draw solution and correlating to them their concentration values.

Schematic of a typical FO test skid is given in Figure 2.13.
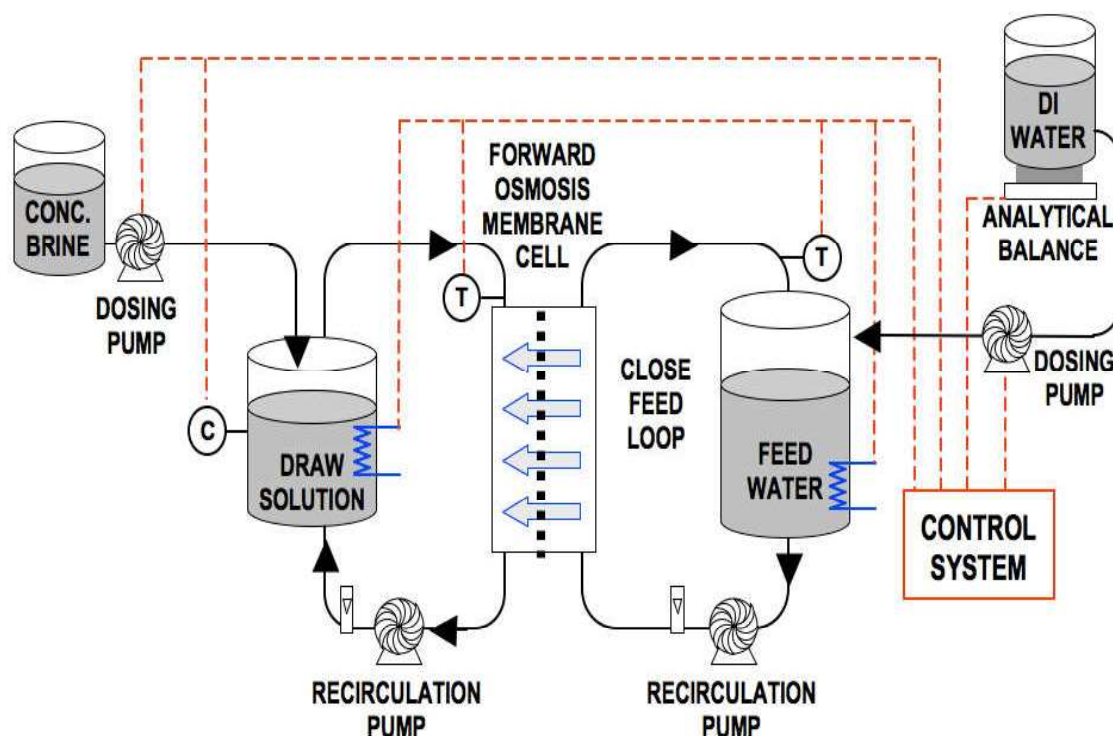
*Figure 2.13: Schematic description of FO membrane performance testing equipment.*

Membrane pieces are put inside the two compartment FO test skid following the AL-FS (active layer facing feed solution) configuration. The two compartments of the shell are filled with measured volume of feed solution (facing the skin side of the membrane) and draw solution (back layer of the membrane in contact with the high concentration draw solution). Flow of solvent from lower concentration feed side to higher concentration draw solution side takes place due to the osmotic pressure gradient between these two solutions. The laboratory test set up for FO experiments are shown in Fig. 2.14. The volume of feed solution is measured prior to starting of experiment and at regular interval to calculate VRF. Active area of the membrane is $7.54cm^2$ and the feed temperature is maintained at $25\pm3°C$. Feed is allowed to flow along one surface of the membrane and draw solution is circulated simultaneously across the other surface to minimize the effect of concentration polarization.

60

All the experiments are carried out in absence of any applied pressure. Scale up facility for testing of FO membranes in 2512 module is presented in Fig. 2.15.



(a)                                                      (b)

*Figure 2.14: Pictorial representation of laboratory facility of two compartment FO test cell: (a) static mode & (b) circulating mode.*



*Figure 2.15: Laboratory facility for testing of FO membranes in spiral module.*

During the course of experiment some solute may back diffuse from highly concentrate draw solution to feed solution side. This back diffusion is mathematically calculated from mass balance.

## 2.5.2. Performance evaluation of RO and NF membranes

Transport properties of the polymeric membranes are evaluated using a cross-flow test cell (Fig. 2.16), at 10bar (for NF) to 15bar (for RO) trans-membrane pressure. The actual test set up is shown in Fig. 2.17. Rectangular membrane samples, with effective membrane area $32cm^2$ are washed thoroughly by de-ionized water followed by placing them in the test cell. The membrane coupons are oriented within the test cell such that their active skin layers face the incoming feed solution during operation. The experiments are accomplished in recycle mode (both permeate and reject streams are circulated back to the feed tank) to maintain a steady feed concentration. Steady state conditions are achieved prior to data collection by pre pressurizing the membranes for long run. Temperature of feed solution is maintained at 25-30$^o$C for all RO/NF performance evaluation experiments. Concentrations of salt in feed as well as permeate solutions are determined by measuring the specific conductance of both the solutions and correlating them with their salinity. All the membrane samples are prepared and tested in triplicate for NF/RO performance evaluation and the averaged out results are calculated. All the data are recorded and reported after achieving the steady state.

Percent solute rejections (SR) of the membranes are evaluated following Eqn. 2.9.

$$SR(\%) = \frac{C_F - C_P}{C_F} \times 100 \qquad (2.9)$$

Where $C_P$ and $C_F$ are the solute concentration of solute in permeate and feed solutions respectively.

The steady-state water permeability ($J_w$) is expressed in terms of L.m$^{-2}$.hour$^{-1}$ (LMH) and can be determined by directly by measuring the permeate flow, volume (V, in L) collected over the time, (T, in day) through a membrane area, (A, in m$^2$) at certain operating pressure using the Eqn. 2.10.

$$J_W = \frac{V}{AT} \tag{2.10}$$

The laboratory set up for performance evaluation of RO/NF membranes under standard condition is shown in Fig. 2.17.
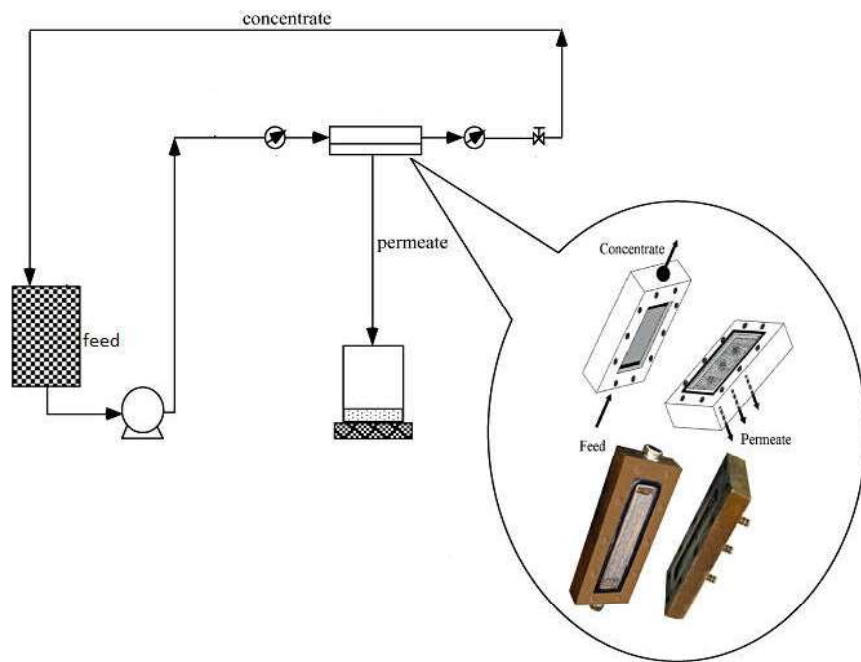


*Figure 2.16: Schematic description of NF/RO membrane performance testing equipment.*
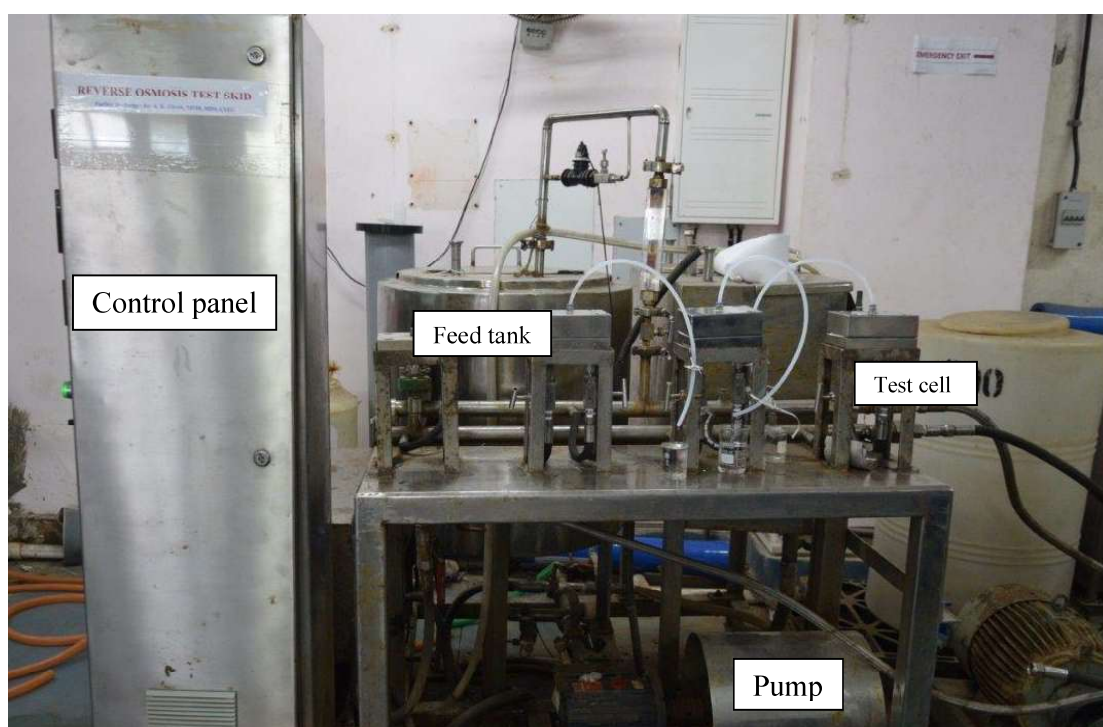
*Figure 2.17: Laboratory testing facility of NF/RO membranes.*

# CHAPTER 3

## DEVELOPMENT OF CELLULOSIC AND POLYAMIDE BASED FORWARD OSMOSIS TYPE MEMBRANES SUITABLE FOR SIMULATED LOW LEVEL RADIOACTIVE WASTE TREATMENT

## 3a. Development of Cellulosic membranes for treatment of simulated ADU filtrate solution

### 3.1a. Introduction

Forward osmosis (FO) being a potential membrane process, is used in many applications nowadays where reverse osmosis (RO) dominated over the eras [153, 154]. Over the past several decades, the application area of FO were confined into desalination of brackish and sea water [194-197], wastewater treatment [198, 199], concentration of pharmaceuticals [200], concentration of fruit juices and liquid food processing [201-203] etc. Very recently it has been reported that FO can also be used to concentrate a stream containing uranium with higher concentration of ammonium nitrate with nominal leaching of uranium to the draw solution side [204]. CA membranes being hydrophilic in nature exhibit modestly higher water fluxes than others but their uses are limited over a narrow range of pH (4.0-8.5) while TFC polyamide membranes being relatively hydrophobic in nature shows lower water permeability than cellulosic membranes, but these membranes have the advantage of being more stable in a wide range of pH and radiation dose owing to their inherent structure. Hence, a low level radioactive solution bearing a moderate pH can be concentrated using cellulosic membranes. One such example is the filtered solution of ammonium diuranate (ADU) precipitate which contains radio contaminants (uranium and its daughter products) and very high concentration of ammonium nitrate (about 40000 ppm) at around pH 7.5. Reverse osmosis (RO) and nanofiltration (NF) membranes had already been used for decontamination of radioactive streams by concentrating the activity in smaller volumes and making the larger volumes suitable for direct disposal [205, 206].

So, FO experiments were conducted to concentrate simulated ADU-filtered solution (containing only uranium as uranyl nitrate and ammonium nitrate) using indigenously

prepared CA, CTA and CA-CTA blend (CAB) membranes in laboratory and their performances are compared. All the membranes were characterized and performances evaluated in terms of volume reduction factor using solution of 40,000 ppm of $NH_4NO_3$ and 20 ppm uranium as feed and 320000 ppm of $NH_4NO_3$ as draw solution. The concentration of uranium was estimated in both feed and draw solution after 5hours of experiment to check the leaching. The effect of nature of draw solutions ($NH_4NO_3$, $NH_4HCO_3$ and $CaCl_2$) on volume reduction for the same system using cellulosic membranes was also evaluated. Effect of concentration of draw solutions was also determined by monitoring volume reduction with CA membranes using different concentrations of two draw solutions ($NH_4NO_3$ and $CaCl_2$). After achieving satisfactory performance with cellulosic membranes in small sheet using forward osmosis test skid, keeping in mind the real application of such system, attempt was made for concentration of the same feed using membrane pouch containing dry $CaCl_2$ salt inside.

## 3.2a. Experimental:

### 3.2.1a. Materials:

Cellulose acetate (CA) (Mn = 50,000) and cellulose triacetate (CTA) (Mn = 72,000–74,000) polymers were procured from Aldrich, India. Solvents like 1,4-dioxane, acetone, formamide and methanol and sodium chloride of analytical reagent grade were purchased locally and used without further purification. Ammonium nitrate, ammonium bicarbonate and calcium chloride of all analytical grades were procured from Thomas, India.

### 3.2.2a. Polymer Dope Solution Preparation:

Polymer casting solution was prepared by dissolution of prerequisite amount of polymer in appropriate solvent. Composition of casting solution for preparation of cellulosic osmosis

membranes are given in Table 3.1a. In brief, the base polymer as well as the solvent mixture required for complete dissolution of the polymer was varied for preparation of three different kind of cellulosic membranes. For CA membranes, prerequisite amount of acetone and formamide solvents were mixed together followed by addition of moisture free polymer beads in a clean glass bottle. The polymer dope solution was kept for agitation until homogeneous solution is formed. Similarly for preparation of CTA membranes, acetone and 1, 4-dioxane were mixed together followed by addition of dry polymer beads. Methanol was added after complete dissolution of polymer by rigorous agitation. For CAB membranes, CA and CTA polymers were dissolved separately in 1, 4-dioxane and acetone mixture maintaining the specified compositions. Both the solutions were then mixed together and methanol was added in a subsequent step to the mixed polymer solution followed by further homogenization of the mixed polymer solution.

All three final viscous dope solutions were kept in rest for overnight under controlled ambient temperature and humidity (maintaining $(25\pm3)^{\circ}$ C temperature and 35-40 % relative humidity)for removal of any trapped air bubbles.

Table 3.1a: Casting solution composition for preparation of cellulosic osmosis membranes.

| Membrane | Composition of Casting Solution (%w/w) | | | | |
|---|---|---|---|---|---|
| | Polymer | Acetone | Dioxane | Formamide | Methanol |
| CA | 23.0 | 46.0 | - | 31.0 | - |
| CTA | 8.6 | 44.4 | 44.0 | - | 3.0 |
| CAB | 5.2 (CA) + 5.2 (CTA) | 36.3 | 47.8 | - | 5.5 |

### 3.2.3a. Membrane Preparation:

Cellulosic membranes were prepared by phase inversion technique (details described in section 2.2.1 of chapter 2). For preparation of membrane over a smooth glass plate, the viscous polymer solution was spread evenly over a nonwoven fabric support (Viledon grade H1006 obtained from M/S. Freudenberg Nonwovens India Pvt. Ltd.) attached to the glass plate, using knife edge under a steady casting shear. The membrane after casting was then kept in air for 30 seconds for evaporation of volatile solvents (acetone and/or methanol) and subsequently immersed in a precipitation bath containing chilled deionized water as non-solvent, maintained at 1-2° C temperature for solvent/ nonsolvent exchange for 40minutes to ensure complete precipitation of the polymer. The gelled membrane was then washed thoroughly by fresh water to ensure complete removal of solvent from the membrane matrices and annealed at 90° C hot water for 15minutes in a subsequent step to prepare membranes with very small pore size, suitable for their application in FO.

### 3.2.4a. Physicochemical Characterization of Membranes:

The membranes were characterized in terms of surface morphology, surface hydrophilicity, surface average roughness and performance evaluation in terms of product permeation rate and solute rejection for NaCl feed under standard brackish water RO testing condition (using 2000 ppm NaCl feed at 1551 kPa pressure).

Surface homogeneity of the membranes were characterized using SEM (Model: CamScan3200LV) images. For imaging purposes, each membrane having an area of 1.0 cm$^2$ was coated with gold-palladium using sputter coater under the optimized conditions (Sputtering time: 100 s, Sputter current: 15 mA) in order to reduce the effect of charging by making them electrically conductive. All the micrographs were recorded employing identical

acceleration voltage of 10 keV and 4000X magnifications when operated in secondary electron mode, for better comparison purpose.

Surface roughness analyses of the membrane (CA, CTA and CAB) skin surfaces were carried out by extracting quantitative information by using an AFM instrument (Make: NT-MDT, Model: SOLVER NEXT, Ireland) in the semi-contact tapping mode. Small membrane pieces of approximate dimension of 1 $cm^2$ were cut from each membrane coupons and the air dried samples are glued onto a metal substrate by double sided tape. The instrument is equipped with a standard silicon nitride cantilever NSG 10 (NT-MDT-Multimode, Ireland) with spring constant of 11.8 N/m and typical resonance frequency of 240 kHz with a nominal tip apex radius of 10 nm with high aspect ratio. 10 μm × 10 μm area of each membrane were scanned in tapping mode in air under ambient atmosphere with a scanning frequency of 0.3 Hz. Any tilt generated by the analyst during handling was removed from the scanned images using a second order polynomial by removing all the curvatures and slopes from the image. NOVA-P9 software was used for the acquisition of image as well as evaluation of surface roughness parameters of the membranes. Surface roughness parameters of the membranes were calculated from the peak-valley profiles of the images and reported in terms of average roughness ($R_a$).

Value of water contact angle indicates the hydrophilicity of membrane surfaces and the static water contact angle onto different membrane surfaces were determined using the sessile drop method by a standard drop shape analyzer system (DSA100, KRüSS GmbH, Germany)with DSA 1v 1.92 software. The hydrophilicity of CA, CTA and CAB membranes were assessed by allowing the formation of a sessile drop in a very slow and steady manner onto each of the membrane surface by depositing 0.6 μl of the probe-solvent (deionized water) with a micro syringe. Average contact angle of each drop formed at membrane-solvent-air interface was calculated by taking the average value of contact angles measured in each second over a total

residence time of 60 s. At least six such measurements maintaining same residence time and drop size were done at different locations of each membrane strip and the wetting coefficient of each membrane is reported. The wetting coefficient (X) is defined as X =cosθ, (where θ is the average contact angle) and is a direct measure of surface hydrophilicity. Generally, if the value of X ranges from 0 to 1, the membrane can be termed hydrophilic in nature.

Characterization of the membranes in terms of their separation behaviour under standard BWRO condition were carried out using 2000 ppm NaCl in DI water as feed under 1551 kPa operating pressure. The feed solution was prepared by dissolving preweighted amount of NaCl in ultra-pure water in order to maintain the desired concentration. The product permeability and solute rejection studies at room temperature were calculated by taking the average value of readings taken for three membranes of each type prepared independently. Concentrations of NaCl in both feed and product solutions were calculated by measuring the specific conductance of the solutions (both feed and permeate) and correlating the same with concentration of salt in aqueous streams. The membrane performances are reported in terms of water permeability (LMH) and salt rejection (%), determined from the measured flux and salt rejection data respectively.

### 3.2.5a. Performance evaluation of Cellulosic membranes:

Performance of CA, CTA and CAB membranes were evaluated in terms of their volume reduction factors (VRF) under FO mode. VRF is defined as $V^i_{feed}/V^f_{feed}$, where $V^i_{feed}$ = initial volume of feed and $V^f_{feed}$ = volume of concentrate feed left at the end of experiment. The average of three readings taken for three membrane coupons with effective membrane area 7.54 cm$^2$ prepared separately of each type are reported. Schematic diagram of FO test set-up is given in Fig. 3.1a. All the experiments were carried out in AL-FS (active layer facing feed solution) mode at 25±3° C in absence of any external pressure. Back diffusion of salt from draw solution side to feed side was determined by mass balance.

Leaching of uranium from feed to the draw solution side was estimated using cyclic stripping voltammeter (Make: Metrohm, Model No. 797 VA Computrace, Switzerland).
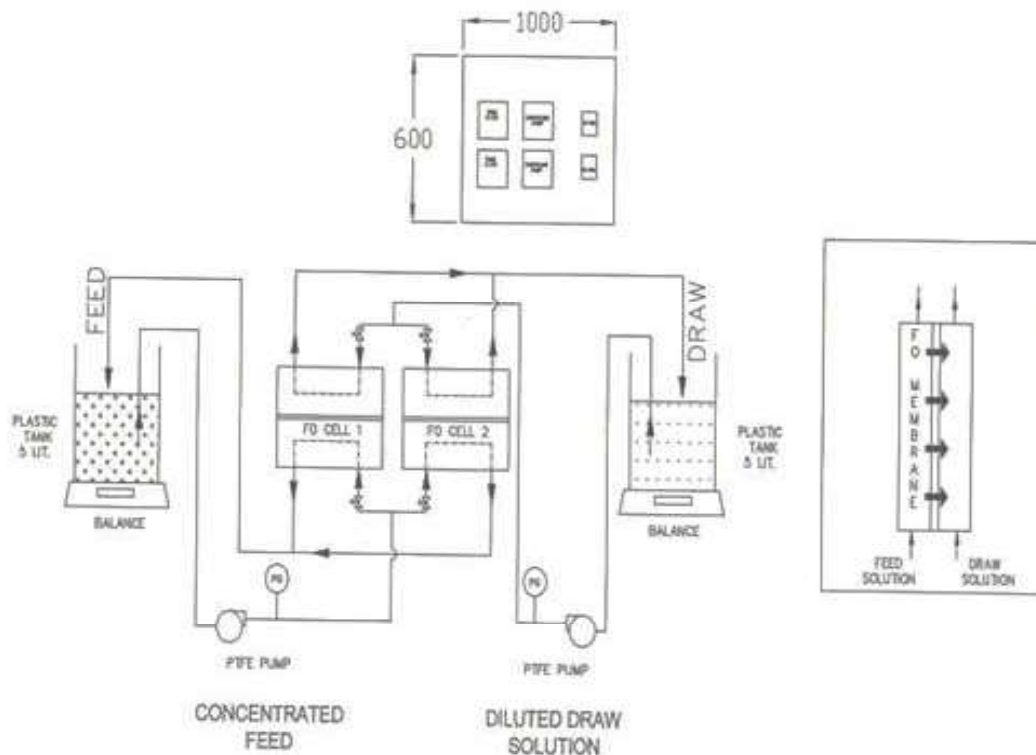


*Figure 3.1a: Schematic of testing set-up used for FO experiment.*

Two pieces of CA membranes (15 cm × 15 cm each) were sealed from 4sides by ultrasonic sealing machines to make a membrane pouch containing 10 g CaCl$_2$ salt inside. The pouch was put inside 2 liters of feed solution for 3 hours and subsequently taken out to collect aqueous CaCl$_2$ solution from the pouch.

## 3.3a. Results and Discussion

### 3.3.1a. Membrane Surface Characteristics and Separation Performance

The cellulosic membranes developed indigenously were characterized in terms of the water contact angle, surface average roughness and performance evaluation under

standard BWRO condition and the results are presented in Fig. 3.2a. The separation data were collected after the product flux gets stabilized over 45 minutes of operation. The measured permeability along-with the solute rejection data for all three membranes is given in the Fig. 3.2a. CA membranes being inherently hydrophilic in nature, because of their intrinsic structure, showed higher water permeability than CTA membranes. Chemical structure of the polymers revealed that all the hydroxylic groups got replaced by acetate groups in CTA where as in CA, two –OH groups per repeating unit are present and these –OH groups being hydrophilic in nature increases the ease of water permeation as compared to CTA membranes. All the membranes were tailor-made with similar salt rejection values for better collation of their performances in FO mode. The permeate water flux collected in mil/min is converted to lt. $m^{-2}$. $h^{-1}$ (LMH) and reported along with % salt rejection and wetting coefficient (X) data for all the membranes (Table 3.2a). The performances of indigenously developed cellulosic membranes are also compared with those of commercial cellulose acetate membranes (**TRISEP SB 50**) in the same table. However, as the data available in literature represents membrane performance under 29 bar operating pressure whereas the indigenously prepared membranes were tested under standard BWRO condition (15 bar operating pressure), permeability per unit operating pressure are also tabulated for better comparison.

Contact angle values of the membranes show that CA membrane was more hydrophilic than CTA membrane, as expected from the chemical structure of the respective polymers. Presence of hydrophilic hydroxyl groups (-OH) in the repeating unit of CA, made them more hydrophilic with lower water contact angle values as compared to CTA membranes where all the –OH groups got replaced by acetate group (-OCOCH$_3$). However CAB membranes were showing the most hydrophilic nature and showed maximum product permeation value in RO mode.

**Table 3.2a:  RO properties and hydrophilicity data of the membranes.**

| Membrane | CA | CTA | CAB | Commercial CA* (TRISEP SB 50) |
|---|---|---|---|---|
| Flux (LMH) | 18.75±1.1 | 12.08±0.68 | 21.13±0.78 | 42.79 (at 29bar) |
| Flux per unit operating pressure (LMH/bar) | 1.25±0.07 | 0.81±0.05 | 1.41±0.05 | 1.48 |
| NaCl rejection (%) | 84.0±0.49 | 87.0±0.47 | 85.9±0.70 | 96 |
| Wetting coefficient | 0.788 | 0.714 | 0.8 | - |

Applied pressure: 1551 kPa; Feed: 2000 ppm NaCl; Feed temperature: 25°C

*https://static1.squarespace.com/static/54e2b7aee4b0902efd671f90/t/5bb643660d9297734
4c956e7/1538671463199/SB50.pdf



*(i)*           *(ii)*
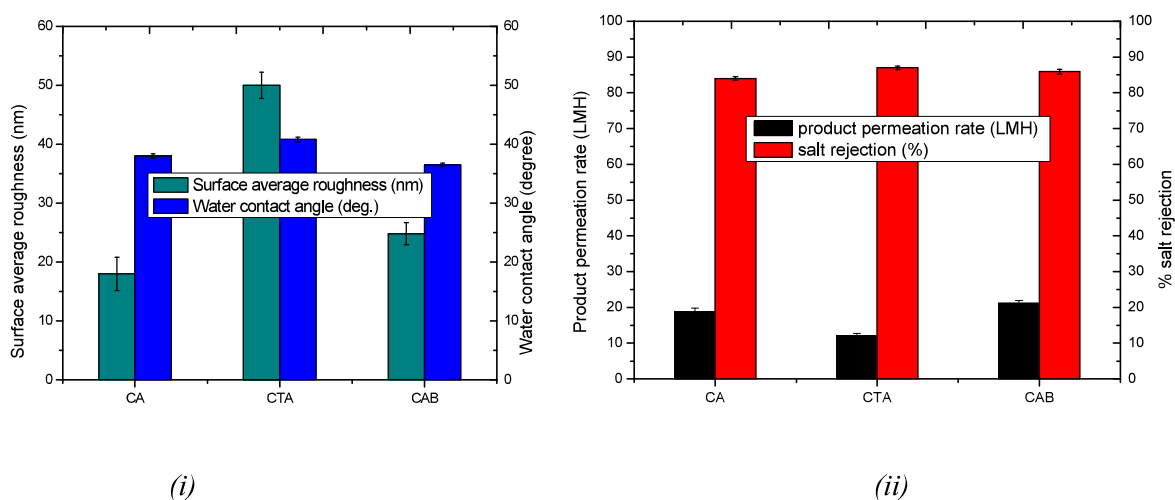
*Figure 3.2a: (i) Characterization data and (ii) Performance in RO mode of the membranes.*

From SEM images (Fig. 3.3a), it is visible that CA membranes had very smooth and homogeneous surface whereas some extent of inhomogeneity is vivid in CTA and CAB membranes. AFM images (Fig. 3.4a) and their corresponding roughness values (Fig. 3.2a) confirms that CTA membrane has rougher surface than both CA and CAB membranes. This may be attributed to the acetate groups replacing the hydroxyl group of CA. CTA membranes showed marginally higher salt rejection value, even after tailor making the all three cellulosic

membranes. Relatively rougher surface of CTA membrane increased its effective surface area and consequently the interaction between feed water and membrane surface enhanced, resulting in lower salt permeability value. CA and CAB membranes showed somewhere intermediate surface characteristics and separation performances under identical operating condition.
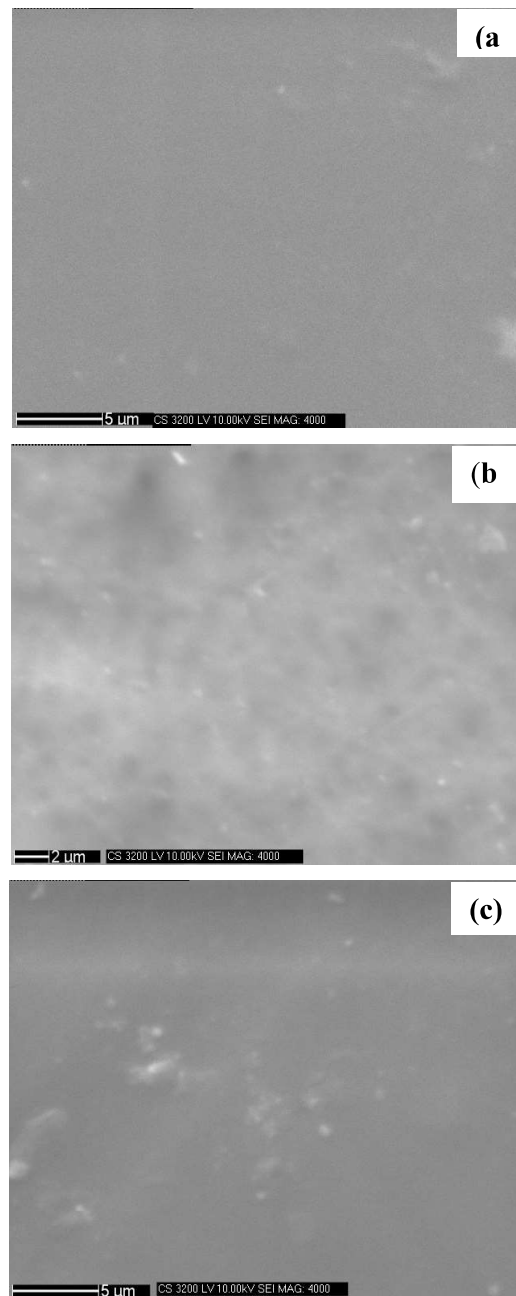


*Figure 3.3a: SEM images of skin surface of (a) CA, (b) CTA and (c) CAB membranes.*
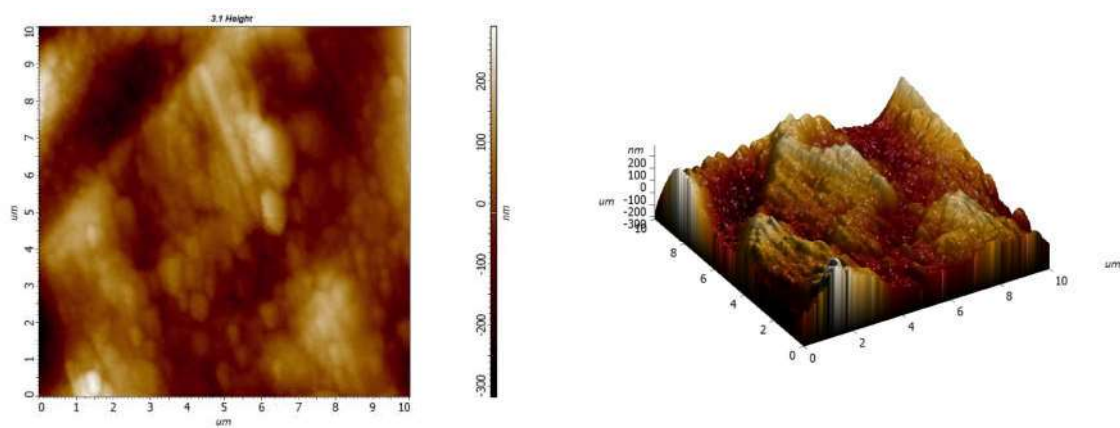
**(a)**
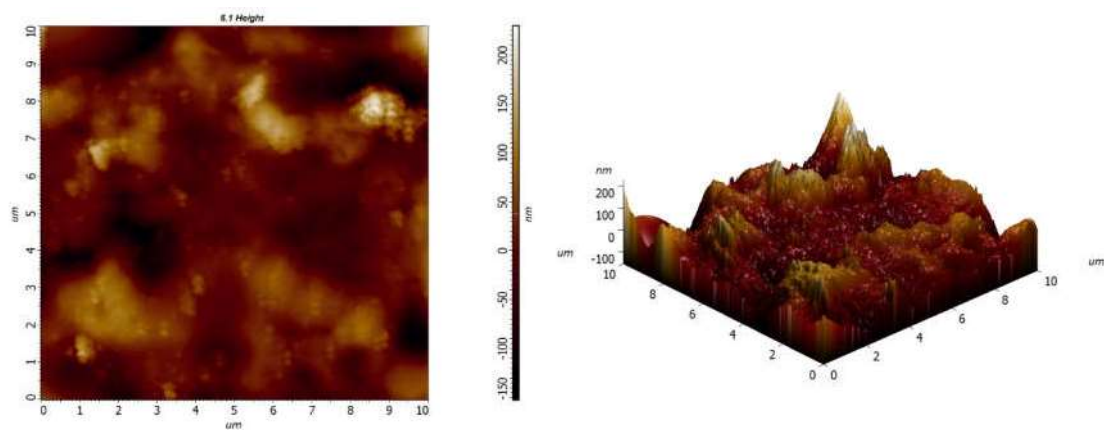


**(b)**
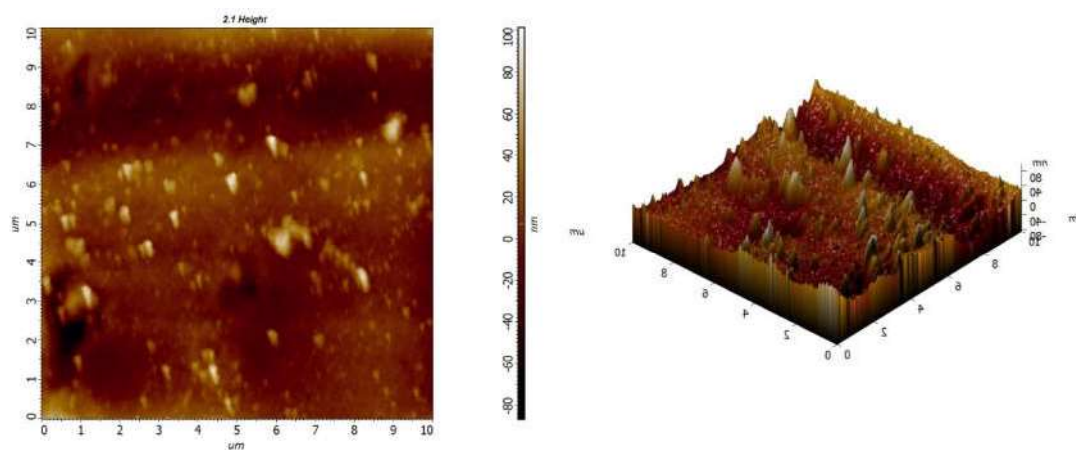


**(c)**

*Figure 3.4a: AFM images of skin surface of (a) CA, (b) CTA and (c) CAB membranes.*

77

### 3.3.2a. Membrane Performance in Forward Osmosis Experiment

Simulated ADU filtrate (as feed) solution was prepared by dissolving pre weighted amount of uranyl nitrate and ammonium nitration into ultrapure water to make the resultant solution with a concentration of 33.0 ppm uranyl nitrate (equivalent to 20 ppm uranium) in 40,000 ppm ammonium nitrate ($NH_4NO_3$). As the concentration of feed solution is quite high, the osmotic engine to be chosen must have very high solubility in water and exert much higher osmotic pressure than the feed solution to make the FO process feasible. Now, as the water solubility of $NH_4NO_3$ is very high [242% (w/w) 30°C], highly concentrated solution of the same can be prepared as the draw solution. Moreover, $NH_4NO_3$ being the major component of the feed solution, its leaching from the highly concentrated draw solution side would not chemically contaminate the feed. Hence, 320000 ppm [4 (M)] of $NH_4NO_3$ was chosen as the draw solution in present study. Performance of all the membranes in terms of VRF as a function of time over a period of 5 hours using simulated ADU feed and 320000ppm $NH_4NO_3$ as draw solution is given in Fig. 3.5a. CA membranes being hydrophilic in nature, showed highest value of volume reduction and the tighter CTA membrane (as observed in RO performance data (Table 3.2a) reduced the ease of transport of water through the membrane as compared to both CA and CAB membranes. Leaching of uranium from feed to draw solution and back-diffusion of $NH_4NO_3$ in the opposite direction are given in Table 3.3a. It is well known that $NH_4NO_3$ is poorly rejected by RO membranes [137]. Mass balance shows that some extent (2.2-3.2%) of back diffusion of $NH_4NO_3$ from draw solution to feed solution is there for all CA, CTA and CAB membranes. The percentage of salt back diffused to the feed side was mathematically calculated from the difference between the actual amount of salt found in the feed side and the amount of salt supposed to be present based on the volume reduction assuming no salt diffused from the dilute feed to highly concentrated draw

solution side. However, leaching of uranium to the draw solution side from feed was found to be very less (0.45−0.56%) for all the membranes (Table 3.3a).

**Table 3.3a: Back-diffusion of $NH_4NO_3$ and leaching of uranium data for all the membranes.**

| Leaching of U from feed (~20ppm) to draw solution after 300 min. | CA | CTA | CAB |
|---|---|---|---|
| | 0.560% (112.03±2.48 ppb) | 0.458% (91.54±3.94 ppb) | 0.552% (110.35±3.30 ppb) |
| **Back-diffusion of $NH_4NO_3$ (320000 ppm) from draw solution to feed after 300 min.** | 3.0% (9600±387.0 ppm) | 2.2% (7040±260.5 ppm) | 3.2% (10240±327.7 ppm) |
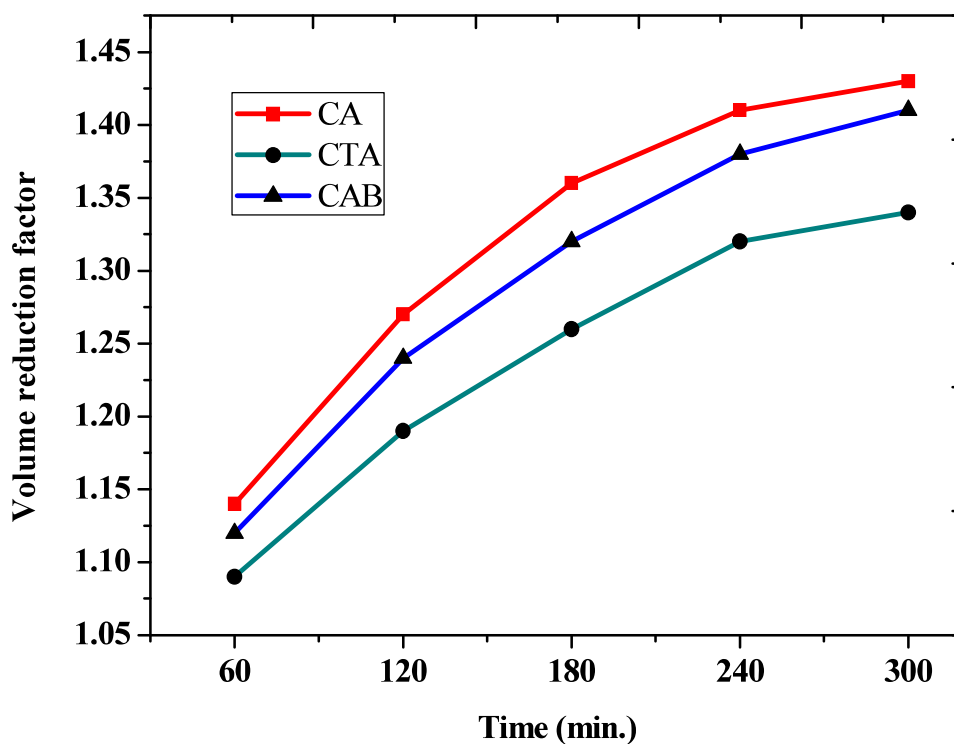


*Figure 3.5a: Plot of change in volume reduction factor as a function of time for all the*

*cellulosic membranes.*

79

### 3.3.3a. Membrane Performance for Different Draw Solutions

As CA membranes had shown better performance than CTA and CAB membranes in terms of VRF with nominal leaching of uranium to the draw solution side, a set of FO experiments using the same feed solution (40,000 ppm $NH_4NO_3$ with 20 ppm uranium) was conducted with CA membrane using three different draw solutions namely, $NH_4NO_3$, $NH_4HCO_3$ and $CaCl_2$ of 4 (M) concentration each. Ammonium bicarbonate ($NH_4HCO_3$) is a widely chosen draw solute and is being used intensively for several applications of FO in particular where the feed is already having high osmotic pressure, e. g. sea water desalination. The major advantages of using $NH_4HCO_3$ as draw solute are (i) it can be prepared easily onsite by simple combination of ammonia and carbon dioxide gases in a specific ratio, (ii) provides high osmotic pressure due to low molecular weight and high water solubility and more importantly, (iii) decomposes off to ammonia and carbon dioxide by mild heating of the diluted draw solution at 65°C making the recovery of pure water really simple. Achilli *et al.* Have studied the suitable choice of draw solutions for different FO applications by selecting 14 different draw solutes and concluded that the draw solutions prepared using $CaCl_2$, $KHCO_3$, $MgCl_2$, $MgSO_4$ and $NaHCO_3$ are preferred over the others in performance point of view [164]. Hence, the bi-monovalent salt $CaCl_2$ was also taken as one of the draw solute. Performance in terms of VRF with CA membrane using simulated ADU filtrate as feed and these three different draw solutions is given in Fig. 3.6a.

Osmotic pressure ($\pi$) of a solution with solute molar concentration (C) at a given temperature T is given by:

$$\Pi = iCRT \dots\dots\dots\dots\dots (1)$$

R=universal gas constant,
 i= van't Hoff factor

If the degree of dissociation is α for a particular species $A_xB_y$ (of molar concentration C) which decomposes in water as:

$$A_xB_y \rightarrow xA^{y+} + yB^{x-}$$
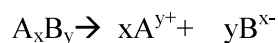
Equilibrium concentration:     $(1-\alpha)C$     $x\alpha C$     $y\alpha C$

Thus, after achieving equilibrium, the total molar concentration of the solution will be:

$$(1-\alpha)C + x\alpha C + y\alpha C = [1+ (x+y-1)\alpha]C = iC \dots\dots\dots (2)$$
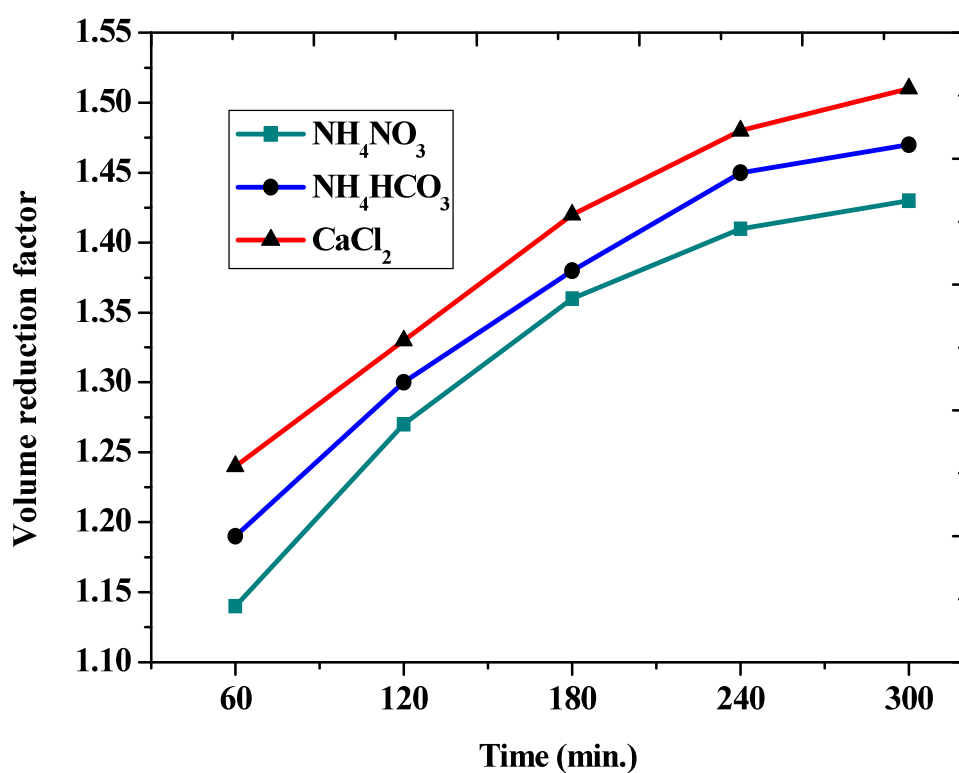


*Figure 3.6a: Plot of change in volume reduction factor as a function of time for different draw solutions (CA membrane).*

Thus the van't Hoff factor ($i$) is a direct measure of total number of ionisable species present in the solution and as the number of ionisable species is three (x=1, y=2 in Equation 2) for $CaCl_2$ and two (x=y=1 in Equation 2) for both $NH_4NO_3$ and $NH_4HCO_3$, the osmotic pressure exerted by $CaCl_2$ was higher than that for $NH_4NO_3$ and $NH_4HCO_3$. Hence, the VRF value was

higher for 4 (M) CaCl$_2$ draw solution than NH$_4$NO$_3$ and NH$_4$HCO$_3$ solutions of the same concentrations because of higher driving force. However, the VRF for NH$_4$HCO$_3$ draw solution was more than NH$_4$NO$_3$ draw solution even though the osmotic pressure of both the solutions were expected to be very close under same concentration.

### 3.3.4a. Membrane Performance as a Function of Concentration of Draw Solution

Performance evaluation in terms of volume reduction was carried out over a range of concentrations of draw solutions in the same system (simulated ADU filtrate containing ~20 ppm uranium in 40,000 ppm NH$_4$NO$_3$ aqueous solution) using CA membrane. For this purpose, NH$_4$NO$_3$ and CaCl$_2$ of three different concentrations [2 (M), 3 (M) and 4 (M)] were used as draw solutions in order to study the effect of concentration of the draw solution as well as the change in chemical nature of the draw solutes. Volume reduction factors of CA membranes as a function of temperature using simulated ADU feed and two different draw solutions of varying concentrations after 5hours of experiment is given in Fig. 3.7a. As expected, the VRF value is more for CaCl$_2$ draw solution than NH$_4$NO$_3$ solution of same concentration because of its higher value of van't Hoff factor. The osmotic pressure gradient between the feed and draw solution increases with increase in draw solution concentration (Equation 1), keeping all other factors same, which in turn increased the volume reduction irrespective of the nature of the draw solute. It can be noticed (Fig. 3.7a) that the increase in volume reduction factor on changing the draw solution concentration from 2 (M) to 4 (M) was more prominent in case of CaCl$_2$ than that of NH$_4$NO$_3$. Staples et al. had critically evaluated the mean activity and osmotic co-efficients of aqueous CaCl$_2$ solutions at 298.15K over the concentration range 0– 10.0 moles. kg−1 [207] which shows that the increase in osmotic co-efficients of aqueous CaCl$_2$ solutions is more for change in concentration from 3.0–4.0 moles. Kg−1 as compared to concentration changes from 2.0–3.0 moles. Kg−1.

Hence, the nonlinear increase in volume reduction factor with $CaCl_2$ in the concentration range 3 (M) to 4 (M) was mainly due to the higher increase of its osmostic pressure than $NH_4NO_3$.
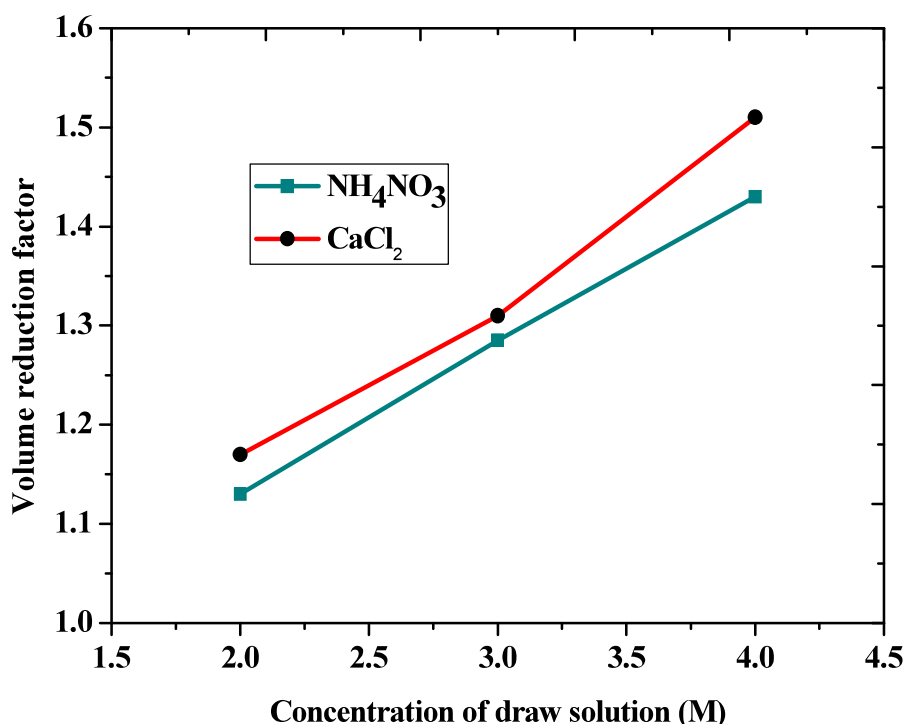


*Figure 3.7a: Plot of change in volume reduction factor as a function of concentration of two different draw solutions (CA membrane).*

### 3.3.5a. Possibility of Using Membrane Pouch as Device for FO Process

The freshly prepared CA membrane pouches of 15 cm×15 cm dimension, were put in 2 liters of simulated ADU filtrate containing ~20 ppm uranium in 40,000 ppm $NH_4NO_3$ aqueous solution. 208 mL of concentrated aqueous solution of $CaCl_2$ had been formed inside the pouch after 3 hours of immersion into the feed. Membrane pouch used as FO device for concentration of simulated ADU filtrate using CA membrane is shown in Fig. 3.8a. However, the bursting pressure of the pouch needs to be known for collection of maximum water from

the feed. The present attempt was just to demonstrate the process to use of FO in a simpler way for concentration of low level radioactive waste.



**Membrane pouch**

**Pouch put in feed**

**Pouch containing almost pure water**

*Figure 3.8a: Membrane pouch used as FO device for concentration of simulated ADU filtrate (CA membrane used).*

## 3.4a. Conclusions

Cellulosic osmosis membranes with similar salt rejecting properties were prepared using cellulose acetate (CA), cellulose triacetate (CTA) and cellulose acetate blend (CAB) [blending of CA and CTA] systems by optimizing all the parameters. Performance of the membranes in terms of volume reduction factor for concentration of simulated ADU increased in the order CTA<CAB<CA with minimal leaching of uranium to the draw solution side for all the membranes. Different draw solutions can be used for the same purpose depending upon the requirement. Increase in draw solution concentration invariably increased the volume reduction at the expense of solute back diffusion to the feed side contaminating it. Membrane pouch can be used as a simple device for concentration of a desired stream with proper choice of the membrane.

## 3b. Development of Polyamide membranes for treatment of simulated ADU filtrate solution

## 3.1b. Introduction

The work discussed so far on development of FO membranes for concentration of low to intermediate level radioactive waste was associated with preparation of cellulosic membranes because of the inherent hydrophilic nature of the polymer. However, the major problems associated with these cellulosic membranes are their poor stability over a range of pH, low glass transition temperature which makes them unsuitable to be used in a membrane based hybrid process operated at elevated temperature and low fouling resistance property of the polymer. With advancement of time, the major breakthrough in membrane science was development of thin film composite polyamide (TFCPA) membranes by Cadotte [174, 175] et al. These composite polyamide membranes are capable of overcoming the backdrops associated with asymmetric cellulosic membranes. Moreover, performances in terms of permeability and solute rejection of a TFCPA membrane can be tailored much more easily than that of asymmetric cellulosic membranes. Thus, as an extension of the work briefed in section (a) of this chapter, TFCPA membranes of aliphatic-aromatic and aromatic-aromatic types were developed indigenously and their performances in terms of VRF for concentration of simulated ADU filtered solution was evaluated.

## 3.2b. Experimental

### 3.2.1b. Materials

Polysulfone (PSf) beads (Mw: 67000-72000, polydispersity: 3.5) were obtained from M/s. Solvay Specialities India Pvt. Ltd., India. AR grade N-methyl pyrrolidone (NMP) was used as solvent for making polysulfone support membranes and was procured from M/s. Sisco Research Laboratories, India. 50% aqueous solution of Polyethylene imines (PEI) [M.Wt.

50,000-100000 Da (PEI-50KDa)] was obtained from M/s. BDH Reagents and Chemicals, Poole, UK and 1, 3- benzene dicarbonyl chloride / isophthaloyl chloride (IPC) was procured from M/s. Aldrich, India.1,3-diamino benzene or *m*-phenylenediamine (MPD) , 1,3,5-benzene tricarboxylic acid chloride or trimesoyl chloride (TMC) and triethyl amine (TEA) all were purchased from M/s. Sigma-Aldrich, India. Isoparaffin/ Isopar-G solvent, used for dissolution of TMC, was procured from M/s. Orion Chem Pvt. Ltd. India. Ammonium nitrate and ammonium bicarbonate of analytical grades were procured from Thomas Baker, India and sodium chloride of analytical grade obtained locally was used without further purification.

### 3.2.2b.Membrane Preparation

TFCPA membranes were prepared in two steps. In the first step the polysulfone support membrane was prepared by phase inversion technique. For preparation of support membrane, a nonwoven fabric (Viledon grade H1006 obtained from M/S. Freudenberg Nonwovens India Pvt. Ltd.) was fixed onto a clean glass plate and the integrally skinned PSf support membrane was prepared in the method explained in section 2.2.2 of chapter 2.

In a second step a polyamide layer of submicron thickness was prepared onto the support polysulfone membrane by in situ polycondensation reaction between amine and acid chloride. For preparation of aliphatic aromatic based TFCPA, pre requisite amount of amine [1.6% polyethylene imine (PEI) for aliphatic-aromatic based membrane and 2% m-phenylene diamine (MPD) for aromatic-aromatic based membrane], was dissolved in EDI water in which the freshly prepared PSf membrane was immersed for 2 minutes. A few drops of TEA, as an acceptor of HCl liberated in the course of polycondensation reaction, were added to the aqueous MPD solution. After taking the membranes out, the excess amine from their surface was removed by squeezing with a soft rubber roller and the amine saturated membranes were dipped into 0.5% solution of acid chloride (IPC in hexane in the former case and TMC in

isopar-G in the latter case) for 1 min. Reaction took place at the interface of water/organic media and a thick PA film is formed. The membrane was heat cured subsequently under IR lamp (90°C) for 15 mins or till the surface looks completely dry. Composition of both membranes is given in Table 3.1b.

**Table 3.1b: Composition of TFCPA Membranes.**

| Membrane | Concentration of Amine (%) | Concentration of Acid chloride (%) |
|---|---|---|
| Aliphatic-aromatic | 1.6 (PEI) | 0.25 (IPC) |
| Aromatic-aromatic | 2 (MPD) | 0.5 (TMC) |

Reaction time: 60 s.; Curing medium: IR lamp (250 W); Curing temp: 90°C; Curing time: 15 mins.

### 3.2.3b. Physicochemical Characterization of Membranes

Both the membranes were characterized in terms of their surface morphology, surface hydrophilicity, surface average roughness and performance evaluation in terms of product permeation rate and NaCl rejection under standard BWRO testing condition.

Surface morphology of the membranes were characterized by acquiring their SEM (Make: ZEISS, Model: GeminiSEM 450, Germany) images. For imaging purposes, each membrane having an area of 1.0 cm$^2$ was coated following the same procedure as explained in section (a) of this chapter. All the micrographs were recorded employing identical acceleration voltage of 5 keV and 50000X magnifications when operated in secondary electron mode, for better comparison purpose.

Surface roughness analyses of the skin surfaces of both PEI/IPC and MPD/TMC based membranes were accomplished by topographical imaging using an AFM instrument (Make:

NT-MDT, Model: SOLVER NEXT, Ireland) in the semi-contact tapping mode. Air dried small pieces of membranes with approximate dimension 1 cm$^2$ were cut and glued subsequently onto a metal substrate by double sided tape. 5 μm × 5 μm area of each membrane were scanned in air under ambient atmosphere with a scanning frequency of 0.3 Hz. Tilt generated as individual error during gluing was removed from the scanned images by applying a second order polynomial. NOVA-P9 software was employed for acquisition of the image as well as evaluation of surface roughness parameters. Quantitative determination of surface roughness of the membranes were carried out and reported in terms of their average roughness values ($R_a$).

Hydrophilicity of the membranes were determined by measuring the water contact angle value onto membrane surfaces using a standard drop shape analyzer system (DSA100, KRüSS GmbH, Germany) with DSA 1v 1.92 software. Static contact angle of sessile drop formed onto each membrane surface was measured following the same procedure as explained in section 3.2.4a of the same chapter and the average values are reported.

Characterization of the membranes in terms of their separation characteristics under standard BWRO condition were carried out in a similar way as elaborated earlier (section 3.2.5a).

### 3.2.4b. Performance evaluation of TFC PA membranes:

Performance in terms of volume reduction factors (VRF) under FO mode of both PEI/IPC and MPD/TMC based membranes were determined at ambient temperature in absence of any external operating pressure. VRF was calculated by measuring the volume of feed solution at the start of experiment and after 5 hours. All the experiments were executed in triplicate placing a membrane piece of membrane (effective area: 7.54 cm$^2$) in two compartment FO cell, skin layer facing the feed solution. Concentration of uranium leached from feed to the

88

draw solution side was determined by cyclic stripping voltammeter (Make: Metrohm, Model No. 797 VA Computrace, Switzerland).

### 3.3b. Results and Discussions

#### 3.3.1b. Membrane Surface Characteristics and Separation Performance

In case of MPD/TMC based membranes, the bifunctional amine moiety (MPD) needs to react with a trifunctional acid derivative (TMC in the present case) to form 3D polymeric network structure. Whereas, PEI, itself being a polymeric amine, is capable of forming polymer networkby reacting with bifunctional IPC.

Characterization data of PEI/IPC and MPD/TMC based membranes, in terms of the water contact angle, surface average roughness and performance evaluation under standard BWRO condition, are presented in Fig. 3.1b. It is evident that MPD/TMC based membranes showed slightly higher value of water permeability as well as solute rejection as compared to PEI/IPC based membranes. During polycondensation reaction the amine molecules need to be diffused from the pores of polysulfone support membranes to react with the acid chloride present in bulk organic solution. Now in case of aliphatic-aromatic membranes, the amine reactant, PEI itself being a polymer, its diffusion from aqueous to organic medium was relatively slower and the acid chloride gets sufficient time to infuse into the pores of PSf. This led to pore clogging of the PSf support membrane (Fig. 3.2b) and the effect can be noticed in slightly lower value of water permeability than MPD/TMC based membrane where none of the reactant molecules are in polymeric form. The same might be the reason behind higher surface roughness value of MPD/TMC based membranes than PEI/IPC based membranes (Fig. 3.2b). Larger active surface area of MPD/TMC based membranes than PEI/IPC based membranes (owing to rougher surface) is the reason behind its slightly higher value of salt rejection under standard BWRO condition. The surface inhomogeneity and rougher

morphology can be well observed from their comparative SEM and AFM images (Fig. 3.3b and Fig. 3.4b).
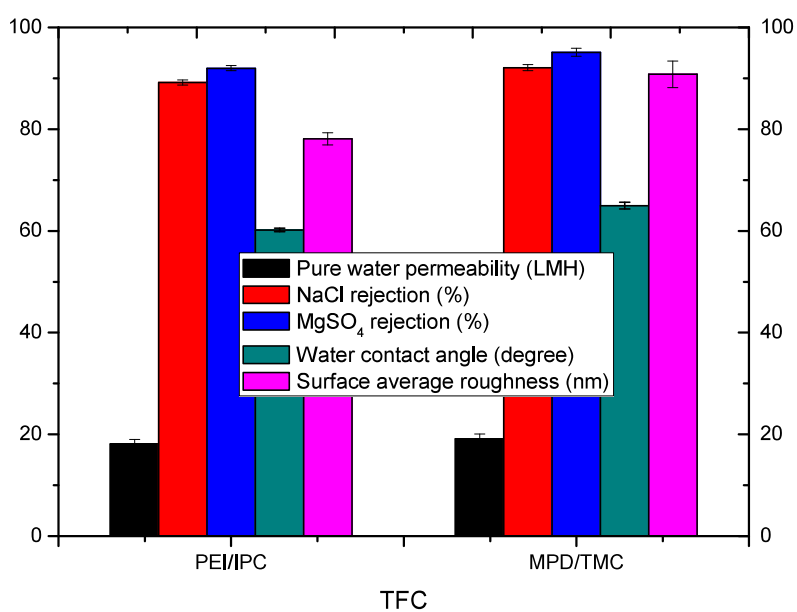


*Figure 3.1b: Performance in RO mode and characterization data of the membranes.*
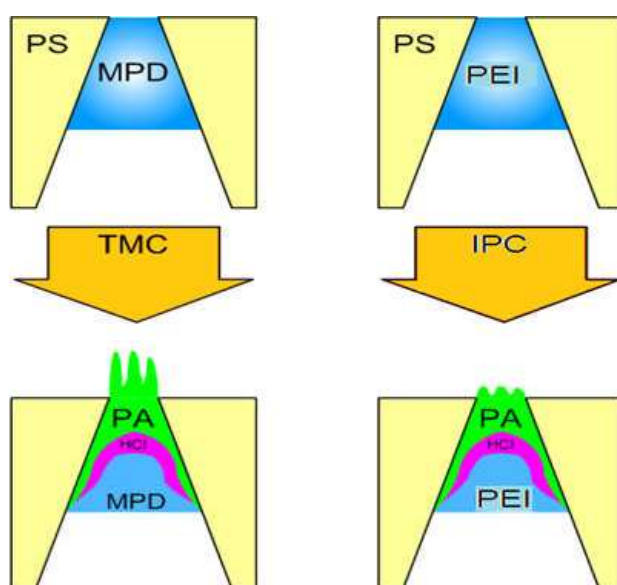


*Figure 3.2b: Schematic Representation of Polyamide Formation.*
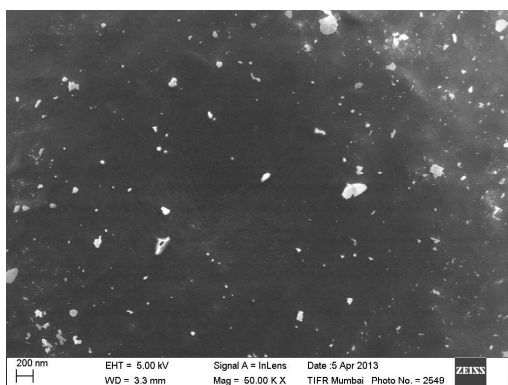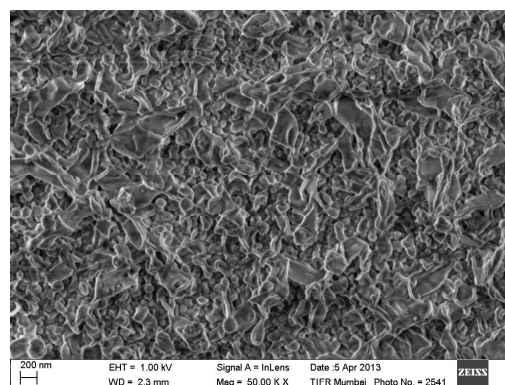
(a)                                                                  (b)

*Figure 3.3b: SEM images of skin surface of (a) PEI/IPC and (b) MPD/TMC based membranes.*
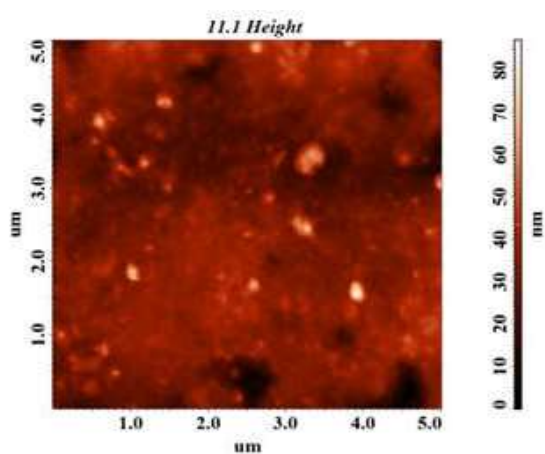


(a)
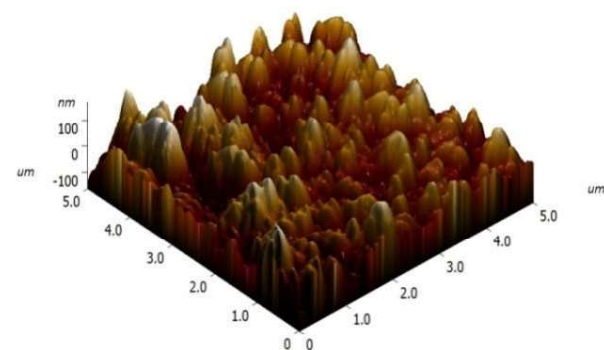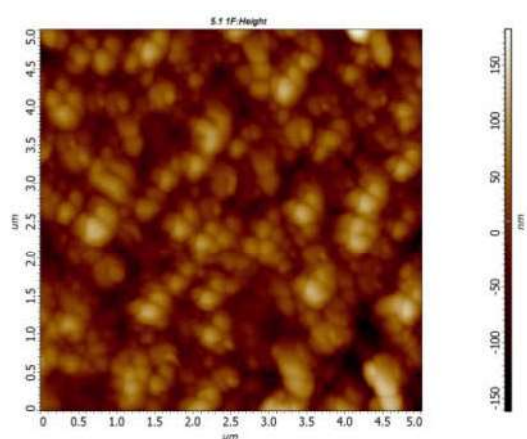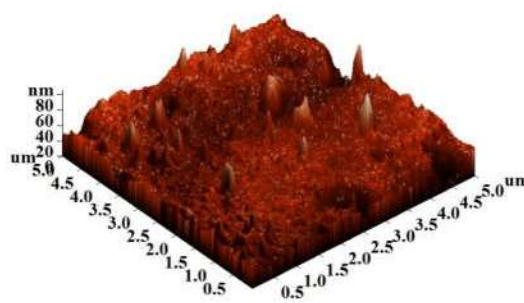


(b)

*Figure 3.4b: 2-D and 3-D AFM images of skin surface of (a) PEI/IPC and (b) MPD/TMC based membranes.*

### 3.3.2b. Membrane Performance in Forward Osmosis Experiment

In order to evaluate membrane performance in FO mode, required amount of uranyl nitrate and ammonium nitrate salts were dissolved into ultrapure water to make the resultant concentration of the feed solution same as that of ADU filtrate (33.0 ppm uranyl nitrate (equivalent to 20 ppm uranium) in 40,000 ppm ammonium nitrate). 320000 ppm [4 (M)] aqueous solution of $NH_4NO_3$ was used as the draw solution, $NH_4NO_3$ was chosen as the osmotic engine for the same reasons as explained in section 3.4.2a of the same chapter. Performance of both the membranes in terms of VRF over time of 5 hours is given in Fig. 3.5b.
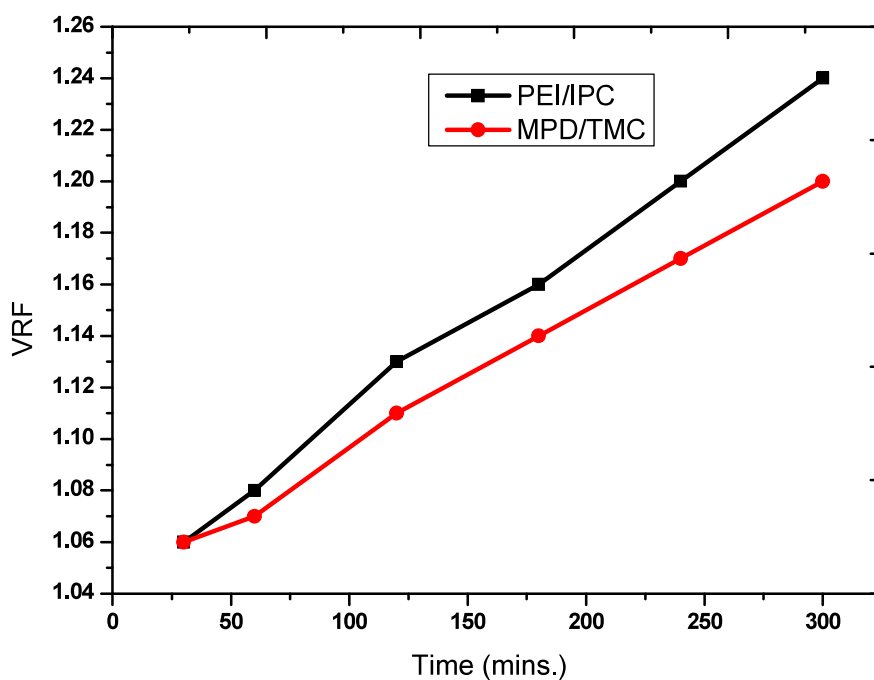


*Figure 3.5b: Plot of change in volume reduction factor (VRF) as a function of time for PEI/IPC and MPD/TMC based membranes.*

Fig. 3.5b shows higher VRF values of PEI/IPC based membranes as compared to MPD/TMC based membranes over the entire range of time. Smaller water contact angle value of PEI/IPC based system (Fig. 3.5b) confirms higher hydrophilicity of the membrane surface as compared to the MPD/TMC based membranes. As no external pressure is operative in FO, hydrophilicity of the membrane surface plays an important role in controlling the VRF value. Leaching of uranium from simulated ADU filtrate to draw solution was determined and found to be very less (~0.5%) (Table 3.3b).

### 3.3.3b. Membrane Performance for Different Draw Solutions

In order to observe the effect of change of draw solute onto membrane performance in terms of their VRF values, both PEI/IPC and MPD/TMC based membranes were exposed to simulated ADU filtrate as feed and two high concentration solutions [5 (M) $NH_4NO_3$ and 4 (M) $(NH_4)_2CO_3$] of inorganic salts as draw solutions. As the number of ionisable species is higher (three) for $(NH_4)_2CO_3$, it was taken in a lower concentration than $NH_4NO_3$ to maintain the osmotic pressure exerted by the draw solutions comparable. VRF of both the membranes with these two different draw solutions were determined in regular time interval over 5hours of experiments (Table 3.2b). A very interesting result was found in this set of experiment. It had been observed that under similar tune of osmotic pressure, performance of the membrane depend on the nature of membrane as well as draw solution. PEI/IPC based membranes showed higher value of VRF when $NH_4NO_3$ was used as the draw solution whereas higher value of VRF was observed with MPD/TMC based membranes using $(NH_4)_2CO_3$ as the draw solution. This anomaly in performances can be revealed from molecular structure (Fig. 3.6b) of the polyamides formed. The aliphatic amine PEI contains primary, secondary and tertiary, all three types of amine groups of which primary amine groups are more prone to react with acid chloride during polycondensation reaction.

**Table 3.2b: Performances of the membranes in terms of VRF as a function of time using different draw solutions.**

| Time (mins) | VRF | | | |
| --- | --- | --- | --- | --- |
| | Draw Solution: NH₄NO₃ | | Draw Solution: (NH₄)₂CO₃ | |
| | PEI/IPC | MPD/TMC | PEI/IPC | MPD/TMC |
| 30 | 1.06±0.023 | 1.06±0.022 | 1.06±0.022 | 1.05±0.028 |
| 60 | 1.08±0.021 | 1.07±0.018 | 1.07±0.026 | 1.07±0.032 |
| 120 | 1.13±0.019 | 1.11±0.019 | 1.08±0.021 | 1.10±0.031 |
| 180 | 1.16±0.024 | 1.14±0.018 | 1.10±0.024 | 1.12±0.026 |
| 240 | 1.20±0.023 | 1.17±0.024 | 1.12±0.022 | 1.15±0.026 |
| 300 | **1.24±0.026** | 1.20±0.019 | 1.15±0.021 | **1.21±0.019** |

A few number of tertiary amine groups are thereby left untouched at the end of reaction and provides some active sites for protonation in mildly acidic $NH_4NO_3$ solution (pH: 5.53). This protonation imparts some extra polar character onto the membrane surface and enhances the surface hydrophilicity favoring water permeability to take place in a faster rate.

On the other hand, TMC being the acid chloride form of tricarboxylic mesitoyl acid, some excess –COCl groups might be present onto the resultant MPD/TMC based polyamide surface which in presence of slightly acidic or alkaline water undergoes hydrolysis to form –COOH. Now, pH of 4 (M) $(NH_4)_2CO_3$ in water (pH: 12.3) confirms the alkaline nature of the solution in which the hydrolysed the –COOH groups, generated from hydrolysis of –COCl groups, gets deprotonated forming carboxylate anions. This negatively charged carboxylates enhances the overall hydrophilicity of aromatic-aromatic based polyamide membranes making the water permeability more feasible.

|      (a)      |      (b)      |
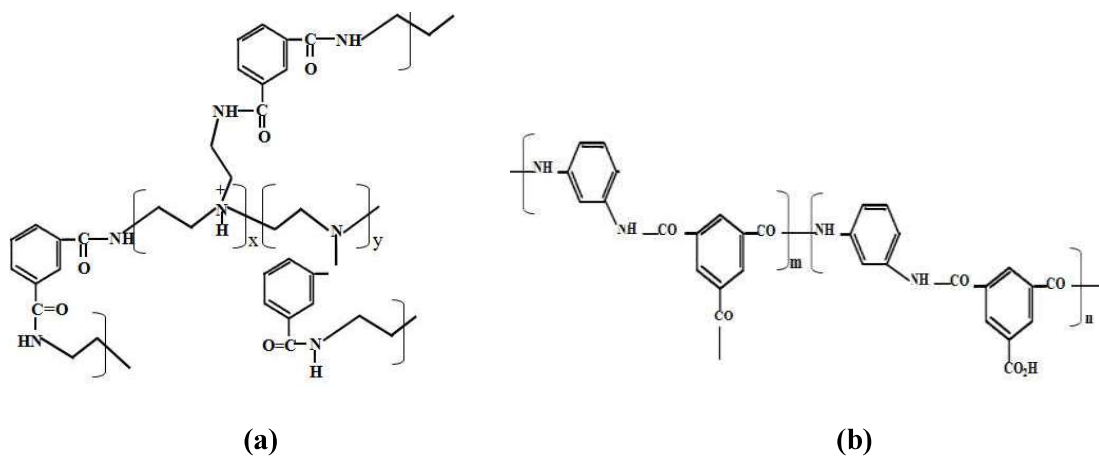
*Figure 3.6b: Molecular structures of Polyamides generated from (a) PEI/IPC and (b)*

*MPD/TMC.*

Determination of uranium concentration (Table 3.3b) in draw solution side after 300minutes of experiment confirms very small amount of leaching from feed to draw solution for both the membranes irrespective of the nature of draw solutions used.

**Table 3.3b: Leaching of U data for both the membranes after 300mins.**

| Draw Solution: $NH_4NO_3$ | | Draw Solution: $(NH_4)_2NO_3$ | |
|---|---|---|---|
| **PEI/IPC** | **MPD/TMC** | **PEI/IPC** | **MPD/TMC** |
| 0.444% | 0.434% | 0.506% | 0.477% |
| ($88.75 \pm 2.73$ ppb) | ($86.781 \pm 2.56$ ppb) | ($101.28 \pm 3.54$ ppb) | ($95.34 \pm 3.14$ ppb) |

## 3.4b. Conclusions

Aliphatic-aromatic and aromatic-aromatic based thin film composite polyamide (TFCPA) membranes with high NaCl rejection under standard BWRO conditions were developed over polysulfone support membrane with PEI/IPC and MPD/TMC based systems after optimization of all the casting as well as coating parameters. Performance of both the membranes in FO mode in terms of VRF for concentration of simulated ADU filtrate solution was evaluated for different draw solutions over a range of time. Performance of TFCPA membranes in terms of VRF was found to be dependent on membrane material as well as nature of draw solute. PEI/IPC based membranes showed higher VRF values in mildly acidic pH whereas MPD/TMC based membranes found to give higher VRF value in moderately alkaline solution. Almost no leaching of uranium from feed to the draw solution side for all the membranes were reported irrespective of the nature of draw solution. Thus, FO can be successfully deployed as an energy efficient process for concentration of low to intermediate level radioactive waste using cellulosic as well as TFCPA membranes.

## 3c. High Flux Thin–film composite polyamide (TFCP) Forward Osmosis membranes for Concentration of Simulated Cesium and Strontium bearing Effluent solution

### 3.1c. Introduction

Cellulosic and polyamide polymers, with their own advantages and disadvantages [194], are being used successfully for development of application specific osmotic membranes. Composite polyamide membranes prepared by deposition of a thin barrier layer onto the support membrane by interfacial polycondensation reaction are more fouling resistant with added advantage of higher mechanical, thermal and pH stability than cellulosic membranes. Aromatic-aromatic MPD/TMC based polyamide membranes are used worldwide for preparation of reverse osmosis membranes for their better product permeability. Also, presence of aromatic ring structure in the polymer backbone makes them potential candidate for long term application in treatment of low to high level radioactive waste. However, in forward osmosis, inflow of water from feed to draw solution side takes place in absence of any external energy source and hydrophilicity of the overall membrane plays the prime role in deciding the membrane performance. From literature [67], it was found that a series of alcohols or hydrophilic reagents or ionic surfactants able to vary physicochemical properties of TFC membrane and also attain the objective of enhancing flux. These phase-transfer catalysts are usually added to the water phase.

With this scientific background, the present work was focused on development of high flux TFC-FO membrane with better radiation stability. For this purpose the most commonly used PSf support membrane of TFC membranes was substituted in this study by relatively hydrophilic polyethersulfone (PES) membrane. For surface modification of polyamide barrier layer, a new formulation of reactant monomers by addition of phenolic compounds into the aqueous amine solution in presence of other additives is illustrated in the trailing section of this chapter. Performance of the indigenously developed TFCFO membranes in terms of

their potential application for concentration of simulated Cs/Sr bearing effluent solution on practical scale was evaluated by rolling the membranes onto a 2512 spiral module. As the operating conditions like flow rate and pressure drop of a laboratory scale membrane process are very much different from those of a spiral module, full-scale membrane processes behave in an altogether different manner from the small laboratory-scale membrane devices [145]. Hence, the present experimental work and its interpretation highlights optimization of preparation and test condition of TFCFO membranes by collecting test data from laboratory-scale trial runs to actual application using 2512 spiral module (representative of full scale processes) under similar test conditions.

## 3.2c. Experimental

### 3.2.1c. Materials

Polyethersulfone (PES) polymer was purchased from M/s. Solvay Specialities India Pvt. Ltd., India. Reagent grade N,N-dimethyl formamide (DMF) & polyvinyl pyrrolidone (PVP) used as solvent and additive for preparation of PES support membrane, were obtained from M/s. Sisco Research Laboratories, India. Monomers used for polycondensation reaction like 1,3-diamino benzene or *m*-phenylenediamine (MPD), 1,3,5-benzene tricarboxylic acid chloride or trimesoyl chloride (TMC) and additives like triethyl amine (TEA) (liquid, 99.5%), (+)-10-champhor sulfonic acid (CSA) (powder, 99.0%) and phenol (ACS reagent, $\geq$99.0% ) were all procured from Sigma-Aldrich, India. Proprietary isoparaffin, Isopar G was procured from M/s. Orion Chem Pvt. Ltd. India. Analytical grade inorganic salts used as draw solutes like calcium chloride and ammonium carbonate are purchased from Thomas Baker, India.

### 3.2.2c. Preparation of membranes

Composite polyamide membranes, with varying concentration of additive (TEA/CSA and/or phenol), were prepared in a step by step reaction in first step of which, PES support membrane is prepared. The support membrane was subsequently coated with a thin polyamide layer in the second step involving in-situ polycondensation reaction.

For preparation of support membrane by phase inversion technique, 20 g of PES & 4 g of PVP was mixed in a hermitically sealed glass bottle prior to addition of 80 g DMF as solvent. The solution was kept under rigorous agitation for several hours until a viscous homogeneous solution is formed. The polymer casting solution was subjected to a mild vacuum for removal of any trapped air bubbles that may lead to formation of defective support membrane in the succeeding stages. Then PES support membranes were prepared using a casting machine (capable of making membranes of 35 cm width and continuous length). Polymer casting solution was first casted onto a rolling non-woven polyester spun bound fabric (M/s. Freudenberg Nonwovens India Pvt. Ltd.) by using a knife edge. The polymer coated fabric was then immediately immersed into the gelling bath containing demineralized water at room temperature. The size of the membranes prepared in a single batch was typically 5 m (length) × 35 cm (width). All the membranes were prepared in an environmentally controlled atmosphere maintaining temperature at 25±3° C and humidity ~40% RH. The membranes obtained by solvent-nonsolvent exchange were washed repeatedly demineralized water and kept in refrigerator cooled water (~6° C) till further use.

Moist PES support membranes were kept in the feeder tank of coating machine, the size of which was maintained the same as the dimensions of support membranes prepared by casting machine. As soon as the electrically controlled coating machine was switched on, the support membrane rolls forward to be immersed in aqueous amine (MPD) solution of preoptimized concentration for 30 seconds. Then excess amine solution from the surface of support

membrane was removed by squeezing them with soft rubber rollers. In the second step, perquisite concentration of TMC solution in isopar solvent was gently sprayed over the amine saturated support membrane for predetermined time. A thin polyamide layer was formed at the surface of polyethersulfone support membrane and the composite membranes were heat cured by putting them in an oven at $90^o$ C for 6 minutes. Finally, the dry TFC membranes were rolled over the collection roller and kept for spiral rolling. In cases where the additives like TEA and CSA were employed, a mixture of 20 g TEA with 40 g CSA was added to 750-800 mL de-ionized water under rigorous stirring. Once the mixture undergoes complete dissolution, more amount of de-ionized water was added to make a solution of total 1000 mL volume in which preweighted amount of MPD and/or phenol was added finally. Both the amine and acid chloride solutions were filtered to ensure complete removal of any undissolved constituent.

### 3.2.3c. Rolling of a 2512 spiral module for FO process

The indigenously developed TFC-FO membrane sheets were rolled over a 2512 spiral module for performance evaluation. The number 2512 stands for the module having diameter of 2.5 inch with 12 inch length. The membranes were sliced and folded, followed by placing 45 mil (1.14 mm) diamond-type polypropylene spacers in between the membrane leaves. A perforated polyvinyl chloride (PVC) tube was used as central tube, centre of which was made blind by placing a block of PVC as depicted in Fig. 3.1c.

The spacer was then glued to the central tube and subsequently coupled with the shaft of winding motor. Two membranes leaves were rolled to comprise one such spiral module. The spacers were used in both interior and exterior of the membrane envelope to sustain the flow channels (Fig. 3.2c) and a tape was winded along the rolled membrane for sealing.
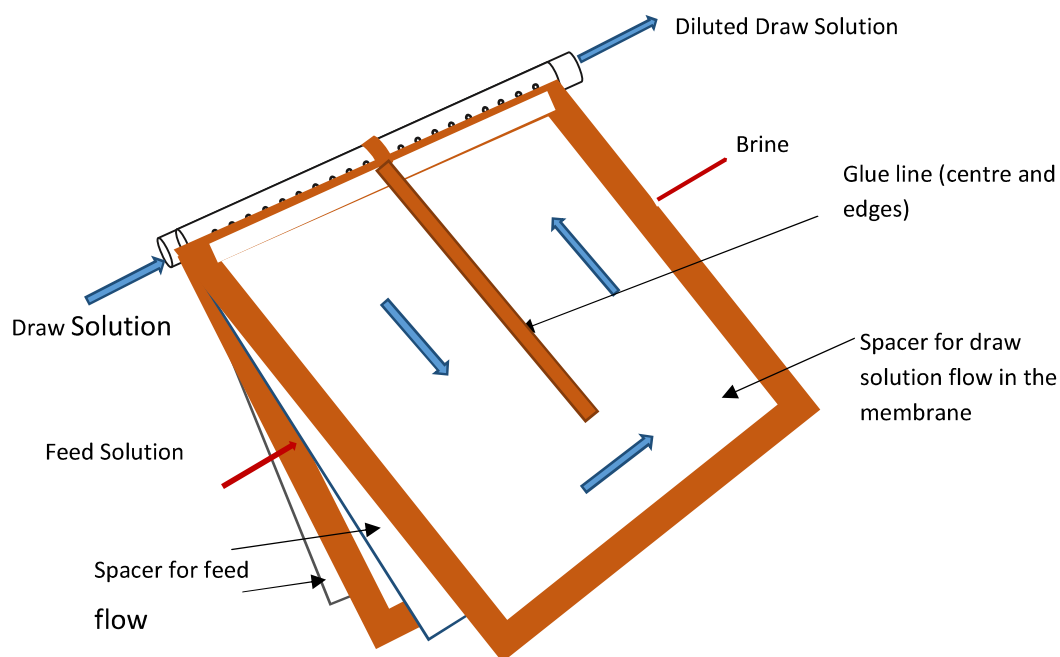
*Figure 3.1c: An illustration of FO module with two envelopes. Spacers were used both inside and outside of the membrane envelope.*
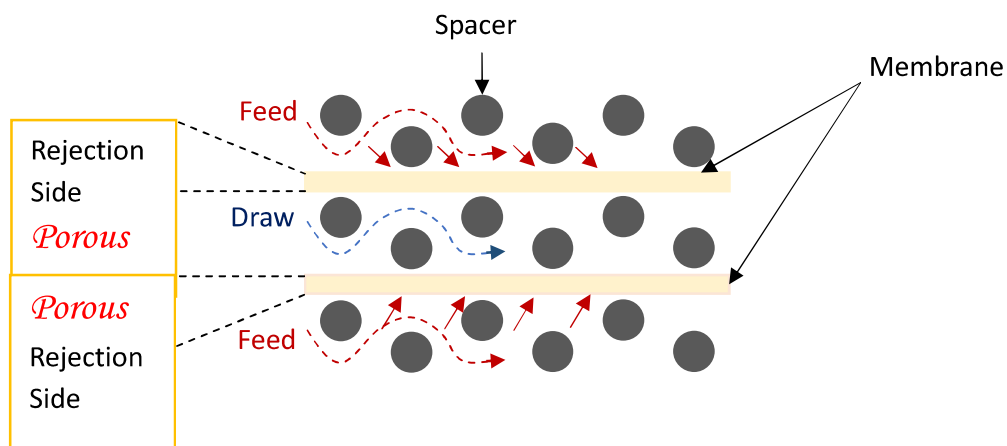


*Figure 3.2c: Cross-sectional view of the FO membrane envelope.*

Open edges of the membranes were trimmed at both sides before attaching the end caps in a final step. The effective membrane area of the standard element was around 0.4 m$^2$. The FO

module was encapsulated by a tubular vessel having four ports (different from the regular three-port vessels used for RO modules).

### 3.2.4c. Physicochemical characterization of membranes

Quantitative idea about the membrane hydrophilicity was obtained by measuring the pure water contact angle using a standard drop shape analysis system (DSA100, KRüSS GmbH, Germany). Static contact angle of the membranes were measured at each second over a total drop-residence time of 60 s in sessile drop mode by forming a drop of 0.6 μL volume onto each membrane surface. Averages of six such measurements along with the standard deviations are reported.

Surface average roughness of all the composite polyamide membranes were measured using an atomic force microscope, AFM (NT-MDT-Multimode 3, Ireland), equipped with standard silicon nitride cantilever at 0.3 Hz scanning frequency in semi contact tapping mode. A second order polynomial function was employed by the software (Nova P9) to remove the tilt generated over the scanned area (5 μm×5 μm).

The TFC polyamide membranes were also characterized in terms of their separation performances (water permeability and back diffusion of salt) in 2512 spiral module under standard FO conditions (de-ionized water as feed and 1.0 M NaCl solution as draw solution in absence of any external operating pressure). The testing set-up used for FO experiment is shown in Fig. 3.3c.

Coupons of approximate 20 $cm^2$ size, were cut from each membrane sheet and tested using two compartment FO test skid. Water permeability obtained as milli Liter/minute (mL/min.) were converted to $L.m^{-2}.h^{-1}$ (LMH) and reported. Back diffusion of NaCl from feed solution to draw solution side was calculated by measuring the solute concentration in either DI water side (feed) or diluted draw solution side at the commencement of experiment.

102
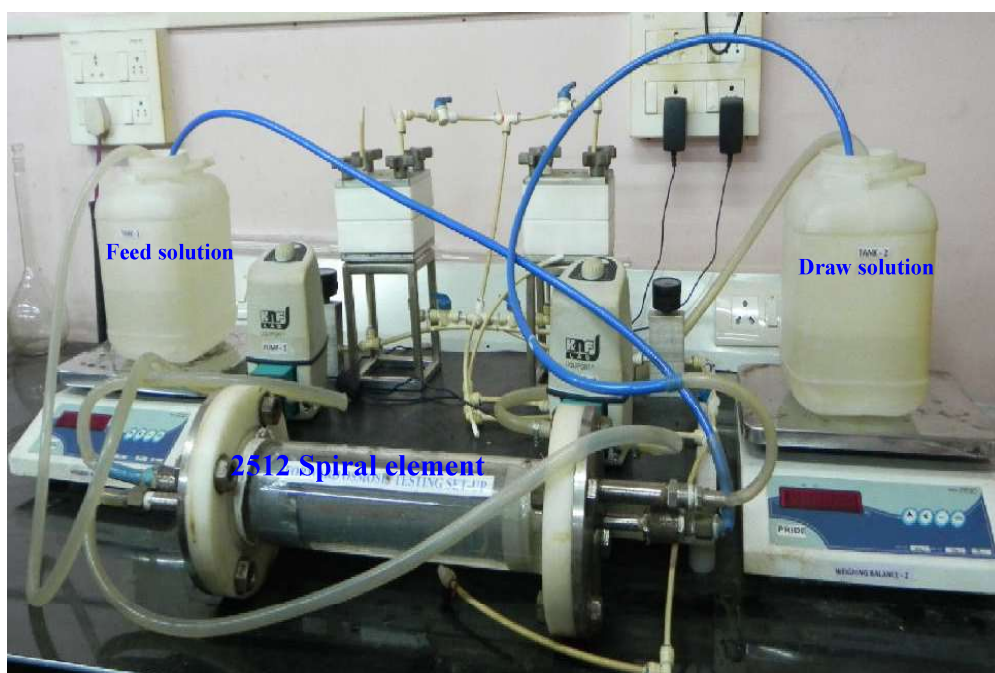
*Figure 3.3c: Experimental set-up used for testing of 2512 spiral FO membrane element.*

### 3.2.5c. Performance evaluation of TFC-FO membranes

Selective TFC-FO membranes were rolled in spiral modules in active layer facing feed side (AL-FS) configuration. The active layer of a membrane, also known as skin layer, is responsible for its separation behavior in terms of solute rejection. In AL-FS configuration, the draw solution is faced by the porous support layer of the membrane, i.e., the draw solution was allowed to flow inside the membrane envelope while feed solution was kept flowing across the outer layer of the membrane envelope. Performance of the TFC-FO membranes in spiral module was evaluated in terms of volume reduction and back-diffusion of draw solute and testing of the membranes were carried out with 500 ppm NaCl with 1ppm $SrCl_2$ & CsCl as feed. A range of concentration of $CaCl_2$ and $(NH_4)_2CO_3$ was used as the draw solution to study the effect of concentration as well as nature of draw solution.

103

Percentage volume reduction was determined by calculating the ratio of initial volume of the feed to the volume of the concentrate feed at the completion of experiment. Average VRF values for each set of experiments were evaluated for three membrane coupons prepared independently and reported along with their standard deviation values.

## 3.3c. Results and Discussions

### 3.3.1c Membrane surface characteristics and separation performance

To study the effect of incorporation of additives into the reactant monomer system on performances of MPD/TMC based TFC-FO membranes, a range of concentrations of phenol was added to amine solution with and without TEA/CSA. Performance of the membranes in terms of water permeability and % back diffusion of draw solute under standard FO condition is presented in Table 3.1c. It can be noted that addition of 6.6% of TEA/CSA salt into MPD solution increased the water permeability from 8.1 LMH to 11.0 LMH as compared to the control TFC membrane. No significant change in solute back diffusion was observed even after incorporation of TES/CSA additive. Both the membranes are showing only 0.70-0.72% diffusion of salt (i.e. ~99.3-99.28% rejection of salt) from higher concentration draw solution to lower concentration feed stream. Addition of TEA/CSA salt in amine solution thereby increased the membrane flux by 1.4 times without any change in rejection performances.

**Table 3.1c:  Effect of additives in amine solution onto composite polyamide membrane performances.**

| Membrane | Additives | FO performance | |
|----------|-----------|----------------|----------------|
| | | Water flux (LMH) | Back diffusion of NaCl (%) |
| TFC-1 | Nil | 8.10±0.8 | 0.70±0.06 |
| TFC-2 | TEA/CSA | 11.0±1.0 | 0.72±0.05 |
| TFC-3 | TEA/CSA + phenol (0.8%) | 14.7±1.1 | 0.75±0.06 |
| TFC-4 | TEA/CSA + phenol (1.2%) | 16.8±1.4 | 0.75±0.08 |
| TFC-5 | TEA/CSA + phenol (1.6%) | 20.1±2.1 | 1.54±0.11 |
| TFC-6 | TEA/CSA + phenol (2.0%) | 27.2±3.0 | 4.25±1.10 |

Addition of 0.8-2% phenol along with TEA/CSA salt into the amine solution further increased the water permeability of TFC membranes. An optimized performance of composite membranes was observed after addition of 0.8-1.6% phenol. Membranes of these composition showed about 53% enhancement in water permeability with equivalent salt rejection (~0.75% back diffusion of draw solute) as compared to the membranes prepared with addition of only TEA/CSA in MPD solution. Addition of phenol beyond 2% concentration made the polyamide film nonuniform resulting in greater flux of the composite membrane at the expense of higher salt back diffusion. At 2% concentration of phenol additive in presence of amine salt (TEA/CSA), phase separation started and the aqueous solution became turbid. Eventually an incomplete coverage of the PES support membrane at the time of polycondensation reaction took place and the membranes showed poor rejection value. Incorporation of phenol into the polycondensaion reaction system may alter the interfacial properties of PES/PA sublayer by changing their polarity and swelling characteristics. As the swelling of TFCPA membrane increases, distance between the molecular chains of both support as well as barrier layer increases and passage of water becomes more favorable. In addition to this, as the membrane surface becomes more polar due to presence of phenolic groups on the skin layer, interaction between water and

membrane surface becomes higher [67]. Both these factors could be the probable reason behind enhancement the water permeation through polyamide membrane in presence of phenolic additives.

All the membranes were instrumentally characterized in terms of their hydrophilicity and surface average roughness. Values of water contact angle (a measure of hydrophilic/hydrophobic character of membrane surface) along with their rms and average roughness of all six composite membranes are given in Table 3.2c.

**Table 3.2c: Contact angle and roughness value of composite polyamide membranes.**

| Membrane | Water contact angle (deg.) | RMS roughness (nm) | Average roughness (nm) |
|---|---|---|---|
| TFC-1 | 65.0±0.4 | 46.26±1.96 | 36.81±1.58 |
| TFC-2 | 63.3±1.0 | 51.85±2.14 | 40.90±1.19 |
| TFC-3 | 62.2±0.7 | 70.77±2.41 | 57.72±2.04 |
| TFC-4 | 60.5±0.8 | 85.69±3.37 | 66.87±2.71 |
| TFC-5 | 68.0±2.7 | 94.91±4.14 | 74.64±2.98 |

Contact angle values show the membranes became slightly more hydrophilic on insertion of additives into the aqueous amine solution. Addition of phenol upto 1.2% increased the membrane surface hydrophilicity as reflected by the gradual decrease in water contact angle values and the membranes showed higher water permeability without much compromise in rejection (Table 3.1c). Further increase in phenol concentration (1.6%) however, made the top layer of polyamide film non uniform and contact angle value increases abruptly.

Pictorial representation of 2D and 3D images of TFCPA membranes are given in Fig. 3.4c. Table 3.2c suggests that increase in phenol concentration in amine solution invariably increased the surface roughness of polyamide membranes. This increasing surface roughness also plays an important role for exerting more hydrophilic character by the membranes.

106
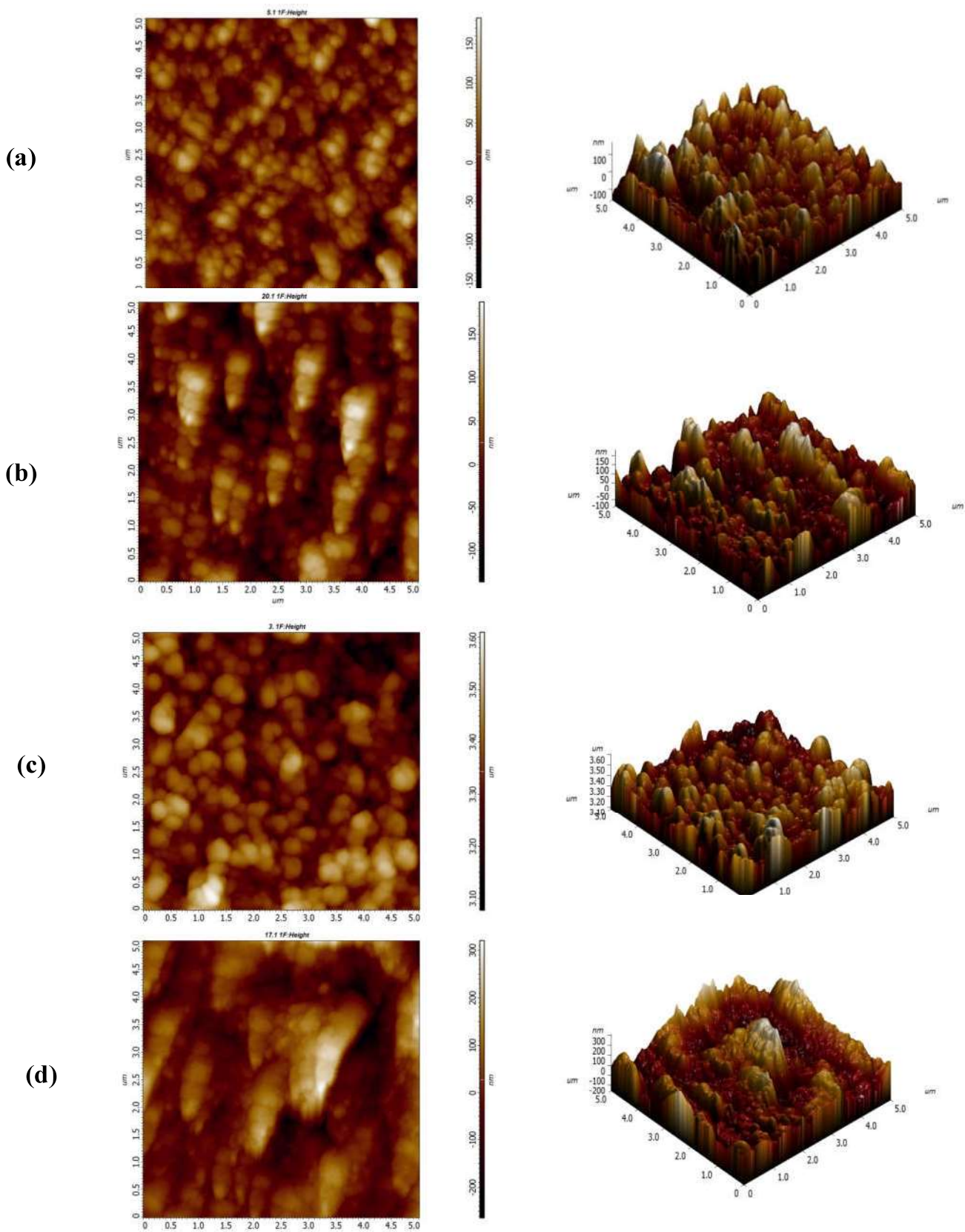
*Figure 3.4c: AFM images (2D & 3D) of (a) TFC-1, (b) TFC-2, (c) TFC-3 & (d) TFC-4 FO membranes.*

The optimized concentration of phenol was thereby found to be 1.2% (in presence of 6.6% TEA/CSA salt) where the TFC membranes (TFC-4) prepared had shown most hydrophilic character with highest performance enhancement in terms of water permeation at moderately low solute back diffusion. Hence, this membrane (TFC-4) was selected for rolling in 2512 spiral module for further studies.

### 3.3.2c. 2512 Spiral module performance (co-relation of pressure with flow rate)

In RO operations, feed pressure is a direct function of its concentration and the relation between product permeation rate and feed pressure plays an important role in process design and operation of RO module. In RO module, only one inlet for feed solution is there, whereas FO modules have two different inlets for flow of feed and draw solution across the membrane surfaces. During operation, as the solvent flows from feed to draw solution side, the feed gets concentrated and the draw solution gets diluted in a typical FO process. In FO spiral module inflow of feed was maintained within the space between the rolled membrane envelopes, facing the polyamide barrier layer while the draw solution flows through the central tube (inner side of the membrane pouches) facing the asymmetric support layer of composite membranes (Fig. 3.1c). This configuration of FO module is very much similar the reported ones in literature [208]. Solvent of the feed solution flowing across the outer layer of membrane pouches diffused into the draw solution present within the membrane envelope and made them dilute. Now, this diluted draw solution had to travel a long path to reach the central tube resulting pressure drop in permeate collection channel. It was thereby absolutely important to determine the effect of 2512 spiral FO module structure onto the flow resistance. Pressure drop in a spiral module (inlet pressure of both feed and draw solution) as a function of solution flow rate is plotted in Fig. 3.5c. The inlet pressure was measured suspending the flow on other side of the membrane. It can be noted from the graphical representation (Fig. 3.5c) that pressure drop increases linearly with increase in flow rate.
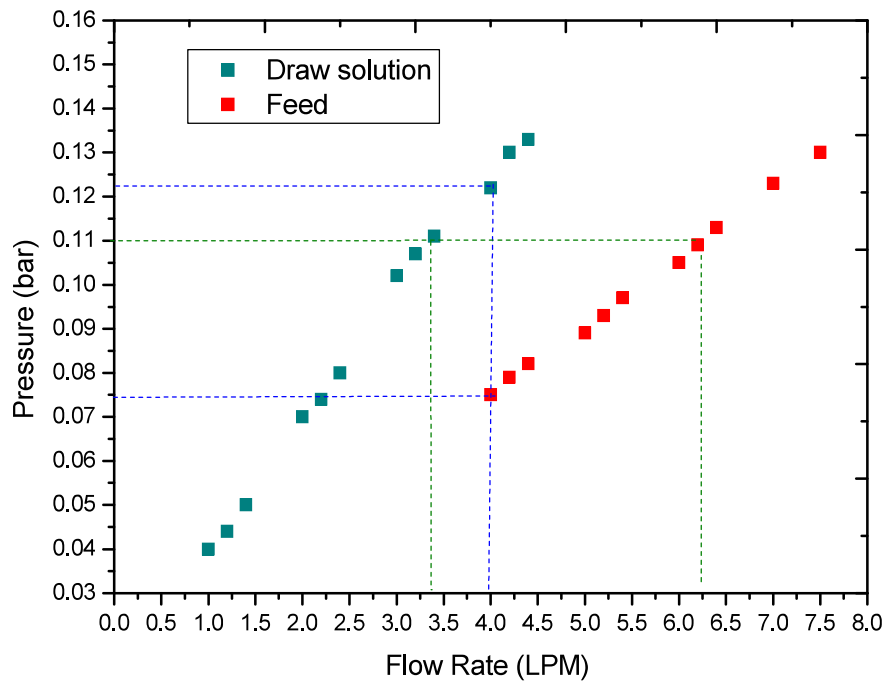
*Figure 3.5c: Flow rate effect on the pressure drop in the FO 2512 spiral module.*

An important point to be noticed is that pressure drop in the draw solution side is much higher than that in feed solution side at a particular flow rate. For example, when the flow rate maintained was 4 LPM, inlet pressure of draw solution and feed solution, as indicated by the blue line, were 0.122 and 0.075 bar respectively. The pressure drop of draw solution is more compare to feed solution because draw solution needs to travel longer path length through more constraint channels. In addition, the change in density and viscosity also contribute towards resultant pressure drop. The parameter to be controlled during operation of a spiral FO module is thereby the inlet pressure and not the solution flow rate. At a fixed inlet pressure, the flow rate of feed solution was found to be much higher than that of the draw solution. The green line in Fig. 3.5c shows that at 0.11bar inlet pressure, the flow rate of feed and draw solutions were 6.25 LPM and 3.3 LPM respectively.

Thus, decrease in flow rate and inlet pressure of the feed solution increased the flow rate of draw solution with decreasing its inlet pressure. A small volume of draw solution is preferred for actual application of FO process to minimize the energy required for recovery of draw

solutes and the flow rate of draw solution side was thereby kept in a lower value than that of the feed side. Accordingly, the inlet pressure on the feed side became higher than the same on the draw solution side. For further application of 2512 FO spiral module, the feed flow was kept constant at 4.5 LPM maintaining the draw solution flow at 1.5 LPM.

### 3.3.3c. 2512 Spiral module performance using different draw solution

Concentration of Sr & Cs bearing simulated radioactive effluent (500 ppm NaCl & 1 ppm $SrCl_2$ & CsCl each) was performed using TFC-4 membrane in 2512 spiral module. Aqueous solutions of two different draw solutes namely, $(NH_4)_2CO_3$ and $CaCl_2$ of 2 (M) concentration each, were used as draw solutions. Both ammonium carbonate $[(NH_4)_2CO_3]$ and calcium chloride $(CaCl_2)$ can deploy very high osmotic pressure because of their extremely high solubility in water as well as larger van't Hoff factor ($i$=3) value. Reports have been available [164] for $CaCl_2$ to be chosen as one of the most preferred draw solutes in FO application. $(NH_4)_2CO_3$, on the other hand, have the added advantage in terms of easy recovery of pure water from diluted draw solution by decomposing off the solute into ammonia and carbon dioxide by mild heating (65°C). Performances of TFC-4 membrane in 2512 spiral module using simulated radioactive solution as feed and two different draw solutions are given in Fig.3.6c.

It can be observed (Fig. 3.6c) that VRF value is slightly higher when $(NH_4)_2CO_3$ was used as draw solute as compared to membrane performances using $CaCl_2$ as draw solute, though the osmotic pressure of both the solutions are theoretically expected to be very close. Back diffusion of $(NH_4)_2CO_3$ was also relatively more than that of $CaCl_2$ might be due to the lower molecular weight and higher solubility of $(NH_4)_2CO_3$ (M. W.= 96.086 g/mol & solubility: 100 g/100 g water at 15°C) than $CaCl_2$ (M. W.= 110.978 g/mol & solubility: 74.5 g/100 g water at 20°C) [209]. Back diffusion of draw solute from higher concentration osmotic engine

110

to feed solution and leaching of Cs & Sr from feed to draw solution were estimated after 240 minutes of experimental run (Table 3.3c).
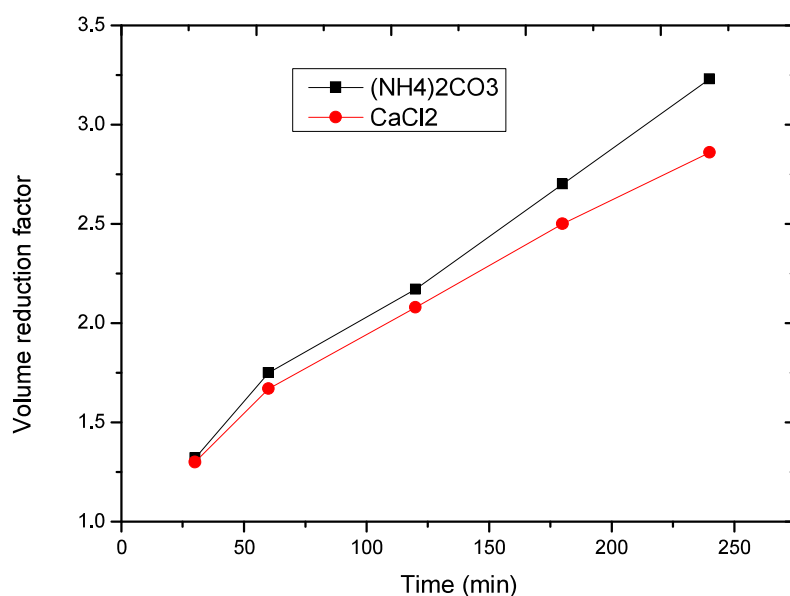


*Figure 3.6c: Volume reduction factor as a function of time for different draw solutions (TFC-4 membrane in 2512 spiral module).*

**Table 3.3c: Back diffusion of draw solutes from draw to feed and leaching of Cs & Sr from feed to draw solution side.**

| Draw solution | Leaching from feed (~1ppm) to draw solution | | Back-diffusion of draw solution (2 M) to feed |
|:---:|:---:|:---:|:---:|
| | Cs | Sr | |
| $CaCl_2$ | 0.021 ppm | 0.018 ppm | 2.6% (5770ppm) |
| $(NH_4)_2CO_3$ | 0.025 ppm | 0.021 ppm | 2.9% (5566ppm) |

111

Effect of concentration of draw solutions onto membrane performance was studied by using four different concentrations [1 (M), 2 (M), 3 (M) & 4 (M)] of $(NH_4)_2CO_3$ and $CaCl_2$ as draw solutions keeping all other parametric variables same. Volume reduction factors of TFC-4 membranes using the same feed (500 ppm NaCl with 1 ppm $SrCl_2$ & CsCl each) in 2512 spiral module configuration were evaluated as a function of draw solution concentration and graphically represented in Fig. 3.6c. VRF values reported were collected after accomplishment of FO testing over a period of 240 minutes. Fig. 3.6c shows that with increase in draw solution concentration, volume reduction factor increases for both the draw solutes irrespective of their chemical nature. The driving force of forward osmosis is osmotic pressure gradient between feed and draw solution. Following van't Hoff theory, osmotic pressure of a solution is directly proportional to molar concentration of the solution and as the draw solution concentration increases, driving force for solvent inflow increases accordingly and higher value of VRF was obtained. A very important point to be noted from Fig. 3.7c is that the VRF value is higher for $(NH_4)_2CO_3$ draw solution than $CaCl_2$ solutions of same concentration over the entire range of concentration.

However, the increase in percent volume reduction on changing the draw solution concentration from 2 (M) to 4 (M) was more in case of $CaCl_2$ draw solute than that of $(NH_4)_2CO_3$. Similar trend was reported in our previous work on concentration of simulated ammonium-diuranate filtered solution by forward osmosis using indigenously developed cellulosic osmosis membranes [210].
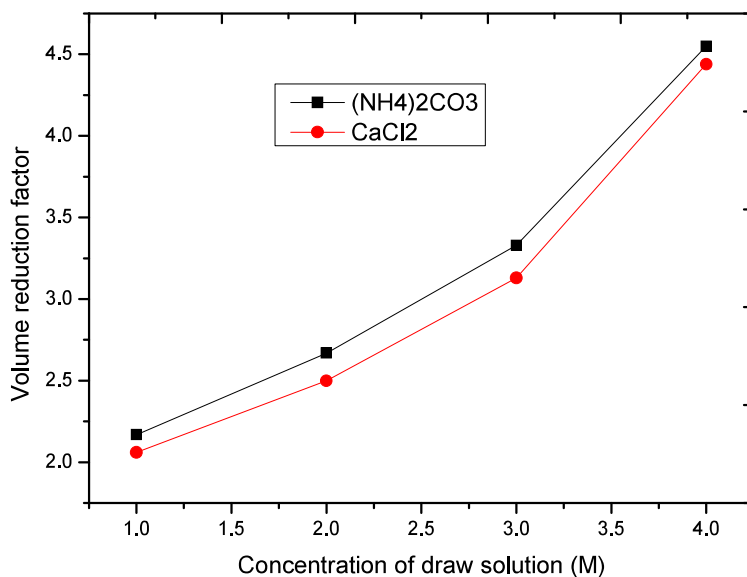
*Figure 3.7c: Percentage volume reduction as a function of concentration of two different draw solutions (TFC-4 membrane in 2512 spiral module).*

The observance is supported from the reports available in literature confirming the increase in osmotic co-efficients of aqueous $CaCl_2$ solutions is more for change in concentration from $3.0 - 4.0$ moles/Kg compared to the same in $2.0 - 3.0$ moles/ Kg range[207]. The increase in VRF was thereby presumably due to the greater increase of osmotic pressure in the concentration range of 3 (M) to 4 (M) for $CaCl_2$ draw solution.

## 3.4c. Conclusions

Thin film composite polyamide membranes suitable for FO applications were indigenously developed by optimising all the casting as well as coating parameters involved in in-situ polycondensation reaction between MPD and TMC over porous PES support membranes. A simple and lucid method for improvement of water permeability of these TFC-FO membranes has been illustrated in the present section of this chapter. Experimental data

collected by the analyst, showed that the additive phenol incorporated in amine solutions not only changed the physicochemical characteristics of membrane, but also capable of enhancing flux of the membranes with a very marginal change in salt rejecting property. Real time application of the TFCFO membranes in larger scale was demonstrated by rolling the optimised membrane in 2512 spiral module. Concentration of cesium and strontium bearing simulated radioactive effluent solution with high volume reduction and minute Cs/Sr leaching was reported with pre-optimised membranes. Judicial choice of draw solution depending upon their on-site availability and reusability is another important factor for its application in practical purpose. Increasing draw solution concentration invariably increased the volume reduction factor at the expense of contamination of feed by greater solute back-diffusion from draw to the feed solution. Thus, FO can be successfully used for treatment of low to medium level radioactive waste by concentrating the activity into a smaller volume and making the larger volume diluted draw solution suitable for direct disposal or reuse.

# CHAPTER 4

## PERFORMANCE ENHANCEMENT OF CELLULOSE TRIACETATE BASED FORWARD OSMOSIS MEMBARNES BY INCORPORATION OF NANOMATERIALS

## 4.1. Introduction

Real time implementation of existing polymeric membranes for water treatment is still restricted by several challenges including trade-off relationship between permeability and selectivity (also called Robeson upper boundary in membrane gas separation) and low resistance to fouling. Development of high performance FO membranes is thereby one of the priority research topics in the FO area. Hydrophilic cellulosic membranes being asymmetric in nature, their thickness cannot be controlled beyond a certain value. Additionally, structure of the pore is beyond the control of individual during preparation of membranes by various methods except in cases of highly expensive track etching method. These two factors make the structural parameter (S) of cellulosic membranes really very high. With intension to compensate the high value of S and tortuosity of the pores, nanoparticles can be incorporated to prepare surface modified nanocomposite membranes.

So objective of this study was to develop high performance CA based FO membranes by incorporation of porous silica nanoparticles and silver nanoparticles to the polymer matrix. Porous silica nanoparticles and silver nanoparticles were expected to provide extra channels for passage of water and lower the overall S value by decreasing tortuosity which can mitigate the effect of internal concentration polarization (ICP).

## 4.2. Experimental

### 4.2.1. Materials:

Cellulose triacetate (CTA) (Mn=72000-74000 Da) polymer was procured from Aldrich, India. Solvents like 1,4-Dioxan, acetone, and methanol of analytical grade were obtained locally and used without any further purification. Maleic acid (Lancaster synthesis) and sodium chloride of analytical grade were procured locally and used without purification. Mesoporous silica nanoparticles (200 nm with pores of 4 nm, specific area: 300-400 $m^2$/g)

117

and nonporous silver nanoparticles (<100 nm, specific area: 5 m$^2$/g) were procured from

Aldrich, India.

**4.2.2. Polymer dope solution preparation**

  Composition of four types of membranes, namely CTA-blank, CTA-silica, CTA-silica-Ag

and CTA-Ag are given in Table 4.1. In brief, the nature and extent of the nanoadditive, *i.e.*,

Silica and/or Ag nanoparticles were varied at the dope solutions comprising of 13 (w/w)% of

CTA and 4.8 (w/w)% of the porogen, maleic acid. Initially, the dispersed nanoparticles in the

solvent mixture comprising of acetone, dioxan and methanol, kept in hermetically sealed

glass bottles were undergone ultrasonic treatment for 15mins, prior to the addition and

subsequent mixing of moisture free CTA and maleic acid, maintaining the specified

compositions. The dope solutions were then kept under rigorous agitation for several hours to

accomplish complete dissolution of polymer in the solvent with homogeneously dispersed

nanoparticles. Once the viscous polymer solution is homogenized, methanol and maleic acid

were added to it and kept in mechanical shaker for 24hours.The resultant viscous dope

solutions were then kept overnight in an environmentally controlled atmosphere maintaining

the (25±3)$^o$C temperature and 35-40 % relative humidity to eliminate any trapped air bubbles

from the solutions.

**4.2.3. Preparation of nanocomposite CTA membranes**

CTA membranes with/without nanoparticles were prepared by solvent/nonsolvent exchange

commonly known as phase inversion technique. The viscous polymer solution was spread

over a nonwoven fabric support (Viledon grade H1006 obtained from M/S. Freudenberg

Nonwovens India Pvt. Ltd.), over a clean glass plate using knife edge under a steady casting

shear. It was then kept in air for 30 seconds for evaporation of volatile solvents like acetone

and methanol followed by immediate immersion of the entire assembly into a precipitation bath containing ultra-pure water as non-solvent, maintained at room temperature (22°-25° C) for solvent/ nonsolvent exchange for 40minutes to ensure complete precipitation of the polymer. To ensure the adequate exchange between solvent and non-solvent followed by complete removal of the pore-former and solvent from the membrane matrices, the resulting membranes were taken out of the water bath and rinsed in fresh water for several times. The gelled membranes were annealed subsequently at 90° C hot water bath for 15 minutes to get pore shrinked membranes suitable for FO applications.

**Table 4.1: Casting solution composition for preparation of cellulosic osmosis membranes.**

| Membrane | Composition of casting solution (% w/w) | | | | | | |
|---|---|---|---|---|---|---|---|
| | Polymer | Acetone | 1,4-Dioxane | Methanol | Maleic acid | Silica-nanoparticle | Ag-nanoparticle |
| CTA-blank | 13.03 | 19.72 | 58.88 | 3.56 | 4.81 | - | - |
| CTA-silica | 13.01 | 19.70 | 58.80 | 3.56 | 4.80 | 0.13 | - |
| CTA-silica-Ag | 12.99 | 19.67 | 58.73 | 3.56 | 4.80 | 0.13 | 0.13 |
| CTA-Ag | 13.01 | 19.70 | 58.80 | 3.56 | 4.80 | - | 0.13 |

Evaporation time: 30s, gelling medium: DI water at room temperature; Annealing: 90°C water for 15mins.

### 4.2.4. Physicochemical characterizations of nanocomposite CTA membranes

The surface morphology of the membranes with and without nanoparticles were analyzed by SEM (Model: (Model: CamScan3 200LV) images. For SEM imaging purposes, each membrane having an area of 1.0 $cm^2$ was coated with gold-palladium using sputter coater

under the optimized conditions of 100 s sputtering time and 30mA sputter current to mitigate the effect of charging by making them electrically conductive. All the micrographs were recorded employing identical acceleration voltage of 20 keV and 1000X magnifications when operated in secondary electron mode, for better comparison purpose.

Surface topographical analyses of the membrane (namely CTA-blank, CTA-silica, CTA-silica-Ag and CTA-Ag) skin surfaces were carried out by extracting quantitative information in the semi-contact mode by using an AFM instrument (Make: NT-MDT, Model: SOLVER next, Ireland). Small squares of approximate dimension of 1 $cm^2$ were cut from each membrane and subsequently glued onto a metal substrate by double sided tape. The rectangular cantilever NSG 10 (NT-MDT, Ireland) is made of piezoelectric $Si_3N_4$ with a spring constant of 11.8 N/m, having a typical resonance frequency of 240 kHz and a nominal tip apex radius of 10 nm with high aspect ratio. The scanning was done onto 5 μm × 5 μm area of each membrane under ambient atmosphere with a scanning frequency of 0.3 Hz. The tilt generated over the scanned area was removed by a second order polynomial using NOVA-P9 software. Acquisition of roughness profile gives the roughness parameters of the membranes which are quantitatively reported in terms of average roughness ($R_a$).

In order to get an idea about change in hydrophilicity of the membranes after addition of nanoparticles, static contact angle measurements at ambient temperature were conducted using sessile drop method. A contact angle measuring instrument (DSA 100 of KRUSS Gmbh, Germany) with DSA 1v1.92 software was employed to assess the hydrophilicity of the skin surface of the membranes, namely CTA-blank, CTA-silica, CTA-silica-Ag and CTA-Ag. The sessile drop was allowed to form in a very slow and steady manner on each of the membrane surface by depositing 0.6 μl of the probe-solvent (deionized water) with a microsyringe. The measurements at the membrane-solvent-air interface were completed by taking average value of contact angles measured in each second over a total residence time of

120

60 s. At least six such measurements maintaining same residence time and drop size were done at different locations of each membrane piece and the averaged out value of contact angle and their standard deviations are reported.

All the membranes were characterized in terms of their product permeation rate & salt rejection under standard brackish water RO testing condition (2000 ppm NaCl feed at 1551 kPa pressure).Product permeation rate of all the membranes with effective membrane area of 25.5 cm$^2$ were determined under cross-flow filtration mode at 1551 bar transmembrane pressure. The steady-state product permeability (L.m$^{-2}$.h$^{-1}$) was determined directly by measuring of the permeate flow, *i.e.*, volume (V in ml) collected over a time period (t in min), through a membrane area (A in cm$^2$) and converting it into L.m$^{-2}$.h$^{-1}$. Prior to all standard BWRO operations, membranes were initially subjected to undergo hydraulic compaction for 4 hours in water at 2585 kPa pressure in order to achieve stabilized performances.

Measurements of salt rejection behaviours of the membranes were carried out using 2000 ppm NaCl in DI water as feed. The test solution was prepared by dissolving prerequisite amount of NaCl in ultra-pure water. The solute rejection studies were carried out at a transmembrane pressure of 15 bar at room temperature. The concentrations of NaCl in both feed and product solutions were measured by measuring the specific conductance of the solutions (feed as well as permeate) and correlating the same with concentration of salt in aqueous media. Separation performance in terms of flux and salt rejection are reported after calculating the average of three readings taken for three different membrane coupons of each type, prepared independently.

### 4.2.5. Performance evaluation of nanocomposite CTA membranes

Volume reduction factor (VRF) is defined as the ratio of initial volume of feed to that at the end of the experiment. To determine VRF of the membranes, UF-filtered water was used as feed and draw solutions were prepared by dissolving pre-weighted amount of NaCl in ultrapure water at varying concentration [(0.5 (M), 1 (M) and 2 (M)]. VRFs were calculated by taking average of three readings taken for three different membranes of each type prepared independently. The effective area of FO membranes during experiment was 7.54 cm$^2$, temperature of feed and draw solution were maintained at 25±3° C. Back diffusion of salt from higher concentration draw solution to lower concentration feed was calculated by mass balance. All the experiments were done under no external pressure in AL-FS mode (active layer facing feed solution) in order to minimize the effect of concentration polarization. The feed was allowed to flow through one side of the membrane while the draw solution was kept flowing across the other side in order to further reduce the effect of concentration polarization.

## 4.3. Results and Discussions

### 4.3.1. Membrane surface characteristics and separation performance

The nanocomposite CTA membranes, fabricated by the familiar technique of non-solvent induced phase inversion process were characterized in terms of their water contact angle, surface average roughness and performance evaluation under standard BWRO condition. The results are given in Table 4.2 and Figure 4.1. Permeate flux and salt rejection data were collected when the recorded data became constant over 45minutes. As the porous silica nanoparticles provide some extra channels for permeation of water as well as salt, flux of CTA-Si membrane was increased at the expense of rejection as compared to the control membrane. CTA-silica-Ag nanocomposite membranes showed some intermediate result between control and CTA-silica nanocomposite membranes.

122

**Table 4.2: Membrane characterization and performance evaluation.**

| Membrane | Flux (lt m$^{-2}$ hr$^{-1}$) | Salt rejection (%) | Water contact angle($^\circ$) |
|---|---|---|---|
| CTA-blank | 14.1±0.23 | 93.6±1.10 | 47.0±2.31 |
| CTA-silica | 18.8±0.34 | 84.4±1.00 | 37.3±2.18 |
| CTA-silica-Ag | 17.2±0.57 | 89.1±0.50 | 44.4±1.71 |
| CTA-Ag | 21.1±0.33 | 93.2±1.00 | 46.7±1.49 |

A very interesting result was obtained from CTA-Ag nanocomposite membranes. No such trade-off between flux and rejection was noticed in this case and the membranes show highest water permeability without any compromise in rejection (over 93% rejection under standard BWRO condition).

Quantitative evaluation of the topographical features of membranes skin surfaces investigated through AFM, finds a distinctive trend in variation of the roughness parameter *i.e.*, average roughness ($R_a$). They vary significantly (~45% enhancement of surface average roughness value on addition of nanoparticles was observed) from a relatively smooth surface profile for the control CTA membranes to progressively rougher surfaces for the nanocomposite CTA membranes, i. e. with impregnation of silica and/or Ag nanoparticles. The result is reflected in the surface average roughness value for the membranes, namely CTA-blank, CTA-silica, CTA-silica-Ag and CTA-Ag which are found to be about 9.035 nm, 13.953 nm, 14.034 nm and 12.478 nm respectively. Surface images of the nanocomposite membranes (Fig. 4.2 & 4.3) confirm impregnation of nanoparticles onto the membrane surfaces without getting leached out in the course of membrane preparation. The images also reveal that the extent of uniform distribution over the membrane surface is more for smaller size Ag-nanoparticles than that of relatively bigger size silica nanoparticles.

Analysis of water contact angle values, presented in the same table (Table 4.2) and Fig. 4.1, derived for the membranes, *i.e.*, CTA-blank (47±0.1°), CTA-silica (37.3±0.4°) CTA-silica-Ag (44.4±0.2°) and CTA-Ag (46.7±0.2°) reveals that hydrophilic nature of the nanocomposite CTA membranes depends on the physicochemical nature of the nanoparticles. Addition of silica nanoparticles onto CTA membranes exhibits noticeable decline in contact angle values because of the inherently hydrophilic nature of silica nanoparticles owing to their chemical structure and makes the membranes more hydrophilic. Ag-nanoparticles, in spite of having weak affinity to polar medium, marginally reduces the water contact angle value of CTA-Ag membranes, probably due to their ability towards generation of hydrated $Ag^+$, when the probe-solvent (water) comes in contact with the Ag-nanoparticles residing at the skin surfaces of the membranes. However, the very small change in contact angle value after impregnation of Ag-nanoparticles as observed in our study for the membranes can be attributed to the effect of nanoparticles aggregation [211]. CTA-silica-Ag membrane shows some intermediate value of water contact angle. Hydrophilicity of the membranes thereby increases in the order CTA-blank < CTA-Ag < CTA-silica-Ag < CTA-silica. However, in spite of being less hydrophilic, CTA-Ag membranes showed highest product permeation rate which may be attributed to the increased porosity and/or changed pore morphology of the membranes caused by impregnated Ag-nanoparticles. Incorporated Ag-nanoparticles into CTA dope solutions were capable of varying the phase behaviors of the polymer dope solutions as well as the dynamics of indiffusion–outdiffusion mechanism of the nonsolvent–solvent system, during the occurrence of phase separation of the polymer [211].
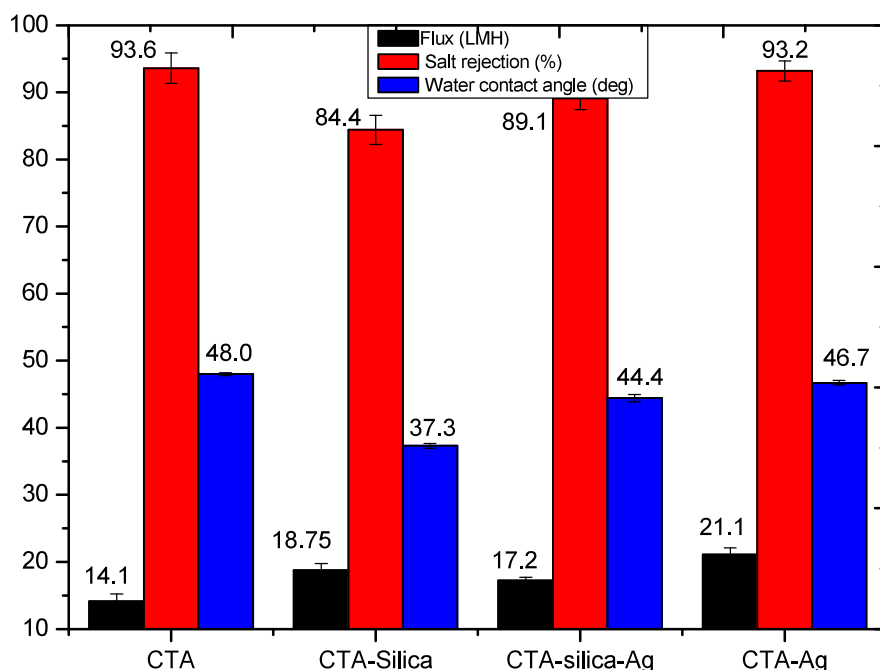
*Figure 4.1: Characterization and performance evaluation of CTA membranes (control and nanoconposite).*

It is an established fact that the formation of phase inversion membranes are regulated by thermodynamic as well as kinetic variations, resulting either instantaneous or delayed demixing during precipitation of the casting polymer solutions [212]. Thus, the presence of Ag-nanoparticles, seems to alter the thermodynamic instability and thereby changes the rate of instantaneous demixing of CTA with the non-solvent water [213-215] resulting in highest water permeability of the membrane with marginal compromise in rejection. CTA-silica membranes being most hydrophilic in nature, showed higher product permeation rate than blank CTA and CTA-silica-Ag nanocomposite membranes in RO mode. In addition to the effect of enhanced hydrophilicity of the overall membrane, porous silica nanoparticles provide some extra channels for passage of water as well as solute, thus flux enhancement

takes place at the cost of salt rejection and the trade-off between flux and rejection is maintained. SEM images show the surface morphology of the membranes. Nanoparticles embedded in the polymer matrix can be noticed in Fig. 4.2. However size of the nanoparticles present on membranes surface suggests that small agglomeration must be there.
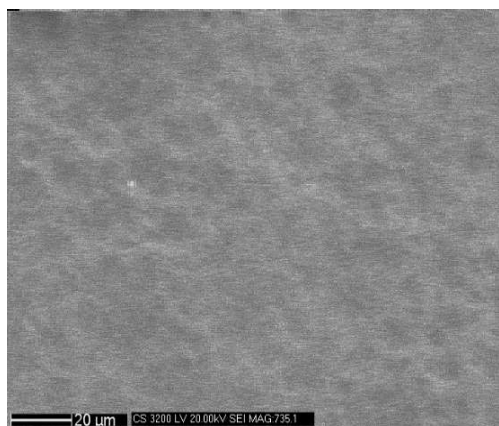


(a)
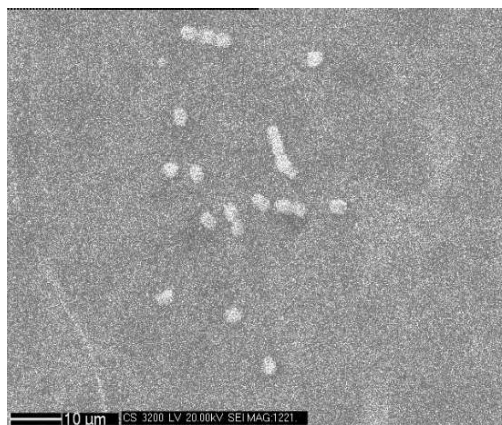


(b)
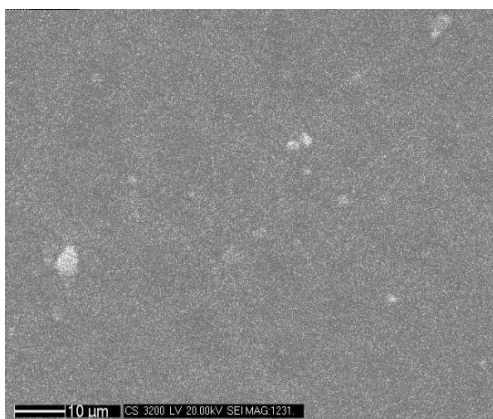


(c)
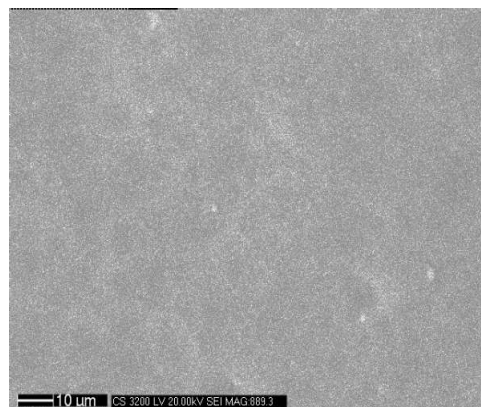


(d)

*Figure 4.2: SEM images of skin surface of (a) CTA-blank, (b) CTA-silica, (c) CTA- silica-Ag and (d) CTA-Ag nanocomposite membranes.*
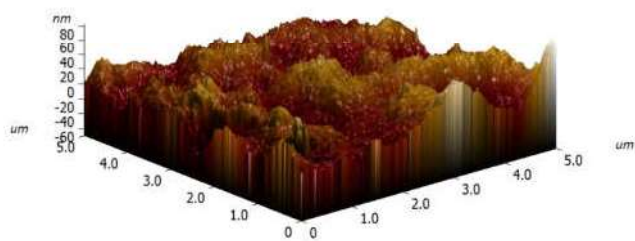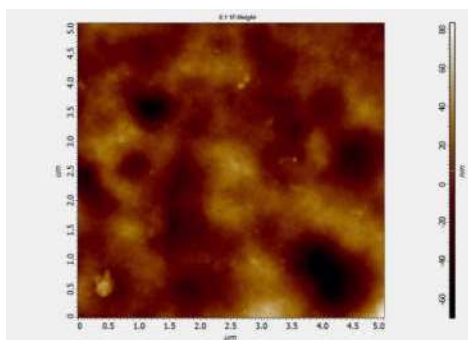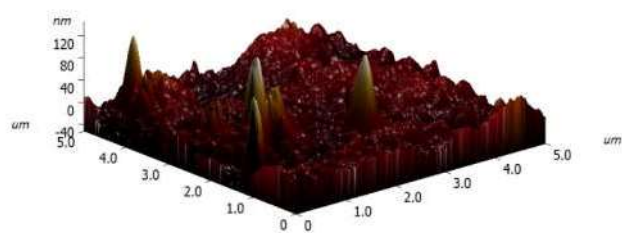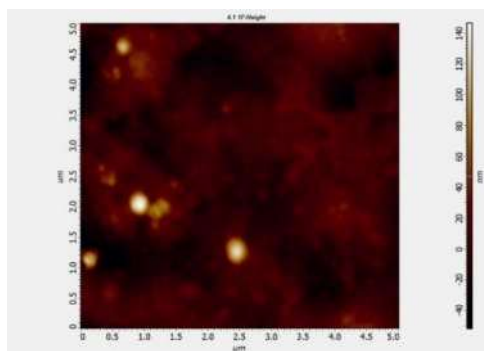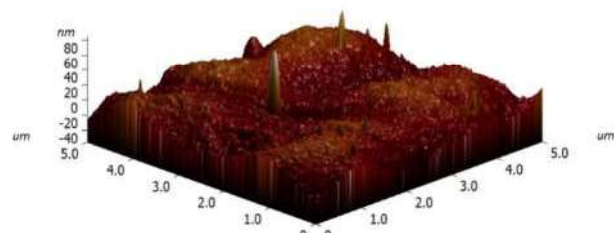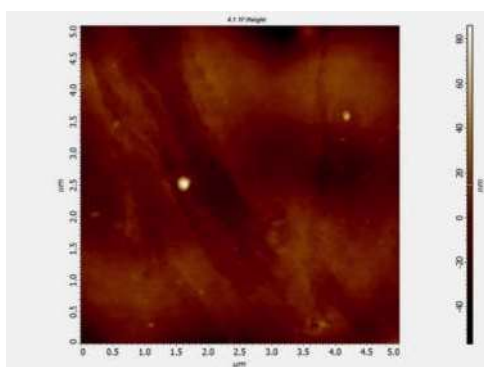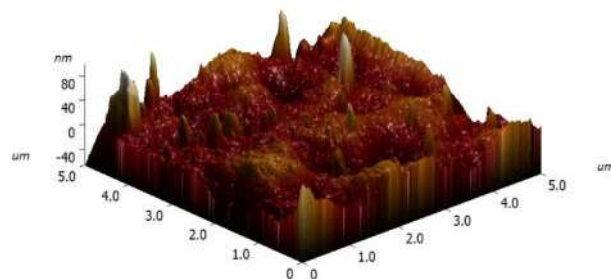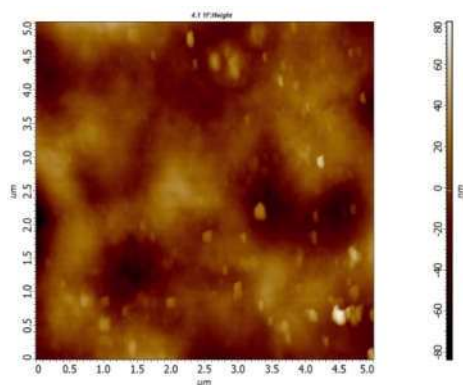
*Figure 4.3: AFM images of skin surface of (a) CTA-blank, (b) CTA-silica, (c) CTA-silica-Ag and (d) CTA-Ag nanocomposite membranes.*

### 4.3.2. Membrane performance in terms of VRF & salt back diffusion in forward osmosis

Volume reduction factor and salt back diffusion of all the membranes for 5 hours of experiment were determined by putting a circular piece of membrane of effective surface area 7.54 cm$^2$ in a two compartment cell using UF-filtered water as feed in one chamber and 0.5 (M) aqueous NaCl solution as draw solution in the other. The mean VRF and back diffusion values were determined by taking the average of three experiments carried out with three independently prepared membrane coupons of each type and the results are given in Table 4.3. All the experiments were carried out in AL-FS mode (active layer facing the feed solution) and the solutions were circulated across the membrane surfaces to minimize the effect of concentration polarization. Results show that the membranes with porous silica nanoparticles gave slightly higher VRF value than the other three membranes. Back diffusion of salt from higher concentration draw solution to lower concentration feed solution increases in the order blank-CTA = CTA-Ag < CTA-silica-Ag < CTA-silica. These results of volume reduction factor and reverse solute flux are in line with the results obtained from RO testing. Tighter CTA membranes show highest hindrance to salt back diffusion while loading of porous silica nanoparticles provide extra channels for passage of water as well as draw solute and increase the ease of leaching with a higher value of VRF.

CTA-Ag membranes have shown the highest value of VRF with only 0.45% back diffusion of draw solute. This result is in line with the observation in RO mode where CTA-Ag membrane shows highest water permeability with maximum salt rejection. However, leaching of salt in FO mode is found to be very less (<2%) for all the membranes. Percentage of salt back diffusion to the feed side is calculated from the difference between actual amount of salt found in the feed solution and the amount of salt supposed to be based on volume reduction assuming no salt is being diffused from feed side (containing pure UF water with

minimal salt concentration) to draw solution side. All the experiments were executed at ambient temperature (25±3° C) and humidity (40% RH) without any external operating pressure.

**Table 4.3: Volume Reduction Factor (VRF) and back diffusion of draw solute through membranes**

| Membrane | Volume reduction factor (VRF) | | | % back diffusion of salt | | |
|---|---|---|---|---|---|---|
| Conc. of NaCl in draw solution (M) | 0.5 | 1.0 | 2.0 | 0.5 | 1.0 | 2.0 |
| CTA | 1.111±0.010 | 1.111±0.030 | 1.220±0.029 | 0.45±0.012 | 0.45±0.013 | 0.77±0.023 |
| CTA-silica | 1.136±0.021 | 1.163±0.032 | 1.220±0.032 | 1.90±0.066 | 1.95±0.058 | 0.77±0.026 |
| CTA-silica-Ag | 1.136±0.033 | 1.136±0.027 | 1.220±0.033 | 1.38±0.048 | 1.32±0.039 | 1.35±0.038 |
| CTA-Ag | 1.230±0.041 | 1.250±0.037 | 1.279±0.028 | 0.46±0.016 | 0.48±0.012 | 0.78±0.020 |

Feed: UF filtered water; Draw solution: 0.5(M) NaCl solution; Membrane area: 7.54cm$^2$

### 4.3.3. Membrane performance as a function of concentration of draw solution

Volume reduction factors of the membranes using UF-filtered water as feed were determined for three different draw solution concentration [0.5 (M), 1 (M) and 2 (M) NaCl] under similar experimental condition as mentioned in section 4.3.2. and the experimental data for 5 hours run is plotted in Fig. 4.4. Forward osmosis being a concentration gradient driven process, takes place in absence of any external pressure and as the concentration of draw solution increases, osmotic pressure difference between the feed and draw solution increases, resulting in higher driving force for water flow to take place. This similar trend is observed

129

for all kinds of membranes. However, the effect is more prominent for blank-CTA membranes than for composite membranes.
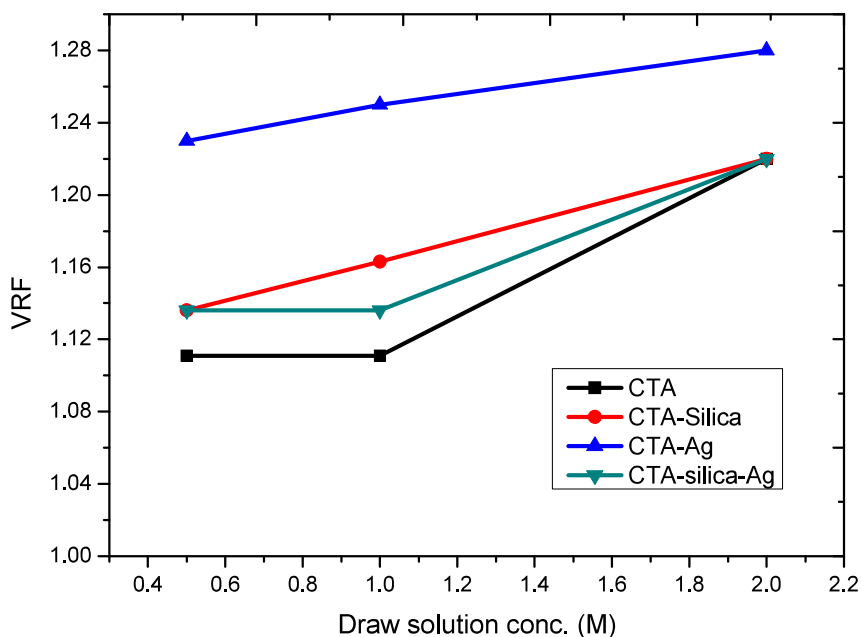


Feed: UF filtered water; Membrane area: $7.54 \text{cm}^2$

*Figure 4.4: Plot of change in volume reduction factor as a function of concentration of draw solutions.*

## 4.4. Conclusions

Composite cellulose triacetate membranes were prepared by incorporation of silica and/or silver nanoparticles with intention to increase the product permeability. Performance of the membrane in terms of volume reduction factor increased in the order CTA-blank < CTA-silica-Ag = CTA-silica < CTA-Ag with <2% salt back diffusion from draw solution side to feed side. Porous silica nanoparticles increase the VRF values at the expense of solute back diffusion by providing extra channels for passage of water as well as draw solutes. CTA-Ag

membranes showed highest water permeability with minimal salt passage both in RO as well as FO mode probably by modifying the solvent mixing-demixing during phase inversion, ensuring some change in core structure of asymmetric CTA membranes by addition of nonporous Ag-nanoparticles. Increase in draw solution concentration increases volume reduction factor but that may result in more back diffusion. The result is more prominent for control CTA membranes. Hence it can be concluded that incorporation of nanoparticles may lead to formation of membranes with enhanced water permeability from low flux asymmetric cellulosic membranes.

# CHAPTER 5

# DEVELOPMENT OF PERFORMANCE ENHANCED ALIPHATIC-AROMATIC BASED THIN FILM COMPOSITE POLYAMIDE MEMBRANES BY ADDITION OF INORGANIC METAL SALTS

# 5a. Performance Enhancement of Aliphatic-Aromatic Based Thin Film Composite Polyamide Membranes by Addition of Iron Salts

## 5.1a. Introduction

An important note about tailoring of membrane performances till date is the worldwide use of MPD and TMC for preparation of polyamide barrier layer of TFC membranes in almost all the cases. However, the problem associated with development of MPD-TMC based membrane is poor stability and limited reusability of monomeric amine. MPD undergoes chemical transformation under ambient condition with continuous change of color of the aqueous solution along with precipitation, resulting in decrease of concentration of the amine stock solution as a function of time. The aliphatic amine PEI, however, has no such handling difficulty and is capable of generating BWRO membranes with equally good salt rejecting properties [216-218]. In spite of these added advantages, very few attempts are reported till date for performance improvement of PEI based TFC-RO membranes because of their poor flux. It is thereby worth trying to develop high performance PEI-IPC based polyamide membranes with enhanced permeability without any compromise in rejection.

Metal ions like calcium, magnesium, copper, zinc etc. are known to form stable complexes with PEI by forming coordinate covalent bonds between tertiary amine groups [219-223] of PEI and metal ions. Incorporation of metal salts in aqueous PEI solution, therefore changes the ratio of free primary, secondary and tertiary amine groups of the polymeric amine and affects the formation of TFC polyamide membranes. Work has been reported explicating the enormous change in performance of TFCRO membranes by presence of inorganic salts like $CuSO_4$ and $FeCl_3$ in amine solution [218]. The present chapter elucidates the role of Fe comprising inorganic salts (in amine solution) as additives onto separation behavior and surface characteristics of PEI-IPC based composite reverse osmosis membranes.

## 5.2a. EXPERIMENTAL

### 5.2.1a. Materials

Polysulfone (PSf) beads were procured from M/s. Solvay Specialties India Pvt. Ltd., India. Reagent grade N-methyl pyrrolidone (NMP), used as solvent for preparation of polysulfone support membrane, was obtained from Sisco Research Laboratories, India. Polyethylene imines (PEI) of M.Wt. 2000 (PEI-2 KDa), M.Wt. 50,000-100000 (PEI-50 KDa), and M.Wt. 600000-1000000 (PEI-600 KDa) (all 50% aqueous solution) were purchased from M/s. Sigma-Aldrich Chemicals, M/s. BDH Reagents and M/s. Fluka A.G. respectively. 1, 3-benzene dicarbonyl chloride or isophthaloyl chloride (IPC) of Aldrich, India make were used. Ferrous sulfate ($FeSO_4.7H_2O$) was procured locally and used without further purification.

### 5.2.2a. Preparation of membranes

Thin film composite polyamide (TFCPA) membranes were prepared in two steps. In the first step polysulfone support membrane was prepared by phase inversion technique. A very thin layer of polyamide was then deposited onto the support membrane by in-situ poly condensation reaction in the second step.

### 5.2.2.1a. Preparation of integrally skinned polysulfone support membrane

20 g of PSf was taken in an airtight glass bottle with subsequent addition of 80 g of NMP as solvent for the polymer. The solution was kept under rigorous agitation for several hours till the polymer beads dissolve completely. A mild vacuum was applied for removal of trapped air bubbles from the polymer solution. The viscous polymer solution was subsequently spread over a nonwoven polyester spun bonded fabric (Viledon grade H1006 obtained from M/s. Freudenberg Nonwovens India Pvt. Ltd.) using a knife edge to maintain uniform thickness. Typical size of the membranes prepared was 15 cm × 10 cm. The whole assembly

136

was immersed, immediately after casting, into a gelling bath containing demineralised water at ambient temperature where the solvent- nonsolvent exchange took place and the polymer was deposited to form integrally skinned polysulfone support membrane. These polysulfone support membranes were checked meticulously for any damages including pinholes and good areas were selected for preparation of composite membranes in the second step.

**5.2.2.2a. Preparation of thin film composite polyamide (TFCPA) membranes by *in-situ* polycondensation reaction**

A submicron layer of polyamide barrier layer was formed over the polysulfone (PSf) support membrane in the second step involving in-situ polycondensation reaction. The reaction takes place between an amine (PEI, in the present case) and an acid derivation (IPC, in this case) at the interface of two immiscible solvents, water and hexane. Water from the surface of wet PSf support membranes was removed by keeping them vertically in air for a while. Reactant solutions were prepared by dissolving pre-requisite amount of PEI and IPC in water and n-hexane respectively. Pre-weighted amount of iron salts were added to the amine solution after complete dissolution of PEI. PSf membranes, after complete removal of surface water were immersed into 2.0% (w/v) aqueous solution of PEI with/without iron sulfate for 120 seconds. Excess amine solution from surface of the membranes was wiped out by squeezing them with soft rubber roller. The amine saturated membranes were submerged into 0.25% (w/v) hexane solution of IPC for 60 seconds where the poly condensation reaction takes place. A very thin layer of polyamide film was formed over the support membrane and the composite polyamide membrane was obtained. The membranes were heat cured under infra-red (IR) lamp for 10 minutes or till the surface looks moisture free. The membranes were stored in desiccators till further use.

### 5.2.3a. Physicochemical characterization of TFCPA membranes

Surface morphology of the membranes (with and without $FeSO_4$) were analyzed by extracting their topographical information using a standard AFM instrument (Make: NT-MDT, Model: SOLVER next, Ireland) in semi contact tapping mode. Small pieces of approximate dimension of $1cm^2$ were cut from each membrane and glued onto a metal substrate by double sided tape. The scanning was done over 10 μm × 10 μm and 5 μm × 5 μm area of each membrane using rectangular cantilever NSG10 (NT-MDT, Ireland) at ambient temperature at 0.3 Hz scanning frequency. The tilt generated due to manual operation of the sample was removed from the scanned area employing a second order polynomial using NOVA-P9 software. Quantitative estimation of surface roughness of different membranes were completed by acquisition of roughness profile and is reported in terms of surface average roughness value ($R_a$).

Effect of addition of iron salts onto surface hydrophilicity of the membranes were determined by measuring their static contact angle value at ambient temperature by employing sessile drop method using a standard contact angle goniometer (DSA 100 of KRUSS Gmbh, Germany) with DSA 1v 1.92 software. A drop of water of 0.6 μl volume was allowed to form very slowly and steadily onto each membrane surface by depositing the probe-solvent with a microsyringe. Contact angle at the membrane-solvent-air surface was measured at each second over a total residence time of 60 seconds and the average value was taken. Mean value of six such operations at six different places of each membrane is calculated and reported with their standard deviations.

### 5.2.4a. Performance evaluation of TFCPA membranes

Performance of composite polyamide membranes were evaluated in terms of water permeability and percentage (%) rejection of salt in a tangential flow type test cell under standard BWRO (Brackish Water Reverse Osmosis) operating condition, i. e. 225 psig (1551 kPa) pressure using 2000 ppm NaCl solution as feed. All the membranes were subjected to hydraulic compaction at 2585 psig pressure to get stabilized data prior to their performance evaluation experiment. A reciprocating pump was used to pump the feed water across a given specimen. The schematic details of the experimental set up and the test cell can be referred to our previous paper [224]. Flux was calculated by taking the average of three readings taken at a regular time interval. Water permeability values obtained as milli Liter /minute (mL/min.) were converted into $L \, m^{-2} \, h^{-1}$ (LMH) and reported. The solute separation data were computed by measuring the specific conductance of feed as well as permeate solutions and converting them to their corresponding concentration values. Similar set of experiments were executed using 2000 ppm $MgSO_4$ solution as feed to determine rejection profile of membranes with a bi-bivalent salt as solute. At least three experiments were run using three membrane coupons prepared independently and the average value is reported.

### 5.3a. Results & Discussions

The amine reactant of the present aliphatic-aromatic based system, PEI, has all three type of amine groups viz. primary, secondary and tertiary in 1:2:1 ratio and it is well established that reactivity of amine groups with acid chloride group increases from secondary to primary and no reaction takes place at all with tertiary amine groups. In contrary, complexation with metal ions is preferred by tertiary amine groups over primary and secondary and these groups are blocked first when some inorganic metal salts are added to the amine solution by forming stable PEI-metal ion complexes. Thus the ratio of amine groups changes upon metal ion

incorporation into PEI solution. The actual photographs of the PEI blank solution, aqueous solution of $Fe^{2+}$ salt and PEI-$Fe^{2+}$ salt solution in small container are shown (Fig. 5.1a).
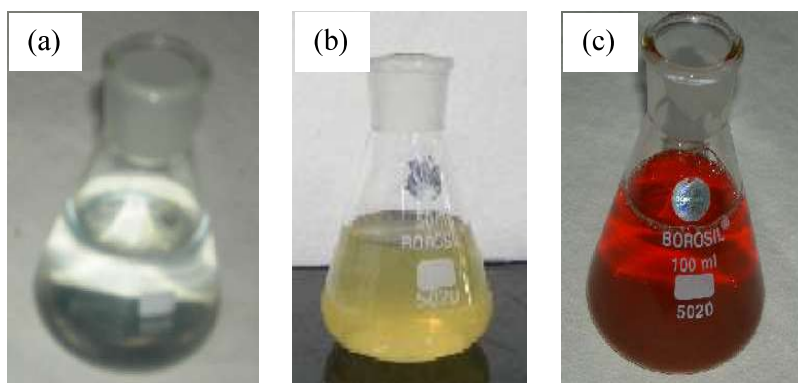


*Figure 5.1a: Pictures of the (a) PEI blank solution, (b) aqueous solution of $Fe^{2+}$ salt and (c) PEI-$Fe^{2+}$ salt solution.*

The abrupt change in color of PEI solution upon addition of a trace amount of [0.8 m(M)] $FeSO_4$ confirms the complexation between PEI and $Fe^{2+}$ and it is thereby the iron complexed PEI which takes part in interfacial polycondensation reaction rather than the PEI itself. The schematic representation of polycondensation reaction between PEI and IPC is given in Fig. 5.2a.
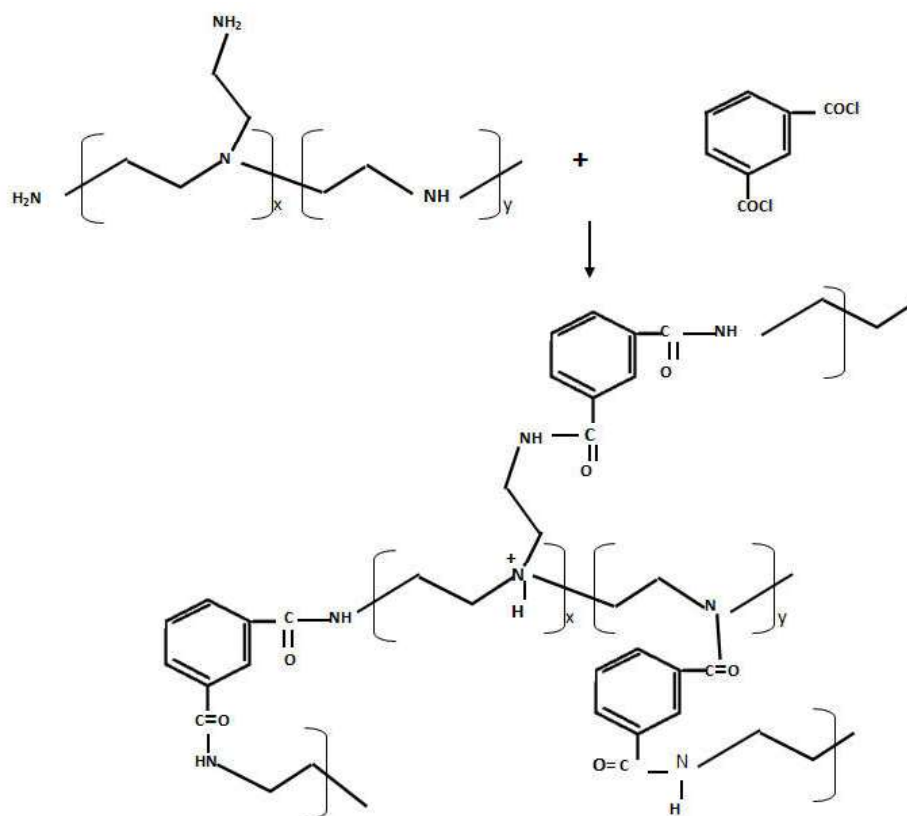
*Figure 5.2a: Reaction schemes of polyamide thin film formation from PEI/IPC system.*

## 5.3.1a. Effect of concentration of $Fe^{2+}$ (as $FeSO_4$) in amine solution on membrane surface characteristics and separation performances

Composite polyamide membranes were prepared from PEI/IPC based system using PEI-50 KDa solution without and with $FeSO_4$ of concentration ranging from 0.10 g/L to 0.78 g/L. Performance of the membranes in terms of pure water permeability and rejection of sodium chloride (NaCl) and magnesium sulfate ($MgSO_4$) along with their physico-chemical characteristics in terms of water contact angle (as a measure of hydrophilic/hydrophobic nature of the membrane surface) and surface average roughness are given in Table 5.1a. 2-D AFM images of control PEI/IPC membranes and the membranes prepared using PEI with two different concentrations of $FeSO_4$ are shown in Fig. 5.3a.

**Table 5.1a: Separation performances and surface physico-chemical characteristics of TFC membranes prepared using different concentration of $FeSO_4$ with PEI-60KDa solution.**

| $FeSO_4$ conc. (g/Litre) | Membrane performance | | | Water contact angle (deg.) | Surface average roughness (nm) |
|---|---|---|---|---|---|
| | PWP ($L.m^{-2}.h^{-1}$) | NaCl Rej. (%) | $MgSO_4$ Rej. (%) | | |
| 0 | 21.1±1.09 | 85.5±0.6 | 90.5±0.2 | 53.0±0.43 | 5.79±0.97 |
| 0.10 [0.36 m(M)] | 29.2±1.18 | 86.0±0.6 | 91.0±0.3 | 52.4±0.76 | 8.98±0.84 |
| 0.22 [0.8 m(M)] | 32.8±1.40 | 89.5±0.5 | 97.0±0.3 | 50.0±0.64 | 10.28±0.69 |
| 0.50 [1.8 m(M)] | 30.2±1.21 | 89.7±0.4 | 97.0±0.4 | 52.0±0.66 | 13.12±1.01 |
| 0.78 [2.8 m(M)] | 28.1±1.32 | 90.0±0.5 | 97.2±0.2 | 53.5±0.74 | 14.02±0.99 |

It is evident from Table 5.1a that addition of iron salts enhances membrane performances in terms of both pure water permeability (PWP) and solute rejection with increase in membrane surface roughness at all concentrations of $FeSO_4$. But there is an optimum concentration [0.22 g/L or 0.8 m(M)] of $FeSO_4$ beyond which the PWP value of composite polyamide membrane decreases with further addition of iron salt. Decrement of water permeability by 4.7 LMH in the range of iron salt concentration 0.22 − 0.78 g/L is associated with marginal increase in NaCl rejection (0.5%). The change in ratio of primary, secondary and tertiary amine groups of PEI due to complexation with $Fe^{2+}$ may be one of the reasons for performance enhancement of composite polyamide membranes.

The interfacial poly-condensation reaction between amine and acid chloride is a self-limiting reaction. Once a thin polyamide film is formed at the interface (generated at the surface of PSf support membrane) of two immiscible solutions, i.e the aqueous solution of amine (residing inside the pores of the support membrane) and organic solution of acid chloride (available in bulk), the amine needs to diffuse through the initially formed polyamide thin layer to react further with acid chloride. Hence, any changes in diffusivity of amine from aqueous to organic medium can influence the rate of the poly-condenstation reaction which in turn has adverse effect on physico-chemical properties of polyamide film. It is a well-known fact that faster reaction gives rougher film as compared to the same formed in a slower reaction [225]. Being a polymeric amine, diffusivity of PEI is normally slow because of its bigger globule size, but as the hydrodynamic volume of PEI is known to decrease with increase in ionic strength of the solution [226], its diffusion becomes faster and the rate of poly condensation reaction increases. Presence of iron salts in amine solution thereby makes the diffusion rate of PEI from aqueous to organic medium faster by increasing the ionic strength of the amine solution and hence rougher surface is formed in composite membrane. The same may be analytically confirmed from AFM images (Fig. 5.3a) and roughness data of the membranes (Table 5.1a). 2D AFM images of the membranes (Fig. 5.3a) also indicate the increase in surface inhomogeneity with addition of iron salts. No significant change in surface hydrophilicity ( as indicated by only 2-3° change in water contact angle of PEI-FeSO$_4$ membranes as compared to control) of the membrane is observed due to addition of metal salts.
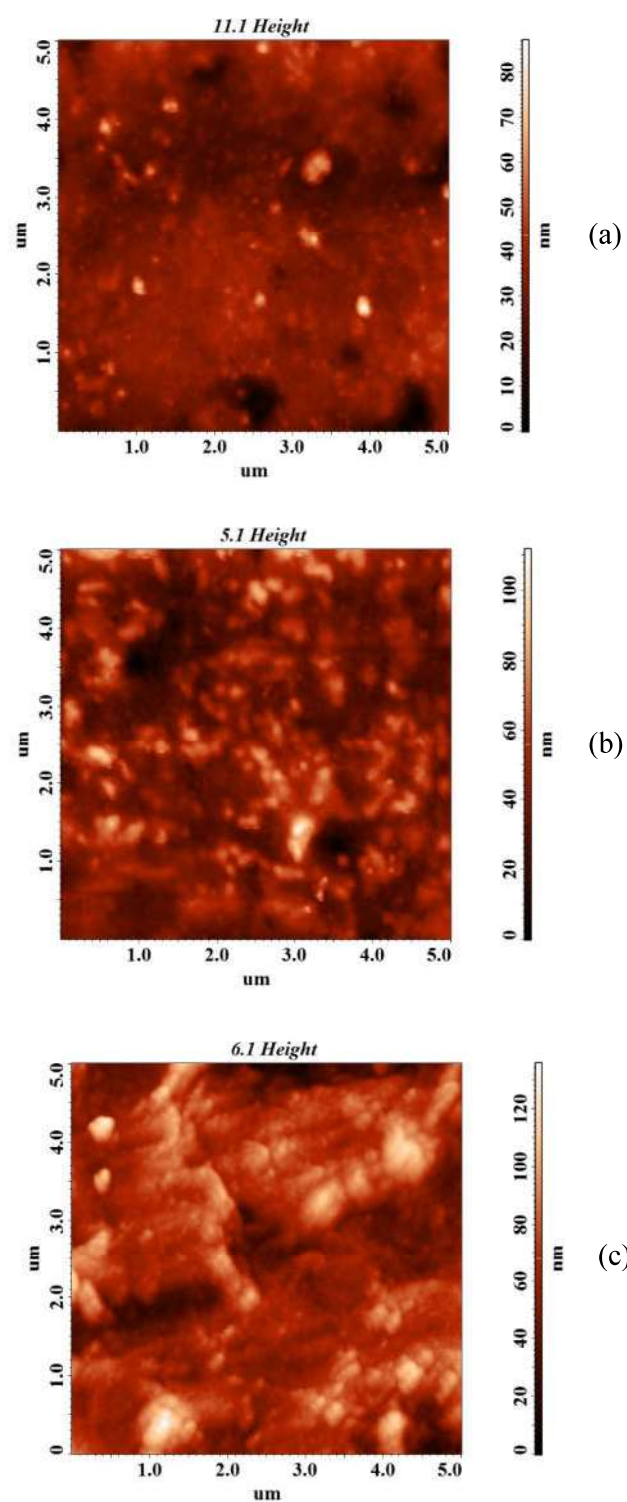
*Figure 5.3a: 2-D AFM images of composite membranes prepared using (a)only PEI, (b)PEI + 0.22 g/L FeSO$_4$ and (c) PEI + 0.78 g/L FeSO$_4$.*

## 5.3.2a. Effect of molecular weight of PEI with addition of iron salt on composite polyamide membrane performances

Three different molecular weights of PEI namely, 2 KDa, 50 KDa and 600 KDa are used to elucidate the effect of molecular weight of PEI onto membrane performance and hydrophilicity on addition of optimized concentration of $FeSO_4$ (0.22 g/L). Performances of composite polyamide membranes, prepared using different molecular weight PEI with and without $FeSO_4$, in terms of water permeability and rejection of sodium chloride (NaCl) and magnesium sulfate ($MgSO_4$) along with their water contact angle value are tabulated in Table 5.2a. It can be seen that the PWP is higher for both low molecular weight PEI (PEI-2 KDa) as well as high molecular weight PEI (PEI-600 KDa) than 50 KDa molecular weight PEI. The performances of thin film composite membranes are actually controlled by compactness and thickness of the thin barrier layer of the membranes. For PEI-2 KDa, the reaction is expected to be faster than higher molecular weight PEI's because of the smaller size of lower molecular weight PEI globules which eventually end up with formation of relatively looser polyamide film. The less compact structure of overall polyamide film is the reason behind higher PWP value of TFCPA membranes at the expense of lower solute rejection. In case of higher molecular weight PEI (PEI-600 KDa), once a thin layer of polyamide film is formed at the interface, it becomes difficult for the PEI-600 KDa globules to penetrate through it for further reaction with acid chloride unless very high reaction time is provided. Hence a thinner polyamide film is formed in this case which gives rise to higher water permeability of the resultant TFC-PA membranes. The compact structure of thin PA layer with high molecular weight restricts the passage of salt when operated under standard BWRO condition, hence higher solute rejection is observed. For intermediate molecular of PEI (PEI-50 KDa), the thickness of polyamide film could be relatively thicker than that formed using higher or lower

molecular weight PEIs, resulting in lower value of PWP as compared to PEI-2 KDa and PEI-600 KDa.

**Table 5.2a: Separation performances and surface physico-chemical characteristics of TFC membranes prepared using PEI of different molecular weight without and with 0.22 g/L FeSO$_4$.**

| Amine solution | Membrane performance | | | Water contact angle (°) |
|---|---|---|---|---|
| | PWP (L.m$^{-2}$.h$^{-1}$) | NaCl Rej. (%) | MgSO$_4$Rej (%) | |
| PEI-2Kda | 28.1±1.59 | 84.0±0.7 | 92.5±0.3 | 49.4±0.61 |
| PEI-2KDa + FeSO$_4$ | 31.2±1.28 | 88.2±0.5 | 98.2±0.4 | 49.0±0.79 |
| PEI-50Kda | 21.1±1.09 | 85.5±0.6 | 90.5±0.2 | 53.0±0.43 |
| PEI-50KDa + FeSO$_4$ | 32.8±1.40 | 89.5±0.5 | 97.0±0.4 | 50.0±0.64 |
| PEI-600Kda | 24.6±1.04 | 88.1±0.5 | 95.6±0.3 | 63.0±0.53 |
| PEI-600KDa + FeSO$_4$ | 25.1±1.10 | 91.2±0.3 | 98.0±0.4 | 61.2±0.73 |

As the rate of poly condensation reaction is expected to be higher with low molecular weight PEI, the polyamide surface becomes rougher. This enhanced roughness of PA barrier layer may be attributed to the higher hydrophilicity of PEI-2 KDa membrane (lower water contact angle value, Table 5.2a) and the effect is reflected in higher difference in separation of NaCl and MgSO$_4$ for PEI-2 KDa based membranes than PEI-50 KDa and PEI-600KDa membranes. Performance enhancement of all the membranes is observed upon addition of ferrous salt irrespective of the molecular weight of amine reactant. It can be seen that (Table 5.2a) the performance enhancement is maximum for PEI-50 KDa based membranes which could again be due to the optimum alteration of ratio of primary, secondary and tertiary amine groups of

146

PEI during complexation and increase in diffusion rate of the amine in presence of salt from aqueous to organic medium.

**5.3.3a. Effect of time of reaction on composite polyamide membrane performances using PEI with and without addition of FeSO$_4$**

The time of polycondensation reaction of in-situ polymerisation reaction is defined as the residence time of amine saturated PSf support membrane within the organic media. Thus, the effect of addition of iron salts on reaction time in terms of membrane performances and surface morphology can be studied by varying this residence time. The membranes selected for this study were prepared using PEI-600 KDa with and without optimized concentration of FeSO$_4$ (0.22 g/L). Performances of TFCPA membranes in terms of water permeability and solute rejection [sodium chloride (NaCl) and magnesium sulfate (MgSO$_4$)] along with their surface average roughness values are given in Table 5.3a.

It can be noted that with increase in reaction time from 15 seconds to 60 seconds, PWP decreases with increase in salt rejection. The same may be expected from conceptual understanding of thin film formation mechanism. For any TFC based membranes some minimum time of reaction is required for formation of thin polyamide layer over the support membrane and the idea of this optimum reaction time for a particular system can be established by checking their solute separation data. Membranes prepared with only PEI (in absence of inorganic additive) reach their highest performance value in terms of separation data for 60 seconds reaction time (checked with 75 seconds also, not mentioned here) whereas the same is around 30 seconds in presence of FeSO$_4$.

**Table 5.3a: Separation performance and surface average roughness characteristics of TFC membranes as a function of time of reaction (with and without $Fe^{2+}$ in PEI solution).**

| Reaction time (s) | Amine solution | Membrane performance | | | Surface average roughness (nm) |
|---|---|---|---|---|---|
| | | PWP (L.m$^{-2}$.h$^{-1}$) | NaCl Rej. (%) | MgSO$_4$Rej. (%) | |
| 15 | PEI | 28.1±1.18 | 73.1±0.6 | 78.5±0.6 | 9.65±2.16 |
| | PEI + Fe$^{2+}$ | 32.8±1.35 | 84.0±0.7 | 91.6±0.6 | 10.84±1.55 |
| 30 | PEI | 27.2±1.45 | 80.3±0.6 | 86.9±0.4 | 10.64±2.10 |
| | PEI + Fe$^{2+}$ | 28.0±1.46 | 89.0±0.6 | 93.0±0.5 | 16.70±2.09 |
| 60 | PEI | 24.6±1.04 | 88.1±0.5 | 95.6±0.4 | 13.50±1.25 |
| | PEI + Fe$^{2+}$ | 25.1±1.10 | 91.2±0.3 | 98.0±0.4 | 16.66±2.04 |

In presence of FeSO4, the hydrodynamic radius of PEI globules become smaller due to complexation and hence their diffusion through the nascent polyamide film becomes more feasible and the self-limiting polycondensation reaction reaches saturation over a smaller time of reaction. 2-D phase images of TFC-PA membranes prepared using PEI and PEI-FeSO$_4$ for 15 seconds of reaction time are shown in Fig. 5.4a.

Because of the faster reaction, the inhomogeneity and surface roughness of the membranes are higher for membranes prepared using PEI-FeSO$_4$compared to the control membranes (Table 5.3a and Fig. 5.4a). AFM images are shown for composite membranes prepared with 15 seconds reaction time, only to show the difference in surface features prior to completion of polycondensation reaction.
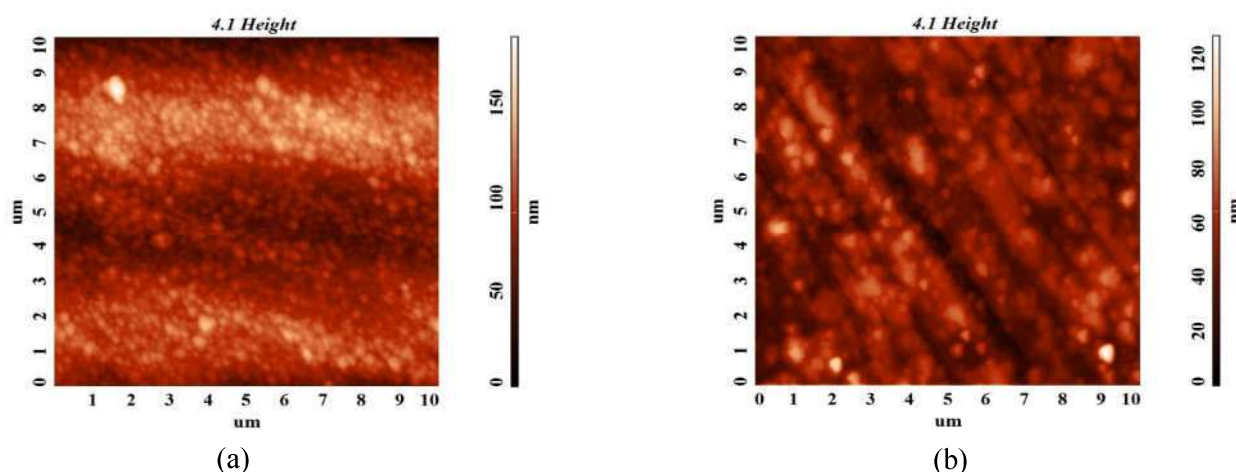
*Figure 5.4a: 2-D AFM images of composite polyamide membranes prepared using (a) only PEI, (b)PEI + 0.22 g/L FeSO₄ (reaction time of 15 seconds).*

## 5.4a. Conclusions

Addition of iron salt with amine reactant has significant impact on performance and physico-chemical characteristics of thin film composite polyamide reverse osmosis (RO) membranes prepared by polycondensation reaction between polyethylene imine and isophthaloyl chloride. Membranes prepared with PEI containing optimized concentration of $FeSO_4$ [0.8m(M)] shows around 56% increase in water permeability with 4% enhancement in salt rejection as compared to the control under standard BWRO condition. Membranes prepared using iron salt incorporated amine solutions were found to be marginally hydrophilic with higher surface roughness and showed performance enhancement in terms of water permeability with slight increment in solute rejection as compared to the control membranes. Performance enhancement was observed for all the TFC-PA membranes irrespective of the molecular weight of polyethylene imine up to a certain optimum concentration of iron salt. Highest enhancement was witnessed for membranes prepared with intermediate molecular weight (50 kDa) PEI. Reaction time required for completion of polycondensation reaction was found to be less when iron salts were added to the amine solution under identical preparation condition.

# 5b. Performance Enhancement of Aliphatic-Aromatic Based Thin Film Composite Polyamide Membranes by Addition of Transition and Non-transition Metal Salts

## 5.1b. Introduction

Motivated by the development of performance enhanced PEI/IPC based TFCRO membranes by incorporation of Fe-salts, as discussed in the earlier section of the same chapter, and keeping in mind that PEI forms very stable complexes with numerous metal ions like copper, nickel, zinc, cobalt, lead, chromium, mercury etc. [221-223], urge had been developed to study the effect of addition of transition as well as nontransition metal salts over a range of concentration onto membrane performances. Complexation of PEI with metal salts decreases the hydrodynamic radius of the polymeric amine molecules and changes the kinetics of polycondensation reaction between amine and acid chloride. Hence, two number of metal suphates from each category, namely copper sulfate & nickel sulfate (transition metal salts) and magnesium sulfate & aluminium sulfate (non-transition metal salts) were chosen for incorporation into the aqueous phase to study the effect of additives on surface characteristics and separation performance of PEI/IPC based thin film composite osmotic membranes.

## 5.2b. Experimental

### 5.2.1b. Materials

Polysulfone (PSf) in beads of weight average molecular weight 67000-72000 Da with polydispersity: 3.5 were purchased from M/s. Solvay Specialities India Pvt. Ltd., India. Reagent grade N-methyl pyrrolidone (NMP) used as solvent for preparation of polysulfone support membranes was obtained from M/s. Sisco Research Laboratories, India. Polyethylene

imines (PEI) of M.Wt. 50,000-100000 (PEI-50 KDa), M.Wt. 2000 (PEI-2 KDa) and M.Wt. 600000-1000000 (PEI-600 KDa) (all 50% aqueous solution) were procured from M/s. BDH Reagents and Chemicals, Poole, UK, M/s. Sigma-Aldrich Chemicals and M/s. Fluka A.G. respectively. 1, 3- benzene dicarbonyl chloride or isophthaloyl chloride (IPC) was acquired from M/s. Aldrich. Metal salts like copper sulfate ($CuSO_4.5H_2O$), nickel sulfate ($NiSO_4.7H_2O$), magnesium sulfate ($MgSO_4.7H_2O$) and aluminium sulfate [$Al_2(SO_4)_3.16H_2O$] were purchased locally and used without further purification.

## 5.2.2b. Membrane preparation

TFCPA membranes with and without metal salts [of a range of concentration from 0.4 m(M) to 2.8 m(M)] were prepared by in-situ polycondensation reaction involving two steps. In the first step asymmetric polysulfone membrane was prepared by phase inversion technique on which a very thin polyamide film was deposited by in-situ polymerisation reaction in the second step. Details of this two-step membrane preparation process are explained elaborately in 5.2.2a section of the same chapter. Re-optimization of the parametric variables was executed to enhance the membrane performances in terms of the permselectivity of control PA membranes.

## 5.2.3b. Physicochemical characterization of composite osmosis membranes

A standard double beam spectrophotometer (Spectroscan UV-2600, Chemito, India) was employed to record the UV/Vis spectra of blank PEI, PEI-$CuSO_4$ & PEI-$NiSO_4$ (0.8 mM concentration of salt in 1.6% aqueous solution of 50 KDa-PEI) solutions after baseline correction using EDI water at ambient temperature in air.

SEM of the optimized TFCPA membranes were recorded by using a standard instrument (Make: ZEISS, Model: GeminiSEM 450, Germany). For imaging purposes, each membrane

having an area of 1.0 cm$^2$ was coated gold-palladium using sputter coater under 15mA sputter current for 100 s in order to minimize the effect of charging of nonconducting polymeric membranes. All the micrographs were recorded employing identical acceleration voltage of 5 keV and 250000X magnifications when operated in secondary electron mode, for better comparison.

Energy dispersive X-ray spectra of selected TFCPA membranes were recorded by employing a standard EDS system (Make: Oxford Instruments, Model: X-Max, UK) coupled with SEM. Water contact angle (as a measure of hydrophilicity) and surface average roughness of all the membranes were measured by employing a standard drop shape analyzer (DSA100 of KRüSS GmbH, Germany) and an atomic force microscope, AFM (Make: NT-MDT, Model: SOLVERNEXT, Ireland) respectively following the same procedure as explained in 5.2.3a.

Dynamic Light scattering (DLS) measurements were performed to monitor the change in PEI globule size after addition of inorganic metal salts. Autosizer 4800 (Make: Malvern Instruments, UK) with Malvern 7132 digital correlator was used for this purpose. He-Ne laser of 632.8 nm wavelength with a power output of 15 mW was used as the optical source. Measurements were made at 90$^\circ$scattering angle and samples were placed in a cylindrical quartz cell of 25 mm diameter inside a peltier controlled water bath.

All the instrumental techniques for physicochemical characterization of membranes and solutions were carried out in an environmentally controlled system maintaining temperature at 25±3° C and ~40% RH.


## 5.2.4b. Performance evaluation of composite polyamide membranes under standard BWRO and FO condition

Performances of thin film composite polyamide membranes were evaluated in terms of their product permeability and percentage (%) rejection of salt in a cross flow test cell under

standard BWRO condition (as elaborated in section 5.2.4a.). Flux values were obtained as volumetric flow rate (ml/min) of permeate from the test cells and are reported in terms LMH. All the membranes are subjected to hydraulic compaction under 2585 kPa pressure prior to their operation under standard BWRO condition. Performance evaluation in terms of salt rejection (S. R.) of all the membranes are determined following the relation % S.R = [(1 − $C_p/C_f$) ×100] where $C_f$ and $C_p$ stands for the salt concentrations in feed and permeate solutions respectively. $C_f$ and $C_p$ are calculated by measuring the specific conductance of feed and permeate samples using a standard laboratory conductivity meter and converting them into their corresponding concentration following a calibration plot of specific conductance of pure salt solutions with precisely known concentrations.

The performance of indigenously developed membranes is also evaluated under standard FO condition using a lab-scale FO test skid. In the two compartment FO cell, DI water is used as the feed solution and 0.5 (M) aqueous solution of NaCl is used as the draw solution. Both the solutions are circulated using two variable speed pumps to minimize the effect of concentration polarization maintain the pressure at 1 bar throughout the course of experiment. Volume reduction factor (VRF= $V^i_{feed}$/ $V^f_{feed}$, where $V^i_{feed}$ and $V^f_{feed}$ stands for the initial volume of feed and final volume of the same at the end of experiment) and back-diffusion of the salt from higher concentration draw solution side to lower concentration feed water is measured after 300 minutes of experiment.


## 5.3b. Results and Discussions

Polyethylenimine (PEI) is a polymeric amine consisting of all three types of amine groups. The ratio of primary, secondary and tertiary amine groups in PEI is typically 1:2:1. A PEI molecule of average molecular weight ($M_W$) 60000 contains around 350 primary amines, 700 secondary amines and 350 tertiary amines and its complexing sites are present in both main

153

chain as well as side chains [227]. On addition of metal salts, the ratio of primary, secondary and tertiary amine group changes due to complexation and the kinetics of polycondensation reaction between amine and acid chloride can thereby be affected. So, the effect of concentrations of different metal ions, effect of molecular weight of the reactant polymeric amine and the role of change of anion keeping the metal cation fixed on the physicochemical characteristics and separation behavior of TFC RO membrane were studied.

## 5.3.1b. Complexation of PEI with metal ions

PEI is known to form moderately stable complexes with various transition metal ions like copper, nickel, zinc, cobalt, lead, chromium, mercury etc. [223, 226, 227]. In the present work, sulfate salts of $Cu^{2+}$, $Ni^{2+}$ $Mg^{2+}$ and $Al^{3+}$ionswere taken to ensure no additional change in thin polyamide film formation caused by the presence of different anions in amine solution. Fig. 5.1b shows the actual colors of PEI solution before and after addition of 0.8 m(M) (millimolar) $CuSO_4$ and $NiSO_4$ individually. PEI solutions remain colorless even after addition of nontransition metal salts like $MgSO_4$ and $Al_2(SO_4)_3$ and hence are not shown in the picture. The intense coloration of PEI solution after addition of$CuSO_4$ and $NiSO_4$ gave some idea about complexation between the amine and incorporated metal salts. The same was confirmed by recording UV-visible spectroscopy of the solutions (Fig. 5.2b). It can be noted that presence of no chromophoric unit in the control PEI solution makes the solution colorless and shows no absorption maxima over the entire range of spectrum (390-1100 nm).

PEI-blank            PEI- Cu            PEI- Ni
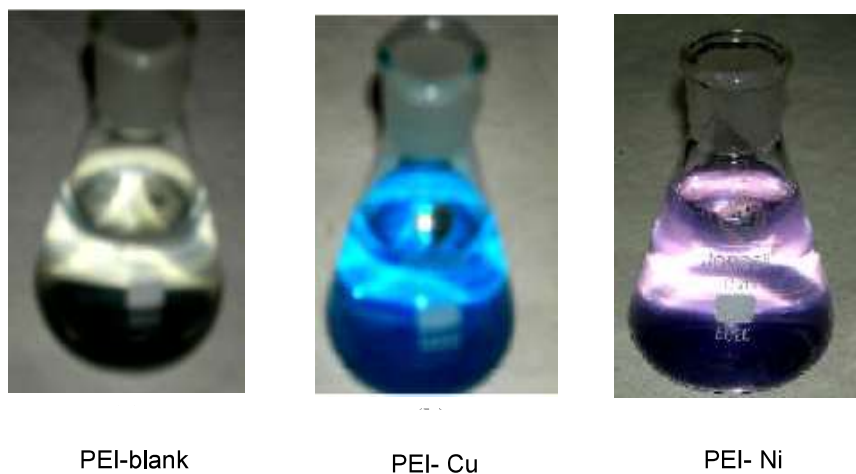
*Figure 5.1b: Photographs of aqueous amine solutions [(a) 1.6% PEI, (b) 1.6% PEI + 0.8 milimolar NiSO$_4$ and (c) 1.6% PEI + 0.8 milimolar CuSO$_4$] used for TFC-PA membrane preparation.*
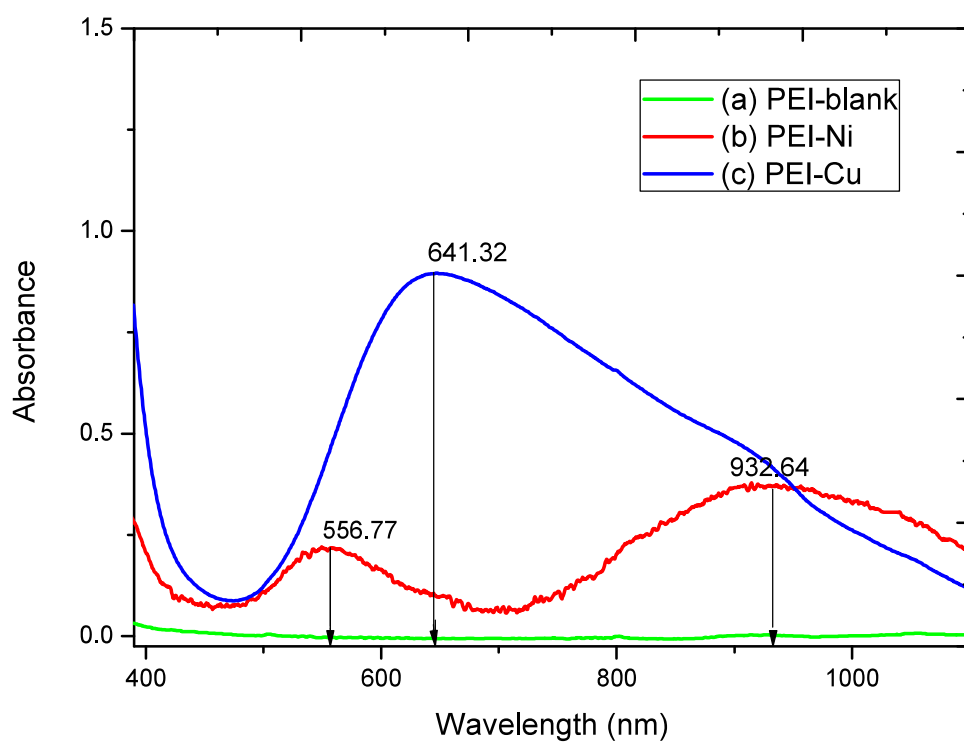


*Figure 5.2b: UV/Visible spectrum of aqueous solutions of (a) 1.6% PEI, (b) 1.6% PEI + 0.8 m(M) NiSO$_4$ and (c) 1.6% PEI + 0.8 m(M) CuSO$_4$.*

155

Upon addition of metal salts like $CuSO_4$ or $NiSO_4$, ligand to metal charge transfer complexes (typically known as LMCT complexes) were formed by formation of co-ordinate covalent bonds owing to donation of electrons from electron rich N-atoms of amine (acting as the ligand) to the vacant d-orbitals of the metal ions and highly colored solutions were generated. Hence absorption maxima (at 641.32 nm for PEI-$CuSO_4$ and at 556.77 nm & 932.64 nm for PEI-$NiSO_4$) recorded in UV-vis spectrophotometer are thus indicative of typical LMCT complex formation between the polymer and the metal salts.

## 5.3.2b. Effect of concentration of different metal ions (as metal sulfate) in amine solution on composite polyamide membrane performances

Composite polyamide membranes were prepared from PEI/IPC based system using 1.6% aqueous solution of PEI with average molecular weight 50 kDa with and without metal salts like $CuSO_4$, $NiSO_4$, $MgSO_4$ and $Al_2(SO_4)_3$. A range of concentration of each metal salts were added to the amine solution and the performance of composite membranes were evaluated (Table 5.1b & Fig. 5.3b) to find the optimum concentration of a particular metal salt at which the resultant TFC-PA membranes show highest permselectivity.

At optimum concentration, highest performance of the TFCPA in terms of water permeability and salt rejection were achieved. Table 5.2b presents the separation performances of TFC-PA membranes at optimum concentration of each metal ion along with the control membrane performances in reverse osmosis (RO) as well as forward osmosis (FO) mode. The performance of the TFC membranes made with MPD/TMC system (with composition used for preparation of commercial TFC membranes) is also included in the same table. . It can be noted that PEI/IPC based TFC membrane has lower water flux than the MPD/TMC based membrane as expected. However, some of the TFC membranes prepared using PEI/IPC system with addition of metal salt in amine solution has comparable or even better separation

performance. All the membranes optimized after incorporation of each metal sulfates were also characterized in terms of their hydrophilicity (by measuring water contact angle) and surface average roughness and the results are illustrated in Fig. 5.4b.

AFM and SEM images of control and optimized metal salt incorporated membranes are depicted in Fig. 5.5b and Fig. 5.6b respectively.

**Table 5.1b: Effect of concentration of different metal ions in amine solution on composite polyamide membrane performances.**

| Conc. of metal ion (mM) | $Cu^{2+}$ | | $Ni^{2+}$ | | $Mg^{2+}$ | | $Al^{3+}$ | |
|---|---|---|---|---|---|---|---|---|
| | Product permeability (LMH) | NaCl rejection (%) | Product permeability (LMH) | NaCl rejection (%) | Product permeability (LMH) | NaCl rejection (%) | Product permeability (LMH) | NaCl rejection (%) |
| 0.0 | 44.1±1.16 | 95.5±0.4 | 44.1±1.16 | 95.5±0.4 | 44.1±1.16 | 95.5±0.4 | 44.1±1.16 | 95.5±0.4 |
| 0.4 | 44.2±1.28 | 86.4±0.3 | 47.6±1.76 | 94.4±0.5 | 46.2±1.52 | 92.4±0.4 | 49.2±1.28 | 93.0±0.2 |
| 0.8 | 44.2±1.76 | 94.0±0.4 | 48.6±1.52 | 96.0±0.3 | 49±1.28 | 92.0±0.3 | 53.6±1.52 | 92.0±0.2 |
| 1.2 | 60.4±1.16 | 83.0±0.2 | 58.4±1.28 | 90.5±0.3 | 53.6±1.58 | 94.4±0.3 | 48.9±2.00 | 94.8±0.4 |
| 2.0 | 64.4±2.00 | 79.6±0.2 | 67.4±1.28 | 82.4±0.2 | 53.8±2.00 | 96.2±0.4 | 48.9±1.76 | 96.1±0.3 |
| 2.8 | 64.6±1.52 | 79.3±0.5 | 91.0±2.60 | 56.5±0.7 | 56.0±2.06 | 91.7±0.5 | Insoluble | - |

Performance of all the membranes in both RO and FO mode follows almost the similar trend. Water permeability of the membranes in RO mode follows the order: blank-TFC < TFC-$CuSO_4$ < TFC-$NiSO_4$ < TFC-$Al_2(SO4)_3$ < TFC-$MgSO_4$. In FO mode however, water

permeation trend becomes slightly different in FO mode and follows the trend: blank-TFC = TFC-CuSO4 < TFC-Al$_2$(SO$_4$)$_3$ < TFC-NiSO4 < TFC-MgSO4. The two transition metal sulfates (CuSO$_4$ and NiSO$_4$) show maximum performance enhancement in terms of permeate flux keeping with almost no compromise in rejection at 0.8 m(M) metal ion concentration.

**Table 5.2b: Summary of the optimum concentration of different metal ions in amine solution on performances of composite polyamide membranes.**

| Membrane | Conc. of metal ion (mM) | RO performance | | | FO performance | |
|---|---|---|---|---|---|---|
| | | Product permeability (LMH) | *NaCl rej.* | *MgSO$_4$ rej.* | *Flux(L.m$^{-2}$.h$^{-1}$)* | *Back diffusion of NaCl (%)* |
| TFC(MPD/TMC) | Nil | 50.4±0.80 | 95.8±0.3 | 98.2±0.3 | 5.21±0.024 | 1.09±0.10 |
| TFC | Nil | 44.1±1.16 | 95.5±0.4 | 97.8±0.2 | 3.7±0.026 | 1.15±0.10 |
| TFC-CuSO$_4$ | 0.8 | 44.2±1.76 | 94.0±0.4 | 97.0±0.3 | 4.4±0.019 | 1.17±0.12 |
| TFC-NiSO$_4$ | 0.8 | 48.6±1.52 | 96.0±0.3 | 98.2±0.2 | 5.0±0.018 | 1.08±0.09 |
| TFC-MgSO$_4$ | 2.0 | 53.8±2.00 | 96.2±0.4 | 98.4±0.3 | 4.8±0.027 | 1.08±0.10 |
| TFC-Al$_2$(SO$_4$)$_3$ | 2.0 | 48.9±1.76 | 96.1±0.3 | 98.5±0.2 | 4.6±0.031 | 1.09±0.11 |

On the other hand, the optimum concentration was found to be higher [2.00 m(M)] for the two nontransition metal sulfates [MgSO$_4$ and Al$_2$(SO$_4$)$_3$] to get maximum separation performance. Fig. 5.3b shows that permeability of the membranes increases invariably with increase in metal ion concentration except in cases of Al$_2$(SO$_4$)$_3$. The interfacial polycondensation reaction between amine and acid chloride is a self-limiting reaction and once a thin polyamide film is formed at the interface of the two immiscible solutions, the amine molecules needs to diffuse through the initially formed polyamide barrier layer to come into contact with the bulk acid chloride solution for further reaction. Diffusion of PEI, a

polymeric amine, is typically slow in absence of any additive but it increases with increasing ionic strength of the solution (as in presence of inorganic metal salts). Also, the hydrodynamic radius of PEI globules in aqueous medium decreases due to complexation [226], and the rate of diffusion from pores of support polysulfone membrane to bulk acid chloride increases. This eventually decreases formation of polyamide inside the support membrane pores and the effect of lower pore clogging is reflected in flux enhancement of the membranes with increase in metal ion concentration.
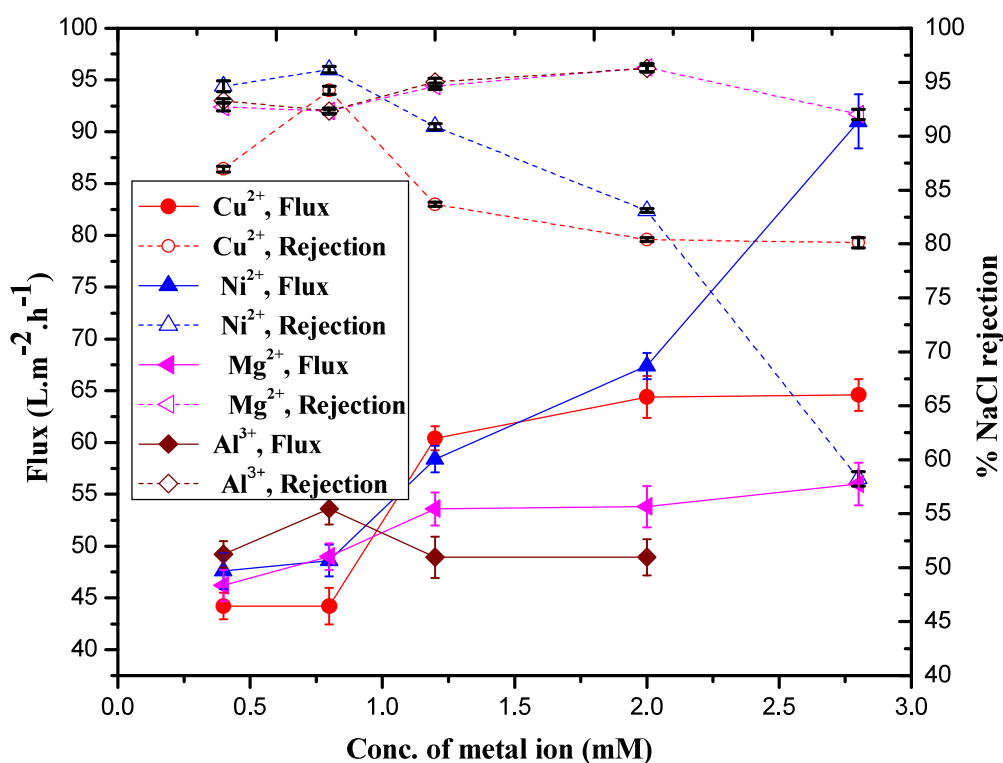


*Figure 5.3b: Effect of concentration of metal ions in amine solution on reverse osmosis membrane performances of composite polyamide membranes.*

As evident from Fig. 5.3b, initially with increase in metal ion concentration, solute rejection of the membranes were increased on addition of metal sulfates upto a certain concentration for all the salts beyond which addition of more metal salts decreases the rejection value drastically. This optimum concentration for attaining highest rejection value was found to be different for different metal salts. The change in ratio of primary, secondary and tertiary amine groups of PEI due to complexation with metal ions might be the reason behind performance enhancement of the membranes. During the poly condensation reaction, HCl is liberated as the by-product and in absence of any external acid acceptor, tertiary amine groups present in PEI acts as acid acceptor whereas primary and secondary amine groups take part in reaction between PEI and IPC. In case if all the tertiary amine groups get blocked due to complexation with metal ions, some of the primary and secondary amine groups then may become protonated by liberated hydrochloric acid and all the sites will not further be available for the condensation reaction. Now, when a metal salt is added to aqueous PEI solution, complexation tendency of the metal ions with the amine group increases in the order primary < secondary < tertiary. Thus the added metal ions block only the tertiary amine groups up to a certain concentration and does not interfere into the polycondensation reaction. Nonetheless, beyond this optimum concentration, PEI starts losing its reaction sites because of blocking of secondary as well as primary amine groups and end up with incomplete reaction for film formation. Thus, for PEI/IPC based membranes, decrease in salt rejection after an optimum metal ion concentration could be because of lack of availability of primary & secondary amine groups (reaction sites) required for completion of polycondensation reaction.
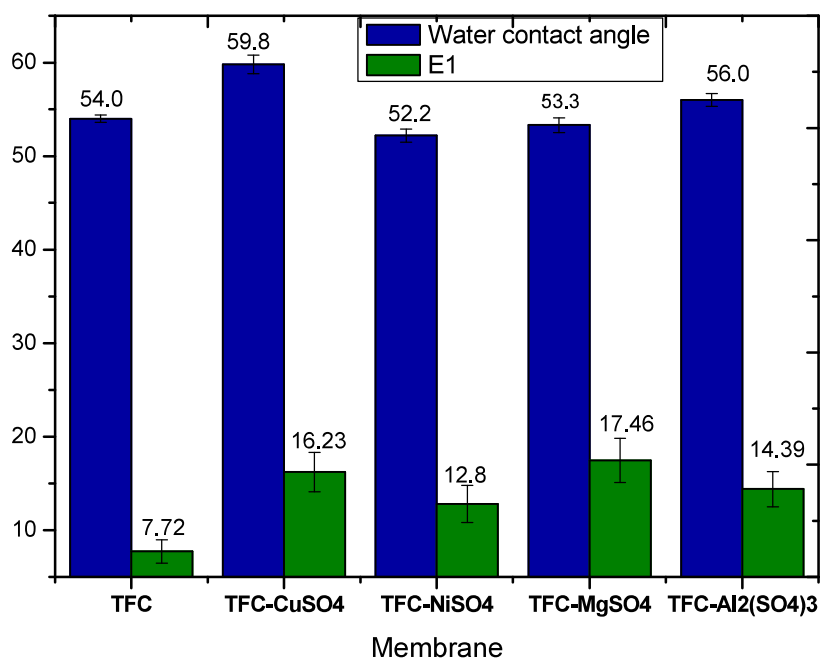
*Figure 5.4b: Physicochemical characterization of TFCPA membranes with and without addition of metal sulfates.*

No remarkable change in hydrophilicity of the membranes was noticed by addition of metal sulfates. Surfaces roughness values (Fig.5.4b) indicate rougher surface of composite membranes prepared in presence metal salts as compared to the control. This may be due to the faster diffusion of smaller size complexed-PEI rather than uncomplexed one making the rate of reaction faster in former case.
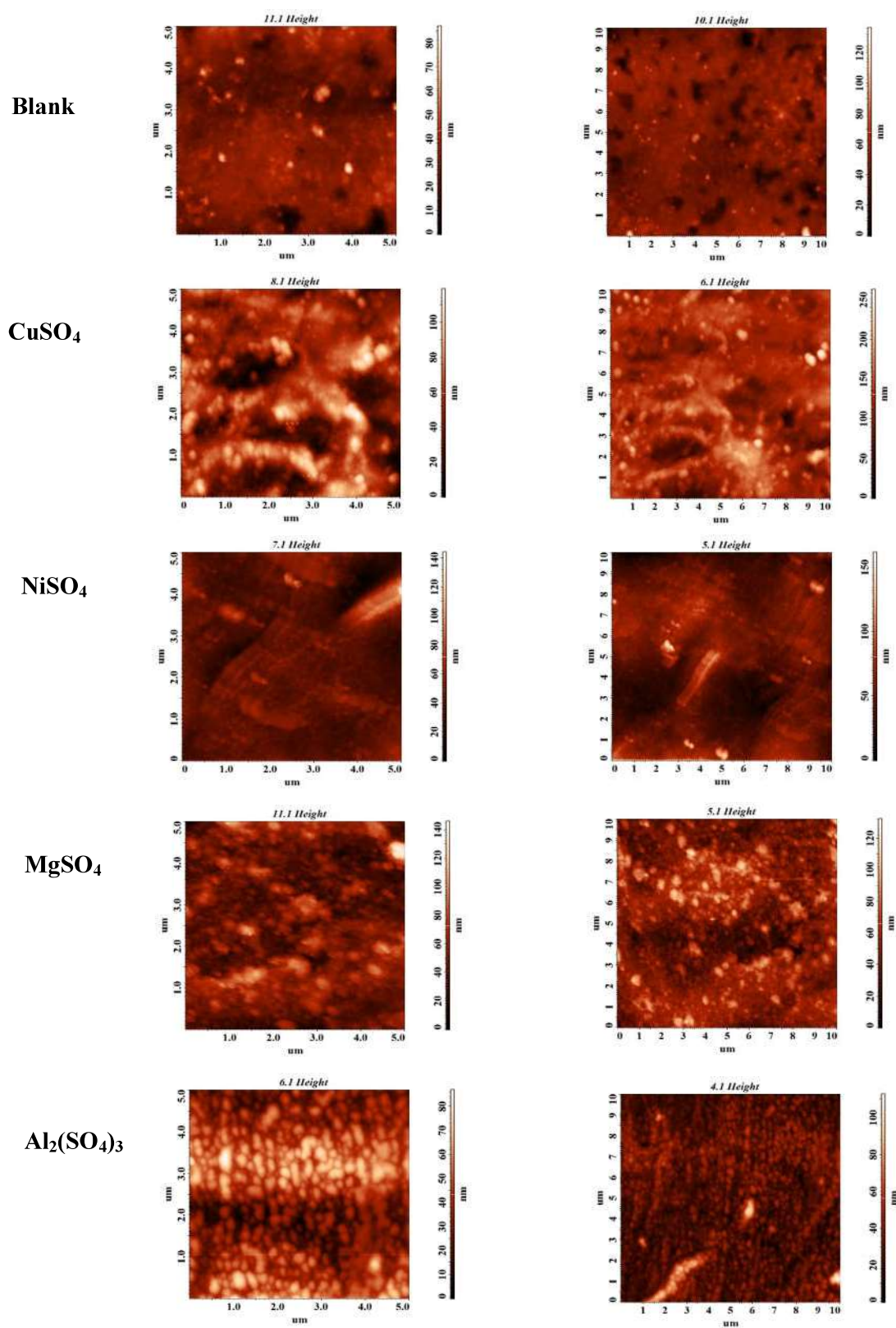
*Figure 5.5b: 2D-AFM surface images of different composite polyamide membranes.*
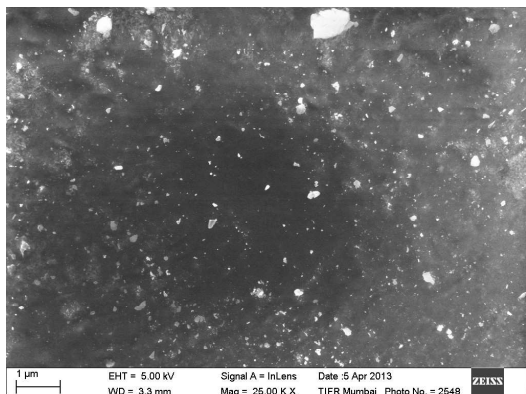
**Blank**



**CuSO$_4$**
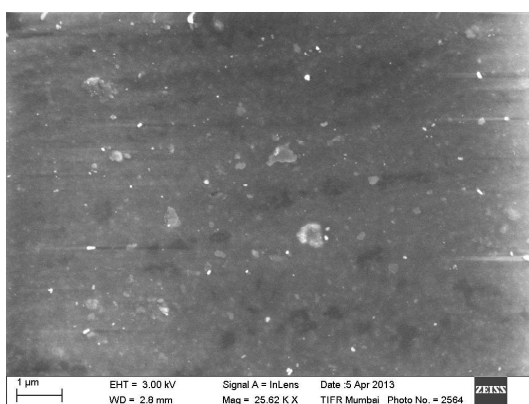


**NiSO$_4$**
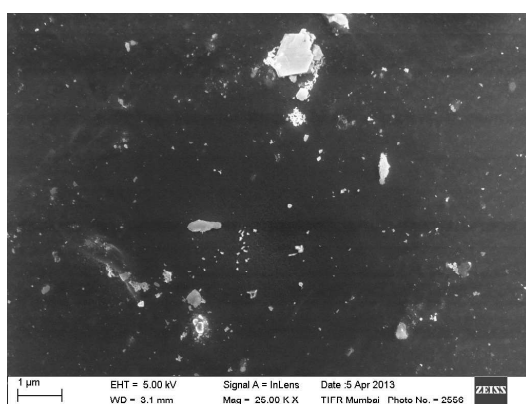


**MgSO$_4$**
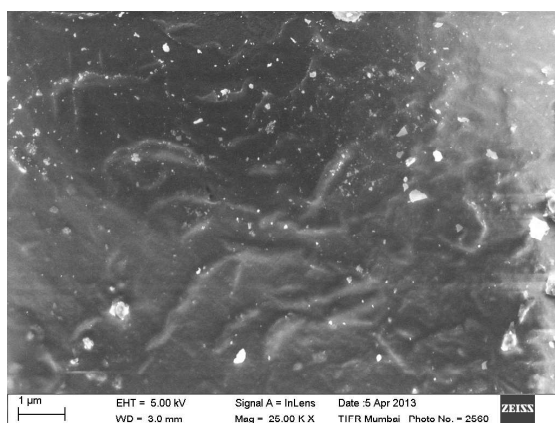


**Al$_2$(SO$_4$)$_3$**

*Figure 5.6b: SEM images of different composite polyamide membranes.*

**5.3.3b. Effect of molecular weight of PEI with same metal ions on composite polyamide membranes**

PEI of two different molecular weights, namely 50 KDa and 600 KDa were chosen to study the change in performance of the membranes after addition of all four different inorganic metal salts at their optimum concentrations. For this purpose, prerequisite amount of different metal salts were added to 1.6% PEI-600 KDa solution and performances of the composite polyamide membranes in terms of permeate flux and NaCl rejection were compared with those prepared using 50 KDa PEI solution keeping all other parametric variables same. Separation performances of the membranes prepared are graphically shown in Fig. 5.7b. It is evident that membranes prepared from higher molecular weight PEI (PEI-600 KDa) shows enhanced performance in terms of both permeate flux and NaCl rejection as compared to those prepared using PEI of average molecular weight (50 KDa) and the trend remains universally same even after addition of metal salts. The results are in accordance with our previous study [228], as discussed in earlier part of the same chapter. However, the increase in flux and rejection of the membranes was relatively small for the membranes prepared after incorporation of transition metal salts (i.e. $CuSO_4$ and $NiSO_4$) than the nontransition metal [$MgSO_4$ and $Al_2(SO_4)_3$] salts. Performance enhancement in terms of product permeability was highest for $MgSO_4$/PEI-600 KDa membranes whereas maximum salt rejection was observed for $Al_2(SO_4)_3$/ PEI-600 KDa membranes.
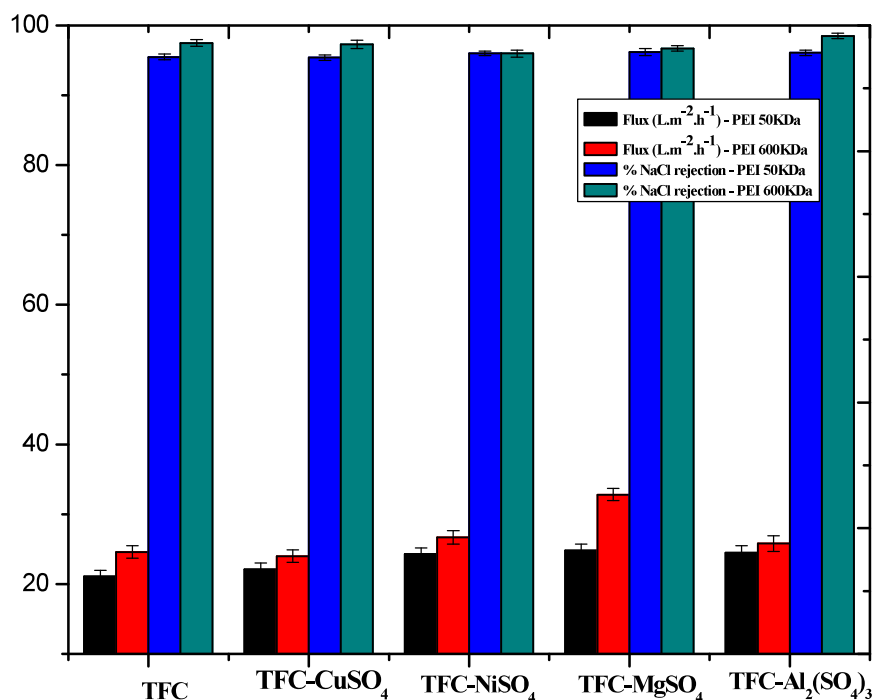
*Figure 5.7b: Effect of molecular weight of the PEI with same metal ions on performances of composite polyamide membranes.*

For in depth understanding of effect of molecular weight of PEI, a batch of TFC-PA membranes were developed using 1.6% aqueous solution of PEI having average molecular weight 2 KDa (PEI-2 KDa) under identical preparation condition keeping the metal ion fixed at its optimum concentration [ 0.8 m(M) $NiSO_4$ was taken in the present study]. Separation performances of the membranes are compared with that of membranes prepared using PEI-50 KDa and PEI-600 KDa (Table 5.3b). It can be noted that the control membranes prepared from both high (600 KDa) and low (2 KDa) molecular weight PEI shows higher product permeability than 50 KDa-PEI (intermediate molecular weight).

**Table 5.3b: Effect of molecular weight of the PEI in presence of NiSO$_4$ (0.8millimolar) on performances of composite polyamide membranes.**

| PEI | Membrane | TFC membrane performance | | |
|---|---|---|---|---|
| | | Product permeability (LMH) | NaCl rej. | MgSO$_4$ rej |
| 2 KDa | TFC | 59.5±1.23 | 94.0±0.3 | 97.0±0.2 |
| | TFC-NiSO$_4$ | 58.3±1.37 | 93.8±0.4 | 96.6±0.3 |
| 50KDa | TFC | 44.1±1.16 | 95.5±0.4 | 97.8±0.2 |
| | TFC-NiSO$_4$ | 48.6±1.52 | 96.0±0.3 | 98.2±0.2 |
| 600KDa | TFC | 49.3±1.17 | 97.5±0.2 | 99.1±0.3 |
| | TFC-NiSO$_4$ | 53.5±1.29 | 96.0±0.4 | 98.4±0.3 |

Because of the bigger size of PEI globules with molecular weight 600 KDa, diffusion of amine through initially formed polyamide film at the water-hexane interface became difficult and a thinner barrier layer was formed in self-limiting polycondensation reaction. This thinner polyamide layer is more compact as compared to the TFC-PA film formed by lower molecular weight PEIs. Thus the membranes prepared using 600 KDa-PEI showed higher flux as well as rejection values. On the other hand, because of smaller globule size of PEI-2 KDa, its diffusion through nascent PA layer was easier and a thicker polyamide film was formed. The less compact thick TFC-PA with overall lower molecular weight showed high product permeability at the expense of lower salt rejection. Addition of NiSO$_4$ enhanced the membrane performances in a similar trend as the control membranes irrespective of the molecular weight of PEI used, i.e. NiSO$_4$/PEI-600 KDa membrane showed both higher product permeability and rejection than NiSO$_4$/PEI-50 KDa membrane whereas NiSO$_4$/PEI-2 KDa membranes gave higher permeability value with lower rejection than NiSO$_4$/PEI-50 KDa membranes.

**5.3.4b Effect of same metal ion with different anions in amine solution on composite polyamide membranes**

To study the role of counter anion on membrane performances keeping the metal cation fixed, two different salts of $Cu^{2+}$ ions and three different salts of $Mg^{2+}$ ions at their optimum concentration corresponding to the sulfate salts [0.8 m(M) for $Cu^{2+}$ and 2 m(M) for $Mg^{2+}$] were added to the aqueous amine solutions. Performance of the TFC membranes prepared from this metal salt incorporated amine solutions in terms of product permeability and solute rejection are tabulated (Table 5.4b) along with their physicochemical characteristics in terms of water contact angle and surface roughness. 3-D AFM images of composite membrane surfaces prepared using different anionic salts of $Cu^{2+}$ and $Mg^{2+}$ are presented in Fig. 5.8b.

**Table 5.4b: Effect of same metal cation with different anions in amine solution on reverse osmosis performances of composite polyamide membranes.**

| Membrane | Conc. of metal ion (mM) | TFC membrane performance | | | Water contact angle (deg.) | RMS roughness (nm) |
|---|---|---|---|---|---|---|
| | | Product permeability (LMH) | NaCl rej. | MgSO₄ rej. | | |
| TFC | Nil | 44.1±1.16 | 95.5±0.4 | 97.8±0.2 | 54.0±0.4 | 7.72±1.23 |
| TFC-CuSO₄ | 0.8 | 44.2±1.76 | 94.0±0.4 | 97.0±0.3 | 59.8±1.0 | 16.23±2.11 |
| TFC-Cu(NO₃)₂ | 0.8 | 61.4±1.26 | 96.6±0.3 | 98.8±0.2 | 53.1±0.8 | 9.91±1.76 |
| TFC-MgSO₄ | 2.0 | 53.8±2.00 | 96.2±0.4 | 98.4±0.3 | 53.3±0.8 | 17.46±2.34 |
| TFC-Mg(NO₃)₂ | 2.0 | 65.5±1.03 | 95.0±0.2 | 97.2±0.3 | 51.8±1.1 | 11.48±1.88 |
| TFC-MgCl₂ | 2.0 | 61.5±1.26 | 93.8±0.3 | 96.0±0.3 | 52.8±0.9 | 8.77±1.77 |

Table 5.4b suggests that as the anion is changed from sulfate to nitrate, keeping the metal ion same, the product permeation of the composite polyamide membrane increases significantly (~25% for $Cu^{2+}$ and 18% for $Mg^{2+}$) for both $Cu^{2+}$ and $Mg^{2+}$ with negligible change (1-2%) in

salt rejection. Also the membranes formed from PEI-metal nitrate solutions tend to be more hydrophilic with smoother surface.

Ionic strength (I.S.) of a solution, containing molar concentration $C_i$ of $i^{th}$ ion with $Z_i$ charge onto it, can be expressed as:

$$I.S. = \sum_i C_i Z_i^2 \qquad \text{.................. (1)}$$

Now sulfate being a bivalent anion, requires to be present in lesser number than monovalent nitrate ions to maintain charge neutrality of a solution containing a particular metal at a fixed concentration and the ionic strength (Eqn. 1) of a solution containing sulfate ion will thereby be always higher than that of a nitrate ion under same concentration. Considering dissociation of equimolecular concentration $(C_i)$ of sulfate and nitrate salts of a bivalent metal ion $(M^{2+})$, ionic strength of the solutions under equilibrium can be calculated following eqn. 1.

$$MSO_4 \rightleftharpoons M^{2+} + SO_4^{2-}$$

$$C_i \qquad C_i \qquad C_i$$

$$(I.S.)_{SO_4} = C_i.2^2 + C_i.2^2 = 8C_i \qquad \text{..................... (2)}$$

$$M(NO_3)_2 \rightleftharpoons M^{2+} + 2NO_3^-$$

$$C_i \qquad C_i \qquad 2C_i$$

$$(I.S.)_{NO_3} = C_i.2^2 + 2C_i.1^2 = 6C \qquad \text{..................... (3)}$$
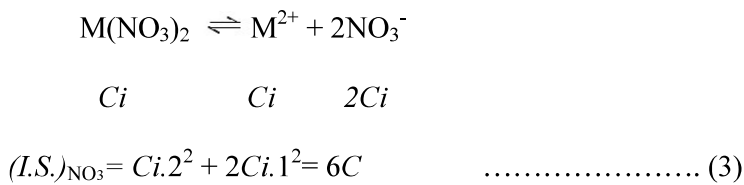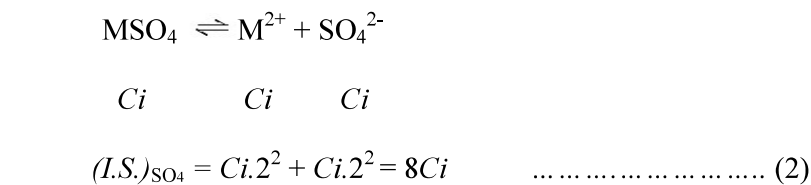
Armstrong et al. reported that increase in ionic strength of a polymer solution decreases the hydrodynamic radius of polymer globules in the solution [226] which in turn facilitates the diffusion of metal ion complexed-PEI molecules through the thin polyamide film for further reaction. A faster reaction typically enhances the surface roughness of the film and the same is reflected in 3D-AFM images (Fig. 5.8b) and average roughness value (Table 5.4b) of the

membranes. As the infusion of PEI became easier in presence of bivalent sulfate ions, a relatively thicker polyamide film was formed and performance enhancement in terms of intrinsic permeability thereby became comparatively less as compared to TFC membranes prepared in presence of metals salts of monovalent anions like nitrate or chloride.
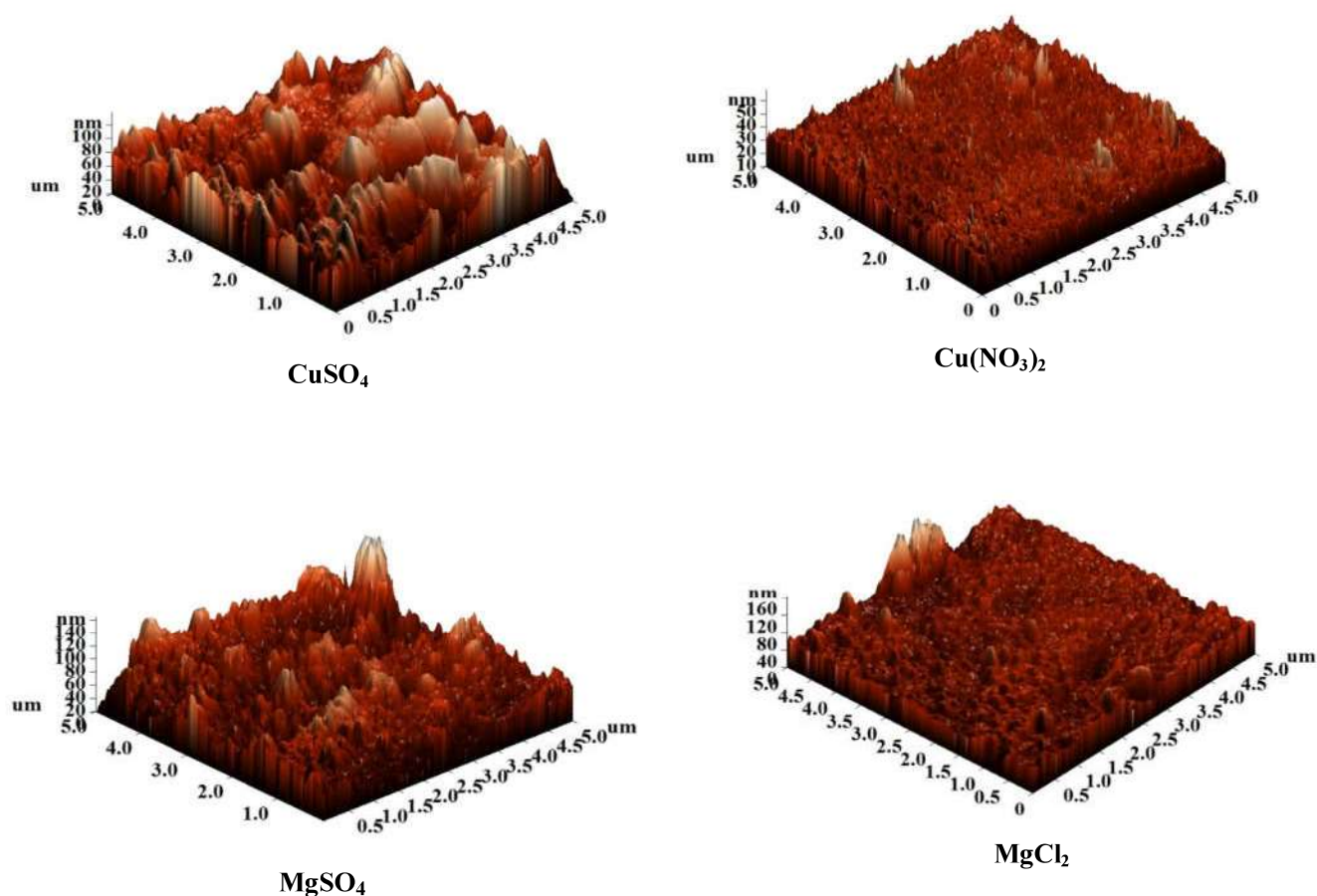


*Figure 5.8b: 3D-AFM surface images of composite polyamide membranes prepared using amine solution with different $Cu^{2+}$ and $Mg^{2+}$ salts.*

Plot of absorbance vs. polymer globule size (Fig. 5.9b), as obtained from dynamic light scattering (DLS) spectra of PEI solutions with and without metal salts ensures decrease in hydrodynamic radius of PEI molecules due to complexation. Average size of PEI globules in absence of any additive is found to be around 316.1 nm and the same is decreased to about 55 nm and 99.9 nm for $CuSO_4$ and $MgSO_4$ complexed PEI respectively.

As the size of PEI globules in presence of complexing agents decreases, diffusion of PEI through polyamide film was facilitated and the probability of polycondensation reaction taking place inside the pores of polysulfone support membrane became less; the effect is reflected in enhancement of permeability of TFC membranes. DLS data shows another important observation on addition of nitrate and chloride salts of the metal ions. Fig. 5.9b shows that size distribution of PEI-$Cu(NO_3)_2$ globules is maximum around 630.8 nm whereas globules of both PEI-$Mg(NO_3)_2$ & PEI-$MgCl_2$ have the maximum distribution around 794.3 nm size.

Because of larger size polymeric amine present in aqueous solution of PEI containing metal salts of monovalent anions, its diffusion in self-limitimg polycondensation reaction becomes highly unfavorable and a thinner polyamide layer is formed. The significant decrease in barrier layer thickness can interpret the reason behind ~50% flux enhancement of TFC membranes on addition of metal salts with monovalent anions as compared to the control.
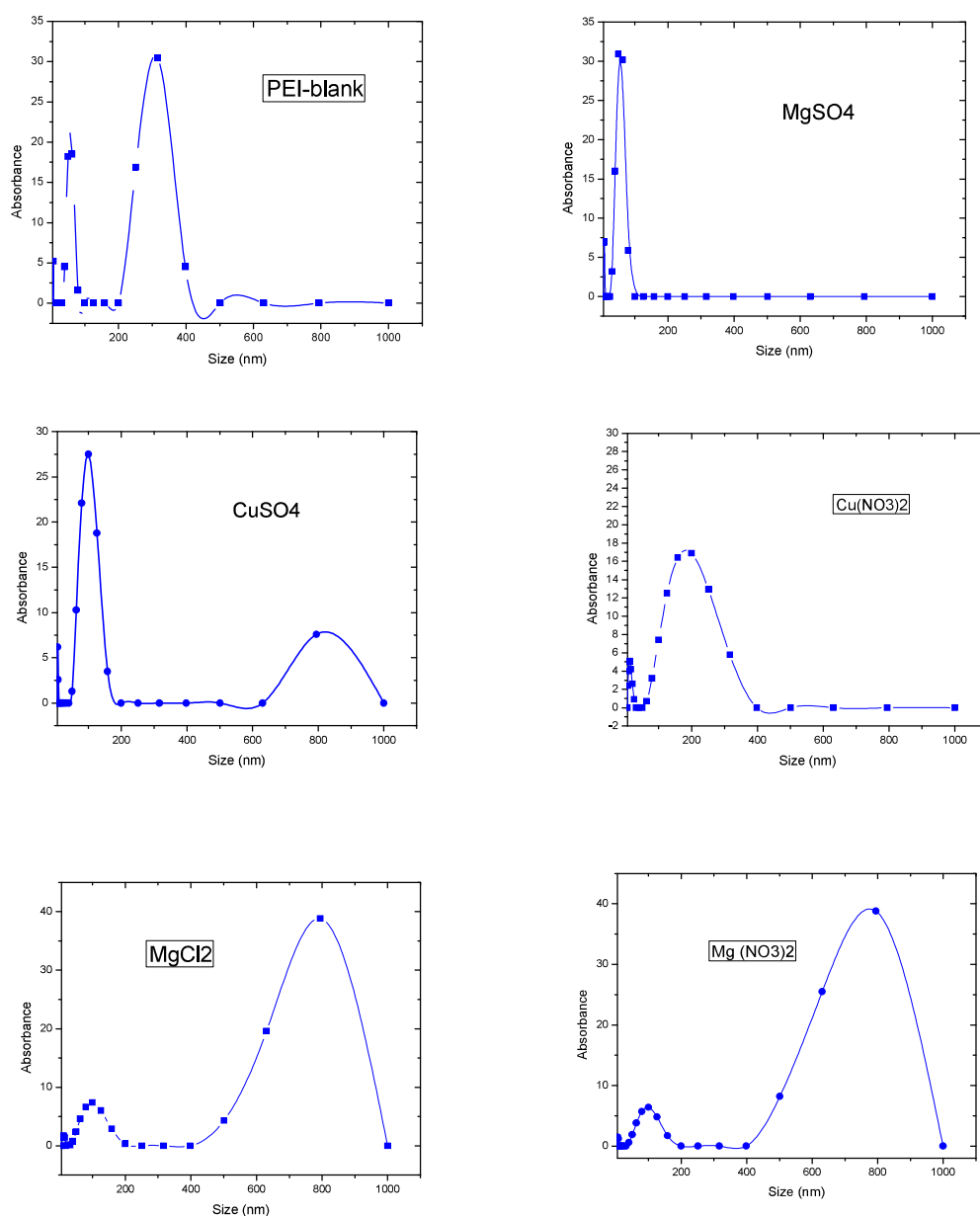
*Figure 5.9b: Absorbance vs size plots of PEI with and without metal salts.*

In order to check if the performance enhancement is due to impregnation of metal ion into the polyamide film, energy dispersive X-ray spectra of control TFC (prepared using blank PEI solution), TFC- $CuSO_4$ (prepared with PEI & 0.8 milimolar $CuSO_4$) and TFC-$Cu(NO_3)_2$ [prepared with PEI + 0.8 milimolar $Cu(NO_3)_2$] membranes were recorded.
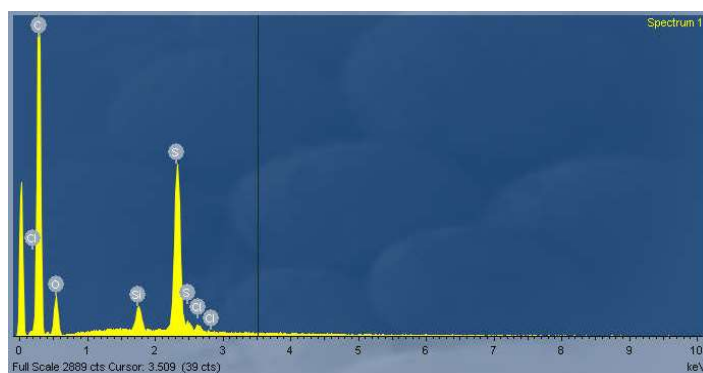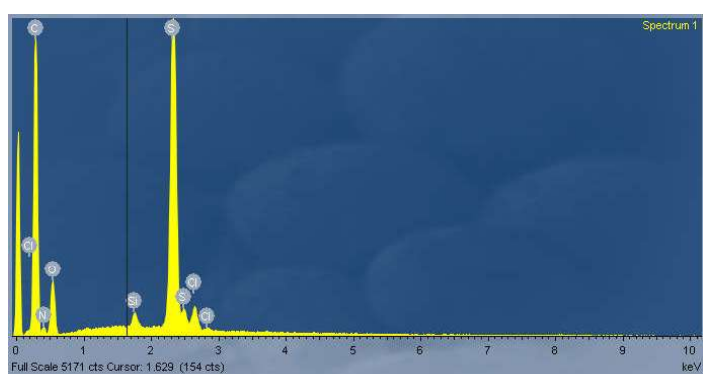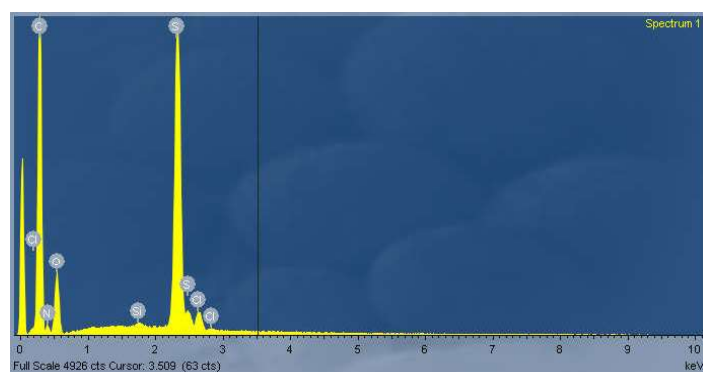
*Figure 5.10b: Energy Dispersive X-ray spectra of [(a) 1.6% PEI, (b) 1.6% PEI + 0.8 milimolar CuSO₄ and (c) 1.6% PEI + 0.8 milimolar Cu(NO₃)₂ used for composite polyamide membrane preparation.*

Fig. 5.10b shows no signal originating from $Cu^{2+}$ in case of both TFC-CuSO$_4$ and TFC-Cu(NO$_3$)$_2$ membranes. As formation of stable complexes between $Cu^{2+}$ and PEI is confirmed from Fig. 5.1b and Fig. 5.2b, it can thereby be concluded that although $Cu^{2+}$-PEI complex

172

took part in polycondensation reaction with acid chloride rather than free PEI, the metal ion got decomplexed in subsequent stages of polycondensation reaction. The decomplexed metal ion was leached eventually either into the aqueous solution inside the pores of support membranes or to the bulk acid chloride solution.

The role of metal ion incorporated in amine solution onto polyamide film formation is conceptually depicted in Fig. 5.11b. The figure illustrates the formation of rougher polyamide layer owing to the faster condensation reaction between smaller size metal-complexed PEI and IPC at the interface as compared to the same by bigger size globules of only PEI.
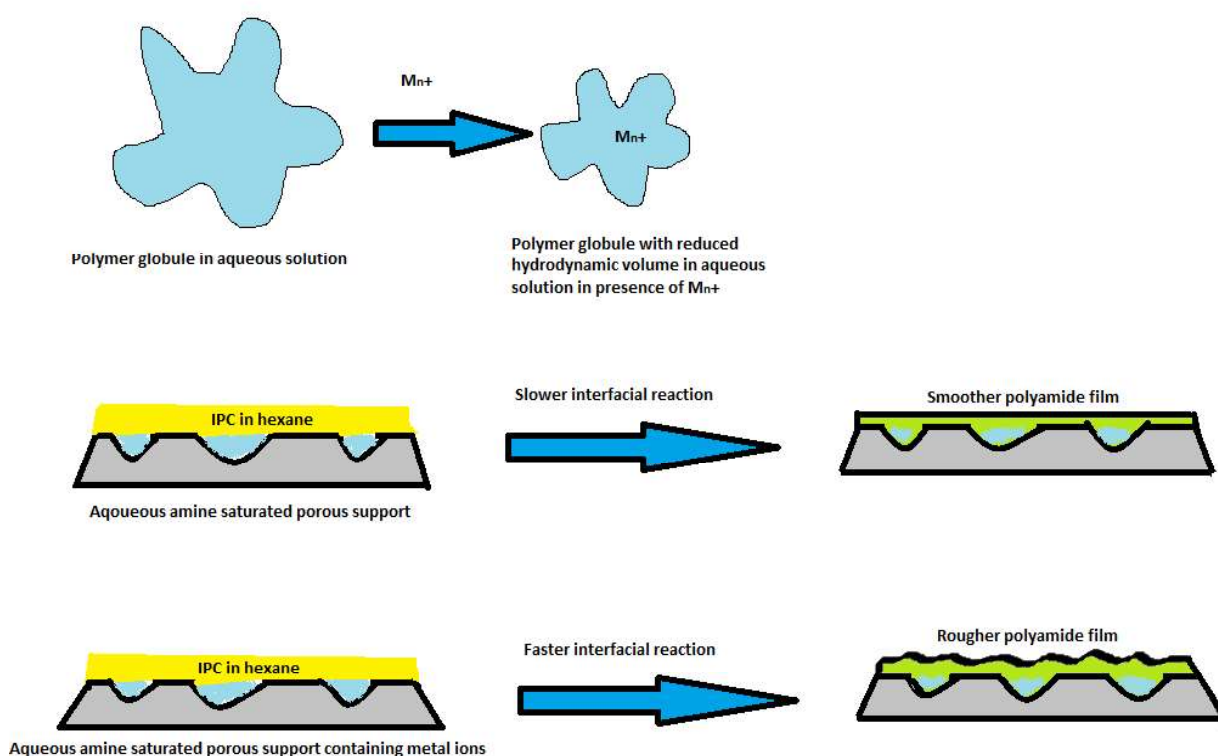


*Figure 5.11b: Conceptual model illustrating role of metal ion in amine reactant*

## 5.4b. Conclusions

Preparation of composite polyamide membranes over polysulfone support membrane by in-situ polycondensation reaction is subjective to the presence of inorganic metal salts in amine solution as complexing agents. Membranes prepared using metal ion impregnated polyethylene imine solutions showed better osmosis performances in terms of product permeability without any compromise in rejection compared to the control membranes (prepared with blank polyethylene imine solution). An optimum concentration of each metal salt was detected up to which the performance enhancement of TFCPA membranes took place. Addition of metal salts beyond this optimum concentration (characteristic of a particular metal salt) deteriorated the separation performance of the membranes extensively. Incorporation of metal salts invariably enhanced the membrane performances irrespective of the molecular weight of the polymeric amine. Univalent nitrate salts of a particular metal ion showed better membrane performance in terms of product flux with slight compromise in rejection as compared to their corresponding sulfate salts. FO experiments with the indigenously developed composite membranes suggest that the membranes can be used as potential candidate in forward osmosis also because of negligible back diffusion of salt from high concentration draw solution to low concentration feed solution. The work elaborated in the current chapter thus provides an effective way to tailor osmotic membranes in achieving high flux without any cost of rejection.

# CHAPTER 6

# DEVELOPMENT OF POLYIMIDE BASED SOLVENT RESISTANT MEMBRANES AND THEIR APPLICATION IN COMPLEXATION NANOFILTRATION USING ORGANIC SOLVENTS

## 6.1. Introduction

The separation processes discussed so far are associated with treatment of aqueous streams in presence of inorganic contaminants. But a number of effluents, especially industrial sewage, that needs to be purified for safe disposal, contain organic pollutants. It was thereby intended to indigenously develop high performance membranes with least swelling in a medium containing harsh polar organic solvents. Since it has amply been illustrated that crosslinking can significantly improve membrane performance in terms of resistance to chemical attack [229-235], Lenzing P-84 polyimide based nanofiltration membranes with different extent of cross linking have been developed for high performance complexation nanofiltration application. All the parametric variables for casting and cross linking of membranes like composition of polymer dope solution, evaporation time, concentration of crosslinker and time of cross linking were optimized to achieve membranes with high organic rejection with prolonged stability in such harsh environment. Cross linked membranes showed up to almost 6 times flux enhancement as compared to their controls with no significant compromise in solute rejection under standard nanofiltration condition. Membranes after cross linking exhibited up to 85% rejection for HCl complexed DMAc. Further complexation of the DMAc/HCl with iron salts containing ferrocyanide ligands resulted in very high rejection (97%) of the organic molecule (confirmed by spectrophotometric analyses).

## 6.2. Experimental

### 6.2.1. Materials

Lenzing P84 (Mn=72000-74000 Da) polymer was procured from HP Polymer GMBH, Austria (Impex chem, India). Reagents like 1,4-Dioxan, and methanol of analytical grade were obtained locally and used without any further purification. Analytical grade sodium chloride and potassium ferrocyanide were procured locally and used without purification.

Ethylene diamine was procured from Merck, India. Organic solvents like N,N-Dimethyl formamide (DMF) and N,N-Dimethyl acetamide (DMAc) of AR grade were procured from M/s. Sisco Research Laboratories, India.

## 6.2.2. Polymer Dope Solution Preparation

Lenzing P 84 polymer was chosen for development of stable SRNF membranes because of its low cost, ease of fabrication, high thermal stability [95], high chemical [236] as well as mechanical [91, 237] stability and most importantly, availability of cross linking sites (Fig. 6.1). Composition of the polymer dope solution is given in Table 6.1. Briefly, 22% (w/w) DMF and 58% 1,4-dioxane were mixed together prior to addition of the polymer into the solvent mixture. The polymer solution in a hermetically sealed glass bottle was put in mechanical shaker until the viscous polymer solution got totally homogenized. The final polymer dope solution was subsequently kept overnight at $(25\pm3)^{\circ}$ C temperature and 35-40% relative humidity to remove any air bubble which might generate some pinholes in the membrane during casting.

### Table 6.1: Polymer dope solution composition.

| % Polymer (w/w) | % N,N-Dimethyl formamide (w/w) | % 1,4-Dioxane (w/w) |
|---|---|---|
| 20 | 22 | 58 |

## 6.2.3. Preparation of Crosslinked Lenzing P84 membrane

## 6.2.3.1. Casting of Lenzing P84 membranes

Solvent resistant nanofiltration membrane was prepared in two steps in laboratory. In the first step, polyimide membranes were prepared by solvent/nonsolvent exchange commonly known

as phase inversion technique. The viscous polymer solution was spread over a clean glass plate using knife edge under a steady casting shear. It was then kept in air for 30 seconds for evaporation of volatile solvent and the entire assembly comprising the casting film was immersed immediately into a precipitation bath containing the non-solvent (ultrapure water) at room temperature (22°-25° C).The whole assembly was kept inside the water bath for 40minutes to ensure adequate exchange between solvent and nonsolvent and complete precipitation of the polymer. The resulting membrane was washed thoroughly to remove any excess solvent and stored in water bath at ambient temperature prior to crosslinking.
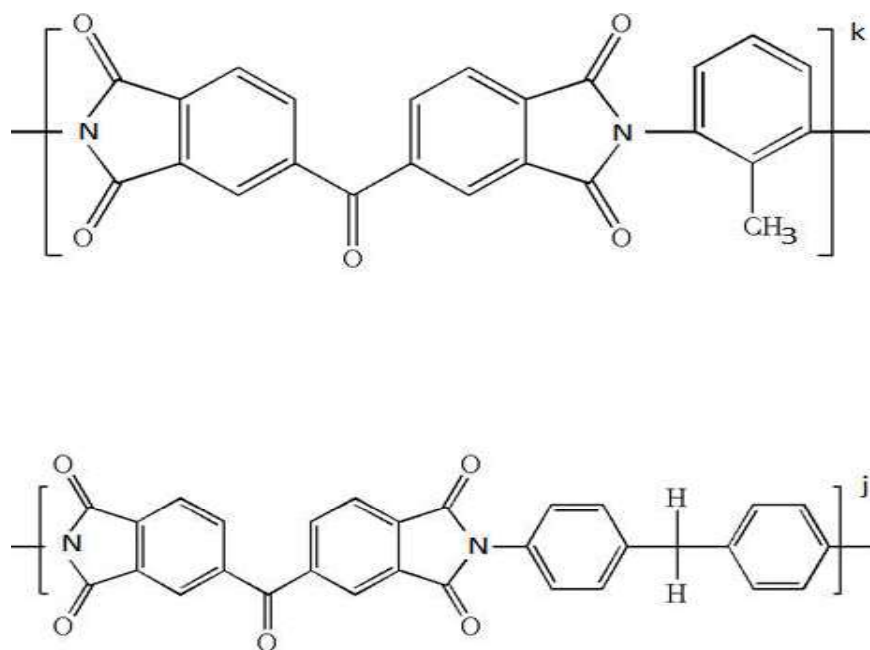


*Figure 6.1: Chemical structure of Lenzing P-84 polymer.*

## 6.2.3.2. Crosslinking of Lenzing P84 membranes

In the second step of membrane preparation, the integrally skinned Lenzing P84 membrane was chemically cross linked to make them stable in harsh organic environment. A solution of preoptimized concentration (3% v/v) of ethylene diamine in methanol was prepared and the

polyimide membrane was dipped into the solution for chemical crosslinking over a range of time (15 mins to 2 hours). Methanol was added to swell the polymer chains and make them more accessible to react with diamine crosslinker ensuring a complete crosslinking of the entire bulk of the membrane [93, 238, 239]. It had been found that crosslinking for more than 45minutes made the polymer extremely brittle and difficult to handle. Crosslinking of Lenzing P84 polymer with ethylene diamine is schematically shown in Fig. 6.2.
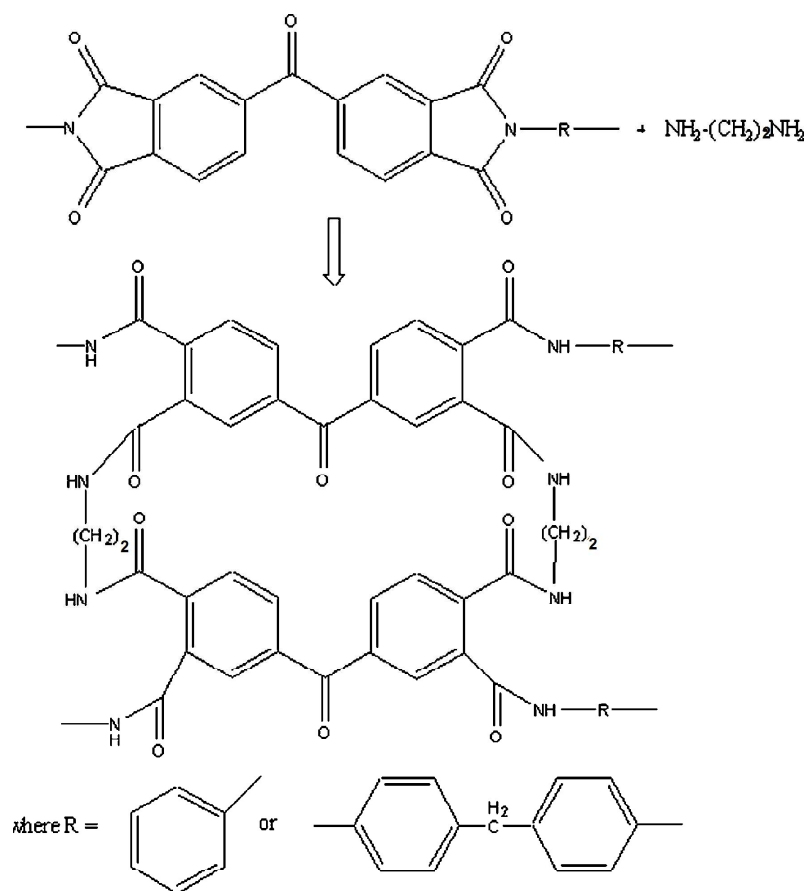


Figure 6.2: Crosslinking of Lenzing P-84 with ethylene diamine.

The membrane was washed thoroughly with methanol and water to remove any unreacted crosslinker and stored in refrigerator cooled water till further use. The thickness of final membrane was measured to be 85 µm. The entire process of casting and crosslinking was

carried out in a controlled environmental atmosphere with temperature $25\pm3^\circ$ C and relative humidity 35-40%.

## 6.2.4. Physicochemical characterizations of P84 membranes before and after crosslinking:

The crosslinked as well as uncrosslinked membranes were characterized in terms of their hydrophilicity, surface morphology, pore size determination, change in glass transition temperature due to crosslinking and separation performance evaluation under standard nanofiltration condition (2000 ppm aqueous $Na_2SO_4$ solution as feed under 10bar operating pressure).

Topographical analyses of optimally crosslinked membrane surfaces along with the control were carried out by extracting their quantitative topographical information in the semi-contact mode by a standard AFM instrument (Make: NT-MDT, Model: SOLVER next, Ireland). Small membrane pieces of approximate dimension of $1cm^2$ were cut from each membrane strip and glued over a metal surface by double sided tape. The rectangular cantilever NSG 10 (NT-MDT, Ireland) made of piezoelectric $Si_3N_4$ with a spring constant of 11.8 N/m, had a typical resonance frequency of 240 kHz and a nominal tip apex radius of 10 nm with high aspect ratio. The scanning of each membrane was done onto 5 $\mu$m $\times$ 5 $\mu$m area under ambient atmosphere with a scanning frequency of 0.3 Hz. Tilt generated because manual stacking of the membrane onto metal plate were removed from the scanned regions using a second order polynomial by removing all the curvatures and slopes from the image and then the resulting best fit was subtracted from it. NOVA-P9 software was used for the image acquisition and evaluation of surface roughness parameters of the membranes. Surface roughness parameters of the membranes were calculated from the height profiles of the images in terms of average roughness ($R_a$) and root mean square roughness ($R_{rms}$).

181

Hydrophilicity of the membrane surfaces before and after crosslinking, was measured using sessile drop method by a standard contact angle measuring instrument (DSA 100 of KRUSS Gmbh, Germany) with DSA 1v 1.92 software. A sessile drop of deionized water with 0.6 μl volume was formed onto each membrane surface very slowly and steadily using a micro syringe. Water contact angles at membrane-solvent-air interface were measured in each second over a total residence time of 60 seconds and the mean value was calculated. Six such measurements of each membrane sample were conducted and the average values are reported. Pore size of the membranes before and after cross linking was determined by Positron annihilation lifetime spectroscopy (PALS), a well-known technique for determination of the free volume of polymer films. Positrons generated from a radioactive source ($^{22}$Na) were subsequently implanted into the polymeric matrices where a fraction of thermalized positrons forms a bound state with an electron and the lifetime of free positron was reduced. The extent of this reduction of Ps lifetime depends on the frequency of collision with nanohole's surface atoms which in turn is a measurement of membrane pore radius.

Dynamic thermo-mechanical analysis (DMTA) was used to determine the change in glass transition temperature (Tg) of the membranes due to cross linking. DMTA measurement was performed on an MCR 102 Rheometer (Anton Paar, Austria) using Solid Rectangular Fixture (SRF) or with Universal Extensional Fixture (UXF). Samples dimensions were 20 mm x10 mm x 1 mm (l x w x t) for all the samples. Temperature sweep was done from 30°C to 400°C to monitor storage modulus in glass and rubbery stages, at 1 Hz frequency and 1% strain.

All the membranes were characterized in terms of their product permeation rate & salt rejection under standard nanofiltration testing condition (2000 ppm $Na_2SO_4$ feed at 10 bar operating pressure). Cross flow filtration mode was operated with a transmembrane pressure of 10 bar on 12.6 cm$^2$ effective membrane area to get the permeation study done. The steady-state water permeation rate was determined by measuring of the permeate flow, *i.e.*, volume

(V in ml) collected during a time period (t in min), through a membrane area (A in cm$^2$) and converting them into L.m$^{-2}$.h$^{-1}$. Prior to the performance evaluation by standard NF operation, all the membranes were subjected to undergo hydraulic compaction for 4 hours in water at 2585 kPa pressure in order to attain steady state performance. Salt rejections of the membranes were calculated by measuring the specific conductance of feed and permeate solutions and correlating them to their concentrations.

### 6.2.5. Performance Evaluation of SRNF Membranes

Lenzing P-84 polymer is stable in nonpolar aprotic solvents like toluene [240] but dissolves instantaneously in organic media containing strong polar aprotic solvents like DMAc, DMF or NMP. Stability of the cross linked membranes were checked gravimetrically by putting a piece of membrane into pure (100%) DMAc for 48 hours. No loss of weight of the membrane pieces crosslinked for 15mins (P84/15) and 30mins (P84/30) confirmed their long term stability in polar aprotic solvents.

The optimally crosslinked membranes were employed for cross-flow permeation experiments with an effective membrane area 14.5 cm$^2$. Measurements were carried out using a range of uncomplexed and complexed aqueous solution of DMAc over a range of concentrations (500-2000 ppm) under three different nitrogen operating pressures, viz. 6 bar, 8 bar and 10 bar at room temperature. In order to increase the organic rejection by the membrane, DMAc was complexed with HCl and the rejection of organics by the membrane was calculated by analysing the total organic carbon (TOC) content of feed and permeate solutions using a standard TOC analyser (ANATOC, SGE analytical science, Australia).

In order to achieve further enhanced rejection by the membrane, the polar aprotic solvent was further complexed by stoichiometric addition of potassium ferrocyanide. Concentration of the complex formed was determined in feed as well as permeate by measuring the absorbance

value at the absorption maxima ($\lambda$max) of the complex using a double beam UV-visible spectrophotometer (Model: Spectrascan 2600, Make: Chemito, India).

## 6.3. Results and Discussions:

### 6.3.1. Membrane Surface Characteristics and Separation Performance:

The complexed polyimide membranes suitable for application in solvent resistant nanofiltration (SRNF) were characterized in terms of the water contact angle, surface average roughness and separation studies under standard NF condition and the results are given in Table 6.2 and Fig. 6.3. Water contact angle of the membranes show that the membranes were moderately hydrophilic and no change in water contact angle is reported due to cross linking for 15 mins. Crosslinking for 30 mins made the membrane brittle on drying which is a must condition to determine the water contact angle accurately, and hence idea of hydrophilicity of P84/30 membrane was beyond the scope of the analyst. Thus no significant change in membrane hydrophilicity due to cross linking indicates any change in hydrophilic character by chemical reaction may be compensated by morphological changes due to crosslinking.

**Table 6.2: Membrane characterization data.**

| Crosslinking time (min) | Permeability (LMH) | Salt rejection (%) | Contact angle (°) | Surface average roughness (nm) | Glass transition temperature (° C) |
|---|---|---|---|---|---|
| 0 | 0.167±0.4 | 90.6±1.2 | 49.38±0.88 | 2.151±0.67 | 319±5.0 |
| 15 | 1.0±0.9 | 94.9±1.3 | 49.9±0.91 | 1.459±0.44 | 310±3.5 |
| 30 | 1.2±0.8 | 90.6±1.5 | Brittle | 1.282±0.43 | 286±4.5 |

Operating pressure: 10bar, Feed: 2000ppm $Na_2SO_4$, Membrane area: 12.6cm$^2$, Feed Temp.: 25°C
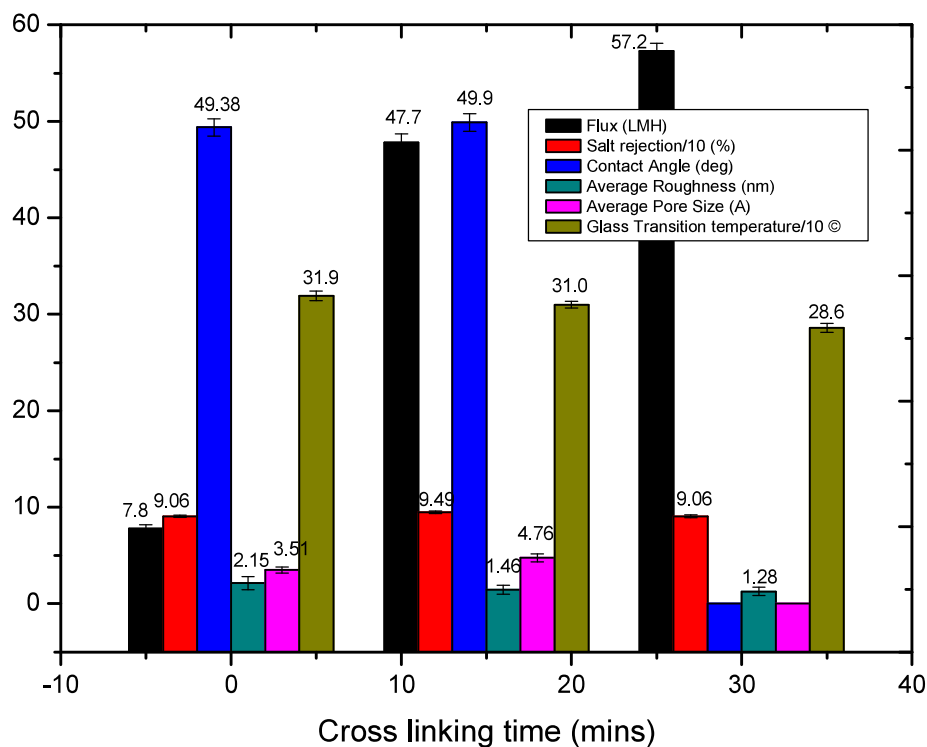
*Figure 6.3: Membrane Characterization Data of crosslinked and uncrosslinked Lenzing P84.*

Surface roughness images (Fig. 6.4) and their corresponding values suggest that the membranes become smoother with increase in crosslinking time keeping the crosslinker concentration fixed. Water permeability and solute rejection data were recorded once the data became constant over 45minutes. All the membranes were showing more than 90% rejection of $Na_2SO_4$ under standard NF condition. Crosslinking for 15 mins marginally increased the solute rejection value as the polymer network became tighter due to higher crosslinking.

Performance evaluation in terms of water permeability shows a very interesting result. Fig. 6.3 elucidates that flux increases around 6 times after treatment of membrane with cross

linker solution for 15-30 mins. For better understanding of flux enhancement of the membranes due to chemical treatment, some idea about the internal structure of the polymer network is to be understood.
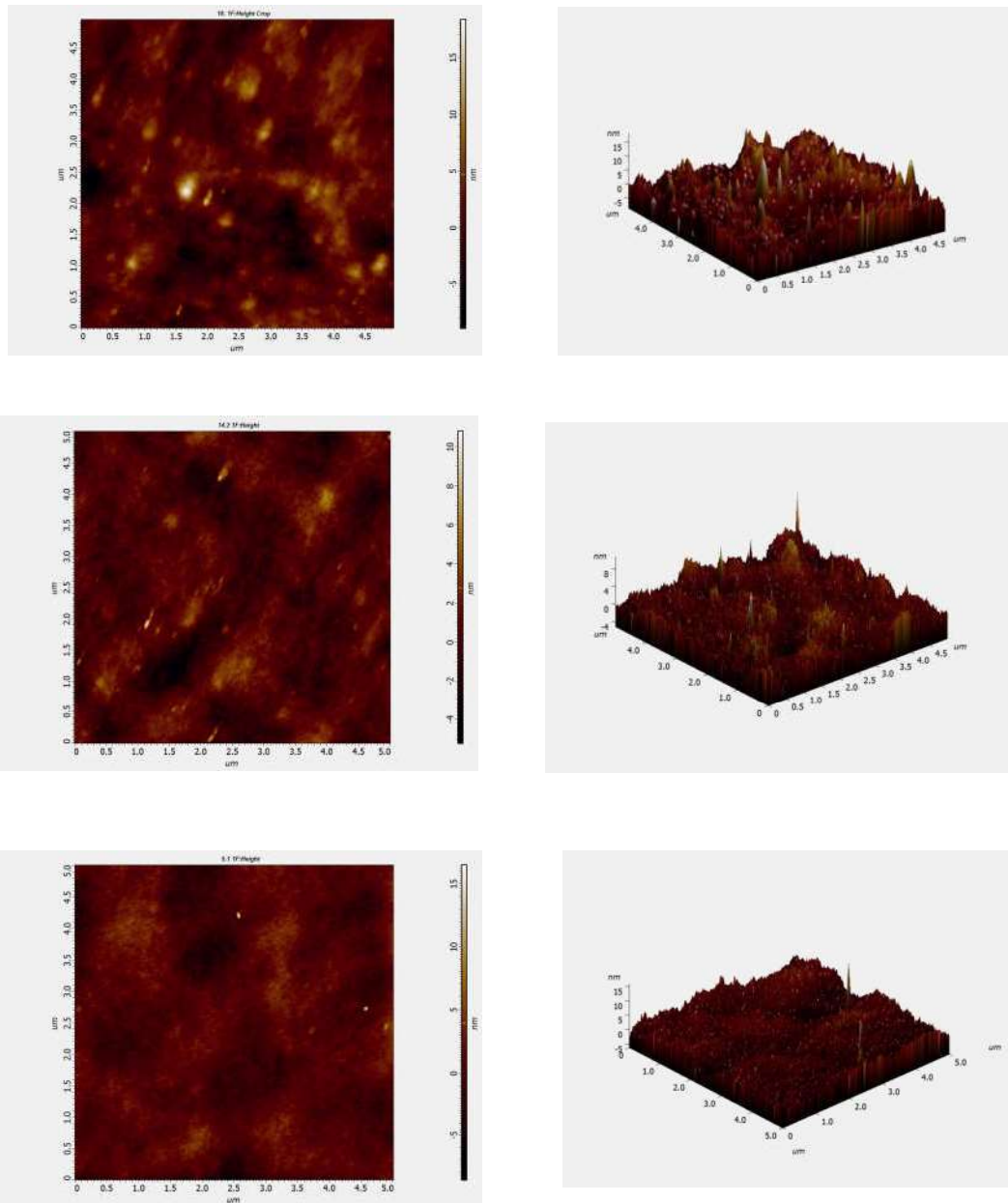


Figure 6.4: AFM images of (a) uncrosslinked, (b) 15mins crosslinked and (c) 30mins crosslinked membranes.

## 6.3.2. Characterization of Internal Structure of the Membrane:

To get some idea about the change in internal polymer structure of the polyimide membranes due to cross linking, glass transition temperature (Tg) of the membranes as a function of crosslinking time was determined. Fig. 6.5 shows subsequent lowering of Tg with increase in time of cross linking. Glass transition temperature of a polymer is defined as the temperature at which it transforms from glassy (more ordered) to rubbery (less ordered) state and is characteristic of a particular polymer. Tg is also a direct measurement of crystalinity of the polymer. A lower the value of Tg of a polymer makes the segmental motion of the polymer chains more feasible at a lower temperature [241-243]. Thus, lowering of Tg by addition of crosslinker might implement some level of molecular relaxation and thereby made the water permeability easier. Moreover, the small molecules of the added crosslinker might intervene into the polymer chains and acted as plasticizer, making more paths to flow water with lower hindrance. This might be another reason for flux enhancement upon addition of ethylene diamine.
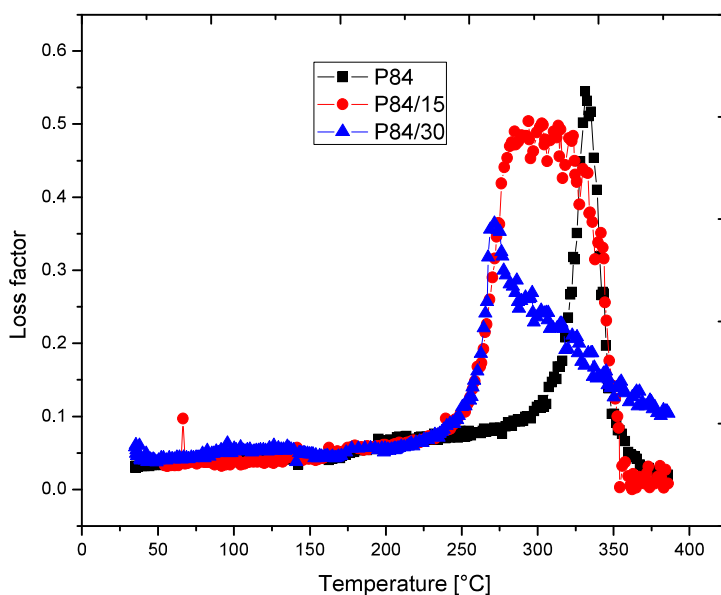


*Figure 6.5: DMTA analysis of uncrosslinked, 15mins crosslinked and 30mins crosslinked membranes.*

Preliminary study by Positron Annihilation Spectroscopy (PALS) showed that treatment with crosslinker enhanced the average pore size of the membranes by 1.4 times probably by merging the smaller pores (Table 6.3). This result is also consistent with the results of Gibbins et al. [244] and Bowen et al. [245] who calculated the pore radius of different SRNF membranes as 5-8 A and 7.2 A respectively (calculated from fluxes based on membrane area, that is, setting the porosity to 100% for the calculation). Thus bigger sized pores generated by chemical treatment during cross linking facilitated the flow of water with lower hindrance resulting in ~6 times flux enhancement. It should be noted that the data presented leads to a rough estimate of the pore size of a membrane, and in reality the pore size distribution should be taken into account.

Table 6.3: Pore size determination data of membranes.

| Crosslinking time (min.) | O-Ps lifetime (ns) | Pore radius (A) |
|---|---|---|
| 0 | 2.76 | 3.51±0.32 |
| 15 | 4.84 | 4.76±0.41 |

### 6.3.3. Complexation Nanofiltration of Polar Aprotic Solvents by Indigenously Developed Membranes:

TOC analysis of the feed and permeate solutions showed that both L84/15 and L84/30 membranes gave rejection up to 60% with 1000 ppm aqueous solution of DMAc under 10bar operating pressure (Fig.6.6). With increase in operating pressure and/or concentration of DMAc in feed solution, permeation of DMAc through the membrane increased and as a result, rejection value dropped down to ~50%.

188
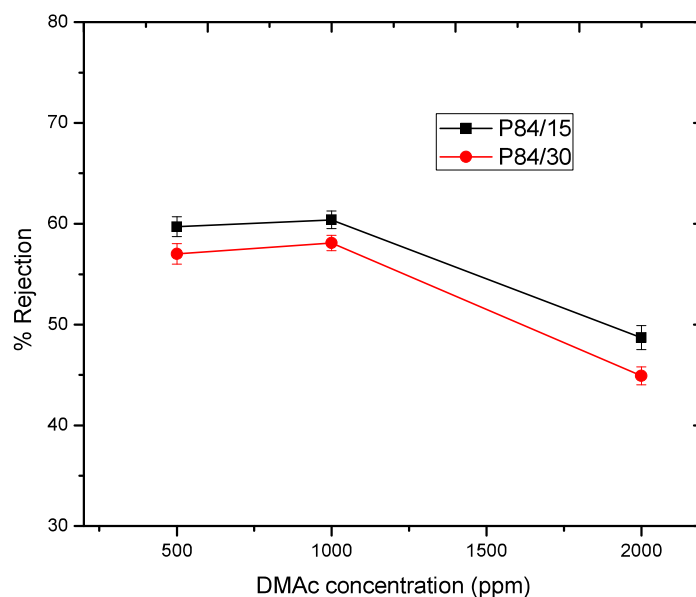
*Figure 6.6: Permeation performance of crosslinked membranes as a function of DMAc concentration*

In order to enhance the rejection, attempts were made for complexation nanofiltration using the same crosslinked polyimide membranes. Complexation nanofiltration was conducted by adding stoichiometric quantity of HCl in 1000 ppm aqueous solution of DMAc and passing it through L84/15 and L84/30 membranes under 10 bar $N_2$ applied pressure. Determinations of concentration of the organics in feed and permeate solution by TOC analyses showed an increment in rejection up to 85% by both the membranes.

A well-known fact about NF membranes is that the separation characteristics of such membranes are conjugated effect of pore size of the membrane as well as interaction between the membrane and solute molecules [246-252]. Fully aromatic polyimides have rigid chains and strong inter chain interactions originate from intra as well as inter chain charge transfer complex (CTC) formation and electronic polarization. The CTC formation and electronic polarization are supported by the strong electron acceptor characteristics of imide [253] groups present in the polymer. The polymer of our concern (Lenzing P84) thereby possesses slight positive surface static charge because of presence of imide groups in its fully aromatic

189

structure. In presence of HCl, DMAc formed a cationic complex (reaction 1) which was rejected strongly by the positively charged membrane surfaces and increased the rejection from 60% to 85%.

$$CH_3CON(CH_3)_2 + HCl \rightarrow \{CH_3CON(CH_3)_2\text{-}H\}^+Cl^- \quad \ldots\ldots\ldots\ldots(1)$$

$$4\{CH_3CON(CH_3)_2\text{-}H\}^+Cl^- + K_4[Fe(CN)_6] \rightarrow \{CH_3CON(CH_3)_2\text{-}H\}^+]_4[Fe(CN)_6]^{4-}$$

$$+4KCl \quad \ldots\ldots\ldots\ldots..(2)$$
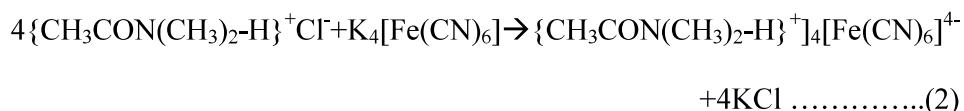
(Intense blue color with $\lambda max = 416.5nm$)

Further increase in rejection using the same membrane was achieved by adding stoichiometric amount of potassium ferrocyanide into the solution containing the DMAc/HCl complex which, on reaction with potassium ferrocyanide generated an intense blue complex (Reaction 2). When the aqueous feed solution containing DMAc-ferrrocyaanide complex was passed through the membranes, because of the very big size of the complex, the same was immensely rejected as indicated by the UV-visible spectrophotometric analysis of feed and permeate solutions. More than 97% rejection (Fig. 6.7) was obtained using the same membrane under identical experimental condition.
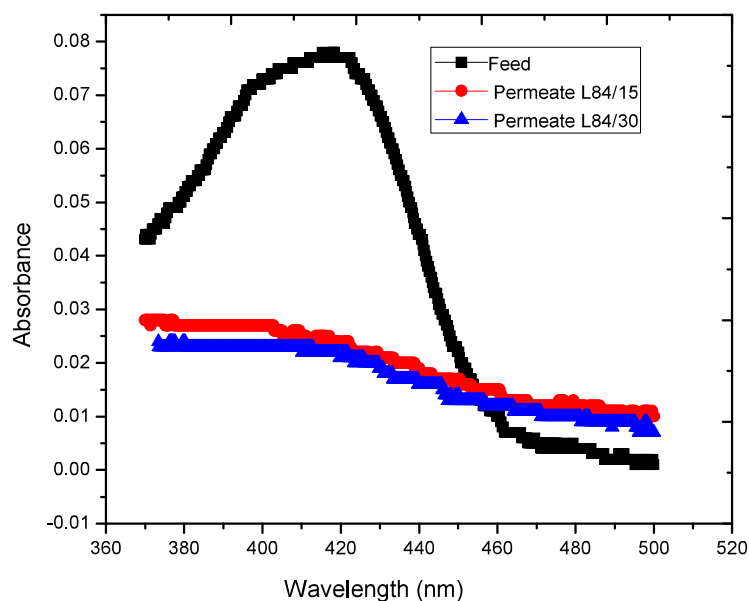
*Figure 6.7: Absorbance vs wavelength plot for Feed (500ppm DMAC/HCl/*

*$K_4[Fe(CN)_6]$ ) and Permeates obtained under 8bar operating pressure using*

*membranes crosslinked for 15mins (Permeate 1) & 30mins (Permeate 2).*

## 6.4. Conclusions:

Stability of commercial Lenzing P84 polymers were successfully enhanced by chemically crosslinking the membranes with pre-optimized concentration of aliphatic diamine crosslinker. Crosslinked polyimide membranes were found to be highly stable even in harsh polar aprotic solvent like DMAc. During optimization of all the parametric variables of indigenously developed membranes, it had been found that the membranes got damaged on treatment with the crosslinker over a longer time. Crosslinked membranes with smoother surface showed 600% increase in water permeability without any compromise in rejection under standard NF condition. This flux enhancement might be attributed to the lower value of Tg and higher pore sizes as observed from internal

structural analyses of the polymeric membranes. These two factors exaggerated the water permeability by reducing the hindrance towards water flow through the membranes. These indigenously developed crosslinked membranes showed upto 85% rejection of DMAc/HCl complex. Further complexation of DMAc/HCl with $K_4[Fe(CN)_6]$ made the rejection value even higher with same membranes under identical experimental condition. Thus, complexation nanofiltration was found to be a very effective way for removal of low concentration organic solvents from aqueous streams using crosslinked PI membranes.

# CHAPTER 7

# CONCLUSIONS AND RECOMMENDATIONS

## 7.1. Conclusions

In this chapter, the summarized results of the entire work pursued as a part of the thesis, is presented. The chapter elucidates the accomplishments and conceptual scientific interpretations unfolded by the present work. The work encompasses development of cellulosic and polyamide based membranes suitable for treatment of different aqueous streams. The objective of the work, as highlighted in the first chapter, was to develop high performance osmotic membranes to mitigate or minimize the typical challenges faced by any researcher in the field of membrane sciences. The most usual shortcomings of any membrane based separation processes are trade of between flux and rejection, stability of the membrane in targeted stream and scale up for actual application. Functional modifications of the membranes, to overcome these obstacles, were practised by changing different parametric variables like altering the polymer solution composition, incorporating nanoparticles or organic/ inorganic additives, crosslinking of membranes. The conclusions & scope of future works are summarized below:

### 7.1.1a. Development of Cellulosic membranes for treatment of simulated ADU filtrate solution

➢ A solution having radioactive effluents needs to be concentrated for its safe disposal and Forward osmosis being an energy efficient process, can successfully be employed for concentration of such aqueous streams containing high value low volume products.

➢ Cellulosic membranes with similar salt rejection properties (>85% under standard BWRO condition) developed from cellulose acetate (CA), cellulose triacetate (CTA) and cellulose acetate blend (CAB-blending of CA and CTA) were employed successfully for concentration of simulated ADU filtrate solution (40,000 ppm $NH_4NO_3$ with 20 ppm U).

➤ Hydrophilic CA membranes with smoother surface showed higher VRF value (1.43) than CTA and CAB membranes under identical experimental condition. All the membranes show nominal leaching of U (~0.5%) from feed to draw solution.

➤ CA membranes show better FO performances in terms of volume reduction factor (1.51) when $CaCl_2$ is used as draw solution as compared to same concentration of $NH_4NO_3$ or $(NH_4)_2CO_3$ because of higher osmotic pressure exerted by $CaCl_2$.

➤ Increase in draw solution concentration from 2 (M) to 4 (M) increased the VRF value almost linearly by enhancing the osmotic pressure gradient between feed and draw solution, at a cost of solute back diffusion.

➤ Membrane pouch, as a simple device can be used for concentration of desired stream with judicial choice of the membrane and draw solute depending upon their on-site availability and requirement of regeneration.

## 7.1.1b. Development of Polyamide membranes for treatment of simulated ADU filtrate solution

➤ The problem associated with cellulosic membranes is their poor stability over a wide range of pH and low Tg which makes them unsuitable to be used in a membrane based hybrid process operating at elevated temperature.

➤ Aliphatic-aromatic and aromatic-aromatic based TFCPA membranes with ~90% salt rejecting property under standard BWRO conditions were prepared by in-situ polymerization reaction between PEI/IPC and MPD/TMC.

➤ The membranes showed lower VRF (1.2 for MPD/TMC & 1.24 for PEI/IPC) value than cellulosic membranes (1.43 for CA) under identical testing condition with similar leaching (~0.5%) of U from feed to draw solution.

➢ PEI/IPC based membranes show higher VRF values when $NH_4NO_3$ was used as draw solution (mildly acidic) whereas MPD/TMC based membranes show higher VRF value with $(NH_4)_2CO_3$ as draw solution (moderately alkaline in nature). This anomaly was well explained by the difference in charge imparted by residual functional groups present on the TFCPA membrane surface.

**7.1.1c. High Flux Thin–film composite polyamide (TFCP) Forward Osmosis membranes for Concentration of Simulated Cesium and Strontium bearing Effluent solution**

➢ High flux TFC based FO membranes prepared over hydrophilic PES support membranes by polycondensation reaction of MPD and TMC in presence of phenol additive.

➢ Addition of phenol upto 1.2% in presence of TEA/CSA salt enhanced the water permeability without any compromise in salt back diffusion (0.75%) in FO mode.

➢ Further addition of phenolic compound resulted in inhomogeneity of membrane surface induced by phase separation of phenol in aqueous amine solution.

➢ The optimized TFCFO membranes rolled over 2512 spiral module showed VRF value as high as 3.23 with acceptable back diffusion (<3%) in high scale concentration of Cs/Sr bearing simulated radioactive effluent solution using $(NH_4)_2CO_3$ draw solution, after optimization of flow rate and pressure drop.

➢ FO process can thereby be used efficiently for confinement of low to medium level radioactive waste into a smaller volume by judicial choice of draw solution and membrane (cellulosic as well as TFCPA).

## 7.1.2. Performance enhancement of cellulose triacetate based forward osmosis membranes by incorporation of nanomaterials

➤ Incorporation of silica and /or silver nanoparticles enhanced the performances of asymmetric cellulosic membranes in terms of water permeability. Porous silica nanoparticles provide extra channels for passage of water as well as solute molecules, the results reflected in higher water permeation at the cost of rejection. Nonporous silver nanoparticles alter the kinetics of solvent/ nonsolvent demixing during phase inversion and CTA-Ag membranes showed higher product permeability with marginal compromise in rejection.

➤ Surface images (SEM and AFM) of nanocomposite membranes confirmed impregnation of nanomaterials onto the polymer matrix without gelling leached in the course of membrane preparation.

➤ Hydropohilic silica nanoparticles exhibited decline in water contact angle value of the nanocomposite membranes (37.3°) as compared to the control (48°). Impregnation of Ag nanoparticles onto the membrane surfaces marginally lowered the water contact angle value (46.7°) owing to generation of hydrated $Ag^+$ in contact water probe solvent.

➤ Performance enhancement in terms of VRF under standard FO condition of the membranes took place in the order CTA-blank< CTA-silica=CTA-silica-Ag< CTA-Ag, the result is in line with the RO performances of control as well as composite membranes. Solute back diffusion varies from 0.45% to 1.9% over the range of draw solution concentration from 0.5 (M) to 2.0 (M).

➤ Increase in draw solution concentration increases the VRF value for all the membranes at the expense of back diffusion.

➤ Thus asymmetric CTA membranes embedded with judicially selected nanoparticles can show enhanced performance in terms of water permeability in FO mode by lowering their structural parameters.

**7.1.3. Development of performance enhanced aliphatic-aromatic based thin film composite polyamide membranes by addition of inorganic metal salts**

➤ Addition of inorganic metal (transition and nontransition) salts into amine reactant adversely affected the performance and physicochemical characteristics of PEI/IPC based TFCPA membranes. Formation of stable complexes between metal salts and PEI (as confirmed by the intense coloration and spectroscopic analyses of the amine solutions) changed the kinetics of polycondensation reaction.

➤ Performance enhancement took place on addition of metal salts upto a certain optimum concentration. This optimum concentration was found to be 2.0 m(M) for nontransition metal salts [$MgSO_4$ and $Al_2(SO_4)_3$] and 0.8 m(M) nontransition metal sulfates ($FeSO_4$, $CuSO_4$ and $NiSO_4$).

➤ Incorporation of an optimum amount of metal sulfates enhances the water permeability up to 50% with slight increase in salt rejection under standard BWRO condition. The membranes prepared with addition of optimized concentration of metal salts showed higher VRF values as compared to the control.

➤ No significant change in hydrophiliity was observed for metal complexed PEI membranes. However, as the kinetics of polycondensation reaction became faster upon addition of metal salts, by decreasing the sizes of PEI globules (confirmed by DLS), rougher PA film was formed.

➤ Performance enhancement upon addition of metal sulfates took place irrespective of the molecular weight of the polymeric amine. Membranes prepared with PEI having intermediate molecular weight (50 kDa) showed higher water permeability than those prepared with PEI of average molecular weights 2 kDa and 600 kDa.Solute rejection of the TFC-PA membranes increased with increase in molecular weight of PEI.

➢ Membranes prepared with monovalent salts like nitrate or chloride found to show higher water permeability with slight or no loss of solute rejection (~95%) under identical condition as compared the corresponding bivalent salts (sulfates) of the same metal cation.

➢ The reaction time required for completion of polycondensation reaction in absence of any complexing agent was found to be higher (60 s) than that for complexed-PEI/IPC based polymerization reaction (30 s) owing to the facilitated diffusion of smaller size polymeric amine through the nascent PA film in presence of metal salts which terminated the reaction over a shorter period of time.

➢ High flux BWRO membranes suitable for desalination of aqueous streams can thereby be developed from PEI/IPC based system by incorporation of inorganic metal salts as complexing agents.

### 7.1.4. Development of polyimide based solvent resistant membranes and their application in complexation nanofiltration using organic solvents

➢ Crosslinkling of lenzing P84 membranes with ethylene diamine made the membranes highly stable in harsh organic environments containing polar aprotic solvent like DMAc.

➢ Crosllinking for 45 minutes or more made the membranes brittle and difficult for handling. An optimum crosslinking of membranes with 3% ethylene diamine in methanol for 15-30 minutes generated smoother membranes with 6times flux enhancement without any compromise in salt rejection (>90%) as compared to the control membrane under standard NF condition.

➢ Increase in pore sizes of the membranes by 1.4 times by merging of smaller pores during crosslinking and some level of molecular relaxation (as reflected in more than 10°C decline in Tg value after crosslinking) might be the reason behind flux enhancement of Lenzing P84 membranes after chemical treatment.

➤ The optimally crosslinked membranes showed ~60% rejection of uncomplexed DMAc from an aqueous solution of 1000 ppm concentration under 10 bar operating pressure. Increase in DMAc concentration as well as operating pressure drops the rejection value to <50%.

➤ Complexation of DMAc with HCl enhanced the rejection of DMAc from 60% to 85% under similar experimental condition. The electronic repulsion between the cationic DMAc/HCl complex and slight positive charges possessed by the imide groups of Lenzing P84 polymer must be the reason behind the increment in rejection. Pure DMAC can be recovered from the concentrated stream by neutralizing it with stoichiometric quantity of NaOH.

➤ Further complexation of DMAc/HCl with $K_4[Fe(CN)_6]$ increased the rejection value up to 97% under identical set of experiment. The bigger size complex formed by reaction between DMAc/HCl and $K_4[Fe(CN)_6]$ is profoundly rejected by the SRNF membranes. Thus, depending upon the requirement (recovery of DMAc or complete removal of organics from the stream) crosslinked lenzing P84 based SRNF membranes can be used successfully for treatment of aqueous streams containing harsh organic solvents.

## 7.2. Recommendations

✓ In the present work, asymmetric nanocomposite membranes were only developed where the nanomaterials were present in the bulk of the polymer matrix. Membranes process being a surface controlled phenomena, attempts can be made to develop membranes (both cellulosic and TFC-PA) with nanoparticles located preferentially onto the membrane surface for still superior performance.

✓ Surface modifications of the indigenously developed membranes by grafting of suitable functional groups are to be endeavored to enhance their fractional rejection.

✓ As the viscosity of a polymer solution plays a major role in physicochemical characteristics as well as performance of the membranes prepared, the same may be measured prior to membrane preparation.

✓ The work discussed in this thesis involves execution of indigenously developed membranes for treatment of simulated radioactive waste. Efforts can be oriented for application of cellulosic as well as polyamide based membranes for concentration of actual radioactive wastes generated in various steps of nuclear power production. Although forward osmosis has the unprecedented advantage of low energy consumption, very few attempts have been reported till date for its relevance in treatment of radioactive waste. Cellulosic membranes being fully aliphatic in nature can be employed for concentration of low to intermediate level radioactive waste, whereas TFC membranes have the potential to be used for treatment of intermediate to high level waste also, because of their higher radiation stability owing to the aromatic ring structure present in polymer backbone. The added advantage of the process is, a simple device like membrane pouch allows no radioactive contamination (unavoidable for any other method) during the process.

✓ Efforts are to be taken up for real time usage of the membranes developed in laboratory to exploit their scope of application in targeted fields. The FO membranes developed from cellulosic (CA, CTA & CAB) as well as polyamide (aliphatic-aromatic & aromatic-aromatic) can successfully be employed for concentration of high value low volume products like fruit juices or pharmaceuticals. The method typically deployed for concentration of any item is evaporation by heating which may cause a loss of sensory (aroma, taste etc.) of the juice and denaturation of nutrients present in food or medicine. Forward osmosis being a naturally occurring process involves no external pressure or temperature during concentration of high

value low volume products like fruit juices or pharmaceuticals, thus refrains the chances of quality degradation of such items.

✓ Density and viscosity of highly concentrated draw solution play an important role in pressure drop of feed and draw solution. In order to isolate the characteristics of the spiral module in terms of pressure drop, an experimental study needs to be carried out using only DI water on both sides of the membranes.

✓ Polyamide based high performance RO membranes must be targeted for desalination of low to medium salinity water to mitigate the dearth of potable water in various parts of the country.

✓ The need of large scale production and application of solvent resistant nanofiltration membranes for decontamination of sewage water disposed by dye and tannery industries is to be taken into account as a viable and sustainable alternative of energy-intensive distillation and evaporation processes or waste generating chromatographic extractions.

# References:

[1] S. Lee, C. Boo, M. Elimelech, S. Hong, Comparison of fouling behavior in forward osmosis (FO) and reverse osmosis (RO), Journal of Membrane Science, 365 (2010) 34-39.

[2] R.L. McGinnis, M. Elimelech, Energy requirements of ammonia–carbon dioxide forward osmosis desalination, Desalination, 207 (2007) 370-382.

[3] C. Schonbein, 11, 402 (1846), Improvements in the Manufacture of Explosive Compounds, British Patent, 11 (1846) 402.

[4] A. Fick, Ueber diffusion, Annalen der Physik, 170 (1855) 59-86.

[5] J. Baranetzky, Diosmotische investigations. Annals of physics and chemistry, Pogg. Ann. physics, 147 (1872) 195-245.

[6] S. Loeb, S. Sourirajan, Sea water demineralization by means of a semipermeable membranes, UCLA Engineering Report, 60 (1960).

[7] S. Sourirajan, Reverse osmosis-a general separation technique, Reverse Osmosis and Synthetic Membranes. NRCC, Ottawa, Canada, (1977) 1-4.

[8] R.C. Ong, T.-S. Chung, J.S. de Wit, B.J. Helmer, Novel cellulose ester substrates for high performance flat-sheet thin-film composite (TFC) forward osmosis (FO) membranes, Journal of Membrane Science, 473 (2015) 63-71.

[9] D. Li, Y. Yan, H. Wang, Recent advances in polymer and polymer composite membranes for reverse and forward osmosis processes, Progress in Polymer Science, 61 (2016) 104-155.

[10] P. Sukitpaneenit, T.-S. Chung, Fabrication and use of hollow fiber thin film composite membranes for ethanol dehydration, Journal of Membrane Science, 450 (2014) 124-137.

[11] J. Su, Q. Yang, J.F. Teo, T.-S. Chung, Cellulose acetate nanofiltration hollow fiber membranes for forward osmosis processes, Journal of membrane science, 355 (2010) 36-44.

[12] R. Wang, L. Shi, C.Y. Tang, S. Chou, C. Qiu, A.G. Fane, Characterization of novel forward osmosis hollow fiber membranes, Journal of membrane science, 355 (2010) 158-167.

[13] S. Chou, L. Shi, R. Wang, C.Y. Tang, C. Qiu, A.G. Fane, Characteristics and potential applications of a novel forward osmosis hollow fiber membrane, Desalination, 261 (2010) 365-372.

[14] N.Y. Yip, A. Tiraferri, W.A. Phillip, J.D. Schiffman, M. Elimelech, High performance thin-film composite forward osmosis membrane, Environmental science & technology, 44 (2010) 3812-3818.

[15] A. Tiraferri, N.Y. Yip, W.A. Phillip, J.D. Schiffman, M. Elimelech, Relating performance of thin-film composite forward osmosis membranes to support layer formation and structure, Journal of Membrane Science, 367 (2011) 340-352.

[16] J. Wei, C. Qiu, C.Y. Tang, R. Wang, A.G. Fane, Synthesis and characterization of flat-sheet thin film composite forward osmosis membranes, Journal of Membrane Science, 372 (2011) 292-302.

[17] Q. Saren, C.Q. Qiu, C.Y. Tang, Synthesis and characterization of novel forward osmosis membranes based on layer-by-layer assembly, Environmental science & technology, 45 (2011) 5201-5208.

[18] S. Chou, R. Wang, L. Shi, Q. She, C. Tang, A.G. Fane, Thin-film composite hollow fiber membranes for pressure retarded osmosis (PRO) process with high power density, Journal of membrane science, 389 (2012) 25-33.

[19] S. Qi, C.Q. Qiu, Y. Zhao, C.Y. Tang, Double-skinned forward osmosis membranes based on layer-by-layer assembly—FO performance and fouling behavior, Journal of membrane science, 405 (2012) 20-29.

[20] S. Belfer, A. Bottino, G. Capannelli, Preparation and characterization of layered membranes constructed by sequential redox-initiated grafting onto polyacrylonitrile ultrafiltration membranes, Journal of applied polymer science, 98 (2005) 509-520.

[21] E. Kiss, J. Samu, A. Toth, I. Bertoti, Novel ways of covalent attachment of poly (ethylene oxide) onto polyethylene: surface modification and characterization by XPS and contact angle measurements, Langmuir, 12 (1996) 1651-1657.

[22] M. Ulbricht, G. Belfort, Surface modification of ultrafiltration membranes by low temperature plasma II. Graft polymerization onto polyacrylonitrile and polysulfone, Journal of Membrane Science, 111 (1996) 193-215.

[23] A.-F. Che, F.-Q. Nie, X.-D. Huang, Z.-K. Xu, K. Yao, Acrylonitrile-based copolymer membranes containing reactive groups: surface modification by the immobilization of biomacromolecules, Polymer, 46 (2005) 11060-11065.

[24] F.-Q. Nie, Z.-K. Xu, Q. Yang, J. Wu, L.-S. Wan, Surface modification of poly (acrylonitrile-co-maleic acid) membranes by the immobilization of poly (ethylene glycol), Journal of membrane science, 235 (2004) 147-155.

[25] B.-H. Jeong, E.M. Hoek, Y. Yan, A. Subramani, X. Huang, G. Hurwitz, A.K. Ghosh, A. Jawor, Interfacial polymerization of thin film nanocomposites: a new concept for reverse osmosis membranes, Journal of Membrane Science, 294 (2007) 1-7.

[26] M.L. Lind, A.K. Ghosh, A. Jawor, X. Huang, W. Hou, Y. Yang, E.M. Hoek, Influence of zeolite crystal size on zeolite-polyamide thin film nanocomposite membranes, Langmuir, 25 (2009) 10139-10145.

[27] J.M. Arsuaga, A. Sotto, G. del Rosario, A. Martínez, S. Molina, S.B. Teli, J. de Abajo, Influence of the type, size, and distribution of metal oxide particles on the properties of nanocomposite ultrafiltration membranes, Journal of membrane science, 428 (2013) 131-141.

[28] E.M.V. Hoek, A.K. Ghosh, X. Huang, M. Liong, J.I. Zink, Physical–chemical properties, separation performance, and fouling resistance of mixed-matrix ultrafiltration membranes, Desalination, 283 (2011) 89-99.

[29] J.S. Taurozzi, H. Arul, V.Z. Bosak, A.F. Burban, T.C. Voice, M.L. Bruening, V.V. Tarabara, Effect of filler incorporation route on the properties of polysulfone–silver nanocomposite membranes of different porosities, Journal of Membrane Science, 325 (2008) 58-68.

[30] L.Y. Ng, A.W. Mohammad, C.P. Leo, N. Hilal, Polymeric membranes incorporated with metal/metal oxide nanoparticles: A comprehensive review, Desalination, 308 (2013) 15-33.

[31] A. Bottino, G. Capannelli, V. D'Asti, P. Piaggio, Preparation and properties of novel organic–inorganic porous membranes, Separation and Purification Technology, 22-23 (2001) 269-275.

[32] A. Razmjou, J. Mansouri, V. Chen, The effects of mechanical and chemical modification of TiO2 nanoparticles on the surface chemistry, structure and fouling performance of PES ultrafiltration membranes, Journal of Membrane Science, 378 (2011) 73-84.

[33] A.K. Ghosh, Tewari, P.K., Next Generation Nanocomposite Ultrafiltration Membranes for Water Purification, Nanotechnology: Recent Trends, Emerging Issues & Future Directions, Nova Publishers, New York, (2014) 349-361.

[34] Y. Wang, F. Wicaksana, C.Y. Tang, A.G. Fane, Direct microscopic observation of forward osmosis membrane fouling, Environmental science & technology, 44 (2010) 7102-7109.

[35] G. Li, X.-M. Li, T. He, B. Jiang, C. Gao, Cellulose triacetate forward osmosis membranes: preparation and characterization, Desalination and Water Treatment, 51 (2013) 2656-2665.

[36] K.Y. Wang, R.C. Ong, T.-S. Chung, Double-skinned forward osmosis membranes for reducing internal concentration polarization within the porous sublayer, Industrial & Engineering Chemistry Research, 49 (2010) 4824-4831.

[37] H.R. Ahn, T.M. Tak, Y.-N. Kwon, Preparation and applications of poly vinyl alcohol (PVA) modified cellulose acetate (CA) membranes for forward osmosis (FO) processes, Desalination and Water Treatment, 53 (2015) 1-7.

[38] F. Kimura-Yeh, H.B. Hopfenberg, V. Stannett, The Preparation and Properties of Styrene Grafted Cellulose Acetate Membranes for Desalination, in: H.K. Lonsdale, H.E. Podall (Eds.) Reverse Osmosis Membrane Research: Based on the symposium on "Polymers for Desalination" held at the 162nd National Meeting of the American Chemical Society in Washington, D.C., September 1971, Springer US, Boston, MA, 1972, pp. 177-203.

[39] U. Merten, Desalination by RO, The M.I.T. Press, Cambridge, (1966).

[40] Y. Nishio, S.K. Roy, R.S.J. Manley, Blends of cellulose with polyacrylonitrile prepared from N,N-dimethylacetamide-lithium chloride solutions, Polymer, 28 (1987) 1385-1390.

[41] J.F. Masson, R.S.J. Manley, Cellulose/poly(4-vinylpyridine) blends, Macromolecules, 24 (1991) 5914-5921.

[42] L. Zhang, G. Yang, L. Xiao, Blend membranes of cellulose cuoxam/casein, Journal of membrane science, 103 (1995) 65-71.

[43] G. Qunhui, Xuejing, Y., Liankai, C. , The synthesis and properties of high cyanoethylation cellulose membrane materials, Technol. Water Treat. (China), 2, 33 (1990) 2(1990) 33.

[44] G. Qunhui, H. Ohya, Y. Xuejing, C. Liankai, H. Jicai, Preparation of ultrafiltration membranes of HCEC and CTA blend, and studies of resistance to microbiological degradation and other properties, Journal of Membrane Science, 100 (1995) 217-228.

[45] M. Sivakumar, Mohan, D., Mohan, V., Lakshmanan, C.M. in Proc. , Indo-French Int. Meet and 13th Nat. Conf. Of Ind. Memb. Soc., (1995).

[46] S. Akhtar, C. Hawes, L. Dudley, I. Reed, P. Stratford, Coatings reduce the fouling of microfiltration membranes, Journal of Membrane Science, 107 (1995) 209-218.

[47] M. Sivakumar, R. Malaisamy, C.J. Sajitha, D. Mohan, V. Mohan, R. Rangarajan, Preparation and performance of cellulose acetate–polyurethane blend membranes and their applications – II, Journal of Membrane Science, 169 (2000) 215-228.

[48] S. Zhang, K.Y. Wang, T.-S. Chung, H. Chen, Y. Jean, G. Amy, Well-constructed cellulose acetate membranes for forward osmosis: minimized internal concentration polarization with an ultra-thin selective layer, Journal of Membrane Science, 360 (2010) 522-535.

[49] W. Fang, R. Wang, S. Chou, L. Setiawan, A.G. Fane, Composite forward osmosis hollow fiber membranes: Integration of RO-and NF-like selective layers to enhance membrane properties of anti-scaling and anti-internal concentration polarization, Journal of membrane science, 394 (2012) 140-150.

[50] J. Su, S. Zhang, H. Chen, H. Chen, Y. Jean, T.-S. Chung, Effects of annealing on the microstructure and performance of cellulose acetate membranes for pressure-retarded osmosis processes, Journal of Membrane Science, 364 (2010) 344-353.

[51] R.C. Ong, T.-S. Chung, B.J. Helmer, J.S. de Wit, Novel cellulose esters for forward osmosis membranes, Industrial & engineering chemistry research, 51 (2012) 16135-16145.

[52] M. Sairam, E. Sereewatthanawut, K. Li, A. Bismarck, A. Livingston, Method for the preparation of cellulose acetate flat sheet composite membranes for forward osmosis—desalination using MgSO4 draw solution, Desalination, 273 (2011) 299-307.

[53] V. Ramachandhran, R.C. Bindal, B.M. Misra, M.P.S. Ramani, Synthesis and Characterisation of Aromatic Polyamide Hydrazide Polymers for Membrane Applications, International Journal of Polymeric Materials and Polymeric Biomaterials, 12 (1989) 271-282.

[54] R.C. Bindal, Ramachandhran,V., Misra B.M., Ramani, M.P.S. , Separation Science & Technology, 25 (1990) 1053.

[55] R.C. Bindal, V. Ramachandhran, B.M. Misra, M.P.S. Ramani, High Solute Rejecting Membranes for Reverse Osmosis: Polyetheramide Hydrazide, Separation Science and Technology, 26 (1991) 597-606.

[56] M.J. Hurndall, R.D. Sanderson, E.P. Jacobs, A.J. Van Reenen, Poly(2-vinylimidazoline) composite reverse osmosis membranes, Desalination, 90 (1993) 41-54.

[57] W. Chan, S. Lam-Leung, C. Ng, Synthesis and characterization of poly (amide-sulphonamide) s with potential for use as membrane materials in reverse osmosis applications, Polymer communications, 32 (1991) 501-503.

[58] R.J. Petersen, Composite reverse osmosis and nanofiltration membranes, Journal of membrane science, 83 (1993) 81-150.

[59] J. Glater, S.-k. Hong, M. Elimelech, The search for a chlorine-resistant reverse osmosis membrane, Desalination, 95 (1994) 325-345.

[60] P. Parrini, Polypiperazinamides: new polymers useful for membrane processes, Desalination, 48 (1983) 67-78.

[61] T. Kawaguchi, H. Tamura, Chlorine-resistant membrane for reverse osmosis. I. Correlation between chemical structures and chlorine resistance of polyamides, Journal of Applied Polymer Science, 29 (1984) 3359-3367.

[62] K. Ikeda, J. Tomaschke, Noble reverse osmosis composite membrane, Desalination, 96 (1994) 113-118.

[63] R. Singh, Characteristics of a chlorine-resistant reverse osmosis membrane, Desalination, 95 (1994) 27-37.

[64] H. Wang, L. Li, X. Zhang, S. Zhang, Polyamide thin-film composite membranes prepared from a novel triamine 3, 5-diamino-N-(4-aminophenyl)-benzamide monomer and m-phenylenediamine, Journal of Membrane Science, 353 (2010) 78-84.

[65] L. Li, S. Zhang, X. Zhang, G. Zheng, Polyamide thin film composite membranes prepared from 3, 4′, 5-biphenyl triacyl chloride, 3, 3′, 5, 5′-biphenyl tetraacyl chloride and m-phenylenediamine, Journal of Membrane Science, 289 (2007) 258-267.

[66] Z. Yong, Y. Sanchuan, L. Meihong, G. Congjie, Polyamide thin film composite membrane prepared from m-phenylenediamine and m-phenylenediamine-5-sulfonic acid, Journal of membrane science, 270 (2006) 162-168.

[67] S. Qiu, L. Wu, L. Zhang, H. Chen, C. Gao, Preparation of reverse osmosis composite membrane with high flux by interfacial polymerization of MPD and TMC, Journal of applied polymer science, 112 (2009) 2066-2072.

[68] A.K. Ghosh, B.-H. Jeong, X. Huang, E.M. Hoek, Impacts of reaction and curing conditions on polyamide composite reverse osmosis membrane properties, Journal of Membrane Science, 311 (2008) 34-45.

[69] L. Zhao, P.C.-Y. Chang, W.W. Ho, High-flux reverse osmosis membranes incorporated with hydrophilic additives for brackish water desalination, Desalination, 308 (2013) 225-232.

[70] X. Lu, S. Romero-Vargas Castrillón, D.L. Shaffer, J. Ma, M. Elimelech, In situ surface chemical modification of thin-film composite forward osmosis membranes for enhanced organic fouling resistance, Environmental science & technology, 47 (2013) 12219-12228.

[71] A. Kulkarni, D. Mukherjee, W.N. Gill, Flux enhancement by hydrophilization of thin film composite reverse osmosis membranes, Journal of Membrane Science, 114 (1996) 39-50.

[72] S. Yu, Z. Lü, Z. Chen, X. Liu, M. Liu, C. Gao, Surface modification of thin-film composite polyamide reverse osmosis membranes by coating N-isopropylacrylamide-co-acrylic acid copolymers for improved membrane properties, Journal of membrane science, 371 (2011) 293-306.

[73] R. Bernstein, S. Belfer, V. Freger, Bacterial attachment to RO membranes surface-modified by concentration-polarization-enhanced graft polymerization, Environmental science & technology, 45 (2011) 5973-5980.

[74] A. Lee, J.W. Elam, S.B. Darling, Membrane materials for water purification: design, development, and application, Environmental Science: Water Research & Technology, 2 (2016) 17-42.

[75] Y. Liu, J. Tan, W. Choi, J.-H. Hsu, D.S. Han, A. Han, A. Abdel-Wahab, C. Yu, Influence of nanoparticle inclusions on the performance of reverse osmosis membranes, Environmental Science: Water Research & Technology, 4 (2018) 411-420.

[76] C. Kong, T. Kamada, T. Shintani, M. Kanezashi, T. Yoshioka, T. Tsuru, Enhanced performance of inorganic-polyamide nanocomposite membranes prepared by metal-alkoxide-assisted interfacial polymerization, Journal of membrane science, 366 (2011) 382-388.

[77] M.T.M. Pendergast, J.M. Nygaard, A.K. Ghosh, E.M. Hoek, Using nanocomposite materials technology to understand and control reverse osmosis membrane compaction, Desalination, 261 (2010) 255-263.

[78] M.M. Pendergast, A.K. Ghosh, E. Hoek, Separation performance and interfacial properties of nanocomposite reverse osmosis membranes, Desalination, 308 (2013) 180-185.

[79] J. Park, W. Choi, S.H. Kim, B.H. Chun, J. Bang, K.B. Lee, Enhancement of chlorine resistance in carbon nanotube based nanocomposite reverse osmosis membranes, Desalination and Water Treatment, 15 (2010) 198-204.

[80] A.-h.M.A. El-Aassar, Improvement of reverse osmosis performance of polyamide thin-film composite membranes using TiO2 nanoparticles, Desalination and water treatment, 55 (2015) 2939-2950.

[81] C. Gao, X. Lu, Z. Bao, Polysulfone amide (PSA) asymmetric RO membrane, Desalination, 83 (1991) 271-278.

[82] J. Hosch, E. Staude, Preparation and investigation of chemically modified porous polyamide ultrafiltration membranes, Journal of Membrane Science, 121 (1996) 71-82.

[83] N.-N. Bui, M.L. Lind, E.M. Hoek, J.R. McCutcheon, Electrospun nanofiber supported thin film composite membranes for engineered osmosis, Journal of Membrane Science, 385 (2011) 10-19.

[84] X. Song, Z. Liu, D.D. Sun, Nano gives the answer: breaking the bottleneck of internal concentration polarization with a nanofiber composite forward osmosis membrane for a high water production rate, Advanced materials, 23 (2011) 3256-3260.

[85] J.T. Arena, B. McCloskey, B.D. Freeman, J.R. McCutcheon, Surface modification of thin film composite membrane support layers with polydopamine: enabling use of reverse osmosis membranes in pressure retarded osmosis, Journal of Membrane Science, 375 (2011) 55-62.

[86] N. Widjojo, T.-S. Chung, M. Weber, C. Maletzko, V. Warzelhan, The role of sulphonated polymer and macrovoid-free structure in the support layer for thin-film composite (TFC) forward osmosis (FO) membranes, Journal of Membrane Science, 383 (2011) 214-223.

[87] K.Y. Wang, T.S. Chung, G. Amy, Developing thin-film-composite forward osmosis membranes on the PES/SPSf substrate through interfacial polymerization, AIChE journal, 58 (2012) 770-781.

[88] X. Li, K.Y. Wang, B. Helmer, T.-S. Chung, Thin-film composite membranes and formation mechanism of thin-film layers on hydrophilic cellulose acetate propionate substrates for forward osmosis processes, Industrial & Engineering Chemistry Research, 51 (2012) 10039-10050.

[89] N. Ma, J. Wei, R. Liao, C.Y. Tang, Zeolite-polyamide thin film nanocomposite membranes: towards enhanced performance for forward osmosis, Journal of membrane science, 405 (2012) 149-157.

[90] S. Darvishmanesh, J. Degrève, B. Van der Bruggen, Mechanisms of solute rejection in solvent resistant nanofiltration: the effect of solvent on solute rejection, Physical Chemistry Chemical Physics, 12 (2010) 13333-13342.

[91] K. Vanherck, G. Koeckelberghs, I.F. Vankelecom, Crosslinking polyimides for membrane applications: a review, Progress in polymer science, 38 (2013) 874-896.

[92] P. Tin, T. Chung, Y. Liu, R. Wang, S. Liu, K. Pramoda, Effects of cross-linking modification on gas separation performance of Matrimid membranes, Journal of Membrane Science, 225 (2003) 77-90.

[93] K. Vanherck, A. Cano-Odena, G. Koeckelberghs, T. Dedroog, I. Vankelecom, A simplified diamine crosslinking method for PI nanofiltration membranes, Journal of Membrane Science, 353 (2010) 135-143.

[94] K. Vanherck, P. Vandezande, S.O. Aldea, I.F. Vankelecom, Cross-linked polyimide membranes for solvent resistant nanofiltration in aprotic solvents, Journal of Membrane Science, 320 (2008) 468-476.

[95] Y.S. Toh, F. Lim, A. Livingston, Polymeric membranes for nanofiltration in polar aprotic solvents, Journal of Membrane Science, 301 (2007) 3-10.

[96] K. Hendrix, K. Vanherck, I.F. Vankelecom, Optimization of solvent resistant nanofiltration membranes prepared by the in-situ diamine crosslinking method, Journal of membrane science, 421 (2012) 15-24.

[97] S. Dutczak, F. Cuperus, M. Wessling, D. Stamatialis, New crosslinking method of polyamide–imide membranes for potential application in harsh polar aprotic solvents, Separation and purification technology, 102 (2013) 142-146.

[98] S.P. Sun, T.S. Chung, K.J. Lu, S.Y. Chan, Enhancement of flux and solvent stability of Matrimid® thin-film composite membranes for organic solvent nanofiltration, AIChE Journal, 60 (2014) 3623-3633.

[99] M. Peyravi, M. Jahanshahi, A. Rahimpour, A. Javadi, S. Hajavi, Novel thin film nanocomposite membranes incorporated with functionalized TiO2 nanoparticles for organic solvent nanofiltration, Chemical Engineering Journal, 241 (2014) 155-166.

[100] M. Namvar-Mahboub, M. Pakizeh, Development of a novel thin film composite membrane by interfacial polymerization on polyetherimide/modified SiO2 support for organic solvent nanofiltration, Separation and Purification Technology, 119 (2013) 35-45.

[101] C. Qiu, S. Qi, C.Y. Tang, Synthesis of high flux forward osmosis membranes by chemically crosslinked layer-by-layer polyelectrolytes, Journal of membrane Science, 381 (2011) 74-80.

[102] P.H. Duong, J. Zuo, T.-S. Chung, Highly crosslinked layer-by-layer polyelectrolyte FO membranes: Understanding effects of salt concentration and deposition time on FO performance, Journal of membrane science, 427 (2013) 411-421.

[103] H. Wang, T.S. Chung, Y.W. Tong, K. Jeyaseelan, A. Armugam, Z. Chen, M. Hong, W. Meier, Highly Permeable and Selective Pore-Spanning Biomimetic Membrane Embedded with Aquaporin Z, small, 8 (2012) 1185-1190.

[104] L. Setiawan, R. Wang, K. Li, A.G. Fane, Fabrication of novel poly (amide–imide) forward osmosis hollow fiber membranes with a positively charged nanofiltration-like selective layer, Journal of Membrane Science, 369 (2011) 196-205.

[105] G. Arthanareeswaran, P. Thanikaivelan, Fabrication of cellulose acetate–zirconia hybrid membranes for ultrafiltration applications: performance, structure and fouling analysis, Separation and Purification Technology, 74 (2010) 230-235.

[106] N. Hamid, A. Ismail, T. Matsuura, A. Zularisam, W. Lau, E. Yuliwati, M. Abdullah, Morphological and separation performance study of polysulfone/titanium dioxide (PSF/TiO2) ultrafiltration membranes for humic acid removal, Desalination, 273 (2011) 85-92.

[107] S. Zhao, P. Wang, C. Wang, X. Sun, L. Zhang, Thermostable PPESK/TiO2 nanocomposite ultrafiltration membrane for high temperature condensed water treatment, Desalination, 299 (2012) 35-43.

[108] I. Sondi, B. Salopek-Sondi, Silver nanoparticles as antimicrobial agent: a case study on E. coli as a model for Gram-negative bacteria, Journal of colloid and interface science, 275 (2004) 177-182.

[109] S.J. Klaine, P.J. Alvarez, G.E. Batley, T.F. Fernandes, R.D. Handy, D.Y. Lyon, S. Mahendra, M.J. McLaughlin, J.R. Lead, Nanomaterials in the environment: behavior, fate, bioavailability, and effects, Environmental toxicology and chemistry, 27 (2008) 1825-1851.

[110] C. Marambio-Jones, E.M. Hoek, A review of the antibacterial effects of silver nanomaterials and potential implications for human health and the environment, Journal of Nanoparticle Research, 12 (2010) 1531-1551.

[111] P. Gunawan, C. Guan, X. Song, Q. Zhang, S.S.J. Leong, C. Tang, Y. Chen, M.B. Chan-Park, M.W. Chang, K. Wang, Hollow fiber membrane decorated with Ag/MWNTs: toward effective water disinfection and biofouling control, Acs Nano, 5 (2011) 10033-10040.

[112] F. Diagne, R. Malaisamy, V. Boddie, R.D. Holbrook, B. Eribo, K.L. Jones, Polyelectrolyte and silver nanoparticle modification of microfiltration membranes to mitigate organic and bacterial fouling, Environmental science & technology, 46 (2012) 4025-4033.

[113] K. Zodrow, L. Brunet, S. Mahendra, D. Li, A. Zhang, Q. Li, P.J. Alvarez, Polysulfone ultrafiltration membranes impregnated with silver nanoparticles show improved biofouling resistance and virus removal, Water research, 43 (2009) 715-723.

[114] X. Liu, S. Qi, Y. Li, L. Yang, B. Cao, C.Y. Tang, Synthesis and characterization of novel antibacterial silver nanocomposite nanofiltration and forward osmosis membranes based on layer-by-layer assembly, Water research, 47 (2013) 3081-3092.

[115] H.-L. Yang, J. Chun-Te Lin, C. Huang, Application of nanosilver surface modification to RO membrane and spacer for mitigating biofouling in seawater desalination, Water research, 43 (2009) 3777-3786.

[116] N. Stafie, D. Stamatialis, M. Wessling, Effect of PDMS cross-linking degree on the permeation performance of PAN/PDMS composite nanofiltration membranes, Separation and purification technology, 45 (2005) 220-231.

[117] L.E. Gevers, S. Aldea, I.F. Vankelecom, P.A. Jacobs, Optimisation of a lab-scale method for preparation of composite membranes with a filled dense top-layer, Journal of membrane science, 281 (2006) 741-746.

[118] L.E. Gevers, I.F. Vankelecom, P.A. Jacobs, Solvent-resistant nanofiltration with filled polydimethylsiloxane (PDMS) membranes, Journal of membrane science, 278 (2006) 199-204.

[119] S.K. Lim, K. Goh, T.-H. Bae, R. Wang, Polymer-based membranes for solvent-resistant nanofiltration: A review, Chinese Journal of Chemical Engineering, (2017).

[120] S. Aerts, A. Vanhulsel, A. Buekenhoudt, H. Weyten, S. Kuypers, H. Chen, M. Bryjak, L. Gevers, I. Vankelecom, P. Jacobs, Plasma-treated PDMS-membranes in solvent resistant nanofiltration: characterization and study of transport mechanism, Journal of membrane science, 275 (2006) 212-219.

[121] E. Florian, M. Modesti, M. Ulbricht, Preparation and characterization of novel solvent-resistant nanofiltration composite membranes based on crosslinked polyurethanes, Industrial & engineering chemistry research, 46 (2007) 4891-4899.

[122] X. Li, P. Vandezande, I.F. Vankelecom, Polypyrrole modified solvent resistant nanofiltration membranes, Journal of Membrane Science, 320 (2008) 143-150.

211

[123] L. Shao, X. Cheng, Z. Wang, J. Ma, Z. Guo, Tuning the performance of polypyrrole-based solvent-resistant composite nanofiltration membranes by optimizing polymerization conditions and incorporating graphene oxide, Journal of Membrane Science, 452 (2014) 82-89.

[124] A.V. Volkov, V.V. Parashchuk, D.F. Stamatialis, V.S. Khotimsky, V.V. Volkov, M. Wessling, High permeable PTMSP/PAN composite membranes for solvent nanofiltration, Journal of membrane science, 333 (2009) 88-93.

[125] K. Goh, W. Jiang, H.E. Karahan, S. Zhai, L. Wei, D. Yu, A.G. Fane, R. Wang, Y. Chen, All-carbon nanoarchitectures as high-performance separation membranes with superior stability, Advanced Functional Materials, 25 (2015) 7348-7359.

[126] X. Li, W. Goyens, P. Ahmadiannamini, W. Vanderlinden, S. De Feyter, I. Vankelecom, Morphology and performance of solvent-resistant nanofiltration membranes based on multilayered polyelectrolytes: study of preparation conditions, Journal of membrane science, 358 (2010) 150-157.

[127] X. Loh, M. Sairam, A. Bismarck, J. Steinke, A. Livingston, K. Li, Crosslinked integrally skinned asymmetric polyaniline membranes for use in organic solvents, Journal of Membrane Science, 326 (2009) 635-642.

[128] X.X. Loh, M. Sairam, J.H.G. Steinke, A.G. Livingston, A. Bismarck, K. Li, Polyaniline hollow fibres for organic solvent nanofiltration, Chemical communications, (2008) 6324-6326.

[129] M. Sairam, X.X. Loh, K. Li, A. Bismarck, J.H.G. Steinke, A.G. Livingston, Nanoporous asymmetric polyaniline films for filtration of organic solvents, Journal of Membrane Science, 330 (2009) 166-174.

[130] A.K. Hołda, B. Aernouts, W. Saeys, I.F. Vankelecom, Study of polymer concentration and evaporation time as phase inversion parameters for polysulfone-based SRNF membranes, Journal of membrane science, 442 (2013) 196-205.

[131] A.K. Hołda, I.F. Vankelecom, Integrally skinned PSf-based SRNF-membranes prepared via phase inversion—Part A: Influence of high molecular weight additives, Journal of Membrane Science, 450 (2014) 512-521.

[132] A.K. Hołda, I.F. Vankelecom, Integrally skinned PSf-based SRNF-membranes prepared via phase inversion—Part B: Influence of low molecular weight additives, Journal of membrane science, 450 (2014) 499-511.

[133] I.B. Valtcheva, S.C. Kumbharkar, J.F. Kim, Y. Bhole, A.G. Livingston, Beyond polyimide: crosslinked polybenzimidazole membranes for organic solvent nanofiltration (OSN) in harsh environments, Journal of Membrane Science, 457 (2014) 62-72.

[134] I.B. Valtcheva, P. Marchetti, A.G. Livingston, Crosslinked polybenzimidazole membranes for organic solvent nanofiltration (OSN): Analysis of crosslinking reaction mechanism and effects of reaction parameters, Journal of Membrane Science, 493 (2015) 568-579.

[135] C. Poinssot, S. Bourg, N. Ouvrier, N. Combernoux, C. Rostaing, M. Vargas-Gonzalez, J. Bruno, Assessment of the environmental footprint of nuclear energy systems. Comparison between closed and open fuel cycles, Energy, 69 (2014) 199-211.

[136] P. Haridasan, P. Pillai, R. Tripathi, V. Puranik, Radiological implications due to thorium in titanium mineral separation and chemical processing, Naturally Occurring Radioactive Material, (2008) 189.

[137] E. Reichmanis, C.W. Frank, J.H. O'Donnell, D.J. Hill, Radiation effects on polymeric materials: a brief overview, in, ACS Publications, 1993.

[138] C. Bowman, E. Arthur, P. Lisowski, G. Lawrence, R. Jensen, J. Anderson, B. Blind, M. Cappiello, J. Davidson, T. England, Nuclear energy generation and waste transmutation using an accelerator-driven intense thermal neutron source, Nuclear Instruments and Methods in

Physics Research Section A: Accelerators, Spectrometers, Detectors and Associated Equipment, 320 (1992) 336-367.

[139] R.L. Keeney, D. Winterfeldt, Managing nuclear waste from power plants, Risk analysis, 14 (1994) 107-130.

[140] V. Hušák, Exposure rate at the surface of syringes containing radioactive material, Journal of Nuclear Medicine, 12 (1971) 574-575.

[141] J.G. Hamilton, The applications of radioactive tracers to biology and medicine, Journal of Applied Physics, 12 (1941) 440-460.

[142] A.L. Rich, E.C. Crosby, Analysis of reserve pit sludge from unconventional natural gas hydraulic fracturing and drilling operations for the presence of technologically enhanced naturally occurring radioactive material (TENORM), NEW SOLUTIONS: A Journal of Environmental and Occupational Health Policy, 23 (2013) 117-135.

[143] P. Pillai, Naturally occurring radioactive material (NORM) in the extraction and processing of rare earths, na, 2007.

[144] K. Raj, K. Prasad, N. Bansal, Radioactive waste management practices in India, Nuclear Engineering and Design, 236 (2006) 914-930.

[145] P. Dey, N. Bansal, Spent fuel reprocessing: a vital link in Indian nuclear power program, Nuclear Engineering and Design, 236 (2006) 723-729.

[146] L. Norlén, Skin barrier formation: the membrane folding model, Journal of investigative dermatology, 117 (2001) 823-829.

[147] M. Elimelech, W.A. Phillip, The future of seawater desalination: energy, technology, and the environment, science, 333 (2011) 712-717.

[148] W.-Y. Ahn, M.-S. Kang, S.-K. Yim, K.-H. Choi, Advanced landfill leachate treatment using an integrated membrane process, Desalination, 149 (2002) 109-114.

[149] A. Cassano, A. Figoli, A. Tagarelli, G. Sindona, E. Drioli, Integrated membrane process for the production of highly nutritional kiwifruit juice, Desalination, 189 (2006) 21-30.

[150] E. Syron, E. Casey, Membrane-aerated biofilms for high rate biotreatment: performance appraisal, engineering principles, scale-up, and development requirements, Environmental science & technology, 42 (2008) 1833-1844.

[151] H.L. Knudsen, R.L. Fahrner, Y. Xu, L.A. Norling, G.S. Blank, Membrane ion-exchange chromatography for process-scale antibody purification, Journal of Chromatography A, 907 (2001) 145-154.

[152] A. Chmielewski, M. Harasimowicz, G. Zakrzewska-Trznadel, Membrane technologies for liquid radioactive waste treatment, Czechoslovak journal of physics, 49 (1999) 979-985.

[153] M.A. Shannon, P.W. Bohn, M. Elimelech, J.G. Georgiadis, B.J. Marinas, A.M. Mayes, Science and technology for water purification in the coming decades, Nature, 452 (2008) 301-310.

[154] T.Y. Cath, A.E. Childress, M. Elimelech, Forward osmosis: principles, applications, and recent developments, Journal of membrane science, 281 (2006) 70-87.

[155] G. Zakrzewska-Trznadel, M. Harasimowicz, Application of ceramic membranes for hazardous wastes processing: pilot plant experiments with radioactive solutions, Desalination, 162 (2004) 191-199.

[156] J. Yin, B. Deng, Polymer-matrix nanocomposite membranes for water treatment, Journal of Membrane Science, 479 (2015) 256-275.

[157] S. Zhao, L. Zou, C.Y. Tang, D. Mulcahy, Recent developments in forward osmosis: opportunities and challenges, Journal of membrane science, 396 (2012) 1-21.

[158] P. Mohapatra, D. Raut, A. Ghosh, A. Reddy, V. Manchanda, Radiation stability of several polymeric supports used for radionuclide transport from nuclear wastes using liquid membranes, Journal of Radioanalytical and Nuclear Chemistry, 298 (2013) 807-811.

[159] V. Ramachandhran, B. Misra, Studies on the radiation stability of ion exchange membranes, Journal of applied polymer science, 32 (1986) 5743-5747.

[160] D.N. Glew, Process for liquid recovery and solution concentration, in, Google Patents, 1965.

[161] R.L. McGinnis, Osmotic desalination process, US Patent, B1 (2002) 6391205.

[162] J. Su, T.-S. Chung, B.J. Helmer, J.S. de Wit, Enhanced double-skinned FO membranes with inner dense layer for wastewater treatment and macromolecule recycle using Sucrose as draw solute, Journal of membrane science, 396 (2012) 92-100.

[163] M.R. Moßhammer, F.C. Stintzing, R. Carle, Evaluation of different methods for the production of juice concentrates and fruit powders from cactus pear, Innovative food science & emerging technologies, 7 (2006) 275-287.

[164] A. Achilli, T.Y. Cath, A.E. Childress, Selection of inorganic-based draw solutions for forward osmosis applications, Journal of membrane science, 364 (2010) 233-241.

[165] K.S. Bowden, A. Achilli, A.E. Childress, Organic ionic salt draw solutions for osmotic membrane bioreactors, Bioresource technology, 122 (2012) 207-216.

[166] Q. Ge, J. Su, G.L. Amy, T.-S. Chung, Exploration of polyelectrolytes as draw solutes in forward osmosis processes, Water research, 46 (2012) 1318-1326.

[167] D. Li, X. Zhang, J. Yao, G.P. Simon, H. Wang, Stimuli-responsive polymer hydrogels as a new class of draw agent for forward osmosis desalination, Chemical Communications, 47 (2011) 1710-1712.

[168] H. Bai, Z. Liu, D.D. Sun, Highly water soluble and recovered dextran coated Fe3O4 magnetic nanoparticles for brackish water desalination, Separation and purification technology, 81 (2011) 392-399.

[169] M.M. Ling, T.-S. Chung, X. Lu, Facile synthesis of thermosensitive magnetic nanoparticles as "smart" draw solutes in forward osmosis, Chemical Communications, 47 (2011) 10788-10790.

[170] Q. Ge, M. Ling, T.-S. Chung, Draw solutions for forward osmosis processes: developments, challenges, and prospects for the future, Journal of membrane science, 442 (2013) 225-237.

[171] A. Razmjou, G.P. Simon, H. Wang, Effect of particle size on the performance of forward osmosis desalination by stimuli-responsive polymer hydrogels as a draw agent, Chemical engineering journal, 215 (2013) 913-920.

[172] C. Charcosset, A review of membrane processes and renewable energies for desalination, Desalination, 245 (2009) 214-231.

[173] E.S. Chian, W.N. Bruce, H.H. Fang, Removal of pesticides by reverse osmosis, Environmental Science & Technology, 9 (1975) 52-59.

[174] J. Cadotte, R. Petersen, R. Larson, E. Erickson, A new thin-film composite seawater reverse osmosis membrane, Desalination, 32 (1980) 25-31.

[175] J.E. Cadotte, Interfacially synthesized reverse osmosis membrane, in, Google Patents, 1981.

[176] I. Kenichi, Tomaschke, J., Noble reverse osmosis composite membrane, Desalination, 96 (1994) 113-118.

[177] M. Hirose, K. Ikeda, Method of producing high permeable composite reverse osmosis membrane, in, Google Patents, 1996.

[178] M.M. Chau, W.G. Light, A.X. Swamikannu, Chlorine-tolerant, thin-film composite membrane, in, Google Patents, 1993.

[179] S.H. Kim, S.-Y. Kwak, T. Suzuki, Positron annihilation spectroscopic evidence to demonstrate the flux-enhancement mechanism in morphology-controlled thin-film-composite (TFC) membrane, Environmental science & technology, 39 (2005) 1764-1770.

[180] S.-Y. Kwak, S.G. Jung, S.H. Kim, Structure-motion-performance relationship of flux-enhanced reverse osmosis (RO) membranes composed of aromatic polyamide thin films, Environmental science & technology, 35 (2001) 4334-4340.

[181] M.L. Lind, D. Eumine Suk, T.-V. Nguyen, E.M. Hoek, Tailoring the structure of thin film nanocomposite membranes to achieve seawater RO membrane performance, Environmental science & technology, 44 (2010) 8230-8235.

[182] H.J. Zwijnenberg, S. Dutczak, M. Boerrigter, M.A. Hempenius, M.W. Luiten-Olieman, N.E. Benes, M. Wessling, D. Stamatialis, Important factors influencing molecular weight cut-off determination of membranes in organic solvents, Journal of membrane science, 390 (2012) 211-217.

[183] S. Darvishmanesh, F. Tasselli, J.C. Jansen, E. Tocci, F. Bazzarelli, P. Bernardo, P. Luis, J. Degrève, E. Drioli, B. Van der Bruggen, Preparation of solvent stable polyphenylsulfone hollow fiber nanofiltration membranes, Journal of membrane science, 384 (2011) 89-96.

[184] H. Zhang, Y. Zhang, L. Li, S. Zhao, H. Ni, S. Cao, J. Wang, Cross-linked polyacrylonitrile/polyethyleneimine–polydimethylsiloxane composite membrane for solvent resistant nanofiltration, Chemical Engineering Science, 106 (2014) 157-166.

[185] S. Basu, M. Maes, A. Cano-Odena, L. Alaerts, D.E. De Vos, I.F. Vankelecom, Solvent resistant nanofiltration (SRNF) membranes based on metal-organic frameworks, Journal of membrane science, 344 (2009) 190-198.

[186] S. Hermans, H. Mariën, C. Van Goethem, I.F. Vankelecom, Recent developments in thin film (nano) composite membranes for solvent resistant nanofiltration, Current Opinion in Chemical Engineering, 8 (2015) 45-54.

[187] K. Khulbe, C. Feng, T. Matsuura, Membrane characterization, Membrane processes. United Nations Educational, Scientific and Cultural Organization, (2010) 131-172.

[188] M. Mulder, Basic principle of membrane technology, Springer Pub., 2nd Edition, Chapter –III (1996) 71–156.

[189] S.K. Sharma, P.K. Pujari, Role of free volume characteristics of polymer matrix in bulk physical properties of polymer nanocomposites: A review of positron annihilation lifetime studies, Progress in Polymer Science, 75 (2017) 31-47.

[190] S. Tao, Positronium annihilation in molecular substances, The Journal of Chemical Physics, 56 (1972) 5499-5510.

[191] M. Eldrup, D. Lightbody, J.N. Sherwood, The temperature dependence of positron lifetimes in solid pivalic acid, Chemical Physics, 63 (1981) 51-58.

[192] P. Kirkegaard, M. Eldrup, Positronfit extended: A new version of a program for analysing position lifetime spectra, Computer physics communications, 7 (1974) 401-409.

[193] N. Selvakumar, H.C. Barshilia, K. Rajam, Effect of substrate roughness on the apparent surface free energy of sputter deposited superhydrophobic polytetrafluoroethylene coatings: A comparison of experimental data with different theoretical models, Journal of Applied Physics, 108 (2010) 013505.

[194] S. Zhao, L. Zou, D. Mulcahy, Brackish water desalination by a hybrid forward osmosis–nanofiltration system using divalent draw solute, Desalination, 284 (2012) 175-181.

[195] S. Phuntsho, S. Hong, M. Elimelech, H.K. Shon, Forward osmosis desalination of brackish groundwater: Meeting water quality requirements for fertigation by integrating nanofiltration, Journal of Membrane Science, 436 (2013) 1-15.

[196] J.R. McCutcheon, R.L. McGinnis, M. Elimelech, Desalination by ammonia–carbon dioxide forward osmosis: influence of draw and feed solution concentrations on process performance, Journal of membrane science, 278 (2006) 114-123.

[197] S. Low, Preliminary studies of seawater desalination using forward osmosis, Desalination and Water Treatment, 7 (2009) 41-46.

[198] A. Achilli, T.Y. Cath, E.A. Marchand, A.E. Childress, The forward osmosis membrane bioreactor: a low fouling alternative to MBR processes, Desalination, 239 (2009) 10-21.

[199] R.W. Holloway, A.E. Childress, K.E. Dennett, T.Y. Cath, Forward osmosis for concentration of anaerobic digester centrate, Water research, 41 (2007) 4005-4014.

[200] C.A. Nayak, N.K. Rastogi, Comparison of osmotic membrane distillation and forward osmosis membrane processes for concentration of anthocyanin, Desalination and Water Treatment, 16 (2010) 134-145.

[201] K.B. Petrotos, P. Quantick, H. Petropakis, A study of the direct osmotic concentration of tomato juice in tubular membrane–module configuration. I. The effect of certain basic process parameters on the process performance, Journal of Membrane Science, 150 (1998) 99-110.

[202] E. Beaudry, K. Lampi, Membrane technology for direct-osmosis concentration of fruit juices, Food Technology, 44 (1990) 121.

[203] K.B. Petrotos, H.N. Lazarides, Osmotic concentration of liquid foods, Journal of Food Engineering, 49 (2001) 201-206.

[204] A. Ghosh, R. Bindal, S. Prabhakar, P. Tewari, Concentration of ammonium diuranate effluent by reverse osmosis and forward osmosis membrane processes, Desalination and Water Treatment, 52 (2014) 432-437.

[205] S. Prabhakar, C. Balasubramaniyan, M. Hanra, B. Misra, S. Roy, A. Meghal, T. Mukherjee, Performance evaluation of reverse osmosis (RO) and nanofiltration (NF) membranes for the decontamination of ammonium diuranate effluents, Separation science and technology, 31 (1996) 533-544.

[206] S. Prabhakar, B. Misra, S. Roy, A. Meghal, T. Mukherjee, Reverse osmosis separation of radiocontaminants from ammonium diuranate effluents, Separation science and technology, 29 (1994) 1001-1010.

[207] B.R. Staples, R.L. Nuttall, The activity and osmotic coefficients of aqueous calcium chloride at 298.15 K, Journal of Physical and Chemical Reference Data, 6 (1977) 385-408.

[208] Y.C. Kim, S.-J. Park, Experimental study of a 4040 spiral-wound forward-osmosis membrane module, Environmental science & technology, 45 (2011) 7737-7745.

[209] CRC Handbook of Chemistry and Physics, 88th ed Editor-in-Chief: David R. Lide (National Institute of Standards and Technology) CRC Press/Taylor & Francis Group: Boca Raton, FL. 2007. 2640 pp. $139.95. ISBN 0-8493-0488-1, Journal of the American Chemical Society, 130 (2008) 382-382.

[210] B. Ghosh, A. Ghosh, R. Bindal, P. Tewari, Studies on Concentration of Simulated Ammonium-diuranate Filtered Effluent Solution by Forward Osmosis Using Indigenously Developed Cellulosic Osmosis Membranes, Separation Science and Technology, 50 (2015) 324-331.

[211] E. Yuliwati, A. Ismail, T. Matsuura, M. Kassim, M. Abdullah, Effect of modified PVDF hollow fiber submerged ultrafiltration membrane for refinery wastewater treatment, Desalination, 283 (2011) 214-220.

[212] P. Van de Witte, P.J. Dijkstra, J. Van den Berg, J. Feijen, Phase separation processes in polymer solutions in relation to membrane formation, Journal of membrane science, 117 (1996) 1-31.

[213] C. Baker, A. Pradhan, L. Pakstis, D.J. Pochan, S.I. Shah, Synthesis and antibacterial properties of silver nanoparticles, Journal of nanoscience and nanotechnology, 5 (2005) 244-249.

[214] H. Strathmann, K. Kock, The formation mechanism of phase inversion membranes, Desalination, 21 (1977) 241-255.

[215] H. Strathmann, K. Kock, P. Amar, R. Baker, The formation mechanism of asymmetric membranes, Desalination, 16 (1975) 179-203.

[216] V. Ramachandhran, A. Ghosh, S. Prabhakar, P. Tewari, Preparation and separation performance studies on composite polyamide membranes using different amine systems and support membranes, Journal of Polymer Materials, 26 (2009) 177-185.

[217] V. Ramachandhran, A. Ghosh, S. Prabhakar, P. Tewari, Separation behavior of composite polyamide membranes from mixed amines: effects of interfacial reaction condition and chemical post-treatment, Separation Science and Technology, 44 (2009) 599-614.

[218] A. Ghosh, R. Bindal, S. Prabhakar, P. Tewari, Effect of Additives in Amine Solution on Performance of Aliphatic-Aromatic and Aromatic-Aromatic Polyamide Composite Reverse Osmosis (RO) Membranes, Journal of Polymer Materials, 28 (2011) 505-515.

[219] A. Ghosh, V. Ramachandhran, S.P. Singh, M. Hanra, M. Trivedi, B. Misra, Preparation and characterization of polysulfone and polyethersulfone membranes for calcium ($Ca2+$) and magnesium ($Mg2+$) separation by complexation ultrafiltration, Journal of Macromolecular Science, Part A, 39 (2002) 557-572.

[220] R.-S. Juang, M.-N. Chen, Measurement of binding constants of poly (ethylenimine) with metal ions and metal chelates in aqueous media by ultrafiltration, Industrial & engineering chemistry research, 35 (1996) 1935-1943.

[221] S. Kobayashi, K. Hiroishi, M. Tokunoh, T. Saegusa, Chelating properties of linear and branched poly (ethylenimines), Macromolecules, 20 (1987) 1496-1500.

[222] A. Von Zelewsky, L. Barbosa, C. Schläpfer, Poly (ethylenimines) as Brønsted bases and as ligands for metal ions, Coordination chemistry reviews, 123 (1993) 229-246.

[223] H. Strathmann, Selective removal of heavy metal ions from aqueous solutions by diafiltration of macromolecular complexes, Separation Science and Technology, 15 (1980) 1135-1152.

[224] A. Ghosh, V. Ramachandhran, M. Hanra, B. Misra, Synthesis, characterization and performance of sulfonated polycarbonate membranes, Journal of Polymer Materials, 15 (1998) 279-287.

[225] P.W. Morgan, S.L. Kwolek, Interfacial polycondensation. II. Fundamentals of polymer formation at liquid interfaces, Journal of Polymer Science Part A: Polymer Chemistry, 34 (1996) 531-559.

[226] R. Armstrong, U. Strauss, Polyelectrolytes, Encyclopedia of polymer science and technology, 10 (1969) 781-861.

[227] J.H. Suh, Polymeric Materials Encyclopedia, Salamone Ed.; CRC Press: Boca Raton, K.C.,, (1996) 4210 and 8230.

[228] B. Ghosh, A. Ghosh, R. Bindal, P. Tewari, Effect of Addition of Iron Salt in Amine Solution on Performance of Polyethylene Imine-Isophthaloyl Chloride (PEI-IPC) based Polyamide-Polysulfone Composite Reverse Osmosis (RO) Membranes, Journal of Polymer Materials, 31 (2014) 29.

[229] B.D. Freeman, I. Pinnau, Polymer membranes for gas and vapor separation: chemistry and materials science, ACS Publications, 1999.

[230] S.A. Stern, Polymers for gas separations: the next decade, Journal of Membrane Science, 94 (1994) 1-65.

[231] C. Dudley, B. Schöberl, G. Sturgill, H. Beckham, M. Rezac, Influence of crosslinking technique on the physical and transport properties of ethynyl-terminated monomer/polyetherimide asymmetric membranes, Journal of Membrane Science, 191 (2001) 1-11.

[232] C. Wright, D. Paul, Feasibility of thermal crosslinking of polyarylate gas-separation membranes using benzocyclobutene-based monomers, Journal of membrane science, 129 (1997) 47-53.

[233] A.F. Ismail, W. Lorna, Penetrant-induced plasticization phenomenon in glassy polymers for gas separation membrane, Separation and purification technology, 27 (2002) 173-194.

[234] K. Saito, T. Kaga, H. Yamagishi, S. Furusaki, T. Sugo, J. Okamoto, Phosphorylated hollow fibers synthesized by radiation grafting and cross-linking, Journal of membrane science, 43 (1989) 131-141.

[235] A. Mika, R. Childs, J. Dickson, B. McCarry, D. Gagnon, Porous, polyelectrolyte-filled membranes: effect of cross-linking on flux and separation, Journal of membrane science, 135 (1997) 81-92.

[236] L.S. White, Polyimide membranes for hyperfiltration recovery of aromatic solvents, in, Google Patents, 2001.

[237] P. Vandezande, L.E. Gevers, I.F. Vankelecom, Solvent resistant nanofiltration: separating on a molecular level, Chemical Society Reviews, 37 (2008) 365-405.

[238] Y. Liu, R. Wang, T.-S. Chung, Chemical cross-linking modification of polyimide membranes for gas separation, Journal of Membrane Science, 189 (2001) 231-239.

[239] L. Shao, T.-S. Chung, S.H. Goh, K.P. Pramoda, Transport properties of cross-linked polyimide membranes induced by different generations of diaminobutane (DAB) dendrimers, Journal of Membrane Science, 238 (2004) 153-163.

[240] L.S. White, Transport properties of a polyimide solvent resistant nanofiltration membrane, Journal of Membrane Science, 205 (2002) 191-202.

[241] Q. Yang, X. Chen, Z. He, F. Lan, H. Liu, The glass transition temperature measurements of polyethylene: determined by using molecular dynamic method, Rsc Advances, 6 (2016) 12053-12060.

[242] C.B. Roth, J.R. Dutcher, Glass transition and chain mobility in thin polymer films, Journal of Electroanalytical Chemistry, 584 (2005) 13-22.

[243] J.C. Jansen, Glass Transition Temperature (T g ), in: E. Drioli, L. Giorno (Eds.) Encyclopedia of Membranes, Springer Berlin Heidelberg, Berlin, Heidelberg, 2016, pp. 1-3.

[244] E. Gibbins, M. D'Antonio, D. Nair, L.S. White, L.M.F. dos Santos, I.F. Vankelecom, A.G. Livingston, Observations on solvent flux and solute rejection across solvent resistant nanofiltration membranes, Desalination, 147 (2002) 307-313.

[245] W.R. Bowen, H. Mukhtar, Characterisation and prediction of separation performance of nanofiltration membranes, Journal of Membrane Science, 112 (1996) 263-274.

[246] C. Bellona, J.E. Drewes, P. Xu, G. Amy, Factors affecting the rejection of organic solutes during NF/RO treatment—a literature review, Water research, 38 (2004) 2795-2809.

[247] X.-L. Wang, T. Tsuru, S.-i. Nakao, S. Kimura, The electrostatic and steric-hindrance model for the transport of charged solutes through nanofiltration membranes, Journal of Membrane Science, 135 (1997) 19-32.

[248] X.-L. Wang, W.-N. Wang, D.-X. Wang, Experimental investigation on separation performance of nanofiltration membranes for inorganic electrolyte solutions, Desalination, 145 (2002) 115-122.

[249] W.R. Bowen, J.S. Welfoot, P.M. Williams, Linearized transport model for nanofiltration: development and assessment, AIChE Journal, 48 (2002) 760-773.

[250] A.E. Childress, M. Elimelech, Relating nanofiltration membrane performance to membrane charge (electrokinetic) characteristics, Environmental Science & Technology, 34 (2000) 3710-3716.

[251] B.S. Lalia, V. Kochkodan, R. Hashaikeh, N. Hilal, A review on membrane fabrication: Structure, properties and performance relationship, Desalination, 326 (2013) 77-95.

[252] M. Ulbricht, Advanced functional polymer membranes, Polymer, 47 (2006) 2217-2262.

[253] D.-J. Liaw, K.-L. Wang, Y.-C. Huang, K.-R. Lee, J.-Y. Lai, C.-S. Ha, Advanced polyimide materials: syntheses, physical properties and applications, Progress in Polymer Science, 37 (2012) 907-974.

# APPENDIX

Experimental details of the indigenously developed membranes with their preparation conditions:

**Table A1: Composition of cellulosic osmosis membranes.**

| Membrane | Composition of Casting Solution (%w/w) | | | | |
|---|---|---|---|---|---|
| | Polymer | Acetone | Dioxane | Formamide | Methanol |
| CA | 23.0 | 46.0 | - | 31.0 | - |
| CTA | 8.6 | 44.4 | 44.0 | - | 3.0 |
| CAB | 5.2 (CA) + 5.2 (CTA) | 36.3 | 47.8 | - | 5.5 |

Evaporation time: 30 s, gelling medium: DI water at 1-2°C, annealing: 90°C hot water for 15mins.

**Table A2: Composition of TFCPA membranes.**

| Membrane | Concentration of Amine (%) | Concentration of Acid chloride (%) |
|---|---|---|
| Aliphatic-aromatic | 1.6 (PEI) | 0.25 (IPC) |
| Aromatic-aromatic | 2.0 (MPD) | 0.50 (TMC) |

Reaction time: 60 s.; Curing medium: IR lamp (250W); Curing temp: 90°C; Curing time: 15 mins.

**Table A3: Composition of TFCFO membranes.**

| Membrane | Additives | |
|---|---|---|
| | TEA/CSA salt (% v/v) | Phenol (% w/v) |
| TFC-1 | Nil | Nil |
| TFC-2 | 6.6 | Nil |
| TFC-3 | 6.6 | 0.8 |
| TFC-4 | 6.6 | 1.2 |
| TFC-5 | 6.6 | 1.6 |
| TFC-6 | 6.6 | 2.0 |

Reactant: 2% MPD in water & 0.1% TMC in isopar-G, Reaction time: 20 s, Curing condition: 90°C in oven for 6 mins.

**Table A4: Composition of nanocomposite cellulose triacetate membranes.**

| Membrane | Composition of casting solution (% w/w) | | | | | | |
|---|---|---|---|---|---|---|---|
| | Polymer | Acetone | 1,4-Dioxane | Methanol | Maleic acid | Silica-nanoparticle | Ag-nanoparticle |
| CTA-blank | 13.03 | 19.72 | 58.88 | 3.56 | 4.81 | - | - |
| CTA-silica | 13.01 | 19.70 | 58.80 | 3.56 | 4.80 | 0.13 | - |
| CTA-silica-Ag | 12.99 | 19.67 | 58.73 | 3.56 | 4.80 | 0.13 | 0.13 |
| CTA-Ag | 13.01 | 19.70 | 58.80 | 3.56 | 4.80 | - | 0.13 |

Evaporation time: 30s, gelling medium: DI water at room temperature; Annealing: 90°C water for 15mins.

**Table A5: Composition of PEI-FeSO$_4$ membranes.**

| Membrane | FeSO$_4$ concentration [m(M)] |
|---|---|
| 1 | 0.36 |
| 2 | 0.8 |
| 3 | 1.8 |
| 4 | 2.8 |

Reactant: 2% PEI (50 kDa) in water & 0.25% IPC in hexane, Reaction time: 60 s, Curing condition: IR lamp (250 W) for 10 mins.

**Table A6: Composition of PEI-metal sulfate membranes.**

| Salts | Metal salt concentration [m(M)] in aqueous amine | | | | | |
|---|---|---|---|---|---|---|
| CuSO$_4$ | 0.0 | 0.4 | 0.8 | 1.2 | 2.0 | 2.8 |
| NiSO$_4$ | 0.0 | 0.4 | 0.8 | 1.2 | 2.0 | 2.8 |
| MgSO$_4$ | 0.0 | 0.4 | 0.8 | 1.2 | 2.0 | 2.8 |
| Al$_2$(SO$_4$)$_3$ | 0.0 | 0.4 | 0.8 | 1.2 | 2.0 | - |

Reactant: 1.6% PEI (50 kDa) in water & 0.25% IPC in hexane, Reaction time: 60 s, Curing condition: IR lamp (250 W) for 10 mins.

**Table A7: Composition of SRNF membranes.**

| Membrane | Crosslinking time (min) |
|---|---|
| P84 | 0 |
| P84/15 | 15 |
| P84/30 | 30 |

Evaporation time: 30s, gelling medium: DI water at 22-25°C, Cross-linker conc.: 3% (v/v).

**Table A8: Effect of casting solution composition for preparation of cellulosic osmosis membranes.**

| Membrane | Composition of Casting Solution (%w/w) | | | | | Membrane performance | |
|---|---|---|---|---|---|---|---|
| | Polymer | Acetone | Dioxane | Formamide | Methanol | Flux (LMH) | % NaCl rej. |
| | CA | | | | | | |
| CA1 | 23.0 | 77.0 | - | - | - | 5.72 | 95.0 |
| CA2 | 23.0 | 66.0 | - | 11.0 | - | 8.46 | 91.2 |
| CA3 | 23.0 | 56.0 | - | 21.0 | - | 13.68 | 85.5 |
| **CA4** | **23.0** | **46.0** | **-** | **31.0** | **-** | **18.75** | **84.0** |
| CA5 | 23.0 | 36.0 | - | 41.0 | - | 24.12 | 73.5 |
| | | | | | | | |
| | CTA | | | | | | |
| CTA1 | 8.6 | 0.0 | 91.4 | - | - | 0.54 | 97.4 |
| CTA2 | 8.6 | 10.4 | 81.0 | - | - | 1.45 | 96.2 |
| CTA3 | 8.6 | 20.4 | 71.0 | - | - | 2.86 | 94.6 |
| CTA4 | 8.6 | 30.4 | 61.0 | - | - | 4.22 | 92.0 |
| CTA5 | 8.6 | 44.4 | 47.0 | - | - | 5.50 | 90.3 |
| CTA6 | 8.6 | 44.4 | 46.0 | - | 1.0 | 8.23 | 89.0 |
| CTA7 | 8.6 | 44.4 | 45.0 | - | 2.0 | 10.18 | 88.1 |
| **CTA8** | **8.6** | **44.4** | **44.0** | **-** | **3.0** | **12.08** | **87.0** |

| | | | | | | | |
|---|---|---|---|---|---|---|---|
| CTA9 | 8.6 | 44.4 | 43.0 | - | 4.0 | 16.02 | 82.5 |
| | | | | | | | |
| | CA+CTA | | | | | | |
| CAB1 | 5.2 + 5.2 | 43.3 | 43.3 | - | 3.0 | 10.56 | 92.0 |
| CAB2 | 5.2 + 5.2 | 40.3 | 46.3 | - | 3.0 | 12.10 | 90.8 |
| CAB3 | 5.2 + 5.2 | 36.3 | 50.3 | - | 3.0 | 13.05 | 90.2 |
| CAB4 | 5.2 + 5.2 | 36.3 | 49.3 | - | 4.0 | 16.11 | 88.5 |
| CAB5 | 5.2 + 5.2 | 36.3 | 48.3 | - | 5.0 | 19.76 | 86.6 |
| **CAB6** | **5.2 + 5.2** | **36.3** | **47.8** | **-** | **5.5** | **21.13** | **85.9** |
| CAB7 | 5.2 + 5.2 | 36.3 | 47.3 | - | 6.0 | 23.20 | 83.0 |

Evaporation time: 30 s ; Gelling medium : DI water at 1-2° C ; Annealing : 90° C hot water for 15minutes.

Applied pressure: 1551 kPa; Feed: 2000 ppm NaCl; Feed temperature: $25^{o}$C